

An investigation into the effect of climate change on eutrophication and surface water quality of Voëlvlei Dam with an emphasis on algal growth

by
Sayed Hanief Ally

*Dissertation presented for the degree of MSc Engineering in the Faculty of
Civil Engineering at
Stellenbosch University*



Supervisor: Mr W. Kamish, Wageed Kamish

March 2013

Declaration

By submitting this thesis electronically, I declare that the entirety of the work contained therein is my own, original work, that I am the owner of the copyright thereof (unless to the extent explicitly otherwise stated) and that I have not previously in its entirety or in part submitted it for obtaining any qualification.

Date: March 2013

بِسْمِ اللَّهِ الرَّحْمَنِ الرَّحِيمِ كَلِمَةُ الشُّكْرِ

انالحمد لله رب العالمين رب العزة و الجلال
نحمده و نعبده و نستعينه و نستغفره و نعوذ بالله من شرور انفسنا و من سيئات اعمالنا
من يهد الله فلا مضل له و من يضل الله فلا هادي له
اشهد ان لا اله الا الله وحده لا شريك له و اشهد ان محمدا عبده و رسوله

أَلَمْ تَرَ أَنَّ اللَّهَ أَنْزَلَ مِنَ السَّمَاءِ مَاءً فَأَخْرَجْنَا بِهِ ثَمَرَاتٍ مُخْتَلِفًا أَلْوَانُهَا وَمِنَ الْجِبَالِ جُدَدٌ
بَيْضٌ وَحُمْرٌ مُخْتَلِفٌ أَلْوَانُهَا وَعَرَابِيٌّ سُودٌ (27) وَمِنَ النَّاسِ وَالْدَّوَابِّ وَالْأَنْعَامِ مُخْتَلِفٌ
أَلْوَانُهُ كَذَلِكَ إِنَّمَا يَخْشَى اللَّهَ مِنْ عِبَادِهِ الْعُلَمَاءُ إِنَّ اللَّهَ عَزِيزٌ غَفُورٌ (28) (الفاطر)

وَهُوَ الَّذِي خَلَقَ مِنَ الْمَاءِ بَشَرًا فَجَعَلَهُ نَسَبًا وَصِهْرًا وَكَانَ رَبُّكَ قَدِيرًا (54) وَيَعْبُدُونَ
مِن دُونِ اللَّهِ مَا لَآ يَنْفَعُهُمْ وَلَا يَضُرُّهُمْ وَكَانَ الْكَافِرُ عَلَى رَبِّهِ ظَهِيرًا (55) (الفرقان)

أَوَلَمْ يَرَ الَّذِينَ كَفَرُوا أَنَّ السَّمَاوَاتِ وَالْأَرْضَ كَانَتَا رَتْقًا فَفَتَقْنَاهُمَا وَجَعَلْنَا مِنَ الْمَاءِ كُلَّ
شَيْءٍ حَيٍّ أَفَلَا يُؤْمِنُونَ (30) (الانبيا)

قُلْ هَلْ نُنَبِّئُكُمْ بِالْأَخْسَرِينَ أَعْمَالًا (103) الَّذِينَ ضَلَّ سَعِيَهُمْ فِي الْحَيَاةِ الدُّنْيَا وَهُمْ
يَحْسَبُونَ أَنَّهُمْ يُحْسِنُونَ صُنْعًا (104) أُولَئِكَ الَّذِينَ كَفَرُوا بِآيَاتِ رَبِّهِمْ وَلِقَائِهِ فَحَبِطَتْ
أَعْمَالُهُمْ فَلَا نُقِيمُ لَهُمْ يَوْمَ الْقِيَامَةِ وَزَنًا (105) ذَلِكَ جَزَاؤُهُمْ جَهَنَّمَ بِمَا كَفَرُوا وَاتَّخَذُوا
آيَاتِي وَرُسُلِي هُزُوعًا (106) (الكهف)

عَنْ أَبِي هُرَيْرَةَ - رضي الله عنه - أَنَّ رَسُولَ اللَّهِ - صَلَّى اللَّهُ عَلَيْهِ وَسَلَّمَ - قَالَ : - إِذَا مَاتَ الْإِنْسَانُ
انْقَطَعَ عَنْهُ عَمَلُهُ إِلَّا مِنْ ثَلَاثٍ : صَدَقَةٍ جَارِيَةٍ ، أَوْ عِلْمٍ يُنْتَفَعُ بِهِ ، أَوْ وَلَدٍ صَالِحٍ يَدْعُو لَهُ - رَوَاهُ مُسْلِمٌ

اما بعد:

من منح الماء كتب له صدق، و من حافظ ذلك الماء له اجر مثل قاسم.
هذا الكنز من عملي تركته ان ينفعي من بعد موتي لالخالفين. يا القارئ الكريم لا تنسني في
دعائك. شكرا كثيرا لعشرتي عند هذا العملي و صبرهم
و الحمد لله رب العالمين و الصلاة و السلام علي خاتم المرسلين

سيد حنيف علي ابن سيد انوار علي ابن سيد حنيف علي
كنية: ابو عبد الله

ABSTRACT

The study of climate change and its effect on the eutrophication of surface waters is a current and critically important study for the well-being of the entire planet. Within the same emission scenario various probable climate change models outcomes are possible that affect the water quality of a body of water. Voëlvlei is an off-channel dam that supplies water to the city of Cape Town in the Western Cape Province of South Africa. Historically, it is a eutrophic dam and with climate change, its water quality is expected to worsen. Four statistically downscaled climate models are used to produce meteorological outputs that drive the hydrodynamic and water quality model. The times simulated were the present day (1971-1990), the intermediate future (2046-2065) and the distant future (2081-2100). The operating procedure was not expected to change for the dam and inflows and withdrawals were kept the same for each of the simulation periods. The water quality model CE-QUAL-W2 version 3.6 was used. The bathymetry was validated with measured data. The model was calibrated for temperature, phosphorus loading, ammonium, nitrite-nitrates and chlorophyll-a concentration. The model was used to predict a present day situation in the dam, which was the basis from which future changes would be assessed. The main driver for algal growth other than nutrients and light was water temperature, which was linked to air temperature. With climate change, the air temperature will raise and enhance algal growth. The limiting nutrient was phosphorus during the winter and the rest of the year nitrogen limits algal growth. In the present day, the dominant algal group was the green algae.

With climate change an increase in the surface water temperature will increase evaporation and cause a decrease in the yield of the dam and further concentrates the algal nutrients. The surface phosphates concentration show increases in all months but especially in autumn. The total algal growth was increased annually and especially during autumn, signalling a seasonal shift and lengthening of the bloom season. The dominant algae however are still the green algae. There will be an increase in the annual concentration of diatoms. The green algae are present in the highest concentrations when compared to diatoms and cyanobacteria. The increase in its nutrients throughout the year as well as the increased water temperature allowed for unabated growth the entire year with peaks earlier in the year during autumn. Cyanobacteria are present at the surface for the entire year at significant concentrations but with intermediate and future climate change their concentrations does not change significantly. The result for cyanobacteria was inconclusive as the inter-variability between the climate models has the greatest variability for cyanobacteria, with 2 models showing an increased concentration and 2 a decreased concentration for intermediate and future time-period. For climate change, the water quality worsens especially during winter. With climate change water quality will worsen earlier in the year confirming a seasonal shift. The modelling of dissolved oxygen proved daunting as the results indicated supersaturation. The concentration of dissolved oxygen does not vary much as would be expected due to the warmer waters.

OPSOMMING

Die studie van klimaatsverandering en die uitwerking daarvan op die eutrofiseering van die oppervlaktewater is 'n huidige en krities belangrike studie vir die welsyn van die hele planeet. Binne dieselfde emissie scenario, is verskeie moontlike uitkomstes van klimaat modelle moontlik en die invloed op die kwaliteit van die oppervlaktewater. Voëlvei is 'n buite-bedding dam wat water verskaf aan die stad van Kaapstad in die Westelike Provinsie van Suid-Afrika. Histories is dit 'n eutrofiese dam en met die verandering van die klimaat sal die kwaliteit van die water na verwagting verswak. Vier statistiese afgeskaalde klimaat modelle word gebruik om meteorologiese toestande te skep en hierdie word dan gebruik as invoer vir die hidrologiese en water kwaliteits model vir die huidige situasie (1971-1990), die intermedieë toekomst (2046-2065) en die verre toekomst (2081-2100). Die bedryfs-proses vir die dam was nie verwag om te verander nie en die invloed en onttrekkings was dieselfde gehou vir elk van die simulasië periodes. Die watergehalte model CE-QUAL-W2 3.6 was gebruik. Die bathymetrie was bevestig met gemete data. Die model was gekalibreer vir temperatuur, fosfor, ammonium, nitriet-nitrate en chlorofil-a konsentrasie. Die model was gebruik om 'n huidige situasie in die dam te simuleer, wat die basis vir klimaatsveranderinge sou wees. Die vernaamste aandrywer vir die alge groei anders as voedingstowwe en lig, was water temperatuur, wat met lugtemperatuur gekoppel was. Met klimaatsverandering word die lugtemperatuur verhoog en alge groei. Die beperkende voedingstof was fosfor gedurende die winter en die res van die jaar was die dam stikstof beperk. Die dominante alge-groep in die huidige situasie was die groen alge.

Met klimaatsverandering styg die temperatuur van die oppervlaktewater, verhoog verdamping, veroorsaak afname in die vlak van die dam en verhoog die konsentrasie van die alge voedingstowwe. Die oppervlak fosfaat konsentrasie verhoog in al die maande veral in die herfs. Die totale alge groei jaarliks en veral gedurende die herfs, 'n teken van 'n seisoenale verskuiwing en verlenging van die blom seisoen. Die dominante alge was nog steeds groen alge. Daar sal 'n toename in die jaarlikse konsentrasie van diatome wees. Die groen alge is in die hoogste konsentrasies vergelyk met diatome en sianobakterië. Die toename in die voedingstowwe deur die loop van die jaar, sowel as die verhoogde watertemperatuur kan vir 'n onverpoosde groei vir die hele jaar, veral in die herfs. Sianobakterië is teenwoordig vir die hele jaar op beduidende konsentrasies, maar met intermedieë en toekomstige klimaat verander die konsentrasies nie veel nie. Die resultaat vir sianobakterië was onoortuigend as gevolg van die inter-veranderlikheid tussen die klimaat modelle, met 2 modelle wat 'n toename in konsentrasie voorspel en 2 'n afname in konsentrasie voorspel. Vir klimaatsverandering, die kwaliteit van die water vererger veral in die winter. Met klimaatsverandering skyf hierdie verswakking van water kwaliteit na vroeër in die jaar, wat bevestig 'n seisoenale skui vir verergering. Die modellering van opgeloste suurstof was uitdagende en die resultate was super-versadig. Die konsentrasie van opgeloste suurstof wissel nie veel as wat verwag sou word as gevolg van die warmer water.

TABLE OF CONTENTS

TABLE OF CONTENTS	V
LIST OF FIGURES	VIII
LIST OF TABLES	X
GLOSSARY	XII
ACRONYMS	XV
1 BACKGROUND	1
2 LITERATURE REVIEW	3
2.1 THE STUDY OF CLIMATE CHANGE	3
2.1.1 A mechanism for climate change	3
2.1.2 Modelling the climate	3
2.1.3 Global Circulation Models (GCM)	4
2.1.4 Anthropogenic emission scenarios	5
2.1.5 A Global Circulation Model projection	7
2.1.6 Regional climate models (RCM)	8
2.1.7 Statistical downscaling to a RCM	9
2.1.8 Uncertainty in the downscaled RCM model	10
2.1.9 The use of climate change models in South Africa	10
2.1.10 The impacts of climate change for Southern Africa	10
2.2 WATER QUALITY IN RESERVOIRS AND RIVERS	12
2.2.1 South African water quality guidelines	12
2.3 EUTROPHICATION	13
2.3.1 A Definition for eutrophication	13
2.3.2 Causes of eutrophication	14
2.3.3 The sources of algal nutrients	14
2.4 FACTORS AFFECTING WATER QUALITY AND ALGAL GROWTH	16
2.4.1 The effect of temperature and solar radiation on algal growth	16
2.4.2 The effect of dissolved oxygen (DO) on algal growth	17
2.4.3 The effect of light and turbidity on algal growth	18
2.4.4 The effect of TDS, conductivity and salinity on algal growth	19
2.4.5 The effect of Nitrogen on algal growth	20
2.4.6 The effect of Phosphorus on algal growth	20
2.4.7 The limiting nutrient concept	21
2.5 TROPHIC STATUS	22
2.5.1 The Trophic Index (TRIX)	22
2.6 TOXIC ALGAE AND THEIR NEGATIVE EFFECTS	23
2.6.1 Human health risks	23
2.7 WATER TREATMENT FACILITY PROBLEMS	24
2.7.1 Aquatic fauna and flora problems	25
2.7.2 Mitigating the effects of eutrophication	25
3 MODELLING THE EFFECT OF CLIMATE CHANGE ON EUTROPHICATION	28
3.1 MODELLING WATER QUALITY	29

3.1.1	A concise history of Water Quality models	29
3.1.2	Hydrodynamic and hydraulic models (H/H)	30
3.1.3	Hydrological and watershed models (H/W)	30
3.1.4	Surface water quality models (SWQ)	30
3.1.5	Groundwater models (GW)	31
3.1.6	Ecological models (E)	31
3.2	A REVIEW OF RELEVANT WATER QUALITY MODELS	32
3.2.1	Model selection	32
3.2.2	BASINS	35
3.2.3	QUAL-2E	36
3.2.4	CE-QUAL-ICM	36
3.2.5	CE-QUAL-RIV1	37
3.2.6	CE-QUAL-W2 version 3.6	37
3.2.7	DUFLOW	38
3.2.8	EFDC	38
3.2.9	ELCOM-CAEDYM	39
3.2.10	EUTROMOD	39
3.2.11	MIKE 11, MIKE 21, MIKE 3	40
3.2.12	WASP5	41
3.3	THE MODEL SELECTION	41
3.4	THE THEORETICAL BASIS FOR CE-QUAL-W2 HYDRODYNAMIC AND WATER QUALITY MODEL	42
3.4.1	The conservation laws of fluid flow	43
3.4.2	Total dissolved solids	46
3.4.3	Generic constituents	47
3.4.4	Phosphates	47
3.4.5	Nitrate-Nitrite	50
3.4.6	Ammonium	51
3.4.7	Dissolved Silica	52
3.4.8	Particulate silica	54
3.4.9	Total Algae	54
3.4.10	Zooplankton	58
3.4.11	Dissolved oxygen	59
3.4.12	Labile Particulate Organic Matter (LPOM)	61
3.4.13	Refractory Particulate Organic Matter (RPOM)	62
3.4.14	Labile Dissolved Organic Matter (LDOM)	62
3.4.15	Refractile Dissolved Organic Matter (RDOM)	63
3.4.16	Labile Dissolved Organic Matter – Phosphorus (LDOM-P)	64
3.4.17	Refractory Dissolved Organic Matter – Phosphorus (RDOM-P)	65
3.4.18	Labile Particulate Organic Matter – Phosphorus (LPOM-P)	65
3.4.19	Refractory Particulate Organic Matter – Phosphorus (RPOM-P)	66
3.4.20	Labile Dissolved Organic Matter – Nitrogen (LDOM-N)	66
3.4.21	Refractory Dissolved Organic Matter – Nitrogen (RDOM-N)	67
3.4.22	Labile Particulate Organic Matter – Nitrogen (LPOM-N)	67

3.4.23	Refractory Particulate Organic Matter – Nitrogen (RPOM-N)	68
3.4.24	Organic Sediments	68
3.4.25	Suspended solids and sedimentation	70
4	BACKGROUND TO VOËLVLEI DAM	71
4.1	SPECIFIC MODELLING REQUIREMENTS FOR THIS STUDY	73
4.1.1	Bathymetry validation	75
4.1.2	Meteorological data	76
4.1.3	Inflow water quantity and quality data	77
4.1.4	The model boundary conditions	78
4.1.5	The initial conditions	78
4.1.6	Model parameterisation	80
4.1.7	The algal temperature-growth relationship	82
4.2	MODEL PERFORMANCE AND VALIDATION	83
4.2.1	Modelled Dam hydraulics	83
4.2.2	Model temperature predictions	84
4.2.3	Ortho phosphorus comparison	85
4.2.4	Ammonium and nitrite-nitrate comparison	86
4.2.5	Chlorophyll-a comparison	87
4.2.6	Conservative tracer tracking	88
4.2.7	Validation of the assumption of complete mixing of Voëlvlei Dam	89
4.3	DWA Target Water Quality Ranges	91
5	THE CLIMATE CHANGE MODELLING RESULTS AND ANALYSIS	94
5.1	THE PRESENT DAY SCENARIO	95
5.1.1	Air temperature	95
5.1.2	Solar radiation	96
5.1.3	Wind-speed and direction	98
5.1.4	Surface water temperature	100
5.1.5	Surface water elevation	102
5.1.6	Algal nutrient inflow concentrations	104
5.1.7	Ortho-Phosphorus concentration	106
5.1.8	Nitrogen concentration	108
5.1.9	Ammonium concentration	108
5.1.10	Nitrate-nitrite concentrations	110
5.1.11	Total nitrogen concentration and the half-saturation constant	112
5.1.12	Identifying the limiting nutrient	113
5.1.13	Dissolved silicon concentration	114
5.1.14	Dissolved oxygen concentration	117
5.1.15	Total algal concentration	121
5.1.16	Diatoms concentration	123
5.1.17	Green algae concentration	125
5.1.18	Cyanobacteria concentration	126
5.1.19	Zooplankton growth	129
5.1.20	Eutrophication level	130
5.2	THE CLIMATE CHANGE SCENARIOS AND EUTROPHICATION LEVELS	132

5.2.1	Air temperature	132
5.2.2	Solar radiation.....	135
5.2.3	Surface water temperature changes	136
5.2.4	Surface water elevations.....	138
5.2.5	Ortho-Phosphorus concentration	140
5.2.6	Ammonium concentration	143
5.2.7	Nitrite-nitrate concentration	144
5.2.8	Dissolved silicon	147
5.2.9	Dissolved oxygen.....	150
5.2.10	Total algae concentration.....	153
5.2.11	Diatom concentration	156
5.2.12	Green algae concentration.....	158
5.2.13	Cyanobacteria concentration	160
5.2.14	The dominant algal group	164
5.2.15	Zooplankton concentration.....	165
5.2.16	Eutrophication level.....	167
6	DISCUSSION	170
7	LIMITATIONS OF THIS STUDY	180
7.1	CE-QUAL-W2 MODEL LIMITATIONS.....	180
7.2	CLIMATE DATA LIMITATIONS.....	180
7.3	INFLOW AND WITHDRAWAL LIMITATIONS	181
7.4	ALGAL GROWTH RATES	181
7.5	GENERAL	182
8	CONCLUSIONS	183
8.1	STUDY LIMITATIONS	183
8.2	WATER QUALITY MODELLING.....	184
9	RECOMMENDATIONS.....	186
10	LIST OF REFERENCES	187
11	APPENDIX	197

LIST OF FIGURES

Figure 1:	A typical grid used when developing a climate model.....	4
Figure 2:	Increasing uncertainties within a climate change scenario development ...	5
Figure 3	The mentioned SRES scenarios for climate change models	6
Figure 4	Changes in temperature, precipitation and pressure for A1B scenario	7
Figure 5	A schematic diagram of downscaling	9
Figure 6	Temperature trends from 1901 to 1950 and predictions to 2100	11
Figure 7	The main factors that affect the trophic states of water-bodies.....	15
Figure 8	Nomogram chart for quick dissolved oxygen calculations	18
Figure 9	Conceptual eutrophication with regards to P in bottom waters	21
Figure 10	The locations of recorded cyanobacteria toxicity events in South Africa ..	24
Figure 11	A typical control volume.....	44
Figure 12	Stress on a control volume	45
Figure 13	Internal fluxes of generic constituents	47
Figure 14	Internal fluxes of phosphorus	48
Figure 15	Internal flux of nitrate/nitrite	50
Figure 16	Internal fluxes of ammonium	51

Figure 17	Internal fluxes of dissolved Silica.....	53
Figure 18	Internal fluxes of particulate Silica.....	54
Figure 19	Internal flux of algae.....	55
Figure 20	Fluxes that affect zooplankton.....	58
Figure 21	Internal flux of dissolved oxygen.....	59
Figure 22	Internal flux of LPOM.....	61
Figure 23	Internal fluxes of RPOM.....	62
Figure 24	Internal fluxes of LDOM.....	63
Figure 25	Fluxes of RDOM.....	64
Figure 26	Zero and first order internal fluxes for organic sediments.....	69
Figure 27	Topographic map of Voëlvlei Dam and surrounds.....	71
Figure 28	Voëlvlei Dam and its inlet canal system.....	72
Figure 29	The 1998 sediment survey of Voëlvlei Dam.....	73
Figure 30	Contour map and 3D shape of Voëlvlei Dam generated as by Surfer.....	74
Figure 31	Segments for Voëlvlei Dam as used by CE-QUAL-W2 (NS direction).....	74
Figure 32	Side and sectional mathematical grid view of Voëlvlei Dam.....	75
Figure 33	Comparison of Voëlvlei Dam volumes.....	76
Figure 34	An example algal growth-temperature relationship.....	82
Figure 35	Surface water level comparison with measured data.....	84
Figure 36	Surface water temperature compared with measured data.....	85
Figure 37	Comparison of simulated phosphate with sampled values.....	86
Figure 38	Comparison of modelled ammonium with sampled values.....	87
Figure 39	Comparison of Nitrite-nitrate with sampled values.....	87
Figure 40	Comparison of chlorophyll-a with sampled values.....	88
Figure 41	Comparison of modelled tracer to sampled values.....	89
Figure 42	Tracer profile at segment 11 for various depths using calibration data.....	89
Figure 43	Vindication of the fully mixed assumption.....	90
Figure 44	Present day air temperature driving Voëlvlei Dam water temperature.....	91
Figure 45	The timeline for climate change study.....	94
Figure 46	Present day mean air temperature predictions.....	96
Figure 47	Present day solar radiation.....	97
Figure 48	Present day solar radiation exceedance for light saturation.....	98
Figure 49	The N-S orientation of Voëlvlei Dam.....	99
Figure 50	Wind-speed and direction over Voëlvlei Dam.....	99
Figure 51	Surface water temperatures at segment 11.....	100
Figure 52	The monthly surface water temperature for segment 11.....	101
Figure 53	Present day surface water temperature exceedance plot.....	102
Figure 54	Present day surface water elevations.....	103
Figure 55	The monthly surface water elevations.....	103
Figure 56	Constituents concentration in the inflow of Voëlvlei Dam.....	105
Figure 57	Dissolved silicon inflow concentration.....	105
Figure 58	Present day ortho-phosphorus concentration at segment 11.....	106
Figure 59	The present day monthly ortho-phosphorus concentration.....	107
Figure 60	The present day ammonium concentration for Voëlvlei Dam.....	108
Figure 61	The monthly present day ammonium concentration.....	109
Figure 62	Present day surface ammonium exceedance plot.....	110
Figure 63	Present day nitrite-nitrate concentrations.....	111
Figure 64	Monthly present day Nitrite-Nitrate concentrations.....	111
Figure 65	Present day surface nitrate-nitrite exceedance plot.....	112
Figure 66	Present day total nitrogen half-saturation exceedance plot.....	113
Figure 67	Present day limiting nutrient from DWA standards.....	114
Figure 68	Present day silicon concentrations.....	115
Figure 69	Monthly present day silicon concentrations.....	115
Figure 70	Present day dissolved silicon half-saturation exceedance plot.....	116
Figure 71	Present day dissolved oxygen concentration.....	117
Figure 72	Monthly dissolved oxygen concentration.....	118
Figure 73	Present day surface dissolved oxygen exceedance plot.....	119
Figure 74	Effect of varied algal growth rates on dissolved oxygen.....	120
Figure 75	CCC present day DO exceedance levels.....	120
Figure 76	Present day total algal concentration.....	121

Figure 77	Monthly mean total algal concentration	122
Figure 78	Present day total algae exceedance plot	123
Figure 79	Present day diatom concentration	124
Figure 80	Monthly diatom concentration.....	124
Figure 81	Present day green algae concentration.....	125
Figure 82	Present day monthly green algae concentration	126
Figure 83	Present day cyanobacteria concentration	127
Figure 84	Present day monthly cyanobacteria concentration.....	127
Figure 85	Present day surface cyanobacteria exceedance, DWA limits with zoom	128
Figure 86	Present day zooplankton concentration	129
Figure 87	Present day monthly zooplankton concentration.....	130
Figure 88	Present day TRIX level.....	131
Figure 89	Climate change air temperature predictions.....	133
Figure 90	Mean monthly incident solar radiation over Voëlvlei Dam	135
Figure 91	Climate change surface water temperature	136
Figure 92	Distant future surface water temperature exceedance	138
Figure 93	Climate change surface water elevations.....	139
Figure 94	Climate change surface phosphate concentration	141
Figure 95	Climate change surface ammonium concentration	143
Figure 96	Climate change surface Nitrite-nitrate concentration	145
Figure 97	Distant future total surface N exceedance	147
Figure 98	Climate change surface dissolved silicon concentration.....	148
Figure 99	Distant future surface dissolved silicon concentration exceedance	150
Figure 100	Climate change surface dissolved oxygen concentration	151
Figure 101	Distant future surface dissolved oxygen DWA limit exceedance plot	153
Figure 102	Climate change surface total algae concentration	154
Figure 103	Distant future surface total algae DWA exceedance plot.....	156
Figure 104	Climate change surface diatom concentration	157
Figure 105	Climate change surface green algae concentration	159
Figure 106	Climate change cyanobacteria concentrations.....	161
Figure 107	Climate change surface cyanobacteria concentration	162
Figure 108	Distant future DWA cyanobacteria exceedance plot.....	164
Figure 109	The effect of climate change on surface algal concentrations (mg/l)	165
Figure 110	Climate change surface zooplankton concentration	166
Figure 111	Climate change effect on the TRIX levels of Voëlvlei Dam.....	168
Figure 112	The mean monthly air temperature effect for Voëlvlei Dam.....	171
Figure 113	The mean monthly surface phosphorus concentration	172
Figure 114	The mean monthly surface ammonium concentration	172
Figure 115	The mean monthly surface Nitrite-nitrate concentration	173
Figure 116	The mean monthly surface dissolved silicon concentration	174
Figure 117	The mean monthly surface dissolved oxygen concentrations.....	174
Figure 118	The mean monthly surface total algae concentrations.....	175
Figure 119	The mean monthly surface diatom concentrations.....	176
Figure 120	The mean monthly surface green algae concentrations	176
Figure 121	The mean monthly surface cyanobacteria concentrations.....	177
Figure 122	The mean monthly surface zooplankton concentrations.....	178
Figure 123	The mean monthly surface TRIX level	178

LIST OF TABLES

Table 1	Summary of water quality for recreational and other use.....	13
Table 2	Selected ranges of P and N as well as their effects	22
Table 3	Categories of TRIX values.....	23
Table 4	A summary of some of the current available models	33
Table 5	Flow gauging stations recording inflow to Voëlvlei Dam	77
Table 6	Summary of the boundary conditions for Voëlvlei Dam	78
Table 7	Constituents modelled and initial values	79
Table 8	Parameters used in water quality model	80

Table 9	The growth-temperature variable values used for this modelling study	83
Table 10	TWQR for the modelled water quality constituents	92
Table 11	TWQR for all algae	93
Table 12	Present day mean air temperature (°C).....	96
Table 13	Present day mean monthly daytime solar radiation (W/m ²)	97
Table 14	Present day mean surface water temperature (°C).....	101
Table 15	Present day mean surface water elevations (masl)	104
Table 16	Present day mean surface ortho-phosphorus concentration (mg/l)	107
Table 17	Present day mean surface ammonium concentration (mg/l).....	109
Table 18	Present day mean surface Nitrite-Nitrate concentration (mg/l)	112
Table 19	Total surface mean monthly nitrogen concentration	113
Table 20	Inflow concentration of dissolved silicon into Voëlvlei	114
Table 21	Present day mean monthly dissolved silicon concentration (mg/l).....	116
Table 22	Present day mean monthly dissolved oxygen concentration (mg/l)	118
Table 23	Present day mean monthly surface total algae concentration (mg/l)	122
Table 24	Present day mean monthly surface diatom concentration (mg/l)	125
Table 25	Present day mean monthly green algae concentration (mg/l).....	126
Table 26	Present day mean monthly surface cyanobacteria concentration (mg/l)	128
Table 27	Present day mean monthly surface zooplankton concentration (mg/l) ...	130
Table 28	Present day monthly mean surface TRIX levels	131
Table 29	Climate change mean monthly air temperature (°C)	134
Table 30	Climate change mean monthly surface water temperature (°C)	137
Table 31	Climate change surface water elevations (m)	140
Table 32	Climate change phosphate concentration (mg/l).....	142
Table 33	Climate change ammonium concentration (mg/l).....	144
Table 34	Climate change nitrite-nitrate concentration (mg/l).....	146
Table 35	Climate change dissolved silicon concentration (mg/l)	149
Table 36	Climate change dissolved oxygen concentration (mg/l)	152
Table 37	Climate change total algae concentration (mg/l)	155
Table 38	Climate change diatom concentration (mg/l)	158
Table 39	Climate change green algae concentration (mg/l).....	160
Table 40	Climate change cyanobacteria concentration (mg/l)	163
Table 41	Climate change zooplankton concentration (mg/l)	167
Table 42	Climate change effect on the surface TRIX level	169
Table 43	Concise summary of water quality	179

GLOSSARY

Adsorption	The adhesion of atoms, ions, biomolecules or molecules of gas, liquid, or dissolved solids to a surface
Algal respiration	A process whereby food molecules are processed to obtain chemical energy
Anoxia	An extreme low level of hypoxia, literally no oxygen.
Anthropogenic	Effects, processes or materials derived from human activities, as opposed to those occurring in biophysical environments without human influence
Benthic	The lower regions of the water-body including the sediment surface
Benthivorous	Animals that feed on organisms living on the bed of the water-body
Biogenic	These are substances produced by the life process such as excretion or secretions
Boreal	Northern hemisphere
Cyanobacteria	Also known as blue-green algae - a phylum of bacteria that obtain energy through photosynthesis. Certain cyanobacteria produce toxins which can be neurotoxins (nerve), hepatotoxins (liver), cytotoxins (tissue), and endotoxins, and can be dangerous to humans and animals.
Desorption	A process whereby a substance is released from or through a surface. The process is the opposite of adsorption.
Detritus	Non-living particulate organic material. It includes the bodies or fragments of dead organisms as well as faecal material.
Dinoflagellates	A type of plankton that has a whip-like tail
El Nino	A globally coupled climate phenomenon whereby warming of the eastern Pacific Ocean causes varying weather conditions in that area (means "the Christ child" in Spanish). El Nino is coupled with La Nina, and is known also as the El Nino Southern Oscillation (ENSO).
Epilimnion	Upper portion of a lake, down to the thermocline
Epiphyton	Organisms attached to immovable substrates in the water-body
Euclidean	Ordinary' distance between 2 points, as measured
Eutrophic	Rich (high in nutrients) and an increased level of water quality problems
Exosphere	The outermost layer of the atmosphere
Extracellular	Outside of the cell
Flocculation	The process whereby particles distributed within a fluid are conglomerated and then removed from the fluid
Holomictic	Lakes that have a uniform temperature and density from top to bottom, allowing the lake waters to mix.
hPa	hectopascals = 100 Pascal's (Pa)
Hydrodynamic	The study of fluids in motion
Hydraulic	The study of the mechanical properties of fluids
Hydrology	The study of movement, distributions and quality of water
Hypertrophic	Excessive levels of nutrients and water quality are almost continuous
Hypolimnetic	Water in the hypolimnion
Hypolimnion	The dense, bottom layer of water in a thermally-stratified lake, below the thermocline. Typically, the hypolimnion is the coldest layer of a lake in

summer, and the warmest layer during winter. It is isolated from surface wind mixing during summer, and usually receives insufficient irradiance for photosynthesis to occur.

Hypoxia	Low levels of oxygen, detrimental to aerobic organisms
Ionosphere	Stretches from 50 to 1,000 km, and the part of the atmosphere that is ionized by solar radiation. It typically overlaps both the exosphere and the thermosphere.
Labile	Adaptable
Lachrymal	The glands that produce tears
Lentic	Refers to standing/stagnant waters or still waters
Lotic	Refers to flowing water, from the Latin <i>lotus</i> , past participle of <i>lavere</i> , to wash. It refers to rivers, springs and streams.
Lymnology, Lymnolytic	Refers to inland waters
Macrophyte	An aquatic plant that grown in or near water
Mesoscale	An area of between 5 and several hundred kilometres for the study of local climate conditions
Mesosphere	A layer extending from the stratopause to 80–85 km.
Mesotrophic	Intermediate level of nutrients with emerging signs of water quality problems
Metalimnetic	Refers to the thermocline
Monomictic	Are dams that are thermally stratified throughout much of the year. The density difference between the warm surface waters and the colder bottom waters prevents these lakes from mixing in summer. During winter the surface waters cool to a temperature equal to the bottom waters then it mixes thoroughly each winter from top to bottom.
Oligotrophic	Low in nutrients, usually no water quality problems.
Orography	The study of the formation and relief of mountains. Can more broadly include hills, and any part of a region's elevated terrain. Orography (also known as <i>oreography</i> , <i>orology</i> or <i>oreology</i>) falls within the broader discipline of geomorphology.
Orthophosphate	A chemical molecule or ion containing 1 phosphate element such as phosphoric acid, H_3PO_4
Perihelion	The point in the orbit of a planet that it is closest to the sun
Periphyton	A complex mixture of algae, cyanobacteria, heterotrophic microbes and detritus that is attached to submerged surfaces in most aquatic ecosystems. It serves as an important food source for invertebrates, tadpoles and some fish.
Planorbid	Air breathing snails
Phytoplankton	Microscopic photosynthesising plankton
Primary production	The production of organic compounds from atmospheric or aquatic carbon dioxide, principally through the process of photosynthesis, with chemosynthesis being much less important. Almost all life on earth is directly or indirectly reliant on primary production.
Radiosonde	A device for use in weather balloons that measures various atmospheric parameters and transmits them to a fixed receiver.

Refractory	Slowly decomposing organics that exert a effect on the dissolved oxygen concentrations
Riparian	The interface between land and a river or stream. Riparian is also one of the fifteen terrestrial biomes of the earth.
Secchi	A measurement of a water-body's turbidity. A disc is mounted on a pole or line, and lowered slowly down in the water. The depth at which the pattern on the disk is no longer visible is taken as a measure of the transparency of the water. This measure is known as the Secchi depth.
Stratopause	The level of the atmosphere which is the boundary between two layers, stratosphere and the mesosphere. The stratopause is 50 to 55 km above the Earth's surface.
Stratosphere	The stratosphere extends from the tropopause to about 51 km. The ozone layer is contained in this layer.
Stochastic	Random.
TDS	Total Dissolved Solids
Thermal stratification	The separation of lakes into three layers: Epilimnion - top of the lake, Metalimnion (or thermocline) - middle layer that may change depth throughout the day, Hypolimnion - the bottom layer of the lake.
Thermocline	A thermocline (sometimes metalimnion) is a thin but distinct layer in a fluid in which temperature changes more rapidly with depth than it does in the layers above or below. In water-bodies, the thermocline may be thought of as an invisible blanket, which separates the upper mixed layer from the calm, deep water below.
Thermosphere	The thermosphere is between 320 and 380 km. The top of the thermosphere is the bottom of the exosphere.
Troposphere	The troposphere begins at the Earth's surface and extends to between 7 km at the poles and 17 km at the Equator, with some variation due to weather.
Tropopause	The atmospheric boundary between the troposphere and the stratosphere
Turbidity	The cloudiness or haziness of a fluid caused by individual particles (suspended solids) that are generally invisible to the naked eye, similar to smoke in air. The measurement of turbidity is a key test of water quality.
Zooplankton	A drifting predatory type of plankton

ACRONYMS

BOD	Biological Oxygen Demand
DOM	Dissolved Organic Matter
DWA	The Department of Water Affairs, previously the Department of Water Affairs and Forestry (DWA)
DWA	The former Department of Water Affairs and Forestry, now DWA
GCM	Global Circulation Model for climate change modelling
HAB	Hazardous Algal Blooms
IIASA	International Institute for Applied Systems Analysis
IPCC	Intergovernmental Panel on Climate Change, established in 1988
MWTP	Municipal Water Treatment Plant
MWWTP	Municipal Waste Water Treatment Plant
N	Nitrogen
NTU	Nephelometric Turbidity Units, used to quantify turbidity
O	Oxygen
OECD	Organisation for Co-operation and Economic Development
P	Phosphorous
POM	Particulate Organic Matter
RCM	Regional Circulation Model for climate change modelling
SLP	Sea Level Pressure
SRES	Special Report on Emissions Scenarios
TWQR	Target Water Quality Range
WWTP	Waste Water Treatment Plant

1 BACKGROUND

The rivers of South Africa differ in water chemistry because of differences in geology and climate, as well as in the nature of the terrestrial vegetation and anthropogenic impacts. Thus, riverine biotas differ in their water quality requirements. Two of the major water quality problems facing water quality managers in South Africa are salinisation of rivers and the eutrophication of both rivers and dams. As a result of the clearing of native vegetation for the preparation of agricultural land, groundwater levels have risen, thereby mobilising the stored salt and causing adverse impacts on farmland, infrastructure, water resources and biodiversity in catchments (Pannell et al., 2006). The Berg River, in particular, has a long history of salinity concerns that have been ascribed to significant quantities of sodium and chloride in the weathered shale, which would leach out under favourable conditions, as well as dryland salinity runoff from irrigated wheat lands and other agricultural practices. An increase in the inflow of plant nutrients into a water-body and favourable prevalent weather conditions may result in an excess growth of periphyton (attached algae) and phytoplankton (floating algae), as well as macrophytes (aquatic plants).

Water quality is influenced by a range of natural factors that include biological, geological, hydrological, meteorological and topographical influences. These factors may vary seasonally according to differences in weather conditions, run-off volumes and water levels. Human (anthropogenic) influences on water quality are mainly due to flow diversions, water abstraction, wetland drainage, dam construction and pollution. The discharges of agricultural, industrial and urban wastewater, as well as the diffuse run-off of agricultural fertilisers and pesticides into catchments, are negative factors influencing water quality (Codd, 2000:52).

Public opinion increasingly supports action to mitigate greenhouse gas emissions, thereby minimising the rate and magnitude of anthropogenic climate change. The majority of the people in many countries now believe that they will see the impacts of climate change in their lifetimes, and that adaptation to the changes is essential for limiting the potential impacts. Continuing to improve how the scientific community assesses and communicates uncertainty to the public and decision makers is crucial to improving the utility of research on climate change both in perception and in reality (Moss, 2007:1).

In recent history, it could be said that the South African policy towards eutrophication had been inadequate. A need was therefore identified in 2000 by the Water Research Commission (WRC) to develop capacity for eutrophication management (Walmsley, 2000). The results of this study included:

- A guide to assess eutrophication-related water quality for rivers, lakes and wetlands;
- An internet based Nutrient Enriched Assessment Protocol (NEAP); and
- A course outline and training material for short course in eutrophication assessment (Rossouw et al., 2008).

Cyanobacteria (blue-green algae) blooms in South African waters are a problem and have existed for many decades. It is argued that the trophic status of major dams in Gauteng was high enough that a regional crisis exists, but that the problem has not reached national crisis status. Algal problems are routinely experienced in 10 dams, of which 5 are situated in the economics and population hub of the country namely Gauteng. In dams such as Hartebeespoort, hypertrophy

exists and severe cyanobacteria problems have been common for decades. Other dams are incipient eutrophic, which was common worldwide and has resulted in eutrophication being identified as the greatest threat to future water supply across the world (Harding, 2006).

The aim of this study was to perform an investigation into the effect of climate change on the surface water quality of Voëlvlei Dam with an emphasis on the surface algal growth for climate change scenarios. The objectives of the study should provide a quantitative analysis of

1. The effect of climate change on air temperature and water temperature;
2. The effect of climate change on algal nutrient dynamics; and
3. The effect of climate change on algal growth and possible algal succession.

In order to meet these aims and objectives a literature review was performed and emphasis was given to:

1. Introduction of the concept of climate change and its effects;
2. Expound on eutrophication and factors affecting it within the context of climate change;
3. Study site selection and characterisation;
4. The water quality model selection;
5. CE-QUAL-W2 capabilities and shortcomings for this study;
6. The model setup, calibration and validation;
7. Performing present day simulations to establish a baseline study;
8. Rerun the simulations with the climate change data and note the changes; and
9. Draw conclusions and present possible recommendations.

Once the literature study was performed, the effect of climate change on the surface water of Voëlvlei Dam may be assessed to ascertain how the eutrophication level changes. Conclusions are drawn and recommendations for future research are made.

2 LITERATURE REVIEW

2.1 THE STUDY OF CLIMATE CHANGE

The study of the climate is necessary to quantify the consequences of future climate on the planet and its subsequent effects, especially on surface water quality. The simulation of future climates is the result of climatological studies that quantify the consequences of deliberate and inadvertent anthropogenic changes to the atmosphere from the present time into the future. It was with this foresight that the Intergovernmental Panel on Climate Change (IPCC, 2007) was established in 1988 by the United Nations Environmental Programme (UNEP) and the World Meteorological Organization (WMO). Climate change, as defined by IPCC, refers to statistically significant variations in climate that persist for an extended period, typically decades or longer. It includes shifts in the frequency and magnitude of sporadic weather events, as well as the slow, continuous rise in global mean surface temperature (IPCC, 2007).

2.1.1 A mechanism for climate change

Gases such as carbon dioxide (CO₂), methane (CH₄), chlorofluorocarbons (CFCs), nitrous oxides (NO_x) and water vapour (H₂O), allow the passage of shortwave solar radiation from the sun onto the earth surface, whilst absorbing the re-radiated radiation from the earth. The occurrence of these gases in the atmosphere has maintained the Earth's surface temperature at an average of 33°C higher than would otherwise have been the case. This heating is essential to sustain life on the planet, and this mechanism has been dubbed the *Greenhouse Effect* (Carter et al, 1994).

2.1.2 Modelling the climate

Forecasting of climate has always been difficult, as much of the motion of the atmosphere is derived from perturbations (cyclones, anticyclones, troughs and ridges), instability of flow and randomness. Numerical models of weather and climate are based on the general mathematical equations describing mass (chemistry), motion, hydrostatic equilibrium and energy balances within the atmosphere, oceans, land and ice, but due to its complexity, a quantitative mathematical solution is likely to be ineffective (Laprise, 2008).

In climate modelling, the planet is usually divided into a 3-dimensional grid (see Figure 1), the basic equations applied to each grid cell and the results evaluated. Atmospheric models calculate predicted winds, heat transfer, radiation, relative humidity and surface hydrology within each grid, and evaluate interactions with the neighbouring point. Due to the climate system being non-linear, its behaviour is chaotic and is difficult to model mathematically.

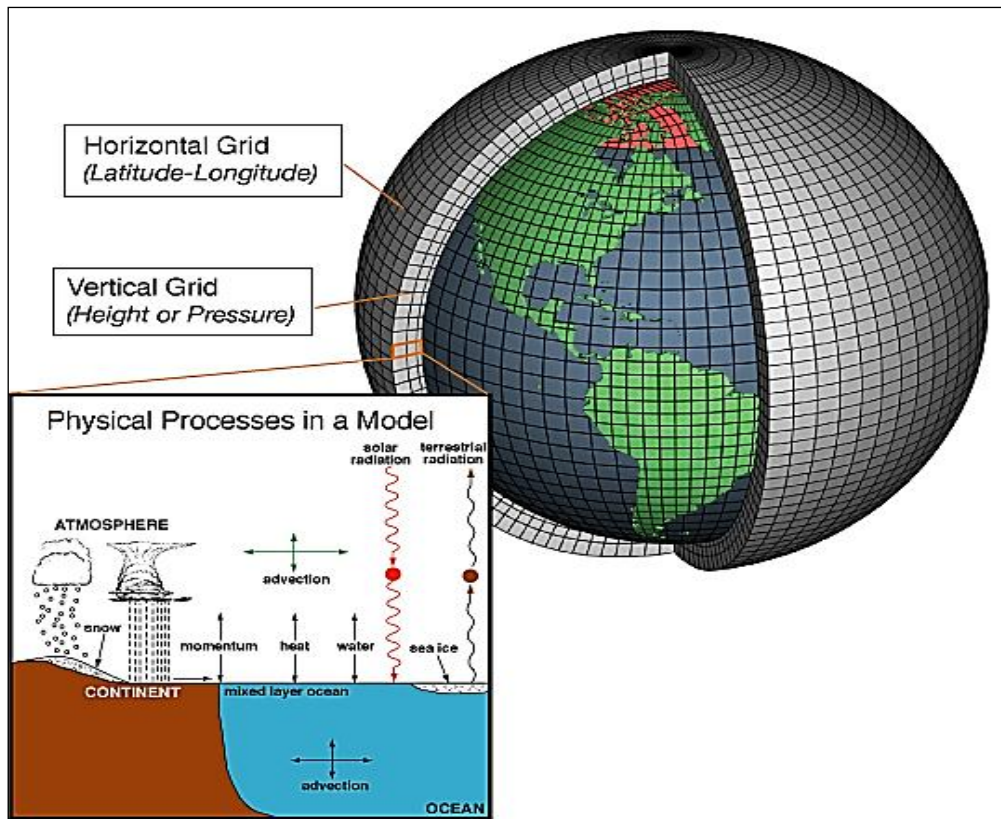


Figure 1: A typical grid used when developing a climate model

Adopted from the NOAA website http://celebrating200years.noaa.gov/breakthroughs/climate_model/welcome.html (2010)

Implementation of climate models requires an understanding of the strengths and weaknesses of the model, as well as an evaluation of the model's output to assess the error and/or bias.

2.1.3 Global Circulation Models (GCM)

The primary reason for developing climate models was to quantify the potential climate change of the future. Model simulations depend on assumptions regarding the anthropogenic emissions of greenhouse gases, which in turn depend on numerous assumptions regarding human behaviour. The predictive ability of these models is becoming more sophisticated, and projections of future climate are becoming consistently more accurate. The problem of unpredictability remains in the assumptions about future changes in atmospheric conditions or boundary conditions.

Different assumptions of socio-economic development and its subsequent emissions and concentration of greenhouse gases introduce uncertainty at the start of a climate change study (see Figure 2). There are many uncertainties concerning future socio-economic conditions, and it is almost impossible to simulate the effects on water resource systems based on future water use, derived from the forecast conditions. Further assumptions about the impact of changes in atmospheric composition enlarge the cumulative uncertainty in quantitative climate change estimates (Fujihara, et al., 2008, Houghton, 2007 and Bergant, et al., 2006).

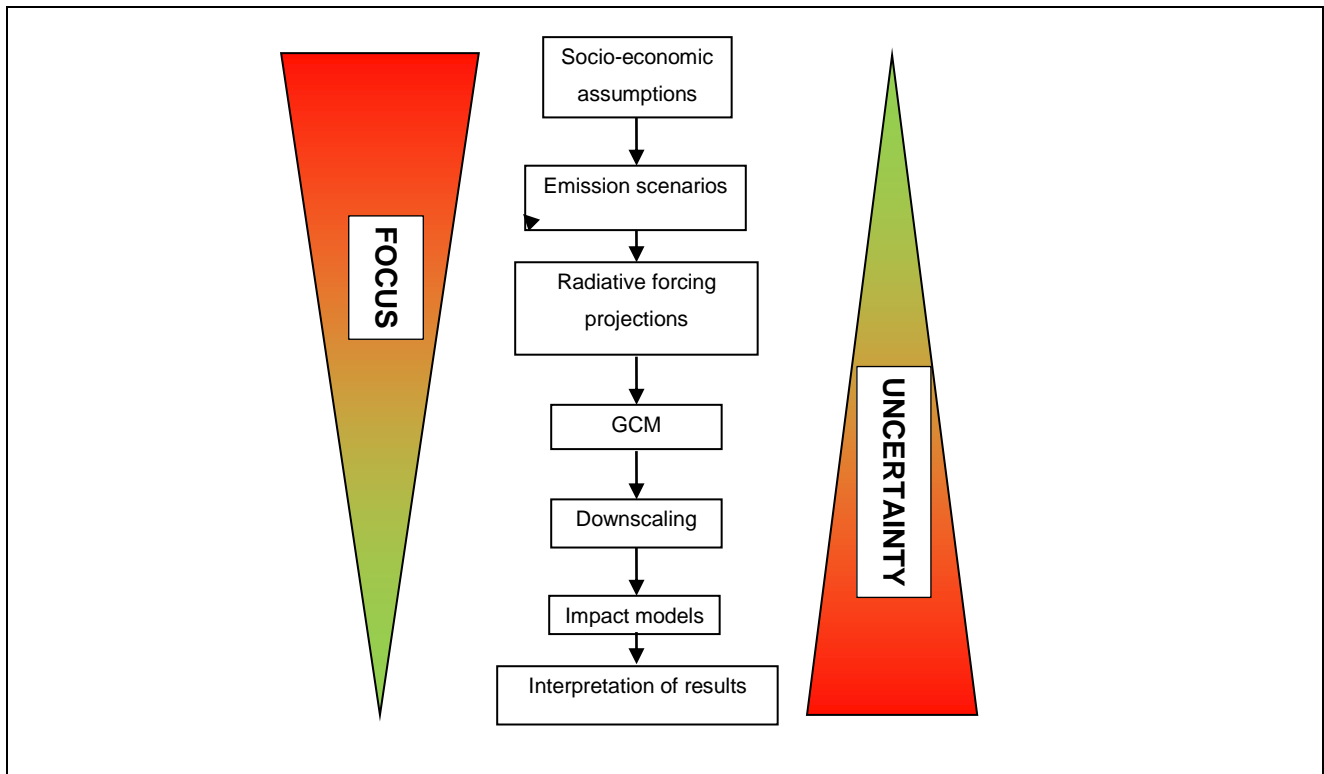


Figure 2: Increasing uncertainties within a climate change scenario development

Adopted from Bergant et al., 2006

Global Circulation Models or General Circulation Models (GCMs) are the tools required to simulate/predict a coupled climate system with hemispheric linkages. GCMs simulate several aspects of the climate components and interactions. The interaction between the different components of ocean layers, land masses, temperature gradients, solar radiation, clouds, ocean currents, trade winds, represent a complex system which requires significant computing resources to produce meaningful forecasts. With the current computing power, most GCMs operate at medium-coarse resolutions and use meshes with spacing in the horizontal of a few hundred kilometres usually about 300 km (May, 2007:60 and Lau et al., 1999), similar to Figure 1, to capture the large-scale circulation flows. These grid sizes are however, insufficient for resolving features such as terrain and land-sea contrasts. Local topography plays a vital role in determining rainfall patterns and a GCM's basic representation of topography is severely limiting in terms of practical use for predicting localised rainfall patterns (Laprise, 2008).

2.1.4 Anthropogenic emission scenarios

The ability to predict future climate is dependent on the future emissions of greenhouse gases. As mentioned before, these rely on assumptions regarding human behaviour, activities, population, economic growth, energy use and sources of energy generation. Several scenarios representing these assumptions were developed by the IPCC in a Special Report on Emission Scenarios (SRES) in 2001. The 35 developed scenarios were categorised into four different storylines, which included estimates of greenhouse gases from all sources namely A1, A2, B1 and B2 scenarios (see Figure 3).

The A1 scenario describes a world of rapid economic growth, a population that peaks mid-century and declines thereafter with the introduction of new, more efficient technologies. The A1 scenario further develops into three groups based on the alternative direction of technological changes in the energy system, namely:

- A1FI: fossil fuel intensive;
- A1T: reliance on non-fossil fuel energy sources; and
- A1B: balanced energy sources.

The A2 scenario describes a heterogeneous world with self-reliance and preservation of local identities. A continuous population growth was experienced with economic development regionally orientated and technological change more fragmented and slow.

The B1 scenario describes a convergent planet with population peaks in the mid-century and declines afterwards (as with A1), but with a rapid change towards a service and information economy, reduction in material intensity and the introduction of clean and resource-efficient technologies. The emphasis was on global solutions to economic, social and environmental sustainability.

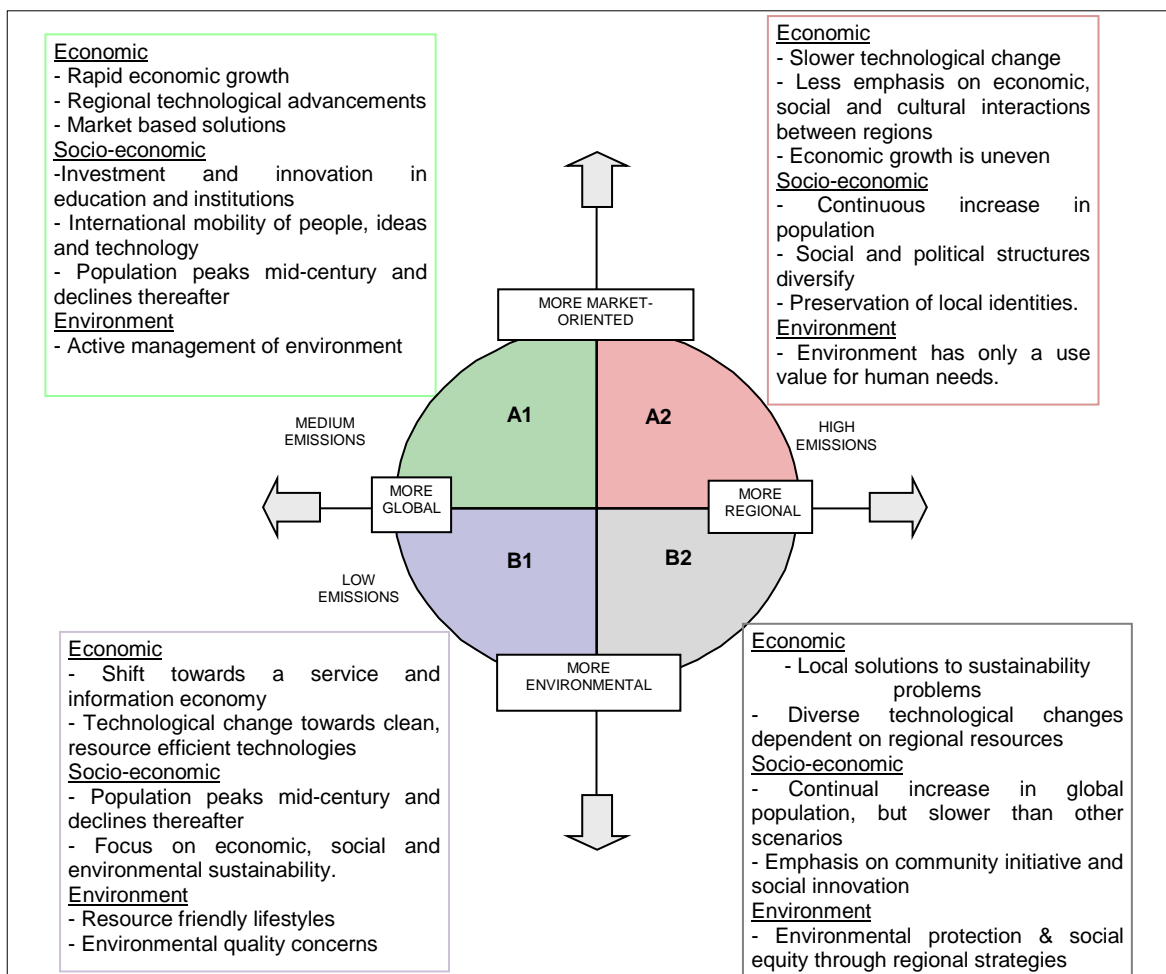


Figure 3 The mentioned SRES scenarios for climate change models

Adopted from IPCC, 2007

The B2 scenario describes a world in which the emphasis is on local solutions to economic, social and environmental sustainability. In this scenario, the world has an increasing population (at a rate slower than A2), intermediate levels of economic change and less rapid and more diverse technological change than in the A1 and B1 scenarios.

All scenarios are equally valid, with no assigned probabilities of occurrence. The SRES scenarios do not include additional climate initiatives such as the United Nations Framework Convention on Climate Change or the emission targets of the Kyoto Protocol (Houghton, 2007:117).

2.1.5 A Global Circulation Model projection

Numerous difficulties exist in the prediction of future climate. For example, GCMs require significant computer processing power, limiting the number of possible results. The behaviour of the sun is also difficult to predict with respect to its random solar flares and its light and heat intensity output. Similarly, short-term disturbances such as El Niño or volcanic eruptions are difficult to predict. The major forces that drive climate such as ocean layers, land masses, temperature gradients, solar radiation, clouds, ocean currents and trade winds are well understood and remain relatively stable.

When Mount Pinatubo erupted in 1991, it provided scientists with an opportunity to test the success of climate model predictions in response to the sulphate aerosols ejected into the atmosphere. The models accurately forecasted the subsequent global cooling of approximately 0.5°C soon after the eruption. Furthermore, the radiative, water vapour and dynamical feedbacks included in the models were quantitatively verified (Rosenzweig et al., 2007 and Hansen et al., 2007). An example of the output from a typical GCM is shown in Figure 4.

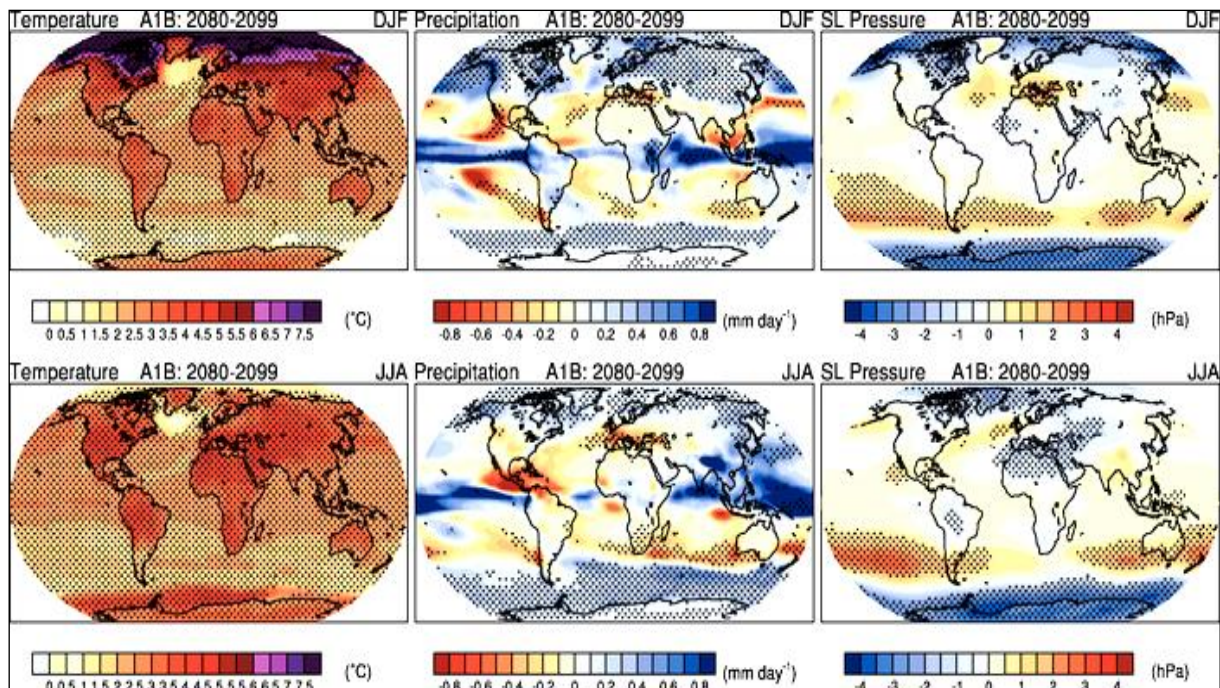


Figure 4 Changes in temperature, precipitation and pressure for A1B scenario

Adopted from Trenberth et al., 2007

Figure 4 shows the surface air temperature ($^{\circ}\text{C}$, left panel), precipitation (mm day^{-1} , middle panel) and sea level air pressure (hPa, right panel) projections for boreal winter (December to February, top panel) and summer (June to August, bottom panel) between 2080 and 2099. The projections were generated based on the A1B scenario, and are represented here as changes in climatic variables for the period 2080 to 2099 relative to those observed between 1980 and 1999. The presence of stippling within the maps denotes areas where the magnitude of the mean exceeds the standard deviation, indicating less variance and a more plausible model for these areas.

In line with projected general global trends, Figure 4 indicates southern Africa will likely experience warming of approximately $3\text{-}4.5^{\circ}\text{C}$ during summer (December to February) and up to 0.4 mm/day less rainfall during winter (June to August), as well as lower sea level air pressure.

2.1.6 Regional climate models (RCM)

In terms of regional changes in climate, GCMs convey little information as their scale is sometimes as large as 300 km^2 and is much larger than the area under investigation. For example, patterns of precipitation are dependent on orographic factors and the surface characteristics of the region, GCMs will therefore be a poor representation of changes at a regional scale because it lacks the necessary detail in surface characteristics. Therefore, outputs from global GCMs have to be *downscaled* to an appropriate spatial resolution to obtain relevant future projections for local-level assessments (See Figure 5). While numerous downscaling techniques exist, they all essentially follow the same basic methodology. The output from GCM simulations are used to provide the initial and driving lateral meteorological boundary conditions for the high-resolution regional climate models. Downscaling may be achieved using statistical downscaling methods, or by incorporating nested numerical mesoscale regional models in the GCM (i.e. dynamic downscaling). The result of the downscaling was Regional Climate Models (RCMs) or limited area GCMs. An increase in resolution results as the RCM accounts for the sub-GCM-grid-scale forcing functions. RCMs produce high resolution simulations of surface variables which in turn are affected by vegetation, land use and topographical features and are thus not an interpolation of GCM results (Landman et al., 2006).

RCMs perform the same task as GCMs but over a restricted area, with the RCM driven at its boundaries by updates from the GCM (Lau et al., 1999; Houghton, 2007 and Tyson and Preston-Whyte, 2000). RCMs can generate reliable descriptions of regional scale water and energy cycles, particularly where complex orography and coastlines regulate the key climate variables (Kim et al., 2008). RCM downscaling of GCMs have improved GCM estimates of precipitation by up to 30%. GCMs provide the large-scale atmospheric patterns whilst the local features (top) influence the climate beyond the resolution of GCMs (Lau et al., 1999).

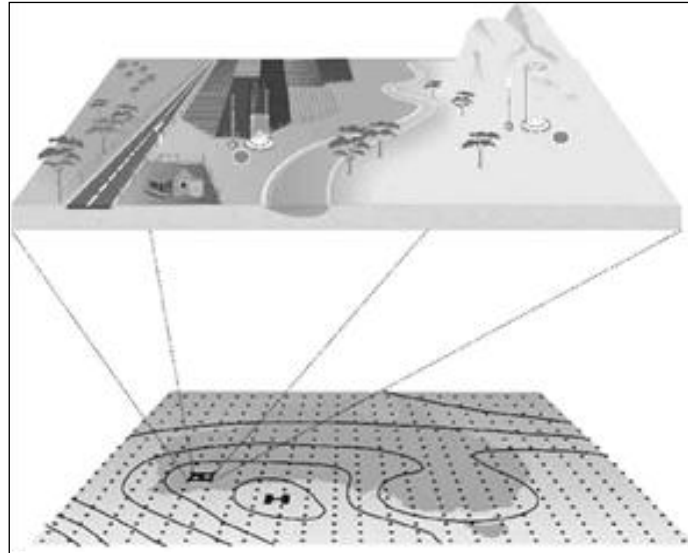


Figure 5 A schematic diagram of downscaling

Adopted from Timbal and McAvaney, 2000

It is important that a RCM produce results consistent with the boundary conditions obtained from the GCM results and should not differ substantially from those produced by the GCM. The RCM variables may drift to their own climatology away from the large-scale forcing data of the GCM when the internal forcing such as local topography was strong or the large scale forcing of the GCM was weak (Laprise, 2008, Houghton 2007).

2.1.7 Statistical downscaling to a RCM

Statistical downscaling has been widely used in weather forecasting. Many variations of statistical downscaling exist, including; empirical, multiple linear regression, and non-linear regression. A multiple linear regression model is a function of large-scale predictor variables (such as temperature and sea level pressure (SLP)) and local scale (mesoscale) predictors such as temperature and precipitation. Scenarios downscaled statistically depend on the assumption that the empirical relationships that link the GCM to the downscaled data was valid under future climate conditions. Large-scale relevant predictors are selected using correlation analysis, partial correlation analysis and scatter plots, and considering physical sensitivity between selected predictors and predictors for the site in question.

Precipitation is modelled as a conditional process in which local precipitation amounts are correlated with the occurrence of wet-days, which in turn are correlated with regional-scale atmospheric predictors. The root mean square (rms) of daily precipitation is averaged over the RCM grid and a precipitation index was computed for each grid box, which is finally distributed over the area of study. (Khan et al., 2006 and Quintana-Seguí et al., 2010).

The advantage of this technique is that it was easily applied. One disadvantage of the statistical method of downscaling is that it relies on the availability of sufficient high resolution data over long periods so that statistical relationships may be established. It was not possible to be sure how

valid the statistical relations are for a climate-changed situation (Houghton, 2007; Quintana-Seguí et al., 2010).

2.1.8 Uncertainty in the downscaled RCM model

Downscaling and bias-correction of a RCM is vital when only one climate model is used for small basins where many interactions are present. The selection of downscaling techniques and the treatment of uncertainties have a significant effect on the results of the RCM. However, the uncertainty relating to the downscaling and bias-correction is lower than the uncertainty in the emissions scenarios and climate modelling, (refer to Figure 2 for uncertainty depictions). Other sources of uncertainty may be feedbacks between the changing climate and vegetation, human adaptations to the new climate (changes in agriculture, water management practices, urbanisation etc.) and other human induced changes of the system. In certain instances, these changes might be more important than the climate change itself (Quintana-Seguí et al., 2010).

This study uses four statistically downscaled RCM A2 models for the Voëlvlei Dam quinary catchment level.

2.1.9 The use of climate change models in South Africa

The use of downscaled climate data from a variety of GCMs to project changes in rainfall, temperature and hydrological regimes under climate scenarios across the country at quinary catchment level (Knoesen et al., 2009) was used as a basis for the identification of impacts on the identified systems.

The Climate Systems Analysis Group based at the University of Cape Town has statistically downscaled four GCMs for use at local level. These have been quality controlled and processed by the School of Bioresource Engineering and Environmental Hydrology at the University of Natal for use in hydrological models, which project environmental climate and hydrological changes. The results of these analyses to be used in this study include; present/ historical conditions (1971-90), intermediate future (2046-2065) and distant future (2081-2100) projections. The four GCMs are:

- CCC (Centre National de Recherches Meteorologiques, France);
- CNRM (Canadian Centre for Climate Modelling and Analysis, Canada);
- ECH (Max Planck Institute for Meteorology, Germany); and
- IPSL (Institut Pierre Simon Laplace, France).

2.1.10 The impacts of climate change for Southern Africa

One of the foremost impacts of climate change concerns regional water resources, particularly in areas with high climate variability. Figure 6 shows the recorded temperature increases for the four cardinal African land regions (Sahara, West, East and Southern Africa) for 1906 to 2005 (black line) and as simulated (red envelope) by climate models incorporating known forcing functions of climate change; and as projected for 2001 to 2100 by climate models (orange envelope). The bars at the end of the orange envelope represent the range of projected changes for 2091 to 2100.

The blue bar represents projections under the B1 scenario where the world was dependent on clean, efficient technology. The orange bar represents the A1B scenario where the world uses a balanced source of energy, and the red bar represents the A2 scenario where the world was heterogeneous with constant population growth and slow technological changes. The black line is dashed where observations are present for less than 50% of the area in the decade concerned.

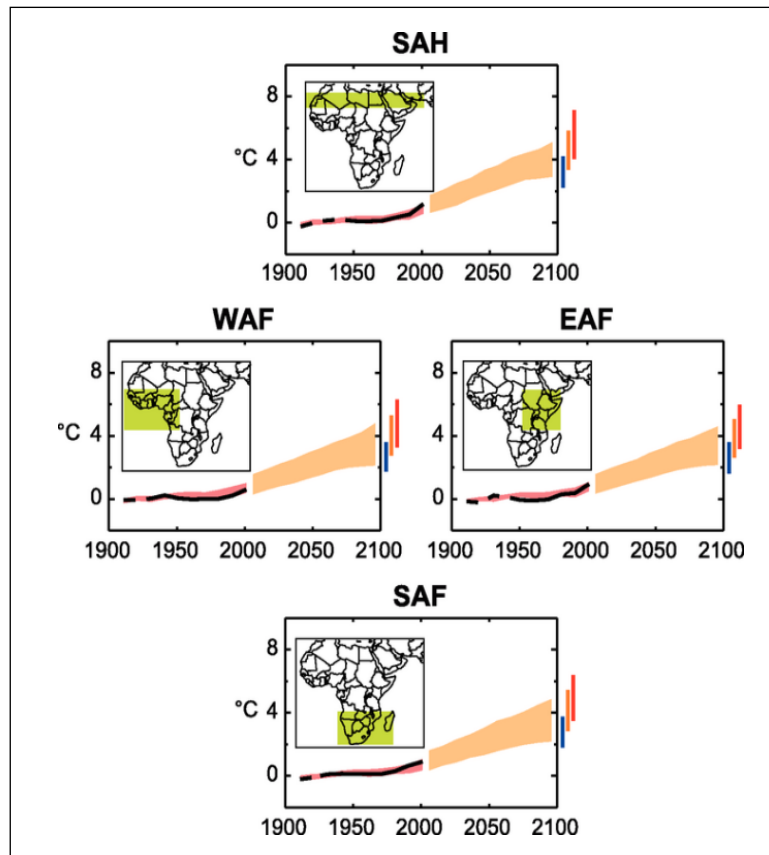


Figure 6 Temperature trends from 1901 to 1950 and predictions to 2100

Adopted from Christensen et al., 2007

Estimates based on observational constraints, such as atmospheric and ocean temperatures indicate that the equilibrium climate sensitivity is greater than 1.5°C with a probable value between 2°C and 3°C. The upper 95% limit remains difficult to predict from current observations without being able to estimate the extent of global dependence on greener technologies and lifestyles.

Figure 4 and Figure 6 support the generally accepted estimations based on modelling and observational studies, which suggest that the equilibrium climate sensitivity is likely to be between 2°C to 4.5°C (IPCC, 2007 and Carter et al., 1994). The effects of climate change on Southern Africa were assessed in the IPCC 4th assessment report (Christensen et al., 2007). The results showed that by the end of 20th century temperature was expected to increase by 2-3.5°C compared to values observed in the years 1980-1999. Increases at the upper limit of this range are expected to occur in the interior, while coastal regions are expected to have increases corresponding to lower limit of that range. Winter (June-August) temperature increases are projected to be greater than those experienced during the summer (December-February) months.

Schulze (2006), using downscaled GCM's and the Agricultural Catchments Research Unit model (ACRU model), identified sensitive regions southern Africa where climate change would have a profound impact on water resources. The winter rainfall region of the Western Cape Province was identified as one of the most vulnerable regions. The A2 models for southern Africa show between a 3-6°C temperature increase for the region.

2.2 WATER QUALITY IN RESERVOIRS AND RIVERS

Water quality is a combination of the physical, chemical, biological and aesthetic characteristics of water. Many of these characteristics are controlled or influenced by constituents that are either dissolved or suspended in water. It is most frequently used with reference to a set of standards against which compliance or fitness of use can be assessed. The most common standards used to assess water quality relate to drinking water, agricultural use, safety for human contact and for the health of ecosystems. Environmental water quality, also called ambient water quality, relates to water-bodies such as lakes, dams, rivers, and oceans. Water quality standards vary significantly due to different environmental conditions, ecosystems, and intended human uses. Toxic substances and high populations of certain microorganisms can present a health hazard for recreational purposes. These conditions may also affect wildlife that uses the water for drinking or as a habitat. Modern water quality regulations generally specify protection of fisheries and recreational use and require as a minimum, maintenance of applicable water quality standards (WHO, 2003 and DWA, 1996).

Lakes, reservoirs and other water-bodies respond directly to climate changes and the variability in these responses will affect water resources, water quality and aquatic ecosystems. Increasing water temperatures may alter the hydrodynamics in lakes, lengthening the thermal stratification period and deepening the thermocline, i.e. the interface between the upper mixed layer and deeper calm layer. These shifts may increase nutrient release from the sediments and lead to alterations in lake nutrient circulation. These changes in climate variables thus directly influence water quality in lakes by altering changes in flow patterns and water temperature. High concentrations of nutrients (phosphates and nitrogen) and expected variability of climate can lead to an increased frequency of phytoplankton blooms and an alteration of the trophic balance. As a result, dissolved oxygen concentrations can fluctuate widely and algal productivity may reach critical (problematic) levels (Komatsu et al., 2007 and IPCC, 2007).

2.2.1 South African water quality guidelines

One of the goals of the Department of Water Affairs (DWA) is to strive to maintain the quality of South Africa's water resources such that they remain within the 'No Effect Range'. For this reason, the No Effect Range in the South African Water Quality Guidelines (2006) is referred to as the Target Water Quality Range (TWQR). DWA Guidelines for water use for recreational and other purposes is shown in Table 1. For each water quality constituent there is a '*No Effect Range*'. This was the range of concentrations or levels at which the presence of a particular constituent would have no known or anticipated adverse effects on the fitness of water for a particular use or on the protection and maintenance of the health of aquatic ecosystems. These ranges were determined by assuming long-term continuous use (lifelong exposure) and incorporate a margin of safety.

Table 1 Summary of water quality for recreational and other use

Constituent of concern	Target concentration or condition	Effect of the constituent
Free floating algae	0-15 mg/l for recreational full contact	At a mean concentration of 15 mg/l nuisance conditions are encountered for <12% of the year
Ammonia (mg NH ₃ /l)	0-1 for human consumption	
Nitrate and nitrite	0-6 mg/l for human consumption	30 mg/l may be hazardous to animal health form ingestion
Phosphorus	Less than 0.025 mg/l	
Total dissolved solid (TDS)	0-450 mg/l for human consumption	No health risk in this range
Conductivity	0-70 mS/m for human consumption	No health risk in this range

Compiled from DWA, 1996

2.3 EUTROPHICATION

2.3.1 A Definition for eutrophication

There have been many definitions for eutrophication and Ahl in 1980 expressed eutrophication as a process leading to nutrient rich conditions irrespective of biological effects. Subsequently the broader definition of eutrophication has been described as anything, including external and internal sources, playing a part in accelerating nutrient loading to a water-body and increasing the nutrient level within the water-body. The composition of the nutrient load was proportionally dependent on conditions determined by man as well as a host of natural factors including geological, topographical and hydrological influences. *In South Africa, eutrophication has been recognised as a priority water quality problem for over 30 years and in a study on the eutrophication status of a number of South African reservoirs, it was found that the extent of eutrophication had increased since the problem was first identified in the 1970's* (Rossouw et al, 2008:1).

Currently, one of the most widely accepted definitions of eutrophication is that of the Organisation for Economic Cooperation and Development (OECD) which describes the process as *“the nutrient enrichment of waters which results in the stimulation of an array of symptomatic changes, amongst which increased production of algae and aquatic macrophytes, deterioration of water quality and other symptomatic changes are found to be undesirable and interfere with water uses”* (Walmsley, 2000:5). Eutrophication is therefore a natural or unnatural process of nutrient enrichment of a water-body and results in the reduction in species diversity at all trophic levels (Codd, 2000:52).

The increase of nutrients within a water-body could result in an increased production of algae and a deterioration of water quality, whereas excessive development of blooms is indicative of uncontrolled eutrophication.

The word trophy (*trophe*) is of Greek origin and literally means nourishment or that which is connected to nutrition. The trophic indices were developed to classify the plant or animal community affected by anthropogenic disturbances and to assess quality status of the aquatic environment. At least four types of trophic statuses can be distinguished namely, oligotrophic, mesotrophic, eutrophic and hypertrophic. The nutrient condition of water and water-bodies are classified as follows:

- Oligotrophic low in nutrients and usually no water quality problems;
- Mesotrophic intermediate level of nutrients with emerging signs of water quality problems;
- Eutrophic rich (high) and an increased level of water quality problems; and
- Hypertrophic excessive levels of nutrients and water quality problems are persistent.

2.3.2 Causes of eutrophication

Generally, eutrophication occurs in water-bodies independent of human activities, but human activities are causing nutrient enrichment of water-bodies to occur at an unprecedented and accelerated rate. Eutrophication was acknowledged as nuisance algae growth in lakes and phosphorus was identified as the nutrient of concern that encouraged eutrophication. Later nitrogen was seen to be limiting in estuarine and coastal waters and opposing views emerged as to which of the two nutrients was the limiting factor for algae growth. In 1987, Denmark was proactive and limited the pressure on the aquatic environment by reducing the load of phosphorus by 80% and that of nitrogen by 50% in its wastewater (Harremoës, 1998:9). Today the numerous incidents of eutrophication are linked to human induced increases of the nutrient loading of a water-body, particularly phosphorus and nitrogen. The solution to the eutrophication problem requires a multi-disciplinary, multi-sector and multi-focal approach to reduce the rate at which water quality is being degraded.

2.3.3 The sources of algal nutrients

A nutrient is defined as a chemical compound or element that is used by plant cells for growth. In the case of eutrophication, the nutrients are mostly inorganic elements assimilated by plants and in conjunction with photosynthesis produce organic material. Once an oversupply of nutrients is prevalent in a water-body the result is a deterioration of water quality and an increase in algal biomass.

A distinction is made between two types of eutrophication namely 'natural' and 'cultural' eutrophication. Natural eutrophication is related to the natural eutrophication of the water-body which is dependent on geology and natural features of the catchments and is a slow process. Cultural eutrophication is directly attributed to man-made influences and is the result of accelerated nutrient addition and premature eutrophication of the water-body. The rate of cultural eutrophication is directly proportional to the amount of nutrients added to the water-body. Figure 7 shows a graphical representation of some of the main nutrients and physical factors that affect the trophic state of a water-body.

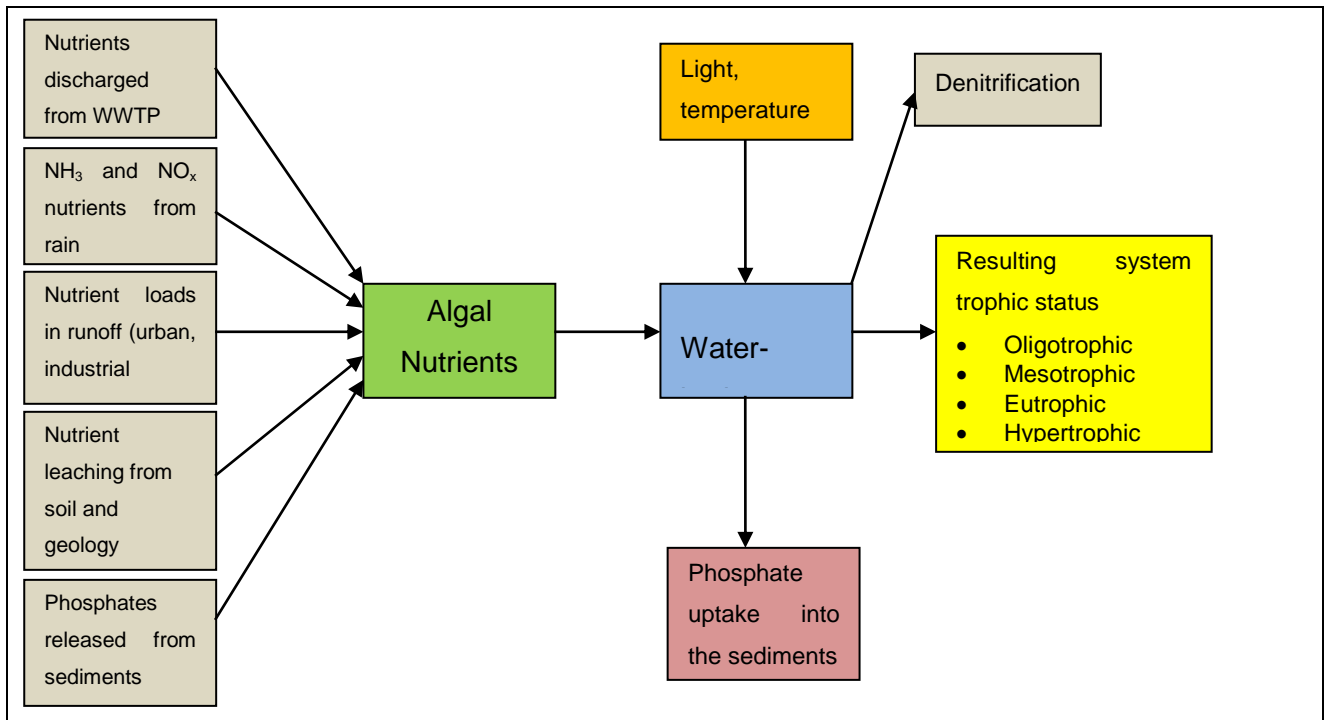


Figure 7 The main factors that affect the trophic states of water-bodies

Algal growth is dependent on a large number of chemical and physical factors. These include temperature, phosphorus, nitrogen, oxygen, hydrogen, carbon, sulphur trace elements and sunlight. Of these aforementioned elements phosphorus (P), nitrogen (N) and light are the critical driving forces for the algal growth process. The nutrients of concern for eutrophication is P as phosphate ions (PO_4^{3-}) and N as nitrate (NO_3) and nitrite (NO_2) as well as ammonium ions (NH_4^+) although they may occur in organic forms, they are utilised by plants in the inorganic form (Dallas and Day, 2004:85). The method of using only phosphate ions to determine the nutrient load by DWA has been critiqued and the accepted scientific standard was to use total amount phosphorus as the determinant for the nutrient load to a water-body (Harding, 2006).

The composition of aquatic plant tissue is $\text{C}_{106}\text{H}_{263}\text{O}_{110}\text{N}_{16}\text{P}$ which is a ratio of C:N:P of 106:16:1. This ratio is the Redfield-Richards ratio and the optimal ratio range of N:P for algal growth is 8:1 to 12:1. It has been observed that P and N are frequently the limiting nutrients in freshwater systems as increases in the levels of these 2 nutrients will raise the probability of eutrophication (Harremoës, 1998). It was generally accepted that the management of N and P inputs to the aquatic environment was paramount to the eutrophication solution (Walmsley, 2000; Owuor et al., 2007).

Cultural eutrophication sources (anthropogenic sources) are point sources and include the nutrient loads from wastewater treatment plants (WWTP) as well as run-off water. Run-off water is literally all spills and effluent bearing nutrients that ultimately flows to the water-body.

2.4 FACTORS AFFECTING WATER QUALITY AND ALGAL GROWTH

Water temperature, pH, available light, turbidity, total suspended solids (TSS), total dissolved solids (TDS), nitrogen, phosphorus, salinity and trace elements influence water quality and algal growth. Water quality and algal growth is dependent on several variables for its lifecycle, such as a conducive environmental conditions and nutrients, which may be categorised into the following for this study.

- Water temperature and direct solar radiation;
- The quantity of dissolved oxygen in the water-body;
- Light penetration, turbidity and suspended solids within the water-body;
- Dissolved solids, salinity and conductivity of the water-body;
- Availability of nitrogen within the water-body; and
- Availability of phosphorus within the water-body.

2.4.1 The effect of temperature and solar radiation on algal growth

The natural thermal or background thermal characteristic of a water-body is dependent on the hydrological, climatological and structural features of its region and catchment area. Natural sources and sinks of heat include solar radiation (usually the dominant source), evaporation and condensation of water vapour at the surface, conduction, heat transfer to and from the air and sediments into the water-body, back-radiation, precipitation, surface run-off as well as groundwater input (Wetzel, 2001).

All organisms have a temperature range at which optimal growth occurs and their life cycles are directly linked to temperature. Temperature primarily affects algal photosynthetic metabolism by controlling the enzyme reaction rate of the algae and an optimum temperature for each species was observed (DeNicola, 1996). Shortwave solar radiation of the wavelength range 400-700 nm is of the greatest importance to aquatic biologists as this wavelength provides the energy that drives photosynthesis (Hauer and Hill, 2007, DeNicola, 1996 and Incropera and Thomas, 1977). This range was known as the photosynthetically active radiation (PAR) range and is measured with photocell equipment systems. In the absence of shortwave solar radiation data, the amount of shortwave radiation which penetrates the water surface to a depth is a function of cloud cover, the total amount of suspended solids (organic and inorganic) and algae present in the water i.e. it is transparency dependent (Cole and Wells, 2008).

Water temperature is primarily determined by direct solar radiation as well as other factors such as latitude, elevation, shading vegetation and morphology (Wetzel, 2001 and DeNicola, 1996). The high specific heat capacity¹ of water makes it susceptible to absorb heat quickly and release it slowly without large temperature changes, contributing to its thermal stability and thus providing a buffer for sudden external temperature changes. Temperature does not limit biomass and primary production but rather sets the upper limit for production when other factors are optimal (DeNicola, 1995). No single temperature is suited for all seasons and organisms to ensure optimum growth.

¹ Specific heat capacity of water $C_p=4.1855 \text{ J}/(^{\circ}\text{K}\cdot\text{mol})$ at 15°C and 1 atmosphere compared to petroleum 2.3, benzene 1.8, asbestos 0.84, clay $0.92 \text{ J}/(^{\circ}\text{K}\cdot\text{mol})$ (Perry, 1985) This implies that a larger amount of heat is required to raise or lower the temperature of water by 1 C

Slight temperature changes that are persistent leads to a preference of one aquatic species over another and the organism profile of a water-body changes. Sudden temperature changes may have proportional effects on the aquatic fauna and flora and will influence the development, growth, size, intra-species selection as well as the age of sexual maturity for at least the duration of the change (Dallas and Day, 2004 and Owuor et al., 2007). Higher water temperatures will promote evaporation from the water surface and change concentrations of organic and inorganic compounds, usually increasing salinity. This change will be important for marine and estuarine waters as the evaporation would increase the salinity as well as being problematic for freshwater purification managers.

The consequences of global warming for some areas are increased solar radiation, light availability, air temperature increase, less rainfall and less cloud-cover as well as a loss of shading riparian vegetation compounding the in-body water-temperature increase. This will promote photosynthesis but inhibit algae and plants that are unable to cope with high light intensity (UV levels) thereby imposing a selection criteria for certain species of plants and animals (Wotton, 1995). There is a shift in the dominance of algal classes from bacillariophyceae (a type of diatom) (<20 C) to chlorophyceae (green algae) (15 -30 C) to cyanophyceae (phylum of cyanobacteria) (>30 C) as the water-body's temperature increases. At temperatures >30 C biodiversity is reduced and cyanobacteria dominates (DeNicola, 1996). Higher temperatures also increase metabolic rates, oxygen demand and CO₂ production by aquatic organisms (Dallas and Day, 2004). This was more pronounced in shallow lakes, as less heat is required to raise the water temperature especially along the banks (DeNicola, 1996).

Cyanobacteria have a wide temperature tolerance but when the water temperature exceeds 20°C rapid increase in the biomass of cyanobacteria may occur if other factors support this (Owuor et al., 2007:9). Cyanobacteria can survive in temperatures up to 75 C (DeNicola, 1996) and dominate in hot-water springs. Anthropogenic causes of thermal pollution into a water-body includes heated industrial effluent discharges, returning heated cooling waters from power stations, inter-basin water transfer (as in the case of Theewaterskloof to the Upper Berg, (Dallas and Day, 2004 and Snaddon and Davies, 1999).

2.4.2 The effect of dissolved oxygen (DO) on algal growth

Dissolved oxygen is essential to the respiratory metabolism of most aquatic organisms and its concentration is determined by atmospheric inputs, photosynthesis, respiration and oxidation (Wetzel, 2001). Thus, the distribution of oxygen within a water-body is the major driving force for the distribution, behaviour and growth of aquatic organisms. In unpolluted water-bodies, the DO concentration is usually above 80% saturation. The diffusion of oxygen from the atmosphere into a water-body is slow and its distribution is controlled by a combination of solubility conditions, barometric pressure, hydrodynamics, photosynthesis and metabolic reactions (Wetzel, 2001). A decrease in dissolved oxygen concentration occurs with higher temperatures as shown in Figure 8. Further depletion of oxygen concentration is due to the higher microbial action at the elevated temperature, which is possible under climate change conditions. The diurnal variations of DO concentration in water-bodies because of photosynthesis and respiration could alter in-lake DO profiles (Hauer and Hill, 2007).

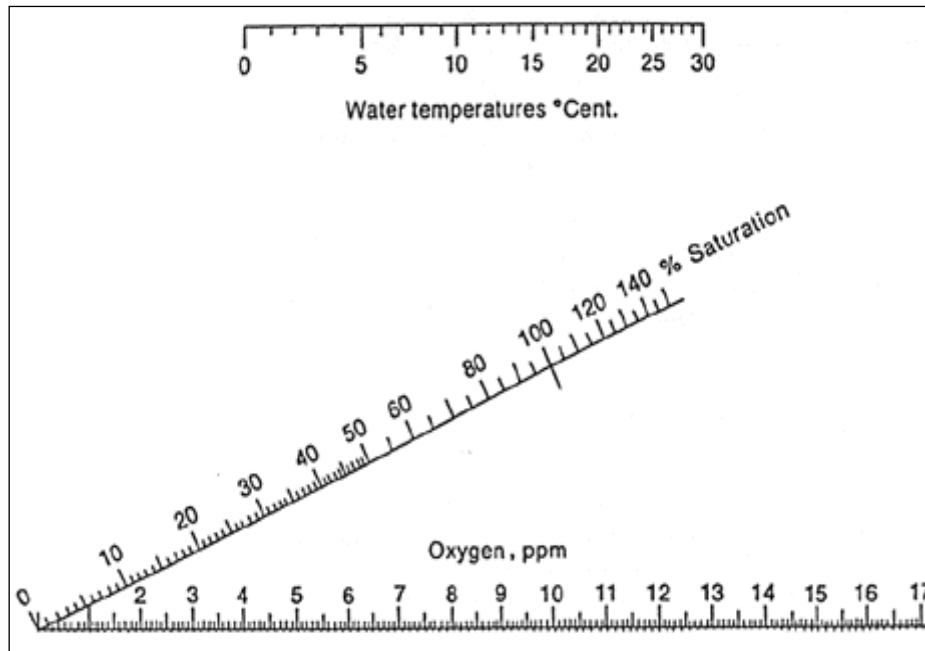


Figure 8 Nomogram chart for quick dissolved oxygen calculations

Adopted from Motimer, 1956 and www.waterontheweb.org

As the temperature, increases due to projected global warming the solubility of oxygen decreases further decreasing the oxygen solubility. Reduced inflow caused by a reduction in rainfall would also decrease the re-aeration potential due to mixing. Increased frequencies of oxygen depletion may occur in the hypolimnion of eutrofied water-bodies where anaerobic decomposition of material occurs (Wotton, 1995 and Wetzel, 2001) which would favour algal species that are tolerant to the lower DO levels.

2.4.3 The effect of light and turbidity on algal growth

The availability of underwater light is an environmental factor that influences species composition and biomass of phytoplankton within the water-body. A reduction in the availability of light limits phytoplankton production. Light penetration into a water-body is directly affected by the turbidity and amount of suspended solids dispersed within the water-body. Turbidity is defined as the property that causes light to be scattered and absorbed. The effect of turbidity is easily seen as it reduces the clarity of water and limits the light penetration, which both has ecological consequences. The scattering of light is caused by suspended matter (silt, clays, plankton, organisms etc.) whilst the light is absorbed by soluble organic compounds. Light penetration is measured using light probes, spectrophotometer, turbidimeter or Secchi disc. The units of turbidity is NTU (Nephelometric Turbidity Units) or in the case of the Secchi disc, meters. The total suspended solids (TSS) is defined as all the particles that are trapped by a 0.45 μm pore size filter (Dallas and Day, 2004 and Rossouw, 2000)

The sources of increased turbidity and algae are limited to hydrology, geomorphology (erosion), quantity of living and non-living matter as well as industrial discharges into the catchment. The effect of turbidity in a water-body is dependent on the total load of solids and the frequency of discharge. If the discharges are infrequent, no negative effects may be presented. In South

Africa, the suspended load may account for 85-95% of the bed load, which enters a water-body, and the remaining is contributed by the bed load (Rossouw, 2000:50). In turbid waters light penetration is reduced, the rate of photosynthesis decreases and at turbidity levels of 5 NTU primary production of photosynthesis is reduced by 3-13% in New Zealand streams (Dallas and Day, 2004).

As a rule of thumb, if the Secchi disc depth is less than 0.2m (i.e. the water is highly turbid) the euphotic (light penetration) zone is very shallow and algal growth is severely inhibited by light availability. If the Secchi depth exceeds 0.8m, light limitation is cancelled out and algal growth is limited by nutrient availability (Rossouw, 2000). Cyanobacteria like *Microcystis*, and other gas vacuolated species with 'swim bladders' can move vertically (passively) within the water column so as to access their ideal light conditions (Owour et al., 2007) whenever the light intensity is too high or low. Such species also adapt to various light intensities by varying its chlorophyll content. The modelling of any motile species is extremely difficult and would require vast computing power and resources beyond the scope of this study.

The apparent benefit of suspended solids is that nutrients, trace elements and toxins adsorb onto the suspended solids and are settled out of the lifecycle or may be transported away.

2.4.4 The effect of TDS, conductivity and salinity on algal growth

The total amount of dissolved organic and inorganic matter as well as the total ions dissolved in water contributes to the total dissolved solids within the water. Natural TDS is determined by geographical location (soil type etc.) and atmospheric conditions. Sources of anthropogenic TDS are from industrial effluents, mining, aquaculture and irrigation. TDS is everything in the water that is not actually water and includes hardness, softness, alkalinity, chlorides, bromides, sulphates, silicates, airborne pollutants and all organic compounds. It also provides a gauging stick of the salinity of water. Conductivity is the ability of water to conduct an electric current and correlates with TDS for the same water type. Tolerance to TDS/salinity is species specific as they are confined to freshwater (<2,000 mg/l), seawater (33,000 - 35,000 mg/l) or estuaries (~0 – 35,000 mg/l) and do not thrive outside these constraints except for limited periods. For South Africa DWA uses the relationship for Western Cape waters where:

$$TDS (mg/l) = conductivity (mS/m) \times 6.6 \text{ or } 5.5 \text{ (Dallas and Day, 2004 and DWA, 1996)}$$

Different algae show varied sensitivities to TDS and the algae that can persist over a wider range of salinities becomes dominant (such as *M. circinale*). Above 250 mg/l of salinity species such as *Cyclotella meneghiniana* and *M. aeruginosa* is excluded from the biomass (Prinsloo and Pieterse, 1994). In addition, increasing salinities should result in the aggregation of photosynthetically inhibited cells and, through prolonged exposure to increasing osmotic stress, produce large, rapidly sinking detritus particles supporting microbial decomposition perpetuating high microbial oxygen demand and anoxia within the water-body (Sellner et al., 1988).

2.4.5 The effect of Nitrogen on algal growth

Nitrogen is an abundant element and is an essential building block of proteins and a constituent of chlorophyll. The sources of N with respect to water quality tests are ammonia (NH_3), ammonium (NH_4^+), nitrites (NO_2^-) and nitrates (NO_3^-) as well as atmospheric N, which is fixed by algae. From the aspect of eutrophication, it is very seldom that nitrogen is the limiting nutrient within a water-body as it is so abundant. Naturally occurring ammonia is produced by the decomposition of organic matter that contains ammonia. Anthropogenic sources of ammonia are from sewage and industrial effluents and may be present as both ammonia and ammonium ions. Nitrite occurs naturally as an anion in fresh and sea waters, whereas anthropogenically it is introduced to receiving waters as wastes from aquaculture, sewage effluents and industrial effluents. Nitrite ions are toxic to fish and causes anoxia during periods of high activity of fish. Nitrate ions are scarce in natural water sources as they are constantly being depleted by the process of photosynthesis, converting nitrates to organic nitrogen. Nitrates are introduced to water from industrial effluents, agricultural runoff and fertilizers. Nitrates are only toxic at high concentrations with respect to its background levels.

High levels of nitrogen as well as phosphorus in freshwaters may favour the growth of toxic *Microcystis* strains over non-toxic ones (Vézic et al., 2002). Cyanobacteria such as *Anabaena* sp. and others can utilise the nitrogen present in the atmosphere for growth and hence it is not seen as limiting for their growth (Dallas and Day, 2004). From an eutrophication management aspect, it is easier to manage and police the anthropogenic loading of a water system so that the subsequent abatement of eutrophication may take place but the case for nitrogen management is not easy or practical as it is abundant in the system. Nitrogen is essential for growth but rarely a limiting growth element for algae.

2.4.6 The effect of Phosphorus on algal growth

Phosphorus is another essential element for all life forms. Phosphorus occurs as orthophosphate (PO_3^{4-}), polyphosphates and organic phosphates. Orthophosphates are considered the immediate available form of P for uptake by algae. The concentration of P is influenced by mineralization, sorption onto suspended material or sediment, desorption, algae uptake and precipitation with calcium or iron. Excessive concentrations of P are the most common cause of eutrophication in freshwater lakes, water-bodies, streams, and in the headwaters of estuarine systems. These high levels of P lead to high algal populations and high respiration rates, causing hypoxia or anoxia in poorly mixed bottom waters and in surface waters during the night under calm, warm conditions. Low dissolved oxygen causes aquatic animal biodiversity to decrease and the release of many materials normally bound to bottom sediments, including various forms of P. This release of P reinforces the eutrophication and is referred to as internal loading. See Figure 9 for a conceptualisation of this phenomenon (Walmsley, 2000: (Dallas and Day, 2004: Correll, 1999).

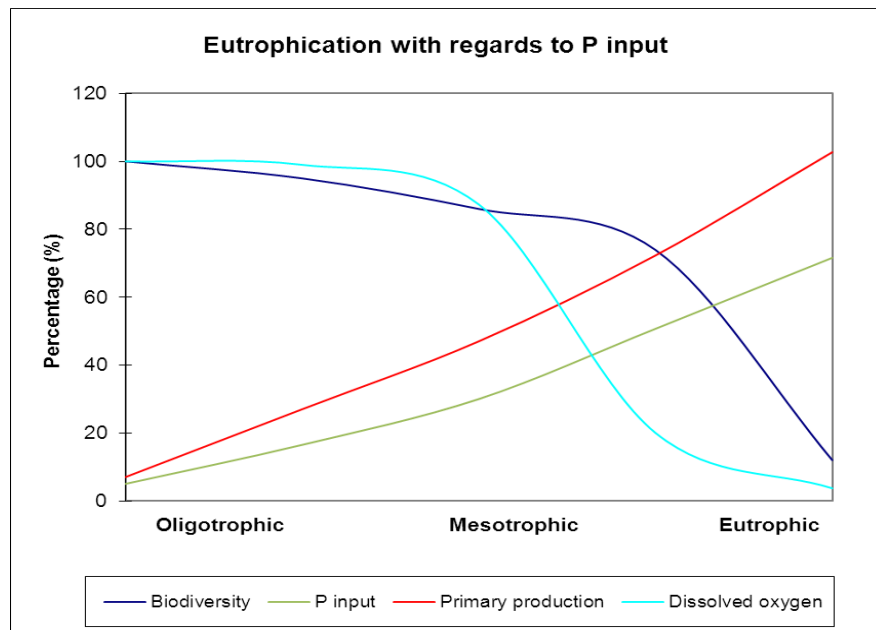


Figure 9 Conceptual eutrophication with regards to P in bottom waters

Adapted from Correll, 1998:262

Anthropogenic activities often result in large loads of P to receiving waters leading to higher primary production as well as a shift in the trophic status of the receiving waters. High primary production leads to high rates of decomposition and depletion of dissolved oxygen in bottom waters. These eutrophic conditions result in fish kills and major shifts in the species composition at all trophic levels. P is released from the decaying matter at in the sediments compounding the amount of available P and this P is available as plant nutrient increasing further the primary production (Correl, 1998).

Phosphate has been considered by many (Walmsley, 2000; Correll, 1999; Rossouw, 2000; Heisler et al., 2008; Harremoës, 1998) as being the constituent of concern for plant nutrient enrichment in water-bodies. The level of P in an aquatic body is determined by DWA and is specific to the water-body and for the Berg River catchment, this is 0.025 mg/l (DWA, 1996 and DWA, 2011). However, this standard has been shown to be inadequate as damage to river systems occurs at P concentration of 20 µg/l and South African water-bodies show a threshold of 35 µg/l above which the frequency of eutrophication problems increase. This decision to limit only ortho-phosphate has been critiqued and the accepted scientific standard is to use total phosphorus as the determinant for load to a water-body (Harding, 2006 and personal communication July 2010). The level of P in effluent discharges into a catchment was fixed in 1985 by the then DWA at 1 mg/l of ortho-phosphate.

2.4.7 The limiting nutrient concept

Algae and macrophytes require about 20 different elements for existence. However, the rate of plant growth is dependent on the concentration and ratios of nutrients present in the water. Plant growth is limited by the nutrient present in the least quantity relative to the growth needs of the plant. This phenomenon is termed the limiting nutrient concept, forming the basis of eutrophication management, i.e. minimise the quantity of the nutrient thus limiting the growth of the plant.

The critical nutrients considered for the growth of algae are N and P (Ahl., 1980:50). South African water quality guidelines recommend that in order to establish the trophic state of a water-body, the inorganic P and inorganic N is to be used. Water-bodies with no water quality problems have ratios of TN:TP (total N : total P) greater than 25-40:1, whilst eutrophic systems have TN:TP ratios of <10:1. Usually if N/P ratio is >10, P is limiting, but if N/P ratio is <10, N is limiting. The TN:TP ratio is affected by turbidity in spite of the nutrient for algal growth being available. TP and TN concentrations below 0.005 mg of P/l and 0.5 mg of N/l are considered low enough that they limit eutrophication, but in the presence of sufficient P, nitrogen fixing compounds can fix atmospheric nitrogen to make up the deficit (Dallas and Day, 2004). See Table 2 for ranges of P and N for South African waters

Table 2 Selected ranges of P and N as well as their effects

Average summer concentrations (mg/l)		Symptoms and effects
Inorganic Phosphate mg/l	Inorganic Nitrogen mg/l	
< 0.005	< 0.5	Oligotrophic conditions with few water quality problems, no nuisance algae or blooms
0.005 - 0.025	0.5 - 2.5	Mesotrophic with moderate, occasional water quality problems, occasional nuisance algae, algal blooms seldom toxic
0.025 - 0.25	2.5 - 10	Eutrophic with frequent water quality problems, frequent nuisance algal growth and may include cyanobacteria
> 0.25	> 10	Hypertrophic with continuous water quality problems, almost constant nuisance algae and cyanobacteria

Adopted from Dallas and Day, :2004:93 and DWA 1996

2.5 TROPHIC STATUS

In order to classify and compare various water-bodies various trophic status indices were devised and applied by various organisations and individuals. Since this study only considers the surface layer of the water-body, a standard applicable to this study is the TRIX index.

2.5.1 The Trophic Index (TRIX)

This index characterises the trophic levels in coastal marine areas and was adopted by the Italian national legislation. It is the linearisation of chlorophyll-a concentration (ChA in $\mu\text{g}/\text{l}$), the absolute dissolved oxygen concentration in percentage (DO %), the total nitrogen ($N_{\text{min}} = N_{\text{nitrate}} + N_{\text{nitrite}} + N_{\text{ammonia}}$ in $\mu\text{g}/\text{l}$) and the total phosphorus (TP $\mu\text{g}/\text{l}$). This is represented mathematically as:

$$TRIX = \frac{(\log(\text{ChA} + a\text{DO}\% + N_{\text{min}} + \text{TP}) + 1.5)}{1.2}$$

From this equation, the following states of marine waters are classified (Table 3).

Table 3 Categories of TRIX values

TRIX value	Trophic category
< 4	Low trophic level
4 - 5	Middle trophic level
5 - 6	High trophic level
6 - 8	Very high trophic level

From Pavluk and bij de Vaate, 2008:3602

The TRIX index was chosen even though it was for marine waters, it was a sufficient measure of the trophic levels of surface waters as no Secchi depth measurements are required. This index was used in conjunction with the DWA limits to establish the present state as well as the effect of climate change on the dam.

2.6 TOXIC ALGAE AND THEIR NEGATIVE EFFECTS

Some of the largest African lakes have been subject to anthropogenic loading for years and the natural balances between the flora and fauna have become disturbed. The easiest visible consequence of this is the water hyacinth and/or the increasing incidence of cyanobacteria blooms throughout Africa (Rossouw et al., 2008). These noxious invasives have spread to southern Africa, resulting in illness, stock losses and disrupting aquaculture.

2.6.1 Human health risks

It was suggested that excessive eutrophication was the major factor for the increased occurrence of harmful algal blooms in recent years. The direct effects of these blooms are toxicity to organisms and discoloration of water or foam production (Du Plessis et al., 2007). A number of species that are linked to blooms has been noted in marine, brackish as well as freshwater. Figure 10 shows the locations for cyanobacteria events within South Africa that directly contributed to loss of livestock and death of wild animals for 2009.

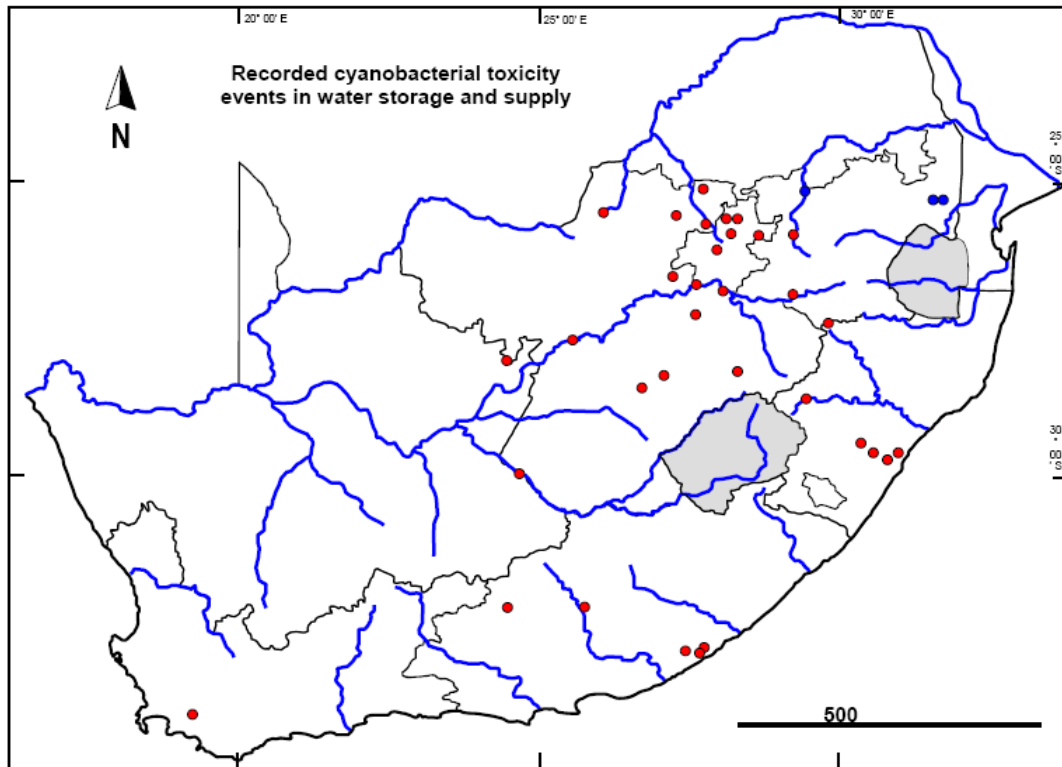


Figure 10 The locations of recorded cyanobacteria toxicity events in South Africa

Adopted from Oberholster et al., 2009. Red dots caused the death of animals, livestock and Blue dots are toxicity events in the Kruger National Park

Cyanobacteria aggregations (blooms, scums and mats) are among the most common and best known symptoms and consequences of anthropogenic eutrophication for surface waters, worldwide (Harding, 2006:8). Overfishing and increased aquaculture alter the food webs which may alter the grazers that feed on harmful algal blooms (HAB) (Heisler et al., 2008:4). Eutrophication, especially an increase in P often leads to significant shifts in phytoplankton species' composition towards bloom-forming cyanobacteria (El Herry et al., 2008:1264). Oceanic cyanobacteria dispersal occurs via natural currents and storms or by dispersal in ballast water exchange or shellfish seeding operations by which algal cells and cysts may be transported.

The common symptoms of cyanotoxin poisoning such as stomach pains, diarrhoea and vomiting are easily confused with gastrointestinal illness and thus not readily linked to cyanotoxins. People who have compromised immune systems or HIV/AIDS are especially at risk as well as children under the age of 5 for whom diarrhoea is the third most important cause of death after HIV/AIDS and low birth weight (Oberholster and Ashton, 2008:8). In Brazil the death of 88 children from over 2000 cases of gastroenteritis was the result of an outbreak of cyanobacteria toxins in drinking water (Oberholster and Ashton, 2008).

2.7 WATER TREATMENT FACILITY PROBLEMS

Once a water-body is eutrophied and toxic blooms occur, an increase in the cost of water treatment is required to render it potable. These increased processing costs could be attributed to changes in odour and taste of the water to be treated. The resulting increases in cyanobacteria, algal and

plant biomass may reduce water quality by increasing the turbidity and particulate matter resulting in the blockage of water filter at the Municipal Water Treatment Plant MWTP (Codd, 2000:52). The treatment is usually to react eutrified water with activated carbon and ozone. Downing and Van Ginkel (2004:30) stated that the additional cost of treating the Voëlvlei Dam amounted to ZAR 60000 per day with the total cost of ZAR 7000000. This was for December 2000 to May 2001 during the time of an *Anabaena* bloom in the dam.

2.7.1 Aquatic fauna and flora problems

It is estimated that the worlds' phytoplankton population consists of approximately 4000 species of which some 200 species cause HABs (Du Plessis et al., 2007). Eutrophication leads to a decrease in dissolved oxygen and subsequent mortality of aerobic aquatic organisms. Amphibians that are exposed to this high nutrient environment are at risk as reduced survivorship, altered feeding and swimming activity, and decreasing growth of and development of the larvae are witnessed. Nutrients increase the density of planorbid snails and likely the intensity of parasite infection resulting in malformations in amphibians affecting species diversity within the water-body (Petlzer *et al*, 2008:186). Eutrophication results in the reduction in species diversity in water-bodies at all animal trophic levels and usually results in the dominance of cyanobacteria (El Herry et al., 2008).

2.7.2 Mitigating the effects of eutrophication

Controlling the trophic state of a water-body is directly linked to controlling the anthropogenic load to the system. Long term eutrophication control would be based on measures aimed at reducing the external loads of nutrients to a water-body. In certain cases, the control of some of these measures may be unfeasible or it may not be possible to lower the levels sufficiently to have the desired effect, such as in the case of temperature. In such cases, the control regimes would target the symptoms of eutrophication without trying to eliminate the problem of nutrient enrichment (Rossouw, 2008). Any attempt to eliminate the effects of eutrophication within a water-body without applying measures to limit the external nutrient load will prove fruitless in the long run.

From an eutrophication management perspective, it is easier to manage and police the anthropogenic loading of a water system so that the subsequent abatement of eutrophication may take place. In order to limit the nutrient loads of return flows and inflows into a water-body the anthropogenic point sources of nutrients must be negated or limited, specifically the N and P inputs (Walmsley, 2000, Owuor et al., 2007).

P is recognised as the fundamental cause of eutrophication for the following reasons:

- Better empirical relations have been observed between algal growth and P concentrations in lakes and water-bodies i.e. it is the key element;
- P availability determines the influence of other nutrients, i.e. it is the limiting nutrient;
- P can be managed more easily (for example than N) because of its chemical and biological properties and it is more easily attenuated at a point source for example at the WWTP;
- Nitrogen plays a secondary role but becomes important at high levels of eutrophication; and
- The removal of P in terms of its availability is the only practical way to combat eutrophication (Rossouw, 2008).

Controlling external nutrient loads to a water-body may include measure such as:

- Modification of products that contain high levels of P and N so as to minimise or eliminate these nutrients into the catchments. Examples of these would be replacing P-based detergents with P free detergents in the industrial and domestic cleaning sectors such as what Denmark did in 1987 by reducing the load of phosphorus by 80% and that of nitrogen by 50% (Harremoës, 1998:9 and Quayle et al., 2010);
- Limiting the discharge levels from WWTP into the catchment with regards to P and N, i.e. setting higher standards as the treatment of domestic effluent is capable of removing up to 95% of the phosphorus ((Dallas and Day, 2004); and
- Control diffuse sources of nutrients in the catchments. The agricultural sector is the main source of diffuse load on the catchment and changes in agricultural practises and fertiliser application would be required to achieve this goal. The timing of the application of fertilizers to avoid the application thereof before heavy rainfall events and avoiding the fertilization of areas susceptible to erosion are some measures that may be adopted (Rossouw, 2008).

Within the water-body some of the techniques to reduce the internal loads of nutrients may include:

- Nutrient trapping by binding nutrients to the sediments and allowing them to settle;
- Selective water depth discharges from water-bodies to extract nutrient rich bottom waters. This may be for treatment and re-assimilation into the water-body or as water for agriculture and aquaculture;
- Aeration of the hypolimnion to reduce the release of nutrient from the sediment;
- Using chemicals to control algal blooms and invasive plants;
- Dredging of the nutrient rich sediments and disposing of them (Rossouw, 2008:11); and
- Biomanipulation of the food chain like the removal of benthivorous fish (like carp) that disturb the sediments facilitating re-suspension of sediments and the nutrients trapped in them.

In the event of an emergency or short term control the following measures are often implemented:

- Physical barriers to contain algal blooms and plants to a specific area or the use of chemicals (FeSO_4 or CuSO_4) to contain the blooms;
- Dissolved air flotation and activated carbon are used by MWTP to treat eutrified water for domestic consumption which is costly; and
- Ozone/UV treatment reduces the concentration of dissolved organic hydrocarbons, halogenated hydrocarbons, polycyclic aromatic carbohydrates, pesticides, dioxins, and (pathogenic) micro-organisms (Rossouw, 2008:11, IPCC, 2007:501)

P is the fundamental element to restrict to achieve a reduction in eutrophication. This should occur ideally at point sources and at WWTPs, which can potentially remove up to 95% of P as well as by modifying current agricultural practices of over-fertilisation and optimising the timing of application of fertilisers.

Thus, algal growth is affected by numerous factors such as light, solar radiation, water temperature and nutrients. Eutrophication is the direct result of over-nitrification of surface waters leading to an excess of algal growth in the water-body and subsequent increased potable treatment costs. It

had been postulated that with climate change, the increased water temperatures would enhance algal growth in water-bodies especially eutrophic surface water. What follows is an investigation into the effect of climate change on eutrophication of surface water.

3 MODELLING THE EFFECT OF CLIMATE CHANGE ON EUTROPHICATION

The general impacts of climate change on southern Africa were assessed in the IPCC 4th assessment report (Christensen et al. 2007). The results indicated that by the end of the 20th century temperature is expected to increase by 2 - 3.5°C compared to values observed in the 1980 - 1999. Results of assessments carried out specifically for South Africa corroborate these results (Schulze, 2006 and Schulze, 2007) .

Changes in temperature and higher ultraviolet light penetration are likely to severely affect freshwater systems, and human populations which rely upon them. Projections of changes in climate (temperature, rainfall and runoff) are extremely difficult to model, and assessing projected climate impacts on freshwater ecosystems is even more challenging, particularly with regard to human influences and responses. The consequences of human-induced impacts include the following effects on aquatic systems, and are likely to be exacerbated with the effects of climate change (Kernan *et al.*, 2007):

- Acidification and eutrophication by sulphur and nitrogen compounds;
- Invasive aquatic species introduction, which alters flow patterns;
- Mobilisation of organic substances from soils;
- Dam building and river diversion;
- Erosion and sedimentation;
- Increased ultra-violet radiation; and
- Habitat fragmentation.

It is important to note that algal blooms, and especially blue green algae, result in many human health-related complications. The impacts of global warming will potentially increase the frequency of toxic algal blooms and this will have a greater chance of human related impacts such as diarrhoea and even potentially toxic algal related fatalities for communities that drink water directly from the river or dam. Management of eutrophication is of particular concern, since this presents severe problems for the treatment of potable water and presents a potential health threat when trihalomethanes (THMs) are formed after chlorination (Kernan et al, 2007).

As previously noted, current climate change models predict climates up to 100 years into the future. They predict higher temperatures of between 3 and 4.5°C and less rainfall for southern west Africa. With the current anthropogenic loading on water-bodies, this would qualitatively result in at least the following:

- Less water inflow into the catchment and the same (present) nutrient loads would result in increased nutrient concentration within the water-body, potentially allowing for greater algal growth because nutrients will be less limiting;
- The climate change would result in lower water levels and increase the rate of decomposition of organic material freeing up more nutrients compounding eutrophication, as well as an increasing in nutrient release from the sediments;
- The lower water levels would result in longer retention times and decreased flushing resulting increased eutrophication and salinity (Jørgensen, 2008);
- Surface water temperature would increase accelerating the growth of algae, specifically those with higher temperature tolerances (usually cyanobacteria) (Cole and Wells, 2008);

- An intervention at the municipal water treatment plant (MWTP) to eliminate the blooms and treat water to potable standards, increasing the cost of treatment;
- Climate change forces higher summer temperatures in the Western Cape and hence faster algal growth and prevalence of more cyanobacteria incidents; and
- Higher water temperature would increase the biological oxygen demand (BOD) resulting in anoxia and species reduction. The dying algae would release their nutrients during decay compounding the situation (Meisner et al., 1987).

Evidently, eutrophication will be adversely affected by the projected climate changes. What are required are predictions of the extent of these changes and the associated changes in water quality so that appropriate mitigating factors may be employed. In order to quantify this potential effect of climate change on water quality a tool is required to simulate the interaction between meteorological driving forces and the water quality response. For this study, the modelling tool selected is a hydrodynamic and water quality model. The ensuing sections will discuss the modelling tools in more detail.

3.1 MODELLING WATER QUALITY

3.1.1 A concise history of Water Quality models

Water quality models have been used for many years to predict the effect of external influences on water quality. Initial water quality variables studied were dissolved oxygen and biological oxygen demand in order to manage the impacts of effluents. Once computers became commercially available (1960's onwards), complex mathematical formulae were applied and calculated parameters now included temperature. As other constituents of water quality is considered important due to their interactive effect on water quality, more complex models were developed and since the 1980's there has been a growing emphasis on hydrodynamic models coupled to water quality processes. Interactions with the sediment are also modelled as well as some form of algal modelling (Nitsche, 2000). With the increasing power of computers, the models being developed now are more complex and computer runtime intensive.

Water quality models may be one dimensional, two-dimensional or three-dimensional, this progression usually indicate the degree of accuracy of the model used. A one-dimensional model will usually oversimplify the hydrodynamics with constant volumes of each segment in the water column. A more accurate representation of the water-body would be obtained using a two-dimensional model, whereas three-dimensional modelling produce results that mimic the real system.

The aim of hydrodynamic water quality modelling is to describe interactions between the hydraulics of a system and its chemical and biological components. A model is an invaluable tool for water quality managers since it can assist in the decision for varying scenarios.

A model for a catchment may be categorised according to the processes they address such as:

- hydrodynamic and hydraulic models (H/H);
- hydrological and watershed models (H/W);
- surface water quality models (SWQ);

- groundwater models (GW);
- ecological models (E).

3.1.2 Hydrodynamic and hydraulic models (H/H)

Hydrodynamic and hydraulic models provide a description of circulation, mixing and density stratification processes that can affect the water quality and transport of constituents of concern within a water-body. These types of models use water-body geometry, boundary conditions, inflows, withdrawals as well as meteorological data to simulate water levels, flow velocities, salinities, temperatures and velocities. Depth, slope of bed, morphology of river channels, surface area, wind-speed, mixing depth, precipitation tidal influences, and temperature and pressure is information on physical properties of water-body required as an input to these models. Physical processes simulated by hydrodynamic models include tidal, wind, and buoyancy or density forcing, and turbulent momentum and mass transport. The spatial dimensions of these models vary from 1-D longitudinal, 2-D in the longitudinal and vertical, 2-D in the horizontal (vertically averaged), to fully 3-D. Hydrodynamic models use numerical solutions for fundamental governing equations for the conservation of momentum and/or mass to predict water movements. Hydrodynamic models such as CH3D-WES are distributed as standalone models and can be coupled internally or externally with WASP5 or CE-QUAL-W2 water quality models. Hydrodynamic models may also form the transport foundation for lake or river mass balance models. They use hydro-meteorological forcing functions to predict the transport that is needed for a constituent mass balance simulation (Limno-Tech, 2002).

3.1.3 Hydrological and watershed models (H/W)

Hydrologic and watershed models are useful for assessing hydrology to manage the water resources of a watershed. This category of models can simulate the generation and dispersion of a constituent of concern from the point of origin to its discharge into receiving waters. These models can be used to quantify total watershed contributions of flow, sediment, nutrients and other constituents of interest. These models require hydro-meteorological data such as rainfall, temperature, humidity and solar intensity. The watershed models evaluate the effects of different land uses and practices, land cover and soil properties on pollutant loadings to water-bodies. Available hydrologic/watershed models vary from simple methods to detailed loading models depending on their capabilities. Simple methods have very limited predictive capabilities and generally provide rough estimates since they are derived from empirical relationships. Detailed models are complex models with greater spatial and temporal resolutions and they use storm events or continuous simulation to predict flow and pollutant concentrations for a range of flow conditions. They include physical processes of infiltration, runoff, pollutant affects, groundwater and surface water interactions. Applications for these models vary depending on data availability and modelling needs (Limno-Tech, 2002).

3.1.4 Surface water quality models (SWQ)

Surface water quality models predict scenarios associated with water quality constituents that result in fish kills, taste and odour problems, human health impacts and other ecosystem disturbances. This category of models includes models that predict dissolved oxygen, nutrient

eutrophication, sediment transport and the fate and transport of constituents. Surface water quality models are used to analyse water quality related problems concerning inputs; reactions and physical transport as well as outputs. The analysis of pollutants in surface waters describes load-response relationships, cause-effect mechanisms, and, in some cases, the impact of pollutants on biota in the system. The parameters simulated include nutrients (generally phosphorus, nitrogen and silicon), dissolved oxygen, biochemical oxygen demand (BOD), chlorophyll, temperature, phytoplankton, zooplankton, and faecal coliforms. These models simulate physical (dilution, advection, and dispersion), chemical, and biological processes (*for example*, nutrient-algal cycle, algal growth and kinetics, DO-BOD cycle, decay, benthic algae, and sediment diagenesis). Eutrophication models predict the production, transformation and decay of phytoplankton biomass in response to changes in nutrients, temperature and light. In some cases, eutrophication and sorbent dynamic models are coupled, which derive and form the basis for the hydrophobic contaminant transport models. The biomass growth rate components of eutrophication model can be linked to a food web bioaccumulation model to predict the contaminant body burden in species (Limno-Tech, 2002).

3.1.5 Groundwater models (GW)

Groundwater models address issues related to water supply, sub-surface contaminant transport, remediation, and mine dewatering. These models can be used for tracking pollutants in the saturated and unsaturated zones as well as evaluating the transport of pollutants due to migration and interactions of groundwater and surface water. Groundwater withdrawals can result in lower river and stream water levels. The hydrology of the watershed can be impacted due to precipitation, runoff, groundwater, surface storage, and river water levels. Coupled watershed and groundwater models can simulate the effect of water fluctuations on groundwater flow and its influence on watershed hydrology. Groundwater models generally require a large amount of information and a complete description of the flow system. Most of the groundwater models require a high level of expertise by the operator (Limno-Tech, 2002).

3.1.6 Ecological models (E)

This category includes a wide variety of models and techniques for the ecological assessment of the aquatic system. It includes habitat and species classification, index systems, as well as toxicological and ecological models that simulate the effect of stressors on habitats. These types of models can examine or predict the status of a habitat, biological population or biological community. Ecological effects models for addressing the impacts of water withdrawals include a wide range of evaluation and assessment techniques that affect the ecosystem structure and function. Changes in water quantity, water quality and sediment dynamics driven by water withdrawals can affect the following components and interactions in an aquatic ecosystem:

- Species habitat;
- Production and diversity of flora;
- Acute and chronic toxicity to any species;
- Population levels;
- Growth of species (that can affect the bioenergetics costs);
- Predator-prey relationships;

- Food web structure;
- Energy flow and nutrient cycling; and
- Bioaccumulation of contaminants.

Specifically, for dealing with issues related to fish species, these effect models should incorporate the effect of hydraulic conditions on:

- Fish stranding under various climatic and diurnal conditions;
- Fish behaviour and shelter-type that can vary with flow conditions;
- Effects on the shift in substrate type, vegetation, and water quality that may affect fish behaviour, recruitment and survival;
- Effects on the activities and bioenergetics of different life-stages and species.

Because of the inherent connection between species and its habitat, the effects models are best suited when used in combination with each other, as well as with other categories of models (Limno-Tech, 2002).

3.2 A REVIEW OF RELEVANT WATER QUALITY MODELS

The water quality models available today are multipurpose and these can be used for river and reservoir modelling, runoff modelling, hydrology and hydrodynamic modelling, water quality modelling, ground water and ecological modelling. The primary purpose behind the conception of the model is used to gauge the performance of the model as well as its applicability from previous applications to the current problem. Of particular concern for this project were the water quality and hydrological/hydrodynamic models and their ability to simulate response to a climate change scenario. The identification of relevant models was based on a literature and web-based search, as well as personal experience. What follows is a description of a method for selecting a model/s for a water quality-related problem with driving inputs from various climate change scenarios.

3.2.1 Model selection

The selection of the appropriate models to address a particular management question was based on many considerations, including management objectives, data availability and available resources. The models presented in Table 4 differ in their capabilities, complexity, and resource requirements. The model inventory provides useful information to support the model selection process. The data needs associated with many of these models may require significant resources to apply them on a site-specific basis; resource and data availability for a given site are critical considerations in the model selection process.

Simple models require less expertise and less data, so they can be used by a wider community, but often they are limited in the management questions that they can credibly address. Complex models generally have high spatial, temporal and process resolutions, require large data sets, and involve extensive computation time. These models, however, can only be used by a limited number of experts. In addition, in some cases, these more complex models have undergone limited field testing and great care should be taken in applying them on a site-specific basis without

rigorous calibration. For selecting models from this inventory, user-specific information for the following factors will help meet the needs:

- A clear definition of the problem must be outlined;
- Define the specific modelling need;
- Resources available: Identify availability of system specific inputs, calibration, and validation data set;
- Identify the availability of modelling expertise, ease-of-use concerns, the model accuracy, and details required;
- Define whether the analysis was required at a screening level or detailed level.

The models reviewed can address one or more system processes, such as hydrodynamics, sediment transport, water quality, or ecological effects. Based on the current inventory, there is no single model that could quantify the ecological impacts for a climate change projection.

For the purposes of this study only water quality, hydrodynamic and hydraulic models was considered to address the effect of climate change on eutrophication and subsequent water quality.

The following models were examined for their suitability in water quality modelling under climate change scenarios. Table 4 provides a summary of some of the popular models for water quality, hydrology and hydrodynamics.

Table 4 A summary of some of the current available models

Model name and description	Type of model	Applicability to this study	Steady state or dynamic	Dimension	Supporting Agency
ALIS Aquatic Landscape Inventory System (ALIS) and associated database	H/W	N	Dynamic	2D	OMNR
AQUATOX Ecosystem Model	E and SWQ	N	Dynamic	2D	USEPA
ATLSS Across Trophic Level System Simulation for the freshwater wetlands of the everglades and big Cypress swamp	H/W and E	N	Dynamic	2D	Coordinated through USGS
BASINS Better Assessment Science Integrating point and Nonpoint Sources(NPSM – Dynamic QUAL2E – Steady state)	H/W and SWQ	Y	Mixed Dynamic and steady state	1-D steady state to 3-D	USEPA and CEAM
QUAL-2E Steady state, one dimensional water quality model	SWQ	Y	Steady state	1-D	USACOE
CE-QUAL-ICM I is a 3-D time variable integrated compartment eutrophication model	H/H and SWQ	Y	Dynamic	3-D	USACOE

CE-QUAL-RIV1 Hydrodynamic & Water Quality Model for Streams	H/H and SWQ	Y	Dynamic	1-D	USACOE
CE-QUAL-W2 2-D laterally averaged hydrodynamic and water quality model	H/H and SWQ	Y	Dynamic	1-D, 2-D	USACOE Portland State University
CH3D-WES Curvilinear Hydrodynamics in Three Dimensions - Waterways Experiment Station	H/H	N	Dynamic	3-D	USACOE
DUFLOW Water quality, hydrodynamic and groundwater model	H/H and SWQ	Y	Dynamic	1-D	Agricultural University of Wageningen
ECOFATE Ecosystem model	H/H and SWQ	N	Dynamic	2-D	Simon Fraser University, Canada (Frank P. Gobas)
EFDC: Environmental Fluid Dynamics Code Hydrodynamics and transport model	H/H and SWQ	Y	Dynamic	1-D to 3-D	Tetra-Tech/Virginia Institute of Marine Sciences
ELCOM-CAEDYM: Estuarine and Lake Computer Model is coupled with Computational Aquatic Ecosystems Dynamic Model	H/H, E and SWQ	Y	Dynamic	3-D	Centre for Water Research, University of Western Australia
EUTROMOD Receiving water model	SWQ	Y	Steady state	1-D	NALMS
GBTOX/GBOCS Green Bay Toxics Model	SWQ	N	Dynamic	3-D	USEPA
HEC-2/HEC-RAS River Analysis System	H/H	N	Steady	1-D (HEC-2)	USACOE
MIKE-11/ MIKE-21/ MIKE-3 Generalised Modelling Package- 1D/ 2D/3D – hydrodynamics	H/H and SWQ	Y	Dynamic	1, 2 and 3D	Danish Hydraulic Institute
RATECON Rate Constant Model for Chemical Dynamics	SWQ	N	Dynamic	1-D	Trent University, Canada (Donald Mackay)
RMA-2V Hydrodynamic analysis model	H/H	N	Dynamic	2-D lateral	USACOE
SAGEM Saginaw Bay Ecosystem Model	SWQ	N	Dynamic	3-D	USEPA
SMPTOX4 Simplified Method Program – Variable-Complexity	H/H and SWQ	N	Steady-state	1-D	USEPA/CEAM

Stream Toxics Model					
WASP5 Water Quality Analysis Simulation Program	SWQ	Y	Dynamic	1-D to 3-D	USEPA

Where H/W is hydrological/watershed model, H/H is hydrodynamic/hydraulic, SWQ is surface water quality, E is ecological effects
Adopted from Limno-Tech, 2002 and Nitsche, 2000.

Most of the models reviewed in the inventory (Table 4) are distributed as stand-alone models, and they generally address one or more aspects of a water quality problem, such as hydrodynamics, sediment transport, water quality, or ecological effects. Model selection is an arduous process and the criteria for selecting include:

- Applicability of the model;
- Cost of the model;
- Support/training in the use of the model;
- Availability of data in the form that the model requires as an input;
- Its ability to model constituents of concern such as phosphates, temperature, oxygen etc.;
- The frequency of the outputs.

The following subsections are descriptions of surface water quality models deemed capable of simulating the effect of climate change on eutrophication as well as the choice of a model for this task.

3.2.2 BASINS

The EPA developed the Better Assessment Science Integrating Point and Nonpoint Sources (BASINS) decision support tool to assess water quality over large watersheds. Its primary purposes are to facilitate examination of environmental information, to provide an integrated watershed and modelling framework and to support analysis of point and nonpoint source management alternatives (Limno-Tech, 2002). The BASINS decision tool includes the Hydrologic Simulation Program-FORTRAN (HSPF) model to simulate the point and nonpoint source runoff and pollution loadings in a watershed. Applications of BASINS includes the identification of impaired surface waters from point and nonpoint pollution, wet weather combined sewer overflows, storm water management issues, and drinking water source protection. BASINS has also been used in urban/rural land-use evaluations, animal feeding operations and habitat management practices.

Data requirements for BASINS are extensive. Much of the necessary data is provided with the software and more detailed, site-specific data can be added if desired. Overcoming the lack of integration, limited coordination, and time-intensive execution typical of more traditional assessment tools, BASINS makes watershed and water quality studies easier by bringing key data and analytical components together "under one roof".

The primary limitation of BASINS corresponds to its extensive resource requirements. There is also concern that providing automated access and/or default values for all model inputs and data will lead to applications that do not adequately describe a specific system. There is lack of data for many watersheds to allow for accurate modelling (Limno-Tech, 2002 and Lee et al, 2010).

3.2.3 QUAL-2E

QUAL-2E is established and widely used although it is a steady state model. It is one of the QUAL series of models and has a two-decade history in water quality management and waste-load allocation studies. Its primary purpose of development was as a water quality management, planning and waste-load allocation tool applicable to conventional pollutants. The model may be used for water quality/eutrophication, far field, stream/river, 1-D, branching, steady flow, steady-state/quasi-dynamic as well as advective/dispersive transport. Twenty-six physical, chemical, and biological properties have to be specified whilst it can predict up to 15 water quality constituent concentrations. Amongst the parameters that were modelled are temperature, salinity, BOD, N, P, Chlorophyll a as well as a 1st order kinetics of constituents. The QUAL2E Windows interface was developed to make the model more user-friendly. It provides input screens to facilitate preparing model inputs and executing the model. It also has help screens and provides graphical viewing of input data and model results. It was widely used and accepted for various solutions to environmental problems. It has a water quality planning tool to aid in developing total maximum daily loads (TMDLs). The model's weakness are that it:

- Is a steady-state model, best suited for low-flow analysis and not wet weather related events;
- Requires significant site-specific data for its proper application; and
- Considers only steady flow and the only time-varying forcing functions are the climatologic variables that primarily affect diurnal temperature and dissolved oxygen.

Documentation for QUAL2E is available at <http://www.epa.gov/ord/webpubs/qua12e/and> further information available at: http://smiq.usgs.gov/cgi-bin/SMIC/model_home_pages/model_home. (Limno-Tech, 2002, Nitsche, 2000 and QUAL 2E manual). Currently a modernised version of QUAL-2E has been released, known as QUAL-2K designed for the Microsoft windows environment. QUAL-2K is programmed in Virtual Basic and Microsoft Excel is used as the graphical user interface. The supporting agency is the USEPA and 2.11b8 is the current version (www.epa.gov/athens/wwqtc/html/qual2k.html, 2013).

3.2.4 CE-QUAL-ICM

CE-QUAL-ICM is a 3 dimensional time-variable integrated-compartment eutrophication model developed by the United States Army Corporation of Engineers (USACOE) and is also is a member of the QUAL family of models. Its primary purpose is to simulate time-varying concentrations of water quality constituents by coupling hydrodynamic and water quality components. Applications of this model include the 3-D model of the Chesapeake Bay where the model was employed to simulate long-term trends in Chesapeake Bay eutrophication (Cercio and Cole, 1995) as well as to assess the water quality impacts of a confined disposal facility in Green Bay, Wisconsin. The model may be applied to most water-bodies in One-Dimensional (1-D), Two-Dimensional (2-D), or Three-Dimensional (3-D) and for unsteady flows. Geometric data to describe the finite difference representation of the water-body have to be defined as well as 140 parameter values needed to specify kinetic interactions. Initial and boundary conditions have to be specified and operators should have extensive modelling experience.

Although the model has full capabilities to simulate state-of-the-art water quality kinetics, it is limited by available data for calibration and verification. In addition, the model may require significant technical expertise in aquatic biology and chemistry to be used appropriately (Cerco and Cole, 1995 and Limno-Tech, 2002). Further Information is available at <http://www.epa.gov/ednrmrl/tools/model/ce-icm.htm> and http://smig.usgs.gov/cgi-bin/SMIC/model_home_pages/model_home

3.2.5 CE-QUAL-RIV1

This model is another member of the QUAL family and its primary purpose is to simulate transient water quality conditions associated with highly unsteady flows that can occur in regulated rivers. This model can handle multiple control structures such as dams. The model consists of two codes: RIV1H, a stand-alone hydraulic routing code and RIV1Q, a water quality code that uses output from RIV1H to provide dynamic water quality simulation. With changes in discharge conditions i.e. for unsteady flows, the model can be used to simulate the concentration of water quality variables. The model can be used to evaluate the ecological impacts caused by change in concentrations under different scenarios of discharge conditions (water use and withdrawals). RIV1H requires river geometry and boundary conditions to perform hydraulic calculations. Geometric data include locations of control structures, streambed elevations, river cross sections and distances between nodes. Boundary conditions include flow rates and stages, lateral inflows or withdrawals and boundary conditions defined by discharge, stage or a stage-discharge rating curve. RIV1Q requires initial in-stream and inflow boundary water quality concentrations, meteorological data for temperature computations as well as rate coefficients.

The model has large resource requirements and requires a trained user whilst not having a user friendly interface as it uses an ASCII input file. It also does not include sediment quality component and may exhibit numerical instability under certain conditions. The model is only applicable to situations where flow is predominantly one-dimensional. It simulates conventional pollutants only and contains limited eutrophication kinetics (Nitsche, 2000 and Limno-Tech, 2002).

3.2.6 CE-QUAL-W2 version 3.6

CE-QUAL-W2 is a two-dimensional (longitudinal-vertical) hydrodynamic and water quality model developed by the Army Corps of Engineers' Waterways Experiment Station (USACOE) and is part of the QUAL family of models. The primary purpose of the model is to simulate time-varying concentrations of water quality constituents by coupling hydrodynamic and water quality subroutines. The model has been applied to many rivers, lakes, reservoirs, and estuaries for nearly 20 years and can simulate temperature, salinity, DO, carbon balance, N, P, Si, phytoplankton, bacteria as well as first-order decay. Geometry data are required to define the finite difference representation of the water-body. Initial and boundary conditions have to be specified and the required hydraulic parameters include horizontal and vertical dispersion coefficients for momentum and temperature/constituents as well as the Chezy coefficient, used to calculate boundary friction. Simulation of water quality kinetics requires the specification of approximately 60 coefficients. Data is required to provide boundary conditions and assess model performance during calibration. Because the model assumes lateral homogeneity, it is best suited for relatively strong longitudinal and vertical water quality gradients; it may be inappropriate for large water-

bodies and has extensive data requirements (Limno-Tech, 2002 and Cole and Wells, 2008). An advantage of this model is that it has previously been used for South African water-bodies and in particular for Voëlvelei Dam.

3.2.7 DUFLOW

Duflow (Dutch flow) is a one-dimensional, non-steady state model for water movement and water quality. Duflow was originally developed to simulate the water movement (both quantitatively and qualitatively) in estuaries in the South-West of the Netherlands. Duflow has a user-friendly graphical interface. It includes 3 models hydrodynamic and water quality module (DUFLOW), the rainfall-runoff module (RAM) and the groundwater module (MODUFLOW). It has 2 predefined water quality components that may be modelled independently. DUFLOW simulates constituents such as N, P, O, sediment-water interaction, 3 algal species and one phytoplankton species. In DUFLOW, flow is modelled using 1-D St-Venant equation, which is solved numerically. Dispersion in DUFLOW can be modelled as a function of the flow velocity. Transport by advection and dispersion is modelled automatically in DUFLOW and the user does not have to make inputs into the implementation of these transport processes. A scenario manager allows the user to see the result of various scenarios such as pollution spills and to compare the results. Its major disadvantage is that it is a 1-D model and cannot describe longitudinal dispersion at low flowrates. Online documentation is available at www.mx-groep.nl/duflow/ (DUFLOW, 2000, Nitche, 2000 and Ritzema, 2010).

3.2.8 EFDC

Environment Fluid Dynamics Computer code (EFDC) is a general purpose modelling package for simulating three-dimensional flow, transport and biogeochemical processes in surface water systems including rivers, lakes, estuaries, reservoirs, wetlands, and coastal region. It was originally developed by Virginia Institute of Marine Science as authorized by USEPA. The EFDC model has been-used for modelling studies in the estuaries of the Chesapeake Bay System, the Indian River Lagoon and Lake Okeechobee in Florida, the Peconic Bay System in New York, Stephens Passage in Alaska, and Nan Wan Bay, Taiwan. The model has also been used to simulate large scale wetlands flow and transport in the Everglades. EFDC is applicable to rivers, lakes, reservoirs, estuaries, wetlands, and coastal regions.

The EFDC model has three primary functional components namely hydrodynamics, water-quality and sediment transport integrated into a single software system. The hydrodynamic model component is based on the three-dimensional shallow water equations and includes dynamically coupled salinity and temperature. The coupled water quality/eutrophication and a sediment/toxicant transport and fate sub-models included in the EFDC can be used to assess the ecological impacts of water quality and water quantity.

Technical expertise is required and the input data to drive the model include open boundary water surface elevation, wind and atmospheric, thermodynamic conditions, open boundary salinity and temperature, volumetric inflows and inflowing concentrations of sediment and water quality state variables. Input file templates are included with the source code and the user's manual to aid in input data preparation. EFDCs' main weaknesses are that considerable technical expertise in

hydrodynamics is required to use the model effectively as well as expertise in eutrophication processes is required to use the water quality component. It also requires extensive computer resources (Limno-Tech, 2002 and Jeong et al., 2010).

Further information is available at <http://www.epa.gov/ednrmrl/tools/model/efdc.htm> and http://smig.usgs.gov/cgi-bin/SMIC/model_home_pages/model_home.

3.2.9 ELCOM-CAEDYM

The Estuarine and Lake Computer Model coupled with an ecological model Computational Aquatic Ecosystem Dynamics Model (ELCOM-CAEDYM) is a three-dimensional hydrodynamic model. ELCOM was primarily developed by the Centre for Water Research, University of Western Australia (www.cwr.uwa.edu.au) to simulate hydrodynamics and transport in stratified water-bodies with spatially-varying wind stress, surface heat exchange, tidal boundaries and multiple inflows (including groundwater sources).

The model solves the three-dimensional Reynolds-averaged, unsteady, hydrostatic, Boussinesq, Navier-Stokes and scalar transport equations on a cartesian mesh. The hydrodynamic algorithms are a semi-implicit, finite-difference approach based on a second-order Euler-Lagrange advection of momentum with an implicit solution of the free surface evolution. Scalar transport uses a conservative discretisation of a flux-limiting third method. Turbulence modelling uses a mixed-layer approach in the vertical with constant eddy viscosities for the horizontal.

CAEDYM consists of a set of subroutines containing a series of equations that describe the major biogeochemical processes influencing water quality. These include primary and secondary production, nutrient (P and N) and metal cycling, oxygen dynamics and the movement of sediment. ELCOM and CAEDYM are coupled such that ELCOM simulates salinity and temperature, passing values for these parameters to CAEDYM for modification of ecological state variables, whilst CAEDYM passes the water quality variables to ELCOM for advective and dispersive processes.

The strength of this model is that it is a coupled system that models hydrodynamics and water quality simultaneously whilst its weaknesses are large data requirements as well as the user having to be proficient in modelling and use of the model. A major disadvantage to these complex models is that a sensitivity analysis over the entire parameter space is impossible and that the establishment of generic parameter values for general plankton models has remained elusive (Hodges and Dallimore, 2006, Chan et al., 2002).

3.2.10 EUTROMOD

Eutrophication model (EUTROMOD) is a spreadsheet-based watershed and lake modelling procedure for eutrophication management, with an emphasis on uncertainty analysis. The spreadsheet uses land and land-use characteristics to estimate surface runoff, sediment and nutrient yields from a watershed. The model estimates nutrient loading, various trophic state parameters, and tri-halo-methane concentration in the lake using data pertaining to land use, pollutant concentrations, and lake characteristics. It predicts growing season average conditions as a function of annual nutrient loadings.

The model was developed using empirical data from the USEPA's national eutrophication survey, with trophic state models used to relate phosphorus and nitrogen loading to in-lake nutrient concentrations. The phosphorus and nitrogen concentrations were then related to maximum chlorophyll level, Secchi disk depth, dominant algal species, hypolimnetic dissolved oxygen status, and tri-halo-methane concentration. EUTROMOD allows for uncertainty analysis by considering the error in regression equations employed, and using an annual mean precipitation and coefficient of variation to account for hydrologic variability.

EUTROMOD simulates total P and N concentrations in the lake based on all inputs, watershed characteristics, land use, precipitation and evaporation. It also generates output on the probability of the blue-green algal dominance, which is directly applicable to evaluate the ecological impacts caused by water withdrawal. EUTROMOD is limited in its application because it is designed for watersheds in the southern United States and it provides predictions only of growing season averages. It is an empirical (not mechanistic) model and its application is limited (Limno-Tech, 2002).

Further information on EUTROMOD is available from through www.nalms.org or <http://www.epa.gov/owow/tmdl/nutrient/linkage.html>.

3.2.11 MIKE 11, MIKE 21, MIKE 3

The MIKE series of models represents a continuous development since the early 1970s by the Danish Hydraulic Institute where MIKE 11 is 1-D, MIKE 21 is 2-D and MIKE 3 is 3-D model. The system has been applied in hundreds of applications and is presently used as the basis for countrywide river models in Bangladesh. The package includes models for rainfall, runoff, hydrodynamics, advection, dispersion, sediments and water quality simulations. The primary purpose of MIKE 21 is to simulate hydraulics, sediment transport and water quality in estuaries, rivers, lakes, estuaries, bays, coastal areas and seas, irrigation systems and similar bodies.

The system consists of five main modules:

- A hydrological module that computes the rainfall-runoff from rural catchments;
- A hydrodynamic module that computes discharges and water level variations in rivers and flood plains. This module solves the full dynamic, diffusive or kinematic wave equations;
- A sediment transport module that simulates sediment transport, dune formation, bed level changes and hydraulic resistance;
- A transport-dispersion module that includes a special description for cohesive sediments; and
- A water quality module that simulates chemical and biological processes.

The constituents that are modelled include hydrodynamics, DO, BOD, nutrients, phytoplankton, temperature, bacteria and toxins. The input data for a MIKE simulation consists of organisational input, initial values, boundary and topographical data. It has a user-friendly model interface, although extensive modelling experience is required. The model is proprietary and in 1999, the cost of MIKE 21 was more than ZAR 100000 (Nitsche, 2000 and Limno-Tech, 2002). See www.dhisoftware.com for more information on the MIKE series of models and current cost.

3.2.12 WASP5

Water Quality Analysis Simulation Program (WASP) is a surface water quality modelling application that has its origins in the Manhattan College of environmental engineering program in the late 60's. It may be used as a 1-D, 2-D or 3-D model and may be coupled with hydrodynamic models. The model simulates time varying processes of advection and dispersion, considering point and diffuse mass loading as well as boundary exchange. WASP5 includes two sub-models for water quality/eutrophication and toxics, namely EUTRO5 and TOXI5. The body of water to be simulated must be divided into a series of completely mixed computational segments. Loads, boundary concentrations, and initial concentrations must be specified for each state variable. Forcing functions such as temperature must also be specified for time and spatially variable parameters.

In TOXI5, up to 12 spatially variable environmental variables, such as pH and light extinction, may be specified as needed. In addition, up to 17 time-variable functions may be used to study diurnal or seasonal effects on pollutant behaviour. In EUTRO5, up to 16 spatially variable environmental parameters, 60 rate constants, and 14 time-variable functions can be specified. The model processes parameters such as temperature, salinity, bacteria, DO, BOD, N, P, phytoplankton, first-order decay, products, process kinetics, equilibrium sorption and re-suspension/deposition. Its strengths are that it provides the flexibility to describe almost any water quality constituent of concern, along with its widespread use and acceptance. The major weaknesses of WASP5 are that:

- It has limited hydrodynamic capabilities with the 1-D RIVMOD-H and DYNHYD5 models;
- There is a potential for instability or numerical dispersion in the user specified computational network;
- Zooplankton dynamics are not simulated in EUTRO5 although their effect may be described by user specified forcing functions that vary in space and time; and
- It has an intermediate-level method for computation of sediment oxygen demand and benthic nutrient fluxes (Limno-Tech, 2002).

Further Information is available for WASP5 at the following web addresses

http://smig.usgs.gov/cgi-bin/SMIC/model_home_pages/model_home

<http://www.epa.gov/ednrmrl/tools/model/wasp5.htm>

<http://www.epa.gov/region4/water/tmdl/tools/wasp.htm>

3.3 THE MODEL SELECTION

The model selection is largely based on the users experience with the model as well as its applicability to the study. To predict the effect of climate change on the water quality and subsequent eutrophication requires both a water quality and hydrodynamic model. Due to the data requirements for a three dimensional model being extensive, a two dimensional model was considered to be sufficiently accurate for this study. Ease of use of the model as well as its previous application is considered advantageous along with any technical support offered. Finally, the price of the model is considered.

The model chosen for this study is CE-QUAL-W2 because of its proven ability to accurately represent hydrodynamics and the ability to represent multiple algal groups. Modelling algae in multiple groups is important because modelling algae as one conglomerate is only a general approximation of actual conditions because kinetic rates are species dependent. A more accurate representation is possible by modelling algae as groups based on different species (Nielsen, 2005). The model had previously been used for Voëlvlei Dam, thus local technical support is available. The model is freely distributed by Portland State University and is used worldwide.

3.4 THE THEORETICAL BASIS FOR CE-QUAL-W2 HYDRODYNAMIC AND WATER QUALITY MODEL

CE-QUAL-W2 is a two-dimensional (longitudinal-vertical) hydrodynamic and water quality model developed by the United States Army Corps of Engineers' Waterways Experiment Station (USACOE) and is part of the QUAL family of models. The primary purpose of the model is to simulate time-varying concentrations of water quality constituents by coupling hydrodynamic and water quality components. The model has been applied to many rivers, lakes, reservoirs, and estuaries for nearly 20 years. The model will simulate water temperature, salinity, DO, carbon balance, N, P, Si, phytoplankton, bacteria as well as first-order decay. Geometry data is required to define the water-body mathematically. The governing equations of state are solved using the finite difference method. Initial and boundary conditions have to be specified and the required hydraulic parameters include horizontal and vertical dispersion coefficients for momentum and temperature/constituents as well as the Chezy coefficient, used to calculate boundary friction. Simulation of water quality kinetics requires the specification of approximately 60 coefficients. Data is required to provide boundary conditions and assess model performance during calibration. Because the model assumes lateral homogeneity, it is best suited for relatively strong longitudinal and vertical water quality gradients; it may be inappropriate for large water-bodies where Coriolis forces are present or where significant lateral gradients exist. The model has extensive data requirements. It allows for user-defined numbers of algal, zooplankton and macrophytes groups (Cole and Wells, 2008).

Amongst the limitations of CE-QUAL-W2 are:

- **Hydrodynamics and transport.** The governing equations are laterally (x-z axis) and layer averaged (bank to bank for rivers). Lateral averaging assumes lateral variations in velocities, temperatures, and constituents are negligible. This assumption may be inappropriate for large water-bodies exhibiting significant lateral variations in water quality. Whether this assumption is met is often a judgment call on the user and depends in large part on the questions being addressed. Eddy coefficients are used to model turbulence. Currently, the user must decide among several vertical turbulence schemes the one that is most appropriate for the type of water-body being simulated. The equations are written in the conservative form using the Boussinesq and hydrostatic approximations. Since vertical momentum is not included, the model may give inaccurate results where there is significant vertical acceleration (Cole and Wells, 2008).
- **Water quality.** Water quality interactions are, by necessity, simplified descriptions of an aquatic ecosystem that are extremely complex. Improvements will be made in the future as better means of describing the aquatic ecosystem in mathematical terms and time for

incorporating the changes into the model become available in this one area (Cole and Wells, 2008).

- **Sediment oxygen demand (SOD).** The model includes a user-specified sediment oxygen demand not coupled to the water column thus does not compute SOD and sediment to water column nutrient fluxes based on organic matter delivery to the sediments. SOD only varies according to temperature. The first order model was tied to the water column settling of organic matter. The model does not have a sediment compartment that models kinetics in the sediment and at the sediment-water interface. This places a limitation on long-term predictive capabilities of the water quality portion of the model (Cole and Wells, 2008).
- **Computer limits.** A considerable effort has been invested in increasing model efficiency including a vertically implicit solution for vertical turbulence in the horizontal momentum equation. However, the model still places computational and storage burdens on a computer when making long-term simulations. Yearlong water quality simulations for a single water-body can take from a few minutes to days for multiple water-bodies in a large river basin. Applications to dynamic river systems can take considerably longer than water-bodies because of much smaller time-steps needed for river numerical stability (Limno-Tech, 2002 and Cole 2008).

In this study, the CE-QUAL-W2 model was applied to Voëlvlei Dam for potential climate induced eutrophication and water quality changes. The model uses a numerical scheme for direct coupling between the hydrodynamic and water quality simulations. It is based on a finite-difference approximation of the laterally averaged equations of motion including the free surface equations, hydrostatic pressure, momentum, continuity, constituent transport and equation of state.

3.4.1 The conservation laws of fluid flow

The model uses laterally averaged equations of motions derived from the three dimensional equations of motion and continuity. The mathematical expression for the general model of fluid flow and heat transfer was developed from the basic principles of conservation of mass, momentum and energy. The governing equations are obtained by performing mass, momentum and energy balance of the fluid (in this case water) about a control volume. The conservation laws of physics state that:

- The mass of a fluid is conserved;
- The rate of change of momentum equals the sum of the forces on the control volume (Newton's second law); and
- The rate of change of energy equals the sum of rate of heat addition and the rate of work done on the control volume (First law of thermodynamics).

Typical behaviour of the fluid was described in terms of velocity, pressure, density and temperature which themselves are considered as averages over a vast number of molecules. The control volume under consideration was thus the smallest possible volume of the fluid that was not influenced by molecular interactions.

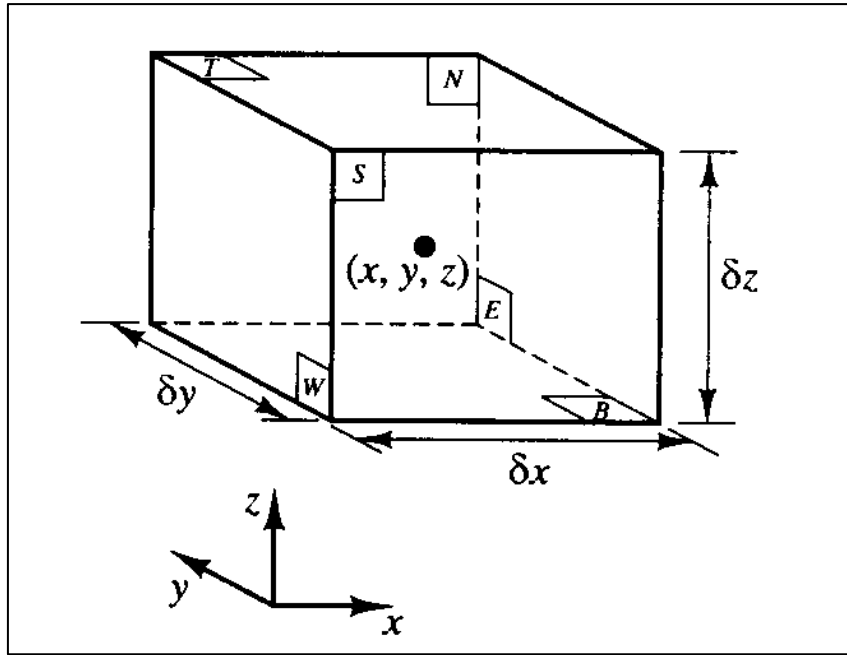


Figure 11 A typical control volume

Adopted from Versteeg and Malalasekera, 1995

The fundamental equation applied is:

$$\text{Rate of increase of mass in volume} = \text{Net rate of flow of mass into the volume} \quad (1)$$

The continuity equation was the mathematical representation of mass conservation on a control volume and was expressed as

$$\frac{\partial \rho}{\partial t} + \nabla(\rho u) = 0 \quad (2)$$

This is the equation describing the unsteady, three-dimensional mass conservation of a compressible fluid. If the fluid was incompressible i.e. density ρ was constant, which water is assumed to be then $\nabla(\rho u) = 0$ or

$$\frac{\partial u}{\partial x} + \frac{\partial v}{\partial y} + \frac{\partial w}{\partial z} = 0 \quad (3)$$

Where u, v and w was the velocity of the fluid in the x, y and z directions respectively.

Momentum and energy conservation describe the changes of properties on a control volume and these properties are a function of position and time. Considering the following figure

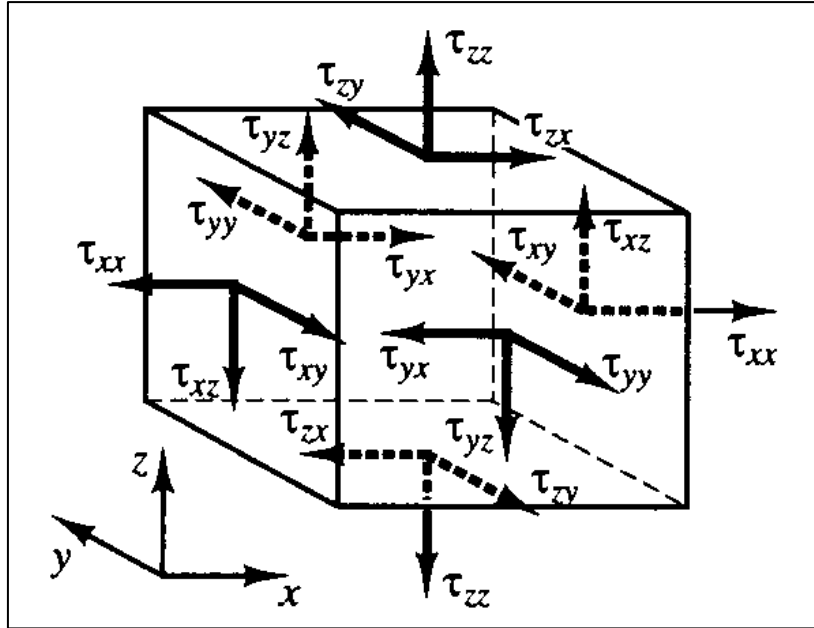


Figure 12 Stress on a control volume

Adopted from Versteeg and Malalasekera, 1995

The equation that describes the momentum conservation in the x direction was derived by setting the rate of change of x-momentum equal to the total force in the x-direction due to surface stresses (T) plus the rate of increase of x-momentum due to internal sources. This was mathematically expressed as for the x, y and z directions. The dam has no slope and hence gravity was excluded for the transport model.

Unsteady acceleration + convective acceleration = pressure gradient + turbulent stresses + source or sinks.

$$\rho \frac{Du}{Dt} = \frac{\partial(-\rho + \tau_{xx})}{\partial x} + \frac{\partial \tau_{yx}}{\partial y} + \frac{\partial \tau_{zx}}{\partial z} + S \text{ and this simplifies to}$$

$$\frac{\partial u}{\partial t} + u \frac{\partial u}{\partial x} + v \frac{\partial u}{\partial y} + \omega \frac{\partial u}{\partial z} = -\frac{1}{\rho} \frac{\partial P}{\partial x} + \frac{1}{\rho} \left(\frac{\partial \tau_{xx}}{\partial x} + \frac{\partial \tau_{xy}}{\partial y} + \frac{\partial \tau_{xz}}{\partial z} \right) + S_x \quad (4)$$

And similarly for the y direction

$$\frac{\partial v}{\partial t} + u \frac{\partial v}{\partial x} + v \frac{\partial v}{\partial y} + \omega \frac{\partial v}{\partial z} = -\frac{1}{\rho} \frac{\partial P}{\partial y} + \frac{1}{\rho} \left(\frac{\partial \tau_{yx}}{\partial x} + \frac{\partial \tau_{yy}}{\partial y} + \frac{\partial \tau_{yz}}{\partial z} \right) + S_y \quad (5)$$

And for the z direction

$$\frac{\partial \omega}{\partial t} + u \frac{\partial \omega}{\partial x} + v \frac{\partial \omega}{\partial y} + \omega \frac{\partial \omega}{\partial z} = -\frac{1}{\rho} \frac{\partial P}{\partial z} + \frac{1}{\rho} \left(\frac{\partial \tau_{zx}}{\partial x} + \frac{\partial \tau_{zy}}{\partial y} + \frac{\partial \tau_{zz}}{\partial z} \right) + S_z \quad (6)$$

The z-momentum equation was simplified and lateral averaging was applied and the laterally averaged equations of state for CE -QUAL-W2 was summarised as follows

The laterally averaged continuity equation is

$$\frac{\partial UB}{\partial x} + \frac{\partial WB}{\partial z} = qB \quad (7)$$

Where

B is the control volume width

U is the laterally averaged velocity in the x direction

W is the laterally averaged velocity in the z direction

q is the net lateral inflow per unit volume

The x momentum equation (U)

$$\frac{\partial UB}{\partial t} + \frac{\partial UUB}{\partial x} + \frac{\partial WUB}{\partial z} = -\frac{B}{\rho} \frac{\partial P}{\partial y} + \frac{1}{\rho} \left(\frac{\partial B\tau_{xx}}{\partial x} + \frac{\partial \tau_{yz}}{\partial z} \right) + S_y \quad (8)$$

The z momentum equation equals zero

$$\frac{1}{\rho} \frac{\partial P}{\partial z} = 0 \quad (9)$$

There are now 3 equations and 3 unknowns U , W and P . This implies that the density was known for the solution of the momentum equations. The equations of state relates the density to temperature and concentration of dissolved substances and was represented as

$$\rho = f(T_w, \varphi TDS, \varphi ISS) \quad (10)$$

Thus, density was a function of temperature, total dissolved solids and inorganic suspended solids. The laterally free water surface equation was defined as

$$B\eta \frac{\partial \eta}{\partial t} = \frac{\partial}{\partial x} \int_{\eta}^h UB dz - \int_{\eta}^h qB dz \quad (11)$$

Where

η is the water surface

From equation 8, any constituent may be substituted for U then the set of equations may be solved numerically. The source/sink term was fully described in the following sections for each constituent of concern. The reader is referred to the user manual of CE-QUAL-W2 for further reading.

CE-QUAL-W2 allows the user to specify which water quality constituents to model in the dam. The omission of any constituent could have a marked effect on the simulated output. The lack of data for certain water quality variables (for example inorganic suspended solids, refractory dissolved organic matter, labile particulate organic matter and labile dissolved organic matter) in the inflows (provided data) immediately limits the model in terms of calculating the external loading of these constituents. The following sections describe the water quality variables sources or sinks and their interaction as used by CE-QUAL-W2 as per user manual. The water quality interactions of the modelled constituents are described in the following sections as taken from Cole and Wells (2008).

3.4.2 Total dissolved solids

Total dissolved solids (TDS) affect water density and ionic strength, thereby affecting water movements, pH, and the distribution of carbonate species. Dissolved solids are normally expressed as TDS in freshwater applications. TDS and salinity as used by the model are not equivalent, salinity is conservative while TDS is not. In the model, however, both are treated conservatively with the rate term set to zero (Cole and Wells, 2008)

3.4.3 Generic constituents

Any number of generic constituents can be defined in the model such that they can settle and decay. The user supplies a zero and/or 1st order decay coefficient with or without an Arrhenius temperature dependence function, and/or a settling velocity. Generic constituents do not interact with the hydrodynamics nor any other water quality state variables as shown in Figure 13.

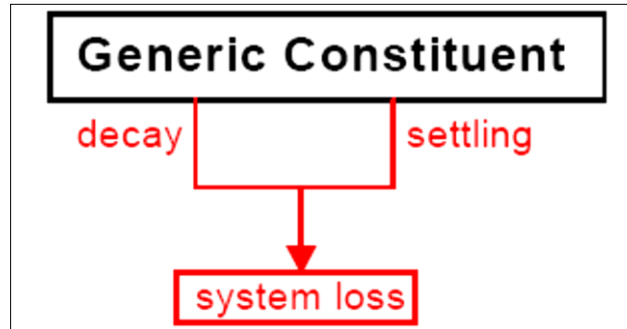


Figure 13 Internal fluxes of generic constituents

Adopted from Cole and Wells, 2008

The governing equation for the source or sink generic constituents is

$$S_g = -K_0 \theta_g^{(T-20)} - K_1 \theta_g^{(T-20)} \Phi_g - \omega_g \frac{\partial \Phi_g}{\partial z} \quad (12)$$

Where:

θ_g = temperature rate multiplier

T = water temperature, °C

ω_g = settling velocity, m s⁻¹

K_0 = zero order decay coefficient, g m⁻³ s⁻¹ at 20°C

K_1 = first order decay coefficient, s⁻¹ at 20°C

Φ_g = generic constituent concentration, g m⁻³

A conservative tracer was included in the model to allow dye study simulations, movements of conservative materials through the water-body, and as an aid in calibrating and testing flow regimes. As a conservative material, this constituent has no internal sources or sinks and the rate term was set to zero. It thus shows whether a source or sink has been omitted from the model (Cole and Wells, 2008).

3.4.4 Phosphates

For the purposes of CE-QUAL-W2 modelling phosphorus was assumed to be completely available as ortho-phosphate (PO₄) for uptake by phytoplankton. Measurements of soluble reactive phosphorus are closest to the form used in the model. The internal fluxes between phosphate and other water quality variables are shown in Figure 14 as used by the model.

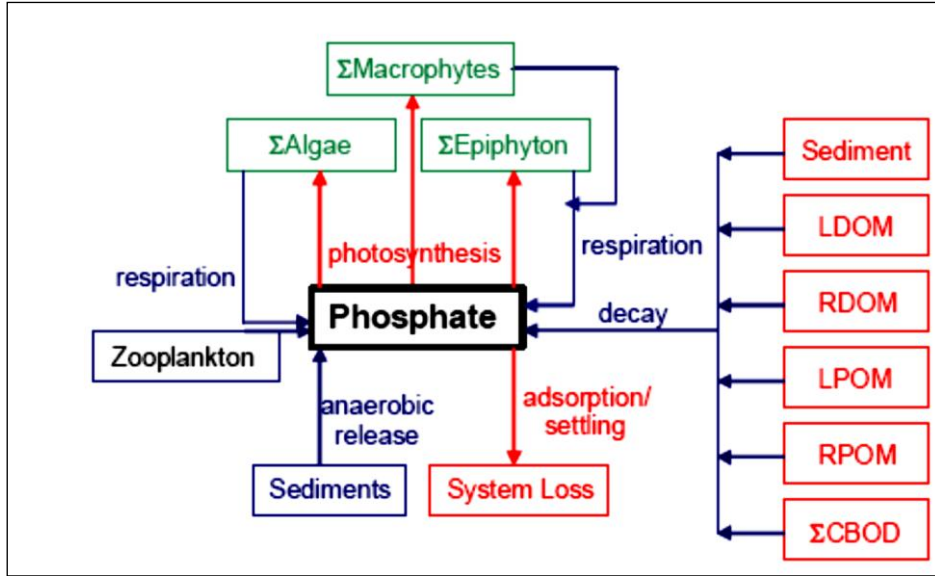


Figure 14 Internal fluxes of phosphorus

Adopted from Cole and Wells, 2008

The rate equation describing the phosphate source/sink is:

$$\begin{aligned}
 s_p = & \sum (K_{ar} - K_{ag}) \delta_p \Phi_a + \sum (K_{er} - K_{eg}) \delta_e \Phi_e + K_{ldom} \delta_p \gamma_{om} \Phi_{ldom} + K_{rdom} \delta_p \gamma_{om} \Phi_{rdom} + K_{lpom} \delta_p \gamma_{om} \Phi_{lpom} + \\
 & K_{pomp} \delta_p \gamma_{om} \Phi_{pomp} + K_s \delta_p \gamma_{om} \Phi_s + SOD \gamma_{om} \frac{A_s}{V_{cell}} + \sum K_{CBOD} R_{CBOD} \delta_{P-CBOD} \Theta^{T-20} \Phi_{CBOD} + K_s \delta_{POM} \gamma_{OM} \Phi_s + \\
 & SOD \gamma_{OM} \frac{A_{sed}}{V} - \frac{P_p (\sum \omega_{ss} \Phi_{ss} + \omega_{pom} \Phi_{poml} + \omega_{pom} \Phi_{pomp} + \omega_{FE} \Phi_{FE})}{\Delta Z} \Phi_p + \sum K_{zr} \delta_{Pz} \Phi_{zoo}
 \end{aligned} \tag{13}$$

Where,

- Δz = model cell thickness, m
- A_{sed} = sediment surface area, m^2
- V = cell volume, m^3
- P_p = adsorption coefficient, $m^3 g^{-1}$
- f_{psed} = fraction of macrophyte phosphorus uptake from sediments
- $\bar{\delta}_{Pe}$ = epiphyton stoichiometric coefficient for phosphorus
- $\bar{\delta}_{Pa}$ = algal stoichiometric coefficient for phosphorus
- $\bar{\delta}_{Pm}$ = macrophyte stoichiometric coefficient for phosphorus
- $\bar{\delta}_{Pz}$ = zooplankton stoichiometric coefficient for phosphorus
- $\bar{\delta}_{POM}$ = organic matter stoichiometric coefficient for phosphorus
- $\bar{\delta}_{P-CBOD}$ = phosphorus/CBOD stoichiometric ratio
- γ_{OM} = temperature rate multiplier for organic matter decay
- Θ = temperature rate multiplier for CBOD decay
- R_{BOD} = conversion ratio for 5-day CBOD to CBOD ultimate
- ω_{ISS} = inorganic suspended solids settling velocity, m/sec
- ω_{Fe} = particulate organic matter settling velocity, $/sec$
- K_{ag} = algal growth rate, $/sec$
- K_{ar} = algal dark respiration rate, $/sec$

- K_{eg} = epiphyton growth rate, /sec
 K_{er} = epiphyton dark respiration rate, /sec
 K_{mg} = macrophyte growth rate, /sec
 K_{mr} = macrophyte respiration rate, /sec
 K_{zr} = macrophyte respiration rate, /sec
 K_{LDOM} = labile DOM decay rate, /sec
 K_{RDOM} = refractory DOM decay rate, /sec
 K_{LPOM} = labile POM decay rate, /sec
 K_{RPOM} = refractory POM decay rate, /sec
 K_{CBOD} = CBOD decay rate, /sec
 K_{sed} = sediment decay rate, /sec
 SOD = anaerobic sediment release rate, $g/m^2/s$
 Φ_P = phosphorus concentration, g/m^3
 Φ_{Fe} = total iron concentration, $g m^{-3}$
 Φ_{ISS} = inorganic suspended solids concentration, $g m^{-3}$
 Φ_a = algal concentration, $g m^{-3}$
 Φ_e = epiphyton concentration, $g m^{-3}$
 Φ_{LDOM} = labile DOM concentration, $g m^{-3}$
 Φ_{LPOM} = labile POM concentration, $g m^{-3}$
 Φ_{RDOM} = refractory DOM concentration, $g m^{-3}$
 Φ_{RPOM} = refractory POM concentration, $g m^{-3}$
 Φ_{CBOD} = CBOD concentration, $g m^{-3}$
 Φ_{sed} = organic sediment concentration, $g m^{-3}$
 Φ_{macro} = macrophyte concentration, $g m^{-3}$
 Φ_{zoo} = zooplankton concentration, $g m^{-3}$

The contribution of algae to the phosphate rate shown in Term 1 of the rate equation 13, K_{ar} (algal respiration) was much smaller than the algal growth rate K_{ag} thus the net effect was the disappearance of phosphates. The contribution of Particulate Organic Matter (POM) and Dissolved Organic Matter (DOM) to phosphates is shown in terms 2 to 5. Organic sediments are accumulated when algae die and settle. Phosphates from these sediments can be released by either a first order or zero order decay rates. These contributions are indicated by terms 6 and 7, respectively.

Phosphates that are adsorbed onto Inorganic Suspended Solids (ISS) and on to Iron (Fe) settle out at the same rate as the particles to which it was attached and was permanently removed from the water column. Phosphates can also be temporarily removed from the water column by adsorbing onto POM – when decay of this material occurs, the phosphates are released back into the water column.

In this study, measured data no ISS or Fe was modelled, implying that phosphates could not be removed from the water column but adhered onto the suspended sediments as $FePO_4$ compounds.

3.4.5 Nitrate-Nitrite

Nitrite is an intermediate product in nitrification between ammonium and nitrate. Nitrate is used as a source of nitrogen for algae and epiphyton during photosynthesis. Preferential uptake of ammonium over nitrate by algae and periphyton is included. The interactions between NO_2+NO_3 and other water quality constituents are shown in Figure 15.

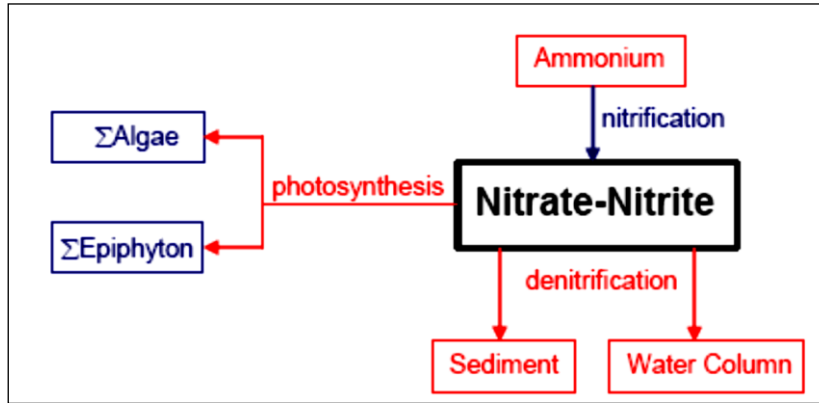


Figure 15 Internal flux of nitrate/nitrite

Adopted from Cole and Wells, 2008

The rate equation describing the NO_2+NO_3 source/sink concentration is:

$$S_{NOx} = K_{NH4} \gamma_{NH4} \Phi_{NH4} - K_{NOx} \gamma_{NOx} \Phi_{NOx} - \omega_{NOx} \frac{\partial \Phi_{NOx}}{\partial Z} - \sum K_{ag} \delta_{Na} \Phi_a (1 - P_{NH4}) - \sum K_{eg} \delta_{Ne} \Phi_e (1 - P_{NH4}) \quad (14)$$

Where

- γ_{NH4} = temperature rate multiplier for nitrification
- γ_{NOx} = temperature rate multiplier for denitrification
- δ_{Ne} = epiphyton stoichiometric coefficient for nitrogen
- δ_{Na} = algal stoichiometric coefficient for nitrogen
- P_{NH4} = ammonium preference factor
- K_{NH4} = nitrification rate, sec^{-1}
- K_{NOx} = denitrification rate, sec^{-1}
- K_{ag} = algal growth rate, sec^{-1}
- ω_{NOx} = sediment transfer velocity, $m \text{ sec}^{-1}$
- Φ_{NH4} = ammonia-nitrogen concentration, $g \text{ m}^{-3}$
- Φ_{NOx} = nitrate-nitrogen concentration, $g \text{ m}^{-3}$
- Φ_a = algal concentration, $g \text{ m}^{-3}$

Nitrification is only allowed to occur if oxygen was present, and denitrification was allowed only if dissolved oxygen is less than a model specified minimum value [O2LIM] of 0.1 mg/l. In the model, the nitrate+nitrite concentration was in units of $\text{NO}_3 + \text{NO}_2$ as N (Cole and Wells, 2008).

3.4.6 Ammonium

Algae use ammonium during photosynthesis to form proteins. The interaction between ammonium and other water quality constituents is shown in Figure 16.

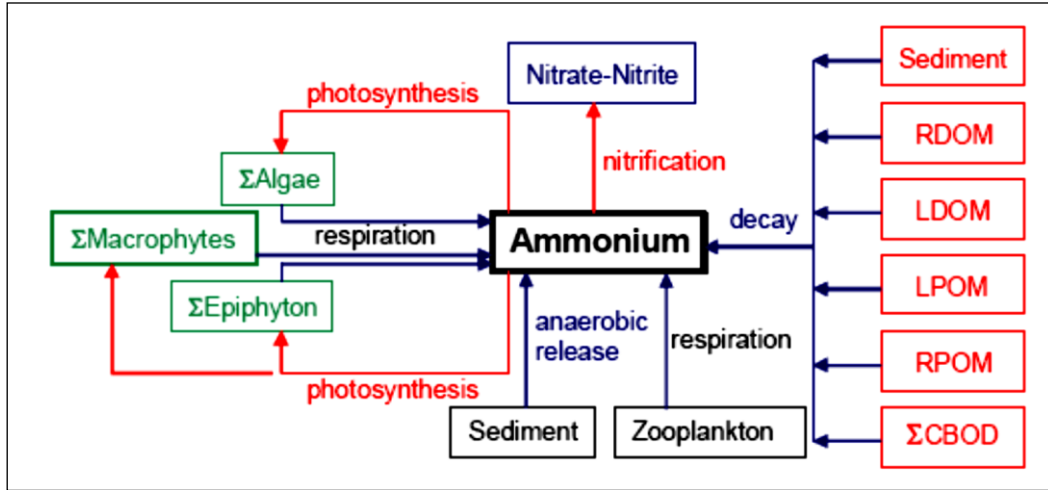


Figure 16 Internal fluxes of ammonium

Adopted from Cole and Wells, 2008

The rate equation describing the ammonium source/sink concentration is:

$$\begin{aligned}
 S_p = & \sum K_{ar} \delta_{Na} \Phi_a - \sum K_{ag} \delta_{Na} \Phi_a P_{NH_4} + \sum K_{er} \delta_{Ne} \Phi_e - \sum K_{eg} \delta_{Ne} \Phi_e P_{NH_4} + K_{ldom} \delta_{Nom} \gamma_{om} \Phi_{ldom} \\
 & + K_{LDOM} \delta_{NOM} \gamma_{OM} \Phi_{LDOM} + K_{RDOM} \delta_{NOM} \gamma_{OM} \Phi_{RDOM} + K_{LPOM} \delta_{NOM} \gamma_{om} \Phi_{LPOM} + \\
 & K_{RPOM} \delta_{NOM} \gamma_{om} \Phi_{RPOM} + K_s \delta_N \gamma_{om} \Phi_s + SOD_{NH_4} \gamma_{om} \frac{A_s}{V} + \sum K_{CBOD} R_{CBOD} \delta_{N-CBOD} \Theta^{T-20} + \\
 & K_{NOx} \gamma_{NOx} \Phi_{NOx} - K_{NH_4} \gamma_{NH_4} \Phi_{NH_4} + \sum K_{zr} \delta_{Nz} \Phi_{zoo}
 \end{aligned} \tag{15}$$

Where

A_{sed} = sediment area, m^2

V = volume of cell, m^3

f_{nsed} = fraction of macrophyte nitrogen uptake from sediments

δ_{Na} = algal stoichiometric coefficient for nitrogen

δ_{Ne} = epiphyton stoichiometric coefficient for nitrogen

δ_{Nm} = macrophyte stoichiometric coefficient for nitrogen

δ_{Nz} = zooplankton stoichiometric coefficient for nitrogen

δ_{NOM} = organic matter stoichiometric coefficient for nitrogen

δ_{N-CBOD} = CBOD stoichiometric coefficient for nitrogen

γ_{NH_4} = temperature rate multiplier for nitrification

γ_{NOx} = temperature rate multiplier for denitrification

γ_{OM} = temperature rate multiplier for organic matter decay

Θ = temperature rate multiplier for CBOD decay

$RCBOD$ = ratio of 5-day CBOD to ultimate CBOD

- P_{NH_4} = ammonium preference factor
 K_{NO_x} = nitrate-nitrogen decay rate, sec^{-1}
 K_{NH_4} = ammonium decay rate, sec^{-1}
 K_{ar} = algal dark respiration rate, sec^{-1}
 K_{ag} = algal growth rate, sec^{-1}
 K_{mg} = macrophyte growth rate, sec^{-1}
 K_{mr} = macrophyte respiration rate, sec^{-1}
 K_{zr} = zooplankton respiration rate, sec^{-1}
 K_{LDOM} = labile DOM decay rate, sec^{-1}
 K_{RDOM} = refractory DOM decay rate, sec^{-1}
 K_{LPOM} = labile POM decay rate, sec^{-1}
 K_{RPOM} = refractory POM decay rate, sec^{-1}
 K_{CBOD} = CBOD decay rate, sec^{-1}
 K_{sed} = sediment decay rate, sec^{-1}
 SOD_{NH_4} = sediment ammonium release rate, $g\ m^{-2}\ sec^{-1}$
 Φ_{ISS} = inorganic suspended solids concentration, $g\ m^{-3}$
 Φ_{NH_4} = ammonium concentration, $g\ m^{-3}$
 Φ_{NO_x} = nitrate-nitrogen concentration, $g\ m^{-3}$
 Φ_a = algal concentration, $g\ m^{-3}$
 Φ_{LDOM} = labile DOM concentration, $g\ m^{-3}$
 Φ_{RDOM} = refractory DOM concentration, $g\ m^{-3}$
 Φ_{LPOM} = labile POM concentration, $g\ m^{-3}$
 Φ_{RPOM} = refractory POM concentration, $g\ m^{-3}$
 Φ_{CBOD} = CBOD concentration, $g\ m^{-3}$
 Φ_{macro} = macrophyte concentration, $g\ m^{-3}$
 Φ_{zoo} = zooplankton concentration, $g\ m^{-3}$
 Φ_{sed} = organic sediment concentration, $g\ m^{-3}$

As with phosphorus, 0-order sediment release only occurs when dissolved oxygen is less than 0.1 mg/l. Either a 0 or 1st-order process or a combination of both may be used for sediment ammonium release. In the model, the ammonia concentration is in units of NH_4 as N (Cole and Wells, 2008).

3.4.7 Dissolved Silica

Dissolved silica is an important component of diatoms, providing the structural skeleton. In many cases, diatoms can be silica limited. Dissolved silica is taken up by algae based on stoichiometric relationships and is produced by the decay of organic matter containing particulate biogenic silica. In addition, dissolved silica is adsorbed onto inorganic suspended solids based on a partitioning coefficient. The interaction between dissolved silica and other water quality constituents is shown in Figure 17.

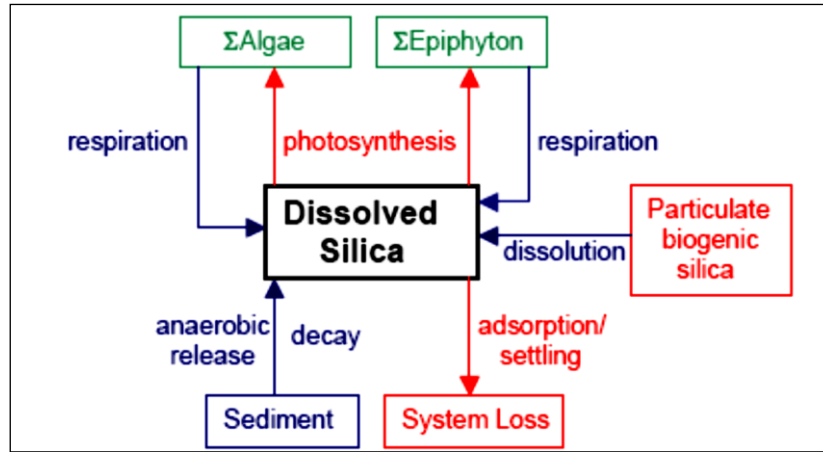


Figure 17 Internal fluxes of dissolved Silica

Adopted from Cole and Wells, 2008

The rate equation describing the dissolved silica source/sink concentration is:

$$\begin{aligned}
 S_{DSi} = & -\sum (K_{ag} - K_{ar}) \delta_{Si} \Phi_a - \sum (K_{eg} - K_{er}) \delta_{Si} \Phi_e \\
 & + K_{sed} \delta_{SiOM} \gamma_{om} \Phi_{sed} + K_{Psi} \gamma_{om} \Phi_{PSi} + SOD \phi_{Si} \gamma_{om} \frac{A_s}{V_{cell}} \\
 & - \frac{P_{Si} (\sum \omega_{ss} \Phi_{ss} + \omega_{POM} \Phi_{POML} + \omega_{POM} \Phi_{POMR} + \omega_{Fe} \Phi_{Fe})}{\Delta Z} \Phi_{DSi}
 \end{aligned}$$

(16)

Where,

- ϕ_{Si} = fraction of SOD for silica release
- Δz = computational cell height, m
- $\bar{\delta}_{Sie}$ = epiphyton stoichiometric ratio for silica
- $\bar{\delta}_{Sia}$ = algal stoichiometric ratio for silica
- $\bar{\delta}_{SiOM}$ = sediment organic matter stoichiometric ratio for silica
- A_{sed} = sediment area, m^2
- V = computational cell volume, m^3
- P_{Si} = silica adsorption coefficient, $m^3 g^{-1}$
- SOD = sediment oxygen demand, $g m^{-2} sec^{-1}$
- ω_{ISS} = inorganic suspended solids settling velocity, $m sec^{-1}$
- K_{ag} = algal growth rate, sec^{-1}
- K_{eg} = epiphyton growth rate, sec^{-1}
- K_{sed} = sediment decay rate, sec^{-1}
- Φ_a = algal concentration, $g m^{-3}$
- Φ_e = epiphyton concentration, $g m^{-3}$
- Φ_{sed} = organic sediment mass, g
- Φ_{ISS} = inorganic suspended solids concentration, $g m^{-3}$
- Φ_{DSi} = dissolved silica concentration, $g m^{-3}$
- Φ_{Fe} = total iron concentration, $g m^{-3}$ (Cole and Wells, 2008)

No inorganic suspended solids or iron (Fe) was modelled in the simulations due to lack of data and therefore silica could not be consumed via this mechanism and this effect could not be quantified.

3.4.8 Particulate silica

Particulate biogenic silica results from diatom mortality. It settles and also dissolves to form dissolved silica. The interaction between particulate silica and other water quality constituents is shown in Figure 18.

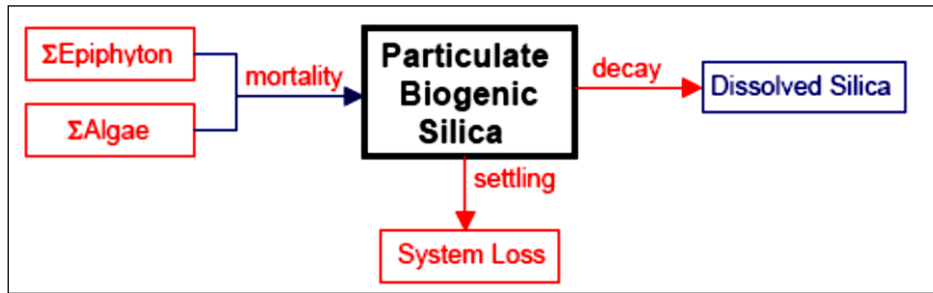


Figure 18 Internal fluxes of particulate Silica

Adopted from Cole and Wells, 2008

The rate equation describing the particulate silica concentration source/sink is:

$$S_{SiP} = P_{am} \delta_{Sia} K_{am} \Phi_a + P_{em} \delta_{Sie} K_{em} \Phi_e - K_{SiP} \gamma_{om} \Phi_{SiP} - \frac{\omega_{SiP} \partial \Phi_{SiP}}{\partial Z} \quad (17)$$

Where,

P_{am} = partition coefficient for algal mortality

δ_{Sie} = epiphyton stoichiometric coefficient for silica

δ_{Sia} = algal stoichiometric coefficient for silica

γ_{OM} = temperature rate multiplier for organic matter

P_{em} = partition coefficient for epiphyton mortality

K_{am} = algal mortality rate, sec^{-1}

K_{em} = epiphyton mortality rate, sec^{-1}

K_{PSi} = particulate biogenic silica decay rate, sec^{-1}

ω_{PSi} = particulate biogenic silica settling rate, $m sec^{-1}$

Φ_e = epiphyton concentration, $g m^{-3}$

Φ_a = algal concentration, $g m^{-3}$

Φ_{PSi} = particulate biogenic silica concentration, $g m^{-3}$ (Cole and Wells, 2009)

3.4.9 Total Algae

Typically, the algal community was represented as a single assemblage or was broken down into diatoms, greens, and cyanobacteria (blue-greens). However, the current version allows for any number of algal groups for simulations through careful specification of the kinetic rate parameters that define the characteristics of each algal group. The internal fluxes between algae with other water quality variables are shown in Figure 19.

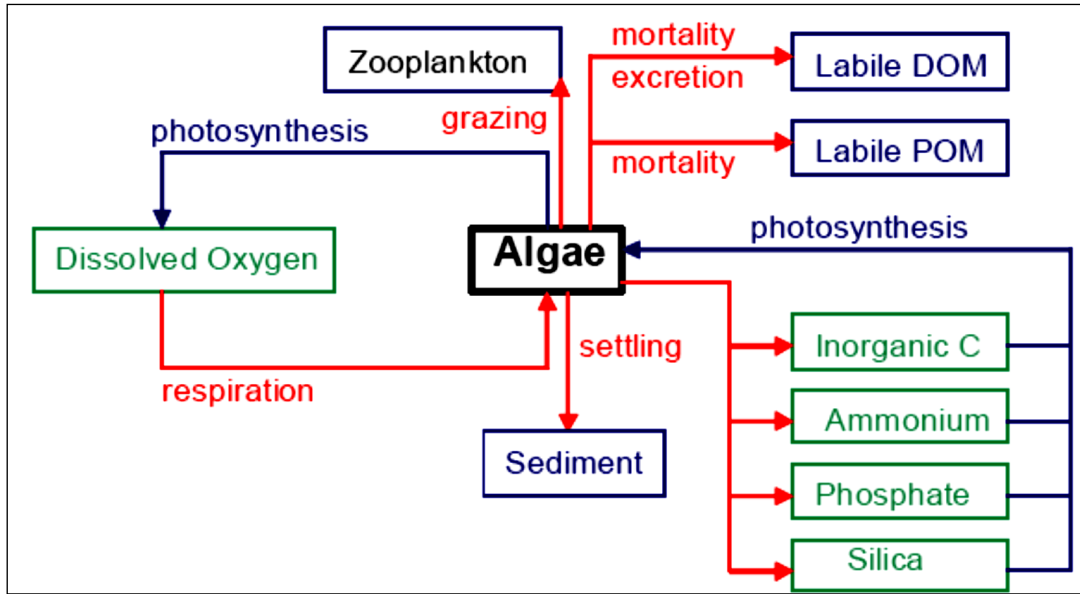


Figure 19 Internal flux of algae

Adopted from Cole and Wells, 2008

It is immediately evident that the modelling of algae demands the inclusion of all related water quality variables. The rate equation for the interaction of algae is,

$$S_{alg} = K_{ag} \Phi_a - K_{ar} \Phi_a - K_{ae} \Phi_a - K_{am} \Phi_a - \frac{\omega_a \partial \Phi_a}{\partial Z} - \sum \left(Z_{\mu} \Phi_{zoo} \frac{\sigma_{alg} \Phi_a}{\sum \sigma_{alg} \Phi_a + \sigma_{pom} \Phi_a + \sum \sigma_{zoo} \Phi_a} \right) \quad (18)$$

Where:

z = cell height

Z_{μ} = net growth rate of a zooplankton species

σ = zooplankton grazing preference factors for various algae types

K_{ag} = algal growth rate, sec^{-1}

K_{ar} = algal dark respiration rate, sec^{-1}

K_{ae} = algal excretion rate, sec^{-1}

K_{am} = algal mortality rate, sec^{-1}

ω_a = algal settling rate, $m sec^{-1}$

Φ_a = algal concentration, $g m^{-3}$

Algal growth rates are computed at each iteration by modifying the maximum growth rate as affected by temperature, light and nutrient availability:

$$K_{ag} = Y_{ar} Y_{af} \lambda_{min} K_{agmax} \quad (19)$$

Where:

Y_{ar} = temperature rate multiplier for rising limb of growth curve

Y_{af} = temperature rate multiplier for falling limb of growth curve

λ_{min} = multiplier for limiting growth factor (it was the minimum of either light, phosphorus, silica or nitrogen calculated at each iteration)

K_{ag} = algal growth rate, sec^{-1}
 K_{agmax} = maximum algal growth rate, sec^{-1}

Thus for each iteration the algal growth rate was a factor of the maximum possible algal growth rate. Rate multipliers (such as γ_{ar} and γ_{af}) for algal growth are computed internally based upon available light, phosphorus, nitrogen and silica. The rate multiplier for light was based upon the Steele function:

$$\lambda_l = \frac{I}{I_s} e^{\left(-\frac{I}{I_s} + 1\right)} \quad (20)$$

Where:

I = available light, $W m^{-2}$
 I_s = saturating light intensity at maximum photosynthetic rate, $W m^{-2}$
 λ_l = light limiting factor

Thus, the expression allows for simulation of photo-inhibition at light intensities greater than the saturation value. However, light penetration decreases with depth:

$$I = (1 - \beta)I_0 e^{-\alpha z} \quad (21)$$

Where:

I_0 = solar radiation at the water surface, $W m^{-2}$
 α = attenuation coefficient which was affected by scattering and turbidity, m^{-2}
 z = depth, m
 β = fraction of solar radiation absorbed at the water surface

The average effect of light on algal growth in a cell was obtained by combining the above two expressions and integrating over the cell depth to obtain

$$\lambda_l = \frac{e}{\alpha \Delta Z} (e^{-\gamma_2} - e^{-\gamma_1}) \quad (22)$$

and

$$\gamma_1 = \frac{(1 - \beta)I_0}{I_s} e^{-\alpha d} \quad (23)$$

$$\gamma_2 = \frac{(1 - \beta)I_0}{I_s} e^{-\alpha(d + \Delta z)} \quad (24)$$

With d = depth at top of model cell,

The fraction of solar radiation, β_{10} , is added directly to the surface layer. The attenuation coefficient, α , consists of a baseline value [EXH2O] to which the effects of inorganic [EXINOR] and organic [EXORG] suspended solids, and algae [EXA] are added.

Rate multipliers limiting maximum algal growth due to nutrient limitations are computed using the Monod relationship:

$$\lambda_1 = \frac{\Phi_i}{P_i + \Phi_i} \quad (25)$$

Where:

Φ_i = phosphorus or nitrate + ammonium concentration, $g\ m^{-3}$

P_i = half-saturation coefficient for phosphorus or nitrate + ammonium, $g\ m^{-3}$

The algal nitrogen preference for ammonium is based upon the following (Cole and Wells, 2008).

$$P_{NH_4} = \Phi_{NH_4} \frac{\Phi_{NOx}}{(K_{NH_4} + \Phi_{NH_4})(K_{NH_4} + \Phi_{NOx})} + \Phi_{NH_4} \frac{\Phi_{NOx}}{(\Phi_{NH_4} + \Phi_{NOx})(K_{NH_4} + \Phi_{NOx})} \quad (26)$$

Where:

P_{NH_4} = ammonium preference factor

K_{NH_4} = ammonia preference half-saturation coefficient, $g\ m^{-3}$

Φ_{NH_4} = ammonium concentration, $g\ m^{-3}$

Φ_{NOx} = nitrate-nitrite concentration, $g\ m^{-3}$

This preference allows algae to use primarily ammonium and gradually switch to nitrate as ammonium concentrations decrease. Algal dark respiration is computed using the rising limb of the temperature function:

$$K_{ar} = \gamma_{ar}\gamma_{af} K_{armax} \quad (27)$$

Where:

γ_{ar} = temperature rate multiplier for rising limb of curve

γ_{af} = temperature rate multiplier for falling limb of curve

K_{armax} = maximum dark respiration rate, sec^{-1}

Algal photorespiration (excretion) is evaluated using an inverse relation to the light rate multiplier:

$$K_{ae} = (1 - \lambda_l) \gamma_{ar}\gamma_{af} K_{aemax} \quad (28)$$

Where:

γ_{ar} = temperature rate multiplier for rising limb of curve

γ_{af} = temperature rate multiplier for falling limb of curve

K_{aemax} = maximum excretion rate constant, sec^{-1}

λ_l = light limiting factor

Excretion rates increase at both low and high light intensities, with excretion products contributing to labile DOM.

Algal mortality was defined as:

$$K_{am} = \gamma_{ar}\gamma_{af} K_{amax} \quad (29)$$

Where:

γ_{ar} = temperature rate multiplier for rising limb of curve

γ_{af} = temperature rate multiplier for falling limb of curve

K_{amax} = maximum mortality rate, sec^{-1}

This mortality rate represents both natural and predator mortality. Algal growth does not occur in the absence of light. Algal growth is not allowed to exceed the limit imposed by nutrient supply over a given timestep. Algal excretion is not allowed to exceed algal growth rates. Similar to inorganic solids, settling algae serve as a source for the layer below. Unlike inorganic solids, algae passing to the sediments accumulate within the sediment compartment. POM is also accumulated in this sediment compartment.

3.4.10 Zooplankton

A multiple zooplankton compartment was adapted from the U.S. Army Corps of Engineers reservoir model CE-QUAL-R1 for the CE-QUAL-W2 model. Zooplankton are assumed to be non-motile and are transported only by advection and dispersion. Zooplankton can graze algae, detritus (POM), and other zooplankton. Losses occur through mortality and respiration as well as sources/sinks as shown in Figure 20.

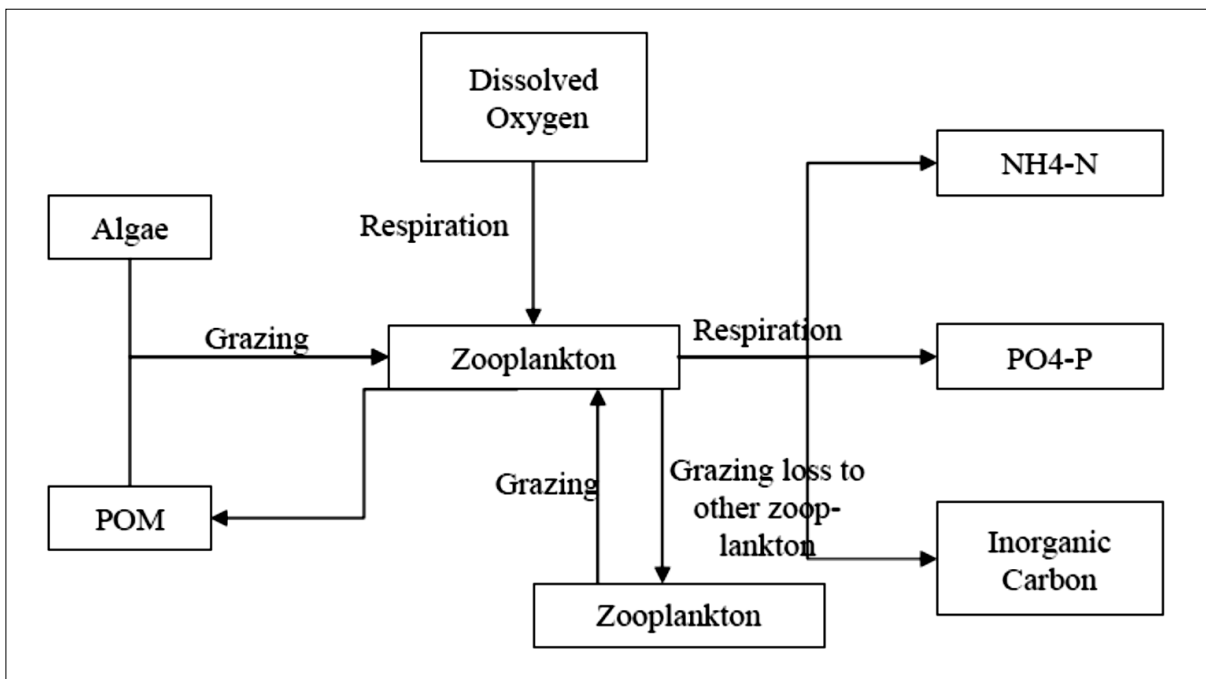


Figure 20 Fluxes that affect zooplankton

Adopted from Cole and Wells, 2008

The growth rate was a function of temperature, the maximum growth rate and a modified Michaelis-Menten equation, which included a low threshold concentration below which zooplankton, did not feed. At dissolved oxygen concentrations below 2 mg/l, feeding stops and the mortality rate was doubled (Cole and Wells, 2008). The source/sink term for zooplankton is:

$$S_{zoo} = \gamma_1 \gamma_2 Z_e K_{z \max} \left(\frac{\left(\sum \sigma_{alg} \Phi_a + \sigma_{pom} \Phi_{lpom} + \sigma_{zoo} \Phi_{zoo} \right) - z_L}{\left(\sum \sigma_{alg} \Phi_a + \sigma_{pom} \Phi_{lpom} + \sigma_{zoo} \Phi_{zoo} \right) + z_{\frac{1}{2}}} \right) \Phi_{zoo} - (1 - \gamma_2) K_{zm} \Phi_{zoo} - \gamma_1 K_{zr} \Phi_{zoo} \quad (30)$$

Where

Φ_{lpom} = Labile particulate organic matter concentration (mg/l)

- Φ_{pom} = Refractory particulate organic matter concentration (mg/l)
- Φ_{a} = Algae concentration (mg/l)
- Φ_{zoo} = Zooplankton concentration (mg/l)
- K_{zm} = Zooplankton mortality rate (d^{-1})
- K_{zmax} = Maximum ingestion rate for zooplankton (d^{-1})
- K_{zr} = Zooplankton respiration rate (d^{-1})
- $Z_{1/2}$ = Half-saturation coefficient for zooplankton ingestion (mg/l)
- Z_{e} = Zooplankton ingestion efficiency
- Z_{L} = Low threshold concentration for zooplankton feeding (mg/l)
- γ_1 = Temperature coefficient for rising limb of curve for zooplankton
- γ_2 = Temperature coefficient for falling limb of curve for zooplankton
- σ_{alg} = Zooplankton preference fraction for algae
- σ_{zoo} = Zooplankton preference fraction for zooplankton
- σ_{pom} = Zooplankton preference fraction for particulate organic matter

3.4.11 Dissolved oxygen

Oxygen is one of the most important elements in aquatic ecosystems. It is essential for higher forms of life, controls many chemical reactions through oxidation, and is a surrogate variable indicating the general health of aquatic systems. CE-QUAL-W2 includes the aerobic and anaerobic processes.

The ability to model anaerobic periods was important since it provides information on potential problems with water quality. Simulations can be used to identify possibilities for both metalimnetic and hypolimnetic oxygen depletion and its impact on various water control management alternatives. If a single variable were to be measured in aquatic systems that would provide maximum information about the system state, it would be dissolved oxygen (Cole and Wells, 2008). The interactions between dissolved oxygen and other water quality constituents are shown in Figure 21.

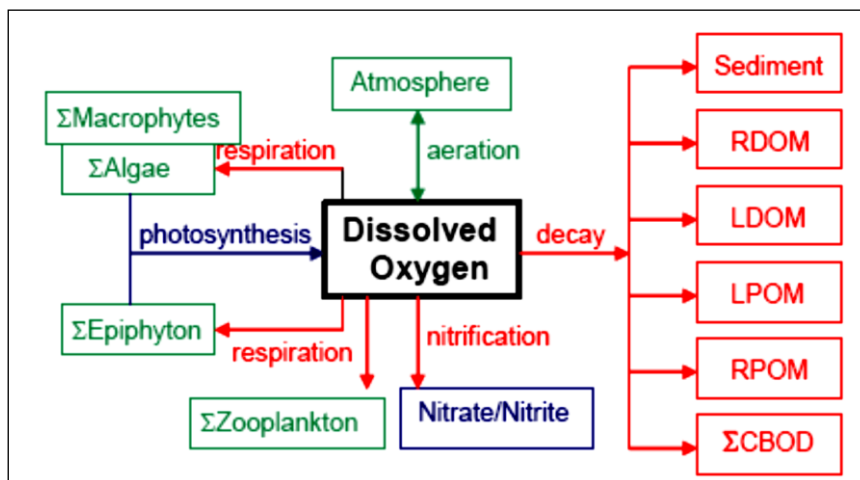


Figure 21 Internal flux of dissolved oxygen

Adopted from Cole and Wells, 2008

The rate equation describing the oxygen concentration is shown in the following equation:

$$\begin{aligned}
S_{DO} = & \sum (K_{ag} - K_{ar}) \delta_{om} \Phi_a + \sum (K_{eg} - K_{er}) \delta_{om} \Phi_e + A_{kt} K_L (\Phi'_{DO} - \Phi_{DO}) \\
& - K_{POMR} \delta_{om} \gamma_{om} \Phi_{POMR} - K_{POML} \delta_{om} \gamma_{om} \Phi_{POML} - K_{LDOM} \delta_{om} \gamma_{om} \Phi_{POML} \\
& - K_{rdom} \delta_{om} \gamma_{om} \Phi_{rdom} - K_s \delta_{om} \gamma_{om} \Phi_s - SOD \gamma_{om} \frac{A_s}{V_{cell}} \\
& - \sum K_{CBOD} R_{CBOD} \Theta^{T-20} \Phi_{CBOD} - K_{NH4} \delta_{NH4} \gamma_{NH4} \Phi_{NH4} + \sum (K_{mg} - K_{mr}) \delta_{ommac} \Phi_{macro} \\
& - \sum K_{zoo} \gamma_{zoo} \delta_{omzoo} \Phi_{zoo}
\end{aligned} \tag{31}$$

Where,

- $\bar{\delta}_{OMa}$ = oxygen stoichiometric coefficient for algal organic matter
- $\bar{\delta}_{OMe}$ = oxygen stoichiometric coefficient for epiphyton organic matter
- $\bar{\delta}_{OMmac}$ = oxygen stoichiometric coefficient for macrophyte organic matter
- $\bar{\delta}_{OM}$ = oxygen stoichiometric coefficient for organic matter
- $\bar{\delta}_{NH4}$ = oxygen stoichiometric coefficient for nitrification
- $\bar{\delta}_{OMzoo}$ = oxygen stoichiometric coefficient for zooplankton
- γ_{NH4} = temperature rate multiplier for nitrification
- γ_{OM} = temperature rate multiplier for organic matter decay
- γ_{zoo} = temperature rate multiplier for zooplankton
- $RBOD$ = conversion from CBOD in the model to CBOD ultimate
- Θ = BOD temperature rate multiplier
- V = volume of computational cell, m^3
- T = temperature, $^{\circ}C$
- A_{sed} = sediment surface area, m^2
- A_{sur} = water surface area, m^2
- K_{ag} = algal growth rate, sec^{-1}
- K_{ar} = algal dark respiration rate, sec^{-1}
- K_{eg} = epiphyton growth rate, sec^{-1}
- K_{er} = epiphyton dark respiration rate, sec^{-1}
- K_{mg} = macrophyte growth rate, sec^{-1}
- K_{mr} = macrophyte dark respiration rate, sec^{-1}
- K_{zr} = zooplankton respiration rate, sec^{-1}
- K_{NH4} = ammonia decay (nitrification) rate, sec^{-1}
- K_{LDOM} = labile DOM decay rate, sec^{-1}
- K_{RDOM} = refractory DOM decay rate, sec^{-1}
- K_{LPOM} = labile POM decay rate, sec^{-1}
- K_{RPOM} = refractory POM decay rate, sec^{-1}
- K_{BOD} = CBOD decay rate, sec^{-1}

For this study no epiphytons, macrophytes and CBOD groups were modelled. No information was available on the Carbonaceous Biological Oxygen Demand (CBOD) concentration and it was subsequently omitted from the oxygen concentration equation.

3.4.12 Labile Particulate Organic Matter (LPOM)

Labile particulate organic matter (LPOM) represents particulate organic material in the water column. When decaying, particulate organic matter is a source of refractory particulate organic matter, nitrogen, phosphorus, and inorganic carbon. A stoichiometric relationship is used for mineralization of ammonium, phosphorus, inorganic carbon and an oxygen demand was exerted as LPOM decomposes. When LPOM settles to the bottom, it accumulates and decays in the sediment compartment if the first order sediment compartment is included in the simulation. The interactions between LPOM and other water quality constituents are shown in Figure 22.

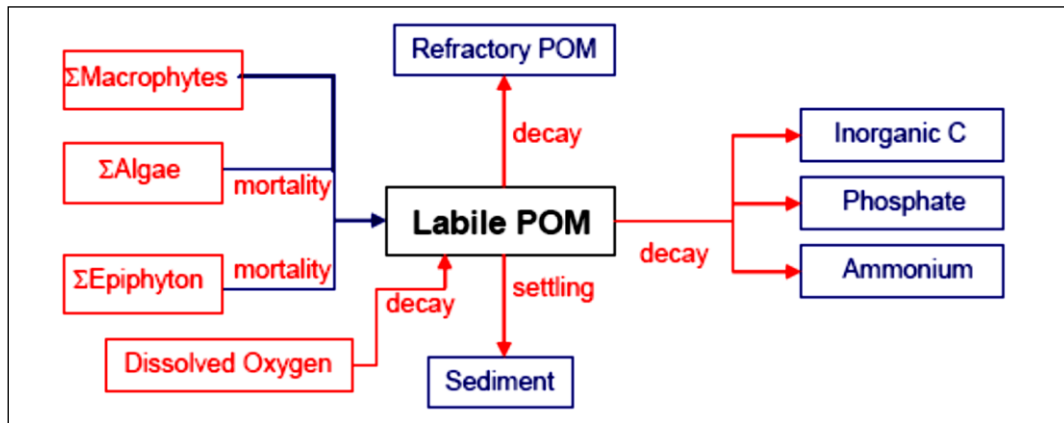


Figure 22 Internal flux of LPOM

Adopted from Cole and Wells, 2008

The rate equation describing the source/sink Labile POM concentration is.

$$\begin{aligned}
 S_{LPOM} = & \sum P_{am} K_{am} \Phi_a + \sum P_{em} K_{em} \Phi_e - K_{lpom} \gamma_{om} \Phi_{ldom} \\
 & - K_{l-r} \Phi_{lpom} - \omega_{pom} \frac{\partial \Phi_{lpom}}{\partial z} + \sum P_{mm} K_{mm} \Phi_{macro}
 \end{aligned} \tag{32}$$

Where,

- P_{am} = partition coefficient for algal mortality
- P_{em} = partition coefficient for epiphyton mortality
- P_{mm} = partition coefficient for macrophyte mortality
- γ_{OM} = temperature rate multiplier for organic matter
- ω_{POM} = POM settling rate, $m \text{ sec}^{-1}$
- K_{am} = algal mortality rate, sec^{-1}
- K_{em} = epiphyton mortality rate, sec^{-1}
- K_{mm} = macrophyte mortality rate, sec^{-1}
- K_{LPOM} = labile POM decay rate, sec^{-1}
- $K_{L \rightarrow R}$ = transfer rate from labile POM to refractory POM, sec^{-1}
- Φ_a = algal concentration, $g \text{ m}^{-3}$
- Φ_e = epiphyton concentration, $g \text{ m}^{-3}$
- Φ_{macro} = marophyte concentration, $g \text{ m}^{-3}$
- Φ_{LPOM} = detritus concentration, $g \text{ m}^{-3}$

POM settling and accumulation in the sediment compartment was handled identically to the algal compartment.

3.4.13 Refractory Particulate Organic Matter (RPOM)

Refractory POM is slowly decaying non-living, organic matter that settles. The source/sink terms are first order decay, the conversion of LPOM to RPOM and sedimentation: The interaction between RPOM and other water quality constituents is depicted in Figure 23.

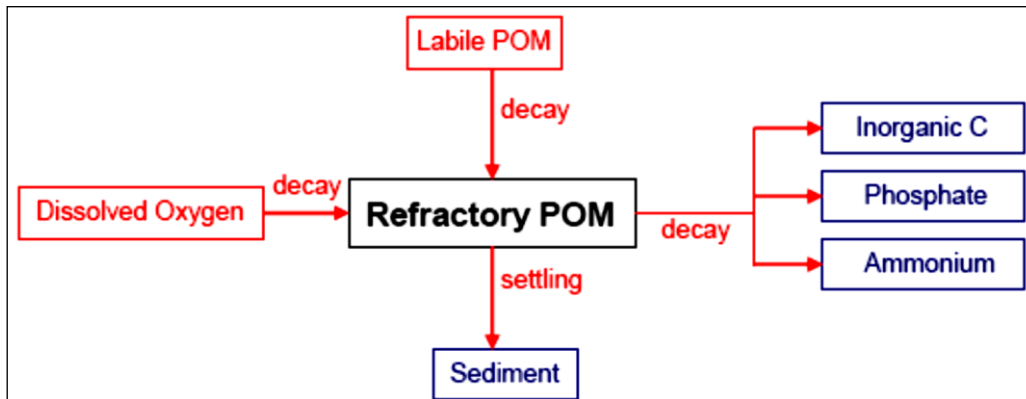


Figure 23 Internal fluxes of RPOM

Adopted from Cole and Wells, 2008

The rate equation describing the concentration of refractory POM is:

$$S_{RPOM} = K_{l-r} \Phi_{lpom} - \gamma_{om} K_{rpom} \Phi_{rpom} - \omega_{pom} \frac{\partial \Phi_{lpom}}{\partial z} \quad (33)$$

Where

γ_{OM} = temperature rate multiplier

$K_{L \rightarrow R}$ = transfer rate from labile POM to refractory POM, sec^{-1}

K_{RPOM} = refractory POM decay rate, sec^{-1}

ω_{POM} = POM settling velocity, m/sec

Φ_{LPOM} = labile POM concentration, $g\ m^{-3}$

Φ_{RPOM} = refractory POM concentration, $g\ m^{-3}$

3.4.14 Labile Dissolved Organic Matter (LDOM)

Because of the importance of dissolved oxygen in aquatic systems, all constituents exerting an oxygen demand must be included in kinetic formulations. This demand is the biochemical oxygen demand (BOD), which includes microbial respiration and metabolism of organic and inorganic compounds. However, production of these materials occurs as well as decomposition, requiring the major components of BOD be modelled individually. One of these constituents was dissolved organic matter (DOM), which is composed of labile and refractory components. DOM is modelled as two separate compartments because of the different decomposition rates of the two groups. The interaction between LDOM and other water quality constituents is shown in Figure 24.

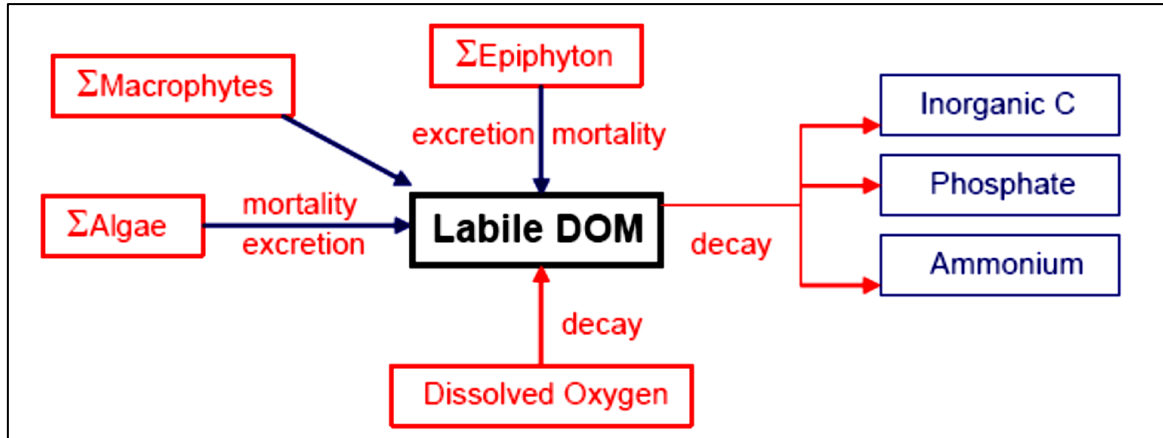


Figure 24 Internal fluxes of LDOM

Adopted from Cole and Wells, 2008

The governing equation is:

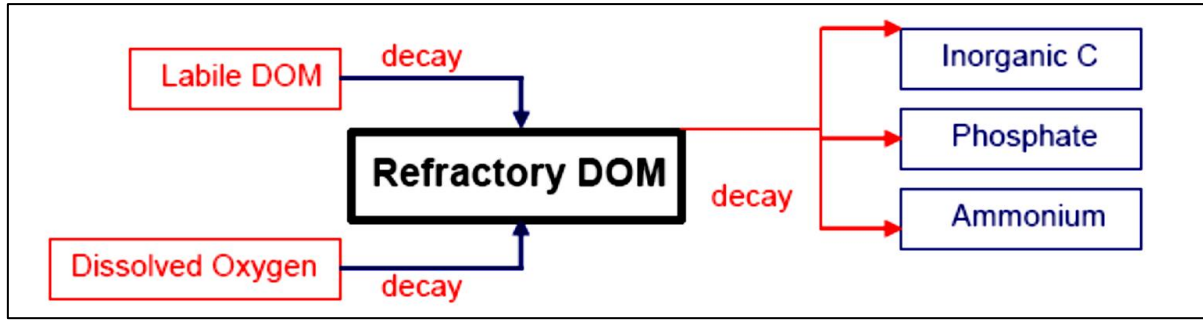
$$\begin{aligned}
 S_{LDOM} = & \sum K_{ae} \Phi_a + \sum (1 - P_{am}) K_{am} \Phi_a + \sum K_{ee} \Phi_e \\
 & + \sum (1 - P_{em}) K_{em} \Phi_e - K_{ldom} \gamma_{om} \Phi_{ldom} - K_{l-r} \Phi_{ldom} + \sum (1 - P_{mm}) K_{mm} \Phi_{macro}
 \end{aligned}
 \tag{34}$$

Where

- P_{am} = partition coefficient for algal mortality
- P_{em} = partition coefficient for epiphyton mortality
- P_{mm} = partition coefficient for macrophyte mortality
- γ_{OM} = temperature rate multiplier for organic matter
- ω_{POM} = POM settling rate, $m \text{ sec}^{-1}$
- K_{am} = algal mortality rate, sec^{-1}
- K_{em} = epiphyton mortality rate, sec^{-1}
- K_{mm} = macrophyte mortality rate, sec^{-1}
- K_{LPOM} = labile POM decay rate, sec^{-1}
- $K_{L \rightarrow R}$ = transfer rate from labile POM to refractory POM, sec^{-1}
- Φ_a = algal concentration, $g \text{ m}^{-3}$
- Φ_e = epiphyton concentration, $g \text{ m}^{-3}$
- Φ_{macro} = macrophyte concentration, $g \text{ m}^{-3}$
- Φ_{LPOM} = detritus concentration, $g \text{ m}^{-3}$

3.4.15 Refractile Dissolved Organic Matter (RDOM)

Refractory DOM is composed of compounds in the aquatic environment that slowly decompose exerting oxygen demand over long periods. Internally, refractory DOM is produced from the decomposition of labile DOM. The source/sink terms is shown in Figure 25.


Figure 25 Fluxes of RDOM

Adopted from Cole and Wells, 2008

The governing rate for RDOM equation is

$$S_{RDOM} = K_{l-r} \Phi_{ldom} - K_{rdom} \gamma_{om} \Phi_{rdom} \quad (35)$$

Where

γ_{OM} = temperature rate multiplier

$K_{L \rightarrow R}$ = transfer rate from labile POM to refractory POM, sec^{-1}

K_{RDOM} = refractory DOM decay rate, sec^{-1}

Φ_{LDOM} = labile DOM concentration, g m^{-3}

Φ_{RDOM} = refractory DOM concentration, g m^{-3}

The CE-QUAL-W2 water quality model allows for the variable stoichiometry of organic matter to the ratios of nitrogen and phosphorus. Eight constituents are required to simulate the amount of nitrogen and phosphorus in labile dissolved organic matter (LDOM), refractory organic matter (RDOM), labile particulate organic matter (LPOM), and refractory particulate organic matter (RPOM). All inputs of organic matter accumulate N and P according to the stoichiometry of the incoming organic matter.

3.4.16 Labile Dissolved Organic Matter – Phosphorus (LDOM-P)

LDOM-P is the amount of phosphorus in labile dissolved organic matter. The rate equation of LDOM-P is:

$$S_{LDOM-P} = \sum K_{ae} \delta_{pa} \Phi_a + \sum (1 - P_{am}) \delta_{pa} \Phi_a + \sum K_{ae} \delta_{pe} + \sum (1 - P_{em}) K_{em} \delta_{pe} \Phi_e + \sum (1 - P_{mm}) K_{mm} \delta_{pm} - K_{LDOM} \gamma_{OM} \Phi_{LDOM-P} - K_{L \rightarrow R} \gamma_{OM} \Phi_{LDOM-P} \quad (36)$$

Where:

P_{am} = pattern coefficient for algal mortality

P_{em} = pattern coefficient for epiphyton mortality

γ_{OM} = temperature rate multiplier for organic matter decay

δ_{P-LDOM} = LDOM stoichiometric ratio for phosphorus

δ_{Pe} = epiphyton stoichiometric coefficient for phosphorus

δ_{Pa} = algal stoichiometric coefficient for phosphorus

δ_{Pm} = macrophyte stoichiometric coefficient for phosphorus

- K_{ae} = algal excretion rate, sec^{-1}
 K_{am} = algal mortality rate, sec^{-1}
 K_{ee} = epiphyton excretion rate, sec^{-1}
 K_{em} = epiphyton mortality rate, sec^{-1}
 K_{mm} = macrophyte mortality rate, sec^{-1}
 K_{LDOM} = labile DOM decay rate, sec^{-1}
 $K_{L\rightarrow R}$ = labile to refractory DOM transfer rate, sec^{-1}
 Φ_a = algal concentration, g m^{-3}
 Φ_m = macrophyte concentration, g m^{-3}
 Φ_e = epiphyton concentration, g m^{-3}
 Φ_{LDOM-P} = labile DOM-P concentration, g m^{-1}

3.4.17 Refractory Dissolved Organic Matter – Phosphorus (RDOM-P)

RDOM-P is the amount of phosphorus in refractory dissolved organic matter. The rate equation of LDOM-P is:

$$S_{RDOM-P} = K_{L\rightarrow R} \Phi_{LDOM-P} - K_{RDOM} \gamma_{OM} \Phi_{RDOM-P} \quad (37)$$

Where:

$$\Phi_{LDOM-P} = \text{labile DOM-P concentration, } \text{g m}^{-3}$$

3.4.18 Labile Particulate Organic Matter – Phosphorus (LPOM-P)

LPOM-P is the amount of phosphorus in refractory dissolved organic matter. The rate equation of LPOM-P is:

$$\begin{aligned}
 S_{LPOM-P} = & \sum P_{am} K_{am} \delta_{pa} \Phi_a + \sum P_{em} K_{em} \delta_{pe} \Phi_e + \sum P_{mm} P_{mpom} K_{mm} \delta_{pm} \Phi_m + K_{zm} \delta_{pz} \Phi_{zoo} \\
 & - K_{LPOM} \gamma_{OM} \Phi_{LPOM-P} - K_{L\rightarrow P} \Phi_{LPOM-P} + K_{zg} (1 - Z_{effc}) \delta_{pz} \Phi_{zoo} - \\
 & K_{zg} \frac{\Phi_{LPOM-P}}{\Phi_{LPOM}} \left(\frac{\sigma_{POM} \Phi_{LPOM}}{\sigma_{alg} \sum \Phi_a + \sigma_{POM} \Phi_{LPOM}} \right) \Phi_{ZOO} - \omega_{POM} \frac{\partial \Phi_{LPOM-P}}{\partial z}
 \end{aligned} \quad (38)$$

Where:

- P_{am} = partition coefficient for algal mortality
 P_{em} = partition coefficient for epiphyton mortality
 P_{mm} = partition coefficient for macrophyte mortality
 P_{mpom} = partition coefficient for RPOM and LPOM from macrophyte mortality
 γ_{OM} = temperature rate multiplier for organic matter
 σ_{alg} = Zooplankton preference fraction for algae
 σ_{pom} = Zooplankton preference fraction for particulate organic matter
 ω_{POM} = POM settling rate, m sec^{-1}
 K_{am} = algal mortality rate, sec^{-1}
 K_{em} = epiphyton mortality rate, sec^{-1}
 K_{zm} = zooplankton mortality rate, sec^{-1}

- K_{mm} = macrophyte mortality rate, sec^{-1}
 K_{LPOM} = labile POM decay rate, sec^{-1}
 $K_{L \rightarrow R}$ = transfer rate from labile POM to refractory POM, sec^{-1}
 Φ_a = algal concentration, g m^{-3}
 Φ_{zoo} = algal concentration, g m^{-3}
 Φ_e = epiphyton concentration, g m^{-3}
 Φ_{LPOM} = LPOM concentration, g m^{-3}
 Φ_{LPOM-P} = LPOM-P concentration, g m^{-3}

3.4.19 Refractory Particulate Organic Matter – Phosphorus (RPOM-P)

RPOM-P is the amount of phosphorus in refractory dissolved organic matter. The rate equation of LPOM-P is:

$$S_{RPOM} = K_{L \rightarrow R} \Phi_{LPOM-P} - K_{RPOM} \gamma_{OM} \Phi_{RDOM-P} + \sum (1 - P_{MPOM}) P_{mm} K_{mm} \delta_{pm} \Phi_m - \omega_{POM} \frac{\partial \Phi_{RPOM-P}}{\partial z} \quad (39)$$

Where:

- P_{mm} = partition coefficient for macrophyte mortality
 P_{mpom} = partition coefficient for RPOM and LPOM from macrophyte mortality
 δ_{pm} = macrophyte stoichiometric coefficient for phosphorus
 γ_{OM} = temperature rate multiplier
 $K_{L \rightarrow R}$ = transfer rate from labile POM to refractory POM, sec^{-1}
 K_{RPOM} = refractory POM decay rate, sec^{-1}
 K_{mm} = macrophyte mortality rate, sec^{-1}
 ω_{RPOM} = POM settling velocity, m/ sec
 Φ_{LPOM-P} = labile POM concentration, g m^{-3}
 Φ_{RPOM-P} = refractory POM phosphorus concentration, g m^{-3}

3.4.20 Labile Dissolved Organic Matter – Nitrogen (LDOM-N)

LDOM-N is the amount of nitrogen in labile dissolved organic matter. The rate equation of LDOM-N is:

$$S_{LDOM-N} = \sum K_{ae} \delta_{Na} \Phi_a + \sum (1 - P_{am}) K_{am} \delta_{Na} \Phi_a + \sum K_{ee} \delta_{Ne} \Phi_e + \sum (1 - P_{em}) K_{em} \delta_{Ne} \Phi_e + \sum (1 - P_{mm}) K_{mm} \delta_{Nm} \Phi_m - K_{LDOM} \gamma_{OM} \Phi_{LDOM-N} - K_{L \rightarrow R} \gamma_{OM} \Phi_{LDOM-N} \quad (40)$$

Where:

- P_{am} = pattern coefficient for algal mortality
 P_{em} = pattern coefficient for epiphyton mortality
 γ_{OM} = temperature rate multiplier for organic matter decay
 δ_{P-LDOM} = LDOM stoichiometric ratio for nitrogen
 δ_{Ne} = epiphyton stoichiometric coefficient for nitrogen

- $\bar{\delta}_{Na}$ = algal stoichiometric coefficient for nitrogen
 $\bar{\delta}_{Nm}$ = macrophyte stoichiometric coefficient for nitrogen
 K_{ae} = algal excretion rate, sec^{-1}
 K_{am} = algal mortality rate, sec^{-1}
 K_{ee} = epiphyton excretion rate, sec^{-1}
 K_{em} = epiphyton mortality rate, sec^{-1}
 K_{mm} = macrophyte mortality rate, sec^{-1}
 K_{LDOM} = labile DOM decay rate, sec^{-1}
 $K_{L \rightarrow R}$ = labile to refractory DOM transfer rate, sec^{-1}
 Φ_a = algal concentration, g m^{-3}
 Φ_m = macrophyte concentration, g m^{-3}
 Φ_e = epiphyton concentration, g m^{-3}
 Φ_{LDOM-N} = labile DOM-N concentration, g m^{-3}

3.4.21 Refractory Dissolved Organic Matter – Nitrogen (RDOM-N)

RDOM-N is the amount of nitrogen in refractory dissolved organic matter. The rate equation of LDOM-N is:

$$S_{RDOM-N} = K_{L \rightarrow R} \Phi_{LDOM-N} - K_{RDOM} \gamma_{OM} \Phi_{RDOM-N} \quad (41)$$

Where

$$\Phi_{LDOM-N} = \text{labile DOM-N concentration, } \text{g m}^{-3}$$

3.4.22 Labile Particulate Organic Matter – Nitrogen (LPOM-N)

LPOM-N was the amount of nitrogen in refractory dissolved organic matter. The rate equation of LPOM-N is:

$$\begin{aligned}
 S_{LPOM-N} = & \sum P_{am} K_{am} \delta_{Na} \Phi_a + \sum P_{em} K_{em} \delta_{Ne} \Phi_e + \sum P_{mm} P_{MPOM} K_{mm} \delta_{Nm} \Phi_m \\
 & + K_{zm} \delta_{Nz} \Phi_{zoo} - K_{LPOM} \gamma_{OM} \Phi_{LPOM-N} - K_{L \rightarrow R} \Phi_{LPOM-N} + K_{zg} (1 - Z_{effc}) \delta_{Nz} \Phi_{zoo} - \\
 & K_{zg} \frac{\Phi_{LPOM-N}}{\Phi_{LPOM}} \left(\frac{\sigma_{pom} \Phi_{LPOM}}{\sigma_{alg} \sum \Theta_a + \sigma_{pom} \Phi_{LPOM}} \right) \Phi_{zoo} - \omega_{POM} \frac{\partial \Phi_{LPOM-N}}{\partial z}
 \end{aligned} \quad (42)$$

Where:

- P_{am} = partition coefficient for algal mortality
 P_{em} = partition coefficient for epiphyton mortality
 P_{mm} = partition coefficient for macrophyte mortality
 P_{mpom} = partition coefficient for RPOM and LPOM from macrophyte mortality
 γ_{OM} = temperature rate multiplier for organic matter
 σ_{alg} = Zooplankton preference fraction for algae
 σ_{pom} = Zooplankton preference fraction for particulate organic matter
 ω_{POM} = POM settling rate, m sec^{-1}
 K_{am} = algal mortality rate, sec^{-1}
 K_{em} = epiphyton mortality rate, sec^{-1}

- K_{zm} = zooplankton mortality rate, sec^{-1}
 K_{mm} = macrophyte mortality rate, sec^{-1}
 K_{LPOM} = labile POM decay rate, sec^{-1}
 $K_{L \rightarrow R}$ = transfer rate from labile POM to refractory POM, sec^{-1}
 Φ_a = algal concentration, g m^{-3}
 Φ_{zoo} = algal concentration, g m^{-3}
 Φ_e = epiphyton concentration, g m^{-3}
 Φ_{LPOM} = LPOM concentration, g m^{-3}
 Φ_{LPOM-N} = LPOM-N concentration, g m^{-3}

3.4.23 Refractory Particulate Organic Matter – Nitrogen (RPOM-N)

RPOM-N is the amount of nitrogen in refractory dissolved organic matter. The rate equation of LPOM-N is:

$$S_{RPOM-N} = K_{L \rightarrow R} \Phi_{LPOM-N} - K_{RDOM} \gamma_{OM} \Phi_{RDOM-N} + \sum P_{mm} (1 - P_{mpom}) K_{mm} \delta_{Nm} \Phi_m - \omega_{POM} \frac{\partial \Phi_{RPOM-N}}{\partial z} \quad (43)$$

Where:

- P_{mm} = partition coefficient for macrophyte mortality
 P_{mpom} = partition coefficient for RPOM and LPOM from macrophyte mortality
 γ_{OM} = temperature rate multiplier
 δ_{Nm} = macrophyte stoichiometric coefficient for nitrogen
 $K_{L \rightarrow R}$ = transfer rate from labile POM to refractory POM, sec^{-1}
 K_{RPOM} = refractory POM decay rate, sec^{-1}
 K_{mm} = macrophyte mortality rate, sec^{-1}
 ω_{RPOM} = POM settling velocity, m/ sec^{-1}
 Φ_{LPOM-N} = labile POM-N concentration, g m^{-3}
 Φ_{RPOM-N} = refractory POM-N concentration, g m^{-3}

3.4.24 Organic Sediments

Organic sediment contributions to nutrients and dissolved oxygen demand are simulated using two methods. The first method uses a constant, or zero-order, release and demand. This method has been frequently used to model sediment demands and nutrient release rates. It does not depend on sediment concentrations or require a separate sediment compartment. However, the formulation was not predictive, as the rates do not vary over time except for the temperature dependence of the decay rate. Therefore, results should be interpreted cautiously when evaluating effects of different nutrient loadings on dissolved oxygen in a water-body.

The second method uses a sediment compartment to accumulate organic sediments and allow their decay. Nutrient releases and oxygen demand are thus dependent upon sediment accumulation – a 1st-order process. However, there is no release of phosphorus or other diagenesis products when overlying water was anoxic since this sediment compartment was labile, oxic decay of organics on the sediment surface. Either of these methods, or a combination, may

be used to simulate effects of organic sediments upon water quality. The zero order process uses a specified sediment oxygen demand and anoxic release rates for phosphorus, ammonium, inorganic carbon, and iron that are temperature dependent. Nutrient releases do not occur when dissolved oxygen concentrations are above a minimum value of 0.1 mg/l nor do they occur if the SOD is set to zero. The sediment contribution to inorganic carbon was computed as a fraction of the sediment oxygen demand. Figure 26 shows the interaction between sediment and other water quality constituents.

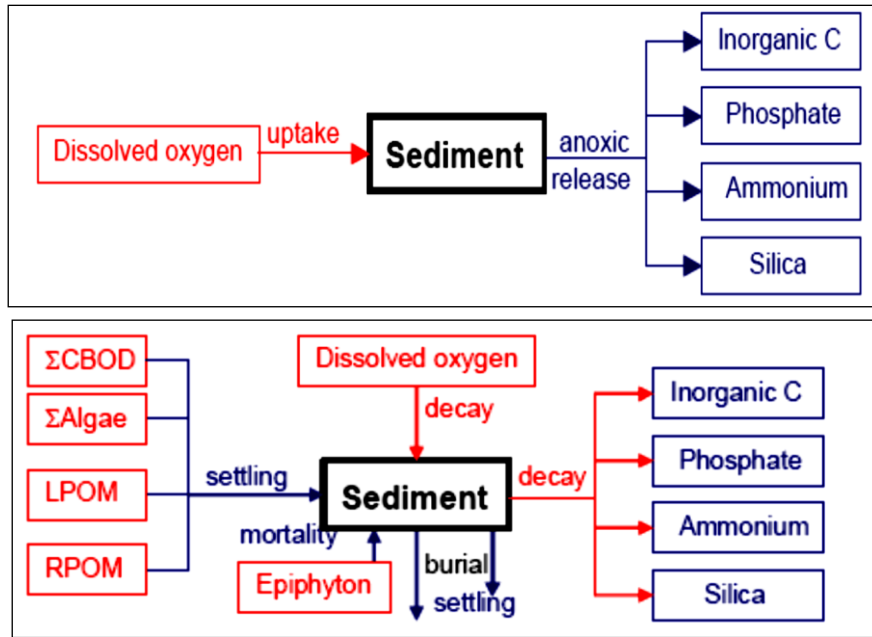


Figure 26 Zero and first order internal fluxes for organic sediments

Adopted from Cole and Wells, 2008

The rate equation describing the sediment concentration is depicted below:

$$\begin{aligned}
 S_{sed} = & \frac{\omega_{POMR} A_{bottom}}{Vol} \Phi_{POMR} + \frac{\omega_{POML} A_{bottom}}{Vol} \Phi_{POML} + \sum \frac{\omega_a A_{bottom}}{Vol} \Phi_a - \\
 & \gamma_{om} K_s \Phi_S + K_{epom} K_{eb} \Phi_e - \frac{\omega_{SED} A_{bottom}}{Vol} \Phi_s + \frac{\omega_{CBOD} A_{bottom}}{Vol} \Phi_{CBOD} - K_{burial} \Phi_S
 \end{aligned}
 \tag{44}$$

Where,

γ_{OM} = rate multiplier for organic matter

Δz = model cell thickness, m

ω_{POM} = POM settling velocity, m sec⁻¹

ω_a = algal settling velocity, m sec⁻¹

ω_{SED} = sediment settling velocity, m sec⁻¹

K_{sed} = sediment decay rate, sec⁻¹

Φ_a = algal concentration, g m⁻³

Φ_{LPOM} = POM labile concentration, g m⁻³

Φ_{RPOM} = POM refractory concentration, g m⁻³

Φ_s = organic sediment concentration, g m⁻³

V_{cell} = volume of computational cell, m^3

A_{bottom} = Area of bottom, m^2

Φ_e = ephyton concentration, $g\ m^{-3}$

K_{epom} = fraction of ephyton that go to particulate fraction and settle into sediment at death

K_{em} = ephyton mortality rate

K_{burial} = sediment burial rate, sec^{-1}

3.4.25 Suspended solids and sedimentation

Suspended solids are important in water quality simulations because of their influence on density, light penetration, and nutrient availability. Increased solids concentrations reduce light penetration in the water column thus affecting temperature that in turn affects biological and chemical reaction rates. Light and nutrient availability largely control algal production (Cole and Wells, 2008).

The lack of data for sedimentation (from inflows or in-dam measurements) was the main reason that inorganic sediments were not modelled. This choice would have a conservative effect on the entire modelling process whereby it could reduce total algal growths thereby presenting the best-case scenario of total algal growth.

4 BACKGROUND TO VOËLVLEI DAM

Voëlvlei Dam is an off-channel storage dam located off the Berg River about 5 km south of Gouda as shown in Figure 27. The catchment of the Dam is relatively small ($\pm 39 \text{ km}^2$) and the dam receives water in two canals which divert water from the Klein Berg, Twenty-Four, and Leeu Rivers (see Figure 28). Historically, water quality in Voëlvlei Dam was regarded as good and an assessment of the trophic status (i.e. degree of nutrient enrichment) by the Institute for Water Quality Studies found that Voëlvlei Dam could be classified as turbid and mesotrophic (i.e. moderately enriched with nutrients) (<http://www.ewisa.co.za/misc/Dams/defaultwcape.htm>, 2012 and http://www.DWA.gov.za/iwqs/rhp/state_of_rivers/berg04/berg3.pdf, 2012).

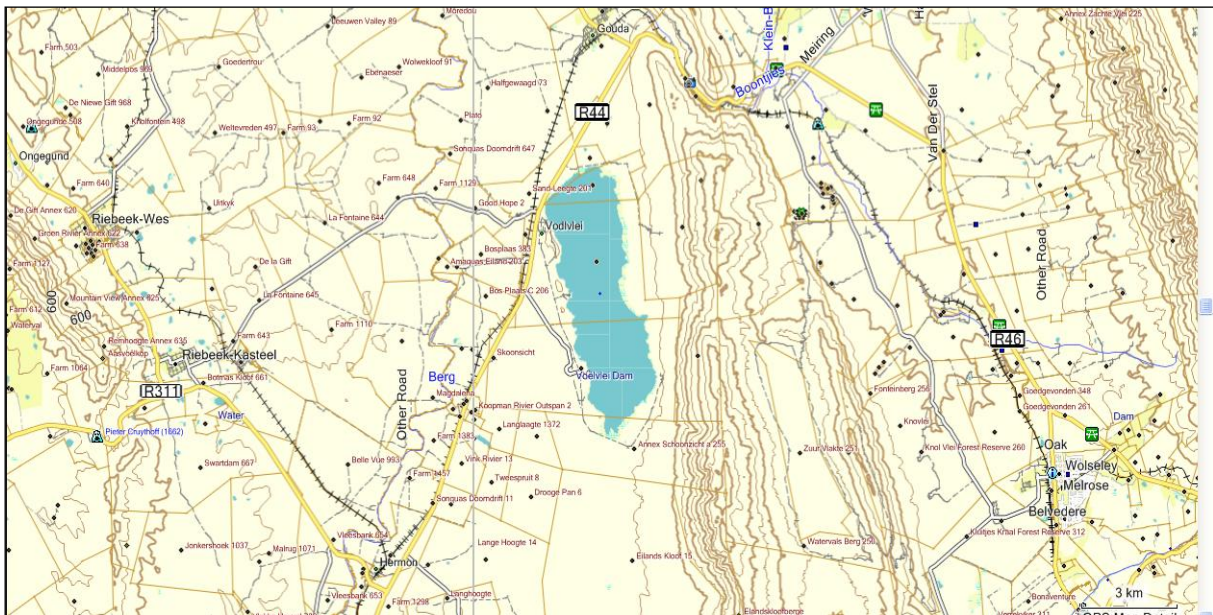


Figure 27 Topographic map of Voëlvlei Dam and surrounds

The Voëlvlei Dam was the first large water supply scheme developed in the Berg River. The first Voëlvlei scheme was completed in 1953 when the natural Vogelvlei Lake was impounded by building a small wall structure. The natural vlei had a catchment of only 40 km^2 and additional water was diverted from the Klein Berg River into a canal to the dam. In 1971, the dam was raised to its present full supply capacity of 172 Mm^3 . The Dam is currently supplied by diverted runoff from the Klein Berg River; Twenty-four Rivers and Leeu River catchments via canals (see Figure 28). The Dam supplies water to Cape Town, the Swartland WTW and irrigation water for downstream users. The water for the Swartland Scheme supplies Riebeeckasteel, Riebeeck Wes and Malmesbury, while the Voëlvlei Water Treatment Works (WTW) supplies Cape Town. The irrigation water is released into the Berg River along with water for the Withoogte Scheme that is then abstracted from Misverstand weir further downstream. The Dam has no spillway infrastructure. (<http://www.ewisa.co.za/misc/Dams/defaultwcape.htm>, 2012 and http://www.DWA.gov.za/iwqs/rhp/state_of_rivers/berg04/berg3.pdf, 2012).

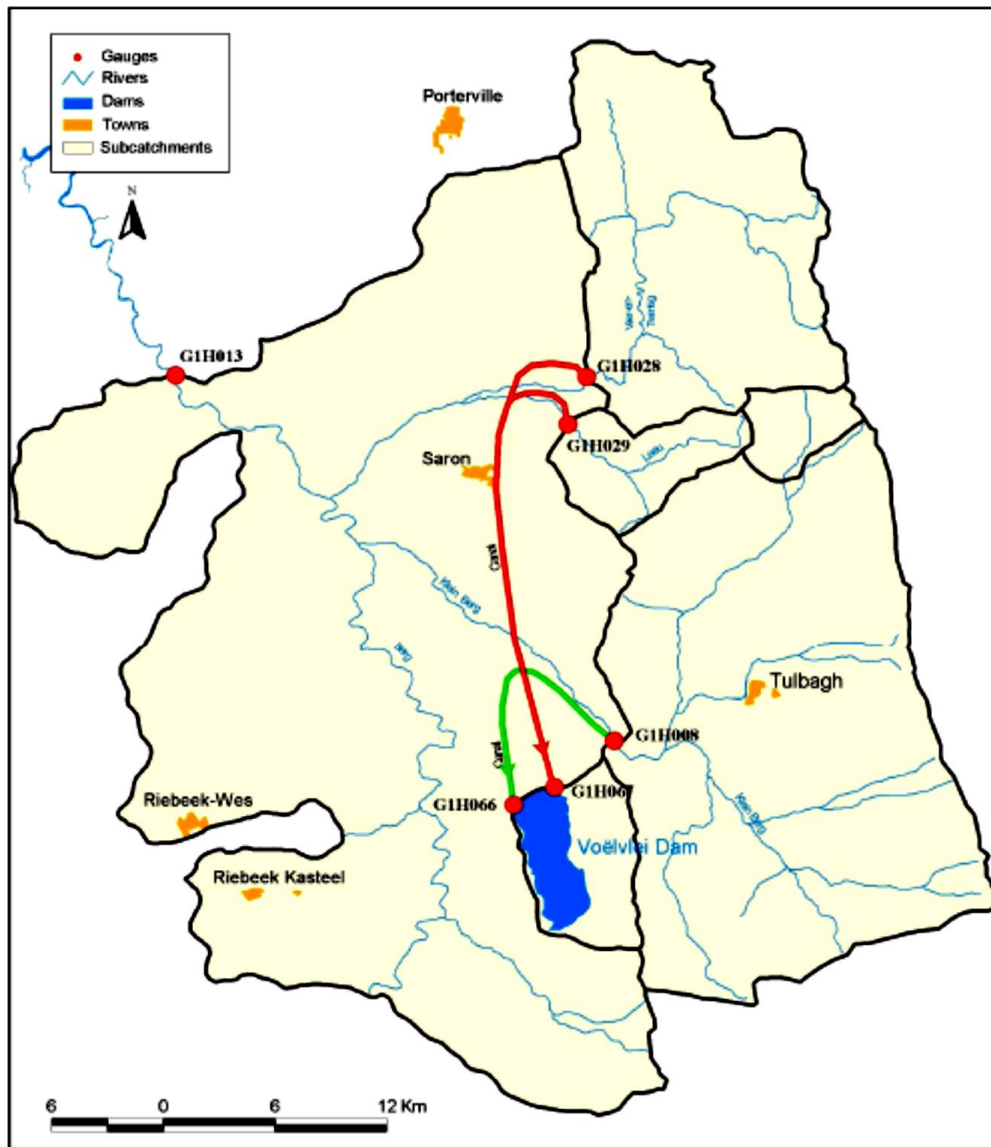


Figure 28 Voëlvlei Dam and its inlet canal system

Adopted from Kamish et al., 2007

The objective of this study was to find any potential links between predicted climate changes and water quality. This effect would probably be seen in eutrophication impacts and not eutrophication itself. It has been postulated that with climate change from the present day to intermediate future and into the distant future that the air temperature would increase by between 2 and 4.5°C for southern Africa and this increase would heat the surface waters sufficiently to amplify the growth of algae within such waters. It was also postulated that all of the three groups of algae namely diatoms, green and cyanobacteria that are currently present, would experience varying rates of increase as a result of the increased water temperature. This increased water temperature would affect the growth of algae by favouring algae with a preference for warmer conditions as a result of the selected temperature growth multipliers which determines algal growth for different water temperatures. It was postulated that cyanobacteria would be the algal group that benefits the most from an increased water temperature with all other factors remaining constant, thereby allowing for an accelerated growth of cyanobacteria and more frequent incidents of harmful algal blooms.

Four downscaled climate models for Voëlvlei were used to establish:

- A baseline study; and
- The effect of climate change on water quality and subsequent eutrophication of the surface water quality of Voëlvlei Dam.

4.1 SPECIFIC MODELLING REQUIREMENTS FOR THIS STUDY

The bathymetric description of the dam is probably the most fundamental data required to construct a numerical grid that is required by the model. The numerical grid is a simplified mathematical description of the volume and shape of the dam. It is essential to construct an accurate description of the dam, as this would determine how well the water level in the dam is modelled. The water level in the dam was linked to water quality modelling and if the initial hydraulic calibration (i.e. volumetric) were not achieved, then water quality calibration would be difficult, if not impossible (Cole and Wells, 2008). In this particular case, the occurrence of algal blooms was of importance, making it vital to simulate the water levels accurately.

Data for construction of the numerical grid was obtained from the DWA – Geomatics Directorate, in the form of a sedimentation survey. Each cross-section had data consisting of X and Y coordinates for the banks of the Dam as well as distances and height above sea level of other points relative to the banks. Sixteen cross-sections, approximately 500 m apart were surveyed in 1998 (See Figure 29).

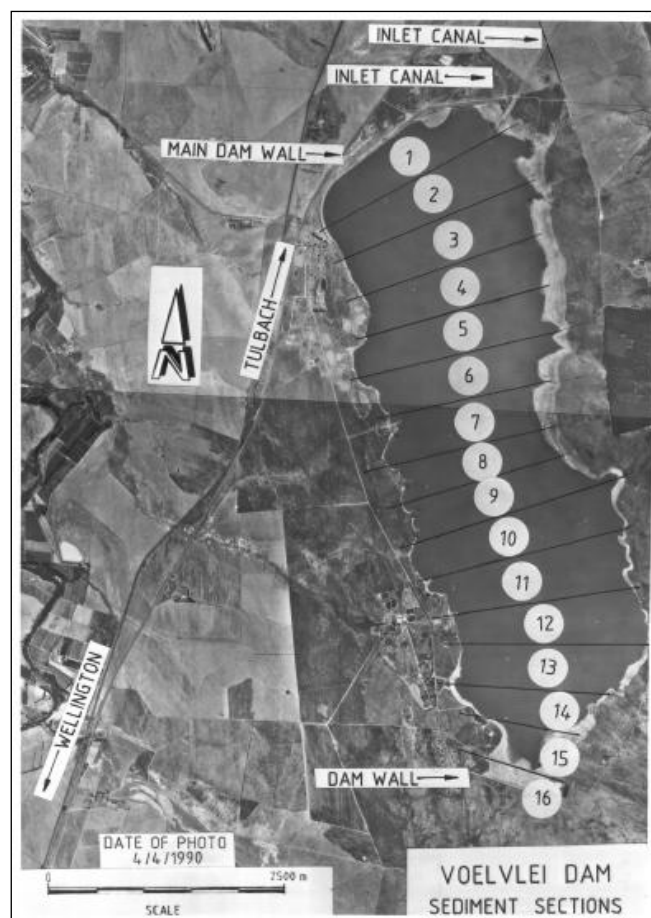


Figure 29 The 1998 sediment survey of Voëlvlei Dam

This original data was transformed into X,Y,Z format and provided for this case study and subsequently imported into the Surfer programme where contours of the Dam were generated (See Figure 30). From this contours the dam was divided into 20 vertical sections of approximately 400m wide. Each of these sections was further vertically divided into layers 0.5 m thick.

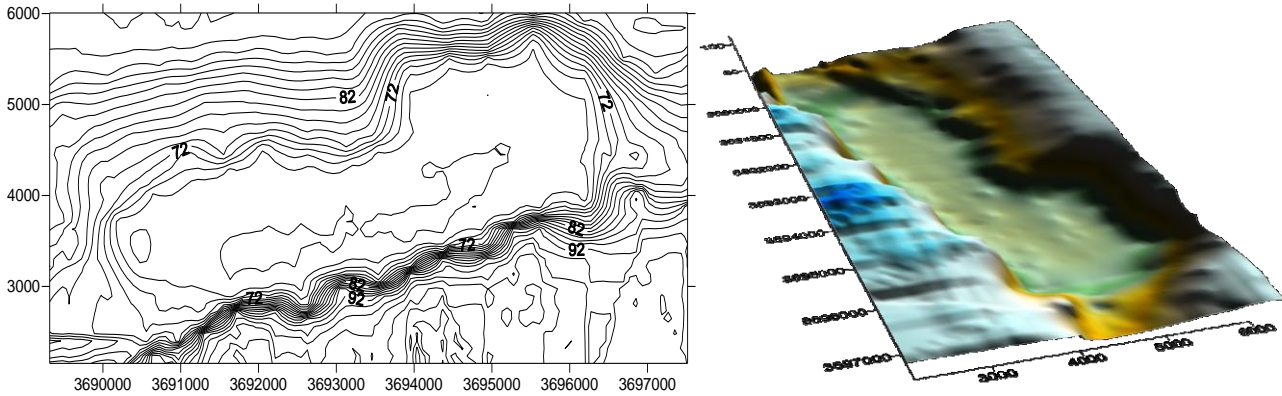


Figure 30 Contour map and 3D shape of Voëlvlei Dam generated as by Surfer

The orientation of a segment was obtained by connecting the mid-point of the cross-section at the maximum supply level of 80m to the mid-point of the following cross-section with the angle being measured, relative to north in a clockwise direction. The figure (Figure 31) below depicts a top view of the segments in a N-S direction (21 to 2) as used by the model CE-QUAL-W2.

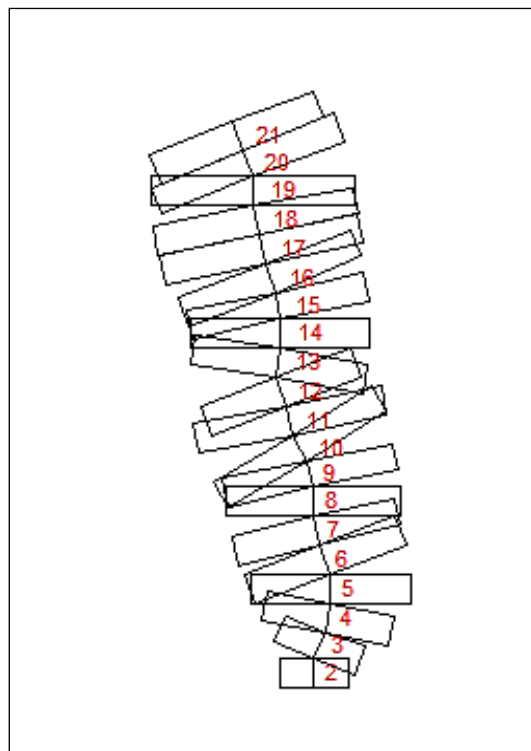


Figure 31 Segments for Voëlvlei Dam as used by CE-QUAL-W2 (NS direction)

The bank to bank width of each cell was then calculated from the following formula :

$$\text{Width} = \frac{\text{Volume in cell}}{\text{length of segment} \times \text{height of segment}} \quad (45)$$

Thereby allocating a width for every segment at 0.5m vertical intervals as shown in Figure 32. Thus, the size of the grid was vertically small so that the accuracy was improved, as the accuracy of the solution was proportional to the number of cells in the grid. The greater the number of cells the greater the accuracy of the result (Versteeg and Malalasekera, 1995).

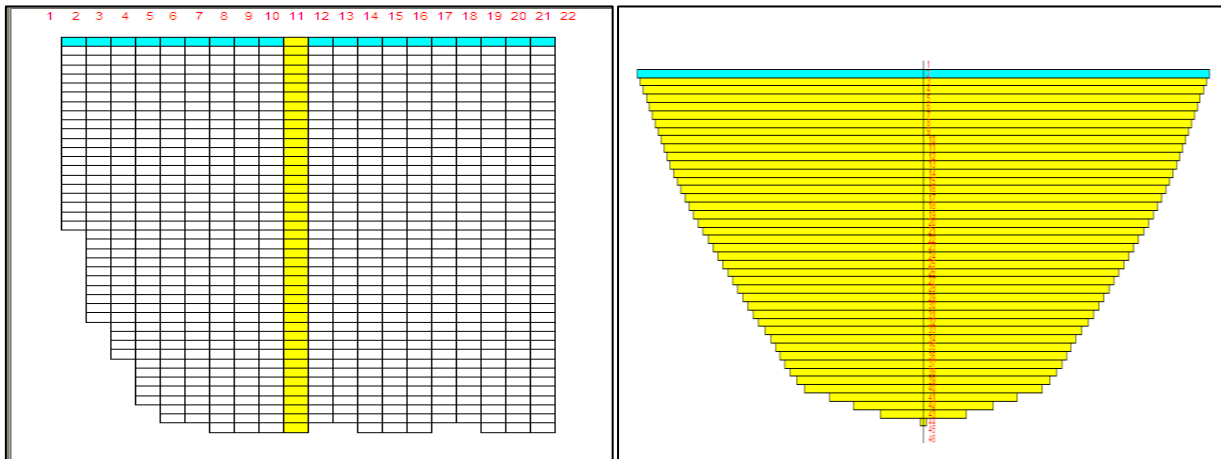


Figure 32 Side and sectional mathematical grid view of Voëlvlei Dam

Using this method, the volume of each cell in the grid was preserved. The entire grid for Voëlvlei Dam was made up of 46 vertical layers and 22 horizontal segments, with segments 1 and 22 as well as layers 1 and 46 representing the boundary cells that have zero width. These cells are required to enable the model to function.

For segments having widths (bank to bank) of less than 30m the numeric algorithms used to solve them are computer time intensive thus, this segment was added to the level above it as this helps increase the timestep, freeing computer time with minimal impact on the volume-area-elevation curves. However, increasing the bottom layers can affect water quality since sediment oxygen demand and nutrient fluxes are dependent on bottom surface areas (Cole and Wells, 2008). It was assumed that this would not be the case as the model had a vertical interval of 0.5m that was considered small.

The segment of concern was segment 11 as this was the withdrawal segment for the MWTP that supplies the city of Cape Town at a maximum withdrawal rate of 230 MI/day and the simulation results will be that of the surface layer.

4.1.1 Bathymetry validation

The mathematical grid was only a representation of reality and should be compared with measured data to ensure that the generated grid is realistic. This is done by comparing the volume-height relationship obtained by the process described before with measured data from DWA's Hydrological Information System (HIS) sediment survey.

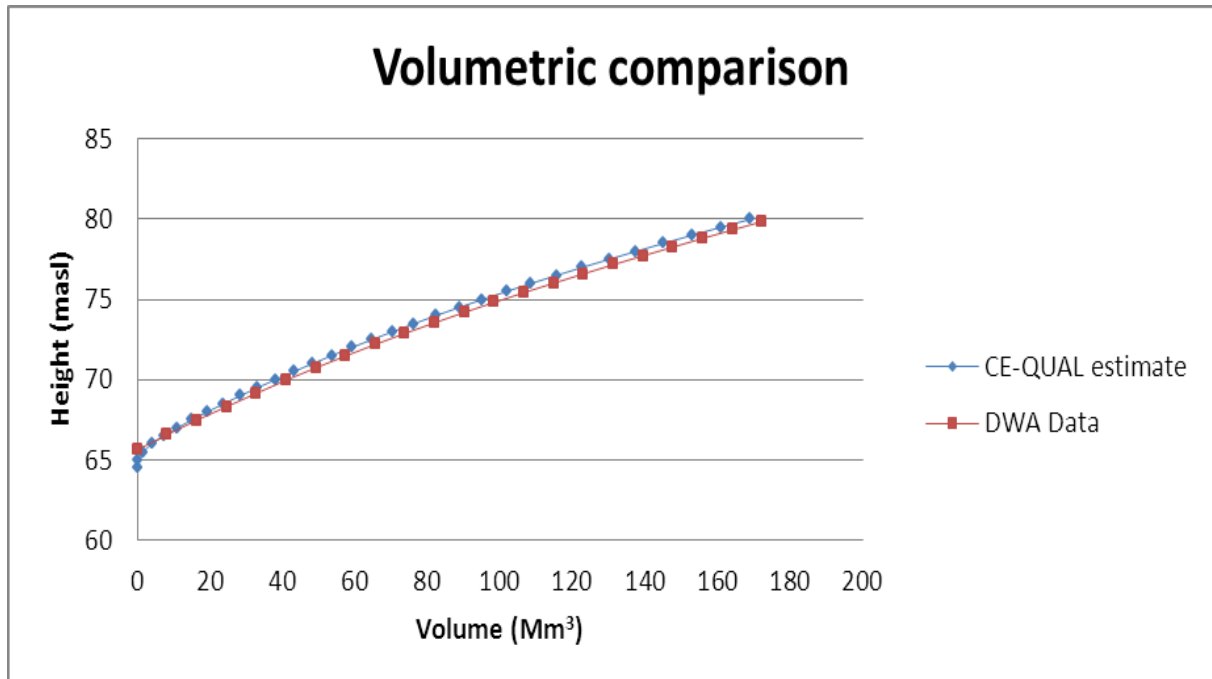


Figure 33 Comparison of Voëlvlei Dam volumes

Figure 33 shows that the model grid agrees well with the actual measured values except for low water levels between 65 and 66 masl where the model underestimates the volume. This was not considered a problem as it was below the minimum operating level.

The major driving forces of CE-QUAL-W2 are the inflows, inflow concentrations and temperature, outflows and meteorological data. In addition, the model also requires calibration data and kinetic data for algal growth and settling. If algae are to be modelled in a system, almost all the water quality variables become important because of the various interactions between the constituents.

4.1.2 Meteorological data

The Climate Systems Analysis Group (CSAG) based at the University of Cape Town has statistically downscaled four GCMs to RCMs for use at local level. These outputs have been quality controlled and processed by the School of Bio-resource Engineering and Environmental Hydrology at the University of Natal for use in hydrological models that project environmental climate and hydrological changes. The results of these analyses to be used in this study are present/ historical conditions (1971-90), intermediate future (2046-2065) and distant future (2081-2100) projections. The four downscaled GCMs were:

- CCC (Canadian Centre for Climate modelling and analysis);
- CNRM (Centre National de Recherche Meteorologi);
- ECHAM5_MPI (Max Planck Institute for Meteorology); and
- IPSL (Institut Pierre Simon Laplace).

The data includes daily minimum and maximum temperature, rainfall, evaporation, solar radiation, minimum and maximum relative humidity and an average wind-speed and wind direction for the country.

Wind-speed and direction was not supplied by CSAG (UCT). CE-QUAL-W2 requires wind-speed and direction as part of its meteorological data input and it was integral for water quality calculations. Thus to overcome this limitation wind-speed and direction was obtained from past data. The recorded wind-speed and direction from 1 January 1971 to 31 December 1971 was repeated for the 20 years of all the simulation periods including the intermediate and future events. This should not be a restriction because the objective is to determine a baseline study and then to determine the relative effect of climate change against this baseline study.

4.1.3 Inflow water quantity and quality data

Inflow to Voëlvlei Dam was diverted from the Twenty-four Rivers, the Leeu River and the Klein Berg River. The daily averaged inflow to the Dam was obtained from the DWA's Hydrological Information System (HIS) database. Details of the flow gauges measuring the inflow are listed in Table 5.

Table 5 Flow gauging stations recording inflow to Voëlvlei Dam

Gauge Number	River	Latitude	Longitude	Period of record
G1H066A01	Klein Berg inlet canal at Voëlvlei Dam	33°21'05"	19°01'12"	1-10-1951 to 14-2-2002
G1H067A01	Twenty- Four Rivers inlet canal at Voëlvlei Dam	33°21'05"	19°01'12"	1-10-1972 to 14-2-2002

Outflows from Voëlvlei Dam consist of abstractions of raw water to supply the Voëlvlei (G1H070M01) and Swartland (G1H068M01) WTW. Water was also released via an outlet canal (G1H065A01) to the Berg River for run-of-river irrigation (DWA, 2002).

The minimum level of operation for the Voëlvlei WTW was 68.33 metres above sea level (masl). No information was available for the minimum draw down level at the Swartland WTW but it was assumed equal to that at Voëlvlei WTW. The minimum draw down level for the Berg River release was 65.62 masl (DWA, 2002). An additional outflow was also operational but flow data for this gauging station (G1H069M01) was only available up to 1982. This pipeline was excluded from the simulation as it was deemed to have too little effect on the water quality. This assumption was confirmed in section 4.2.1.

Inflow water quality data was not as readily available as flow data, and was at best measured only on a weekly basis. For a graphical layout of where pertinent water quality monitoring stations are located for the Voëlvlei Dam system, refer to Figure 28. Although a reasonably good water quality record exists at gauging station G1H029Q01, it was not used. This was because the volume of water diverted from the Twenty-Four Rivers River was substantially greater than that diverted from

the Leeu River and it was therefore assumed that the water quality of the Twenty-Four Rivers River would be more representative of the water quality entering the Dam at G1H067Q01. Similarly, gauging station G1H008Q01 was representative of the water quality at G1H066Q01, due to its dilution effect.

Since no future inflow and outflow data was available it was proposed to use the current Department of Water Affairs Hydrological Information System (DWA HIS) databases' flow-data from 1 January 1971 until 31 December 1990's (present scenario) for each of the subsequent intermediate and future simulations. This would assume that demand and allocation of the water resource does not change for the future simulation periods.

In summary, this modelling should produce a calibrated, verified present day scenario. Assuming no subsequent change in the annual operation and anthropogenic loadings to the dam, the CEQUAL-W2 model predicted the change in surface water quality due to climate change, which in essence was a change in meteorological data. The inflows, withdrawal and wind-speed and direction remained the same for all the model runs.

4.1.4 The model boundary conditions

The water quality of all the inflowing canals was not measured and it was assumed that water quality at upstream monitoring points could be used to describe the boundary conditions at these inflows. These inflows were modelled as tributaries that were evenly distributed into Segment 21.

The modelled outflows from the Dam consisted of the Berg River irrigation release (segment 6) and two lateral withdrawals for the water treatment works as well as evaporation which was calculated based on the air temperature, dew point temperature and wind-speed. Table 6 summarises the flow boundary conditions.

Table 6 Summary of the boundary conditions for Voëlvlei Dam

Inflow/outflow	Segment	Layer
Tributary 1 inflow	21	Evenly distributed
Tributary 2 inflow	21	Evenly distributed
Withdrawal 1 (Voëlvlei WTW)	11	68.33 masl
Withdrawal 2 (Swartland WTW)	18	68.33 masl
Release (Berg river irrigation modelled as a withdrawal)	6	65.62 masl
Evaporation	All active surface segments	Top surface

4.1.5 The initial conditions

The dates of the modelling study for the four climate change scenarios are:

- Present day (1/1/1971-31/12/1990);
- Intermediate future (1/1/2046-31/12/2065); and

- Distant future (1/1/2081-31/12/2100).

In each of the modelling periods under study, Julian day 1 was 1 January for each of the respective climate change scenario dates. An initial condition of temperature and concentration profiles, the number of inflows and outflows and the type of water modelled (saltwater or freshwater) was determined by the user. These conditions are typically measured values from the previous day or any day closest to the start of the simulation. These conditions were initialised in the 'control' file and the 'vertical profile' input files of the model. Meteorological and flow data was available for the years 1996 to 1997, it was decided that initial runs would be used to quantify the outputs and determine if further more rigorous calibration would be required.

It was assumed that reservoir was completely mixed (as it was relatively shallow with winds along it axis) and that a single value initial condition for concentration would be a good initial guess. The in-lake conditions were obtained from the DWA (HIS) database on the date closest to the start date of the simulation period. The constituents that were modelled with initial conditions are listed in Table 7.

Table 7 Constituents modelled and initial values

Constituent	Initial Value
Total dissolved solids (TDS)	50 mg/l
Generic tracer	35 mg/l
Age	0.0 /day
Phosphates	0.022 mg P/l
Ammonium	0.073 mg N/l
Nitrates and nitrites	0.119 mg N/l
Dissolved Silica (DSI)	0.4 mg/l
Particulate Silica (PSI)	0.0 mg/l
Labile dissolved organic matter (LDOM)	0.7 mg/l
Refractory dissolved organic matter (RDOM)	2.0 mg/l
Labile particulate organic matter (LPOM)	0.1 mg/l
Refractory particulate organic matter (RPOM)	0.0 mg/l
Diatoms	1 mg/l
Green Algae	2 mg/l
Cyanobacteria	0.5
Zooplankton	0.1 mg/l
Dissolved oxygen (DO)	10 mg/l
Total inorganic carbon (TIC)	10 mg/l
Alkalinity (CaCO ₃)	0.1 mg/l
Temperature	14.3 °C

4.1.6 Model parameterisation

The model required a set of input parameters to run, which are measured or taken from literature. All the model parameters used in this study are listed in Table 8. Many parameters need to be defined and parameter values were chosen from literature but in most cases, this was a range of possible parameter values. Without being able to measure these values, parameters were chosen and the model was allowed to run thereby presenting a possible solution. In many instances inflow concentrations for inorganic suspended solids, labile organic matter, refractory organic matter, particulate silica and inorganic carbon was not found and these were taken from literature.

Table 8 Parameters used in water quality model

Symbol	Model Parameters	Value
Parameters affecting diatom growth		
K_{ag}	Maximum algal growth rate	5 day ⁻¹
K_{am}	Maximum algal mortality rate	0.1 day ⁻¹
K_{ae}	Maximum algal excretion rate	0.04 day ⁻¹
K_{ar}	Maximum algal respiration rate	0.05 day ⁻¹
h_n	Algal half-saturation constant for nitrogen limited growth	0.01 mg/l
h_p	Algal half-saturation for phosphorus limited growth	0.002 mg/l
h_p	Algal half-saturation for silicon limited growth	0.08 mg/l
AS	Algal settling velocity	0.5 m day ⁻¹
ALGP	Stoichiometric equivalent between algal biomass and phosphorus	0.01
ALGN	Stoichiometric equivalent between algal biomass and nitrogen	0.072
ALGC	Stoichiometric equivalent between algal biomass and carbon	0.4
ALSI	Stoichiometric equivalent between algal biomass and silica	0.2
ACHLA	Ratio between algal biomass and chlorophyll-a	0.8 mg algae/ μ g chl a
ASAT	Light saturation intensity at maximum photosynthetic rate	61.2 Wm ⁻²
Parameters affecting green algae growth		
K_{ag}	Maximum algal growth rate	4.1 day ⁻¹
K_{am}	Maximum algal mortality rate	0.1 day ⁻¹
K_{ae}	Maximum algal excretion rate	0.04 day ⁻¹
K_{ar}	Maximum algal respiration rate	0.05 day ⁻¹
h_n	Algal half-saturation constant for nitrogen limited growth	0.14 mg/l
h_p	Algal half-saturation for phosphorus limited growth	0.38 mg/l
h_p	Algal half-saturation for silicon limited growth	0 mg/l
AS	Algal settling velocity	0.18 m day ⁻¹
ALGP	Stoichiometric equivalent between algal biomass and phosphorus	0.012
ALGN	Stoichiometric equivalent between algal biomass and nitrogen	0.066

Symbol	Model Parameters	Value
<i>ALGC</i>	Stoichiometric equivalent between algal biomass and carbon	0.49
<i>ALSI</i>	Stoichiometric equivalent between algal biomass and silica	0
<i>ACHLA</i>	Ratio between algal biomass and chlorophyll-a	0.8 mg algae/ μ g chl a
ASAT	Light saturation intensity at maximum photosynthetic rate	81.6 Wm ⁻²
Parameters affecting cyanobacteria growth		
<i>K_{ag}</i>	Maximum algal growth rate	1 day ⁻¹
<i>K_{am}</i>	Maximum algal mortality rate	0.1 day ⁻¹
<i>K_{ae}</i>	Maximum algal excretion rate	0.04 day ⁻¹
<i>K_{ar}</i>	Maximum algal respiration rate	0.05 day ⁻¹
<i>h_n</i>	Algal half-saturation constant for nitrogen limited growth	0 mg/l
<i>h_p</i>	Algal half-saturation for phosphorus limited growth	0.011 mg/l
<i>h_p</i>	Algal half-saturation for silicon limited growth	0 mg/l
AS	Algal settling velocity	0.1 m day ⁻¹
<i>ALGP</i>	Stoichiometric equivalent between algal biomass and phosphorus	0.007
<i>ALGN</i>	Stoichiometric equivalent between algal biomass and nitrogen	0.08
<i>ALGC</i>	Stoichiometric equivalent between algal biomass and carbon	0.45
<i>ALSI</i>	Stoichiometric equivalent between algal biomass and silica	0
<i>ACHLA</i>	Ratio between algal biomass and chlorophyll-a	0.8 mg algae/ μ g chl a
ASAT	Light saturation intensity at maximum photosynthetic rate	60 Wm ⁻²
Other parameters affecting all algal growth		
EXH20	Extinction of pure water	0.45 m ⁻¹
EXOM	Extinction due to organic suspended solids	0.1 m ⁻¹
BETA	Fraction of incident solar radiation absorbed at water surface	0.45
Parameters affecting ammonia nitrification and sedimentary phosphorus		
NH4DK	Maximum ammonia nitrification rate	0.12 day ⁻¹
NH4R	Sediment release rate under anaerobic conditions (as a fraction of the sediment oxygen demand (SOD))	0.001
PARTP	Phosphorus partitioning coefficient for suspended solids	0.5
PO4R	Sediment release rate of phosphorus under anaerobic conditions (as a fraction of the sediment oxygen demand (SOD))	0.001
SEDDK	First order sediment decay rate	0.1 day ⁻¹
Parameters affecting dissolved and particulate organic matter		
LDOMDK	Labile Dissolved Organic Matter (DOM) decay rate	0.1 day ⁻¹
RDOMDK	Refractory DOM decay rate	0.001 day ⁻¹
LRDDK	Labile DOM to refractory DOM decay rate	0.001 day ⁻¹
LPOMDK	Labile particulate organic matter (POM) decay rate	0.08 day ⁻¹

Symbol	Model Parameters	Value
RPOMDK	Refractory POM decay rate	0.001 day ⁻¹
LRPDK	Labile to refractory POM decay rate	0.01 day ⁻¹
POMS	POM settling rate	0.1 m day ⁻¹
Stoichiometric coefficients		
O2NH4	Oxygen stoichiometry for nitrification	4.57
O2OM	Oxygen stoichiometry for organic matter decay	1.4
O2AR	Oxygen stoichiometry for algal respiration	1.1
O2AG	Oxygen stoichiometry for algal primary production	1.4

All the values have been adopted from Cole and Wells, 2008, Bowie et al., 1985, Nielsen, 2005, Litchman, 2000, De Nobel et al., 1997, Goldman and Carpenter, 1974, Vuren and Grobbelaar., 1982, Holm and Armstrong, 1981, Lin and Schelske, 1979 and EPA-660/3-75-005.

4.1.7 The algal temperature-growth relationship

The lower, maximum lower, upper and maximum upper temperature used in defining the curve that determined the effects of temperature on algal rates are shown in Figure 34. Also specified is the fraction of maximum algal rates that occurs at the specified temperatures. The CE-QUAL-W2 default values are shown. When including multiple algal groups, the temperature rate coefficients are one of the most important parameters determining algal succession (Cole and Wells, 2008). Diatoms would have much lower temperatures and cyanobacteria would have higher values.

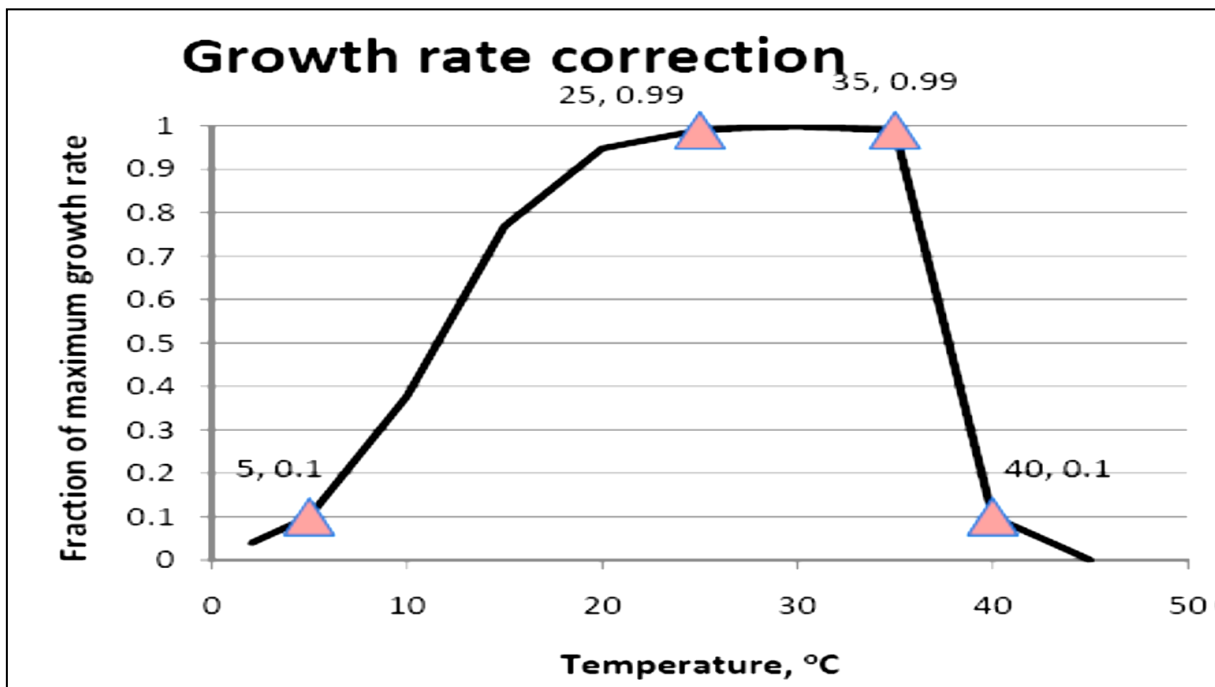


Figure 34 An example algal growth-temperature relationship

Adopted from Cole and Wells, 2008

Table 9 The growth-temperature variable values used for this modelling study

Temperature (°C)	Diatoms	Green Algae	Cyanobacteria
Lower temperature AT1	4	5	5
Lower temperature for maximum algal growth AT2	20	20	24
Upper temperature for maximum algal growth AT3	25	25	31
Upper temperature for algal growth AT4	28	32	38

Adopted from Nielsen, 2005, Cole and Wells, 2008, Bowie et al., 1985, Tsujimura and Okubo, 2003, Tamiya et al., 1965 and Talling, 1955.

The choice of parameters was a daunting task since the literature values are reported as ranges rather than singular values. It was known that laboratory sampled growth constants vary for the same species for an in-situ condition. Ideally, growth constants should be collected in-situ but even this could not be sufficient, as algae are capable of adapting their growth characteristics. Thus, the parameters used for this study were chosen from literature and iteratively this was improved upon by running the model and comparing to actual data, then calibrating to improve the result.

Ideally, the following process should be applied in practice:

- Build model and validate hydraulics and hydrodynamics;
- Compare algal growth to measured data, adapt and rerun to confirm;
- Use model to predict future scenario;
- Measure the data in-situ in the future scenario;
- Compare this to the predicted data and modify model to calibrate;
- Use this new parameters to predict next future scenario; and then
- Repeat the process.

This process could be repeated on a short time scale such as a month so that the measured data would be available within a month and subsequent validation and calibration may be performed.

4.2 MODEL PERFORMANCE AND VALIDATION

4.2.1 Modelled Dam hydraulics

Although the bathymetry of the dam was well captured by the model as shown by the volume-height relationship in Figure 33 it was still necessary to check the hydraulic performance of the dam. Sampling data of water quality variables from the DWA HIS database was composite surface measurements and no profile data was available. The water volumetric balance for the dam was developed from the inflows and outflows that are measured daily. An outflow from the Dam (ICS pipeline) was not monitored but was small in relation to the Berg River outflow and the abstractions for the Voëlville and Swartland WTW. The meteorological data was obtained from the weather station at the dam and inflow data for this simulation period was obtained from the DWA HIS database. The daily water levels in Voëlville Dam were obtained from the DWA HIS database for

the annual period of 1 September 1996 to 30 August 1997 and were used to compare the measured levels to the modelled output from CE-QUAL-W2 for the same period. The results are shown graphically in Figure 35.

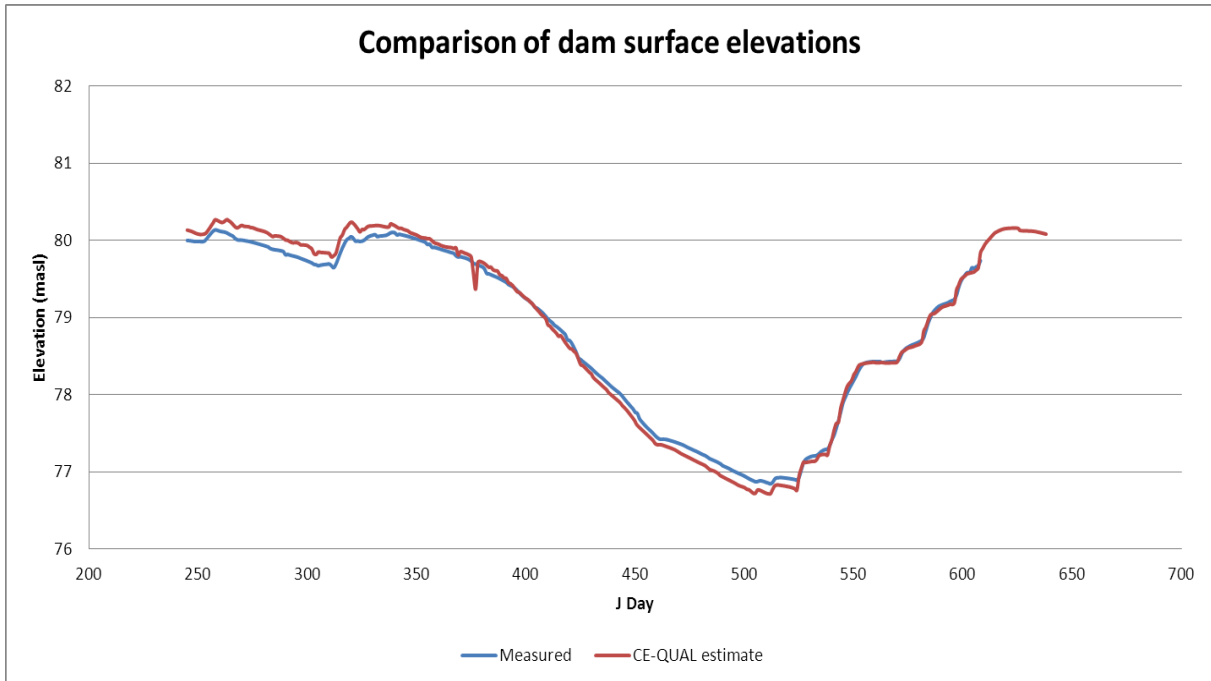


Figure 35 Surface water level comparison with measured data

It was seen that the model agrees relatively well with the surface water elevations measurement and that the overall trend was followed closely. The additional outflow to the pipeline that was excluded from the simulation could explain the discrepancy in surface water levels. The trend between the measured data and the simulated output was good enough to accept that the bathymetry that had been constructed for the dam was hydraulically calibrated for the model. The climate change scenario modelling study would attempt to show differences in algal growth thus any discrepancies will not be compounded rather carried through each modelling scenario.

4.2.2 Model temperature predictions

Water temperature data for the dam surface, close to the dam wall (Segment 21) was measured by the DWA on a scheduled basis and the model output temperature was compared to this. This comparison would provide an indication of the hydrodynamics of the dam. This could only be done for surface water temperature, as no vertical profile temperature data was available.

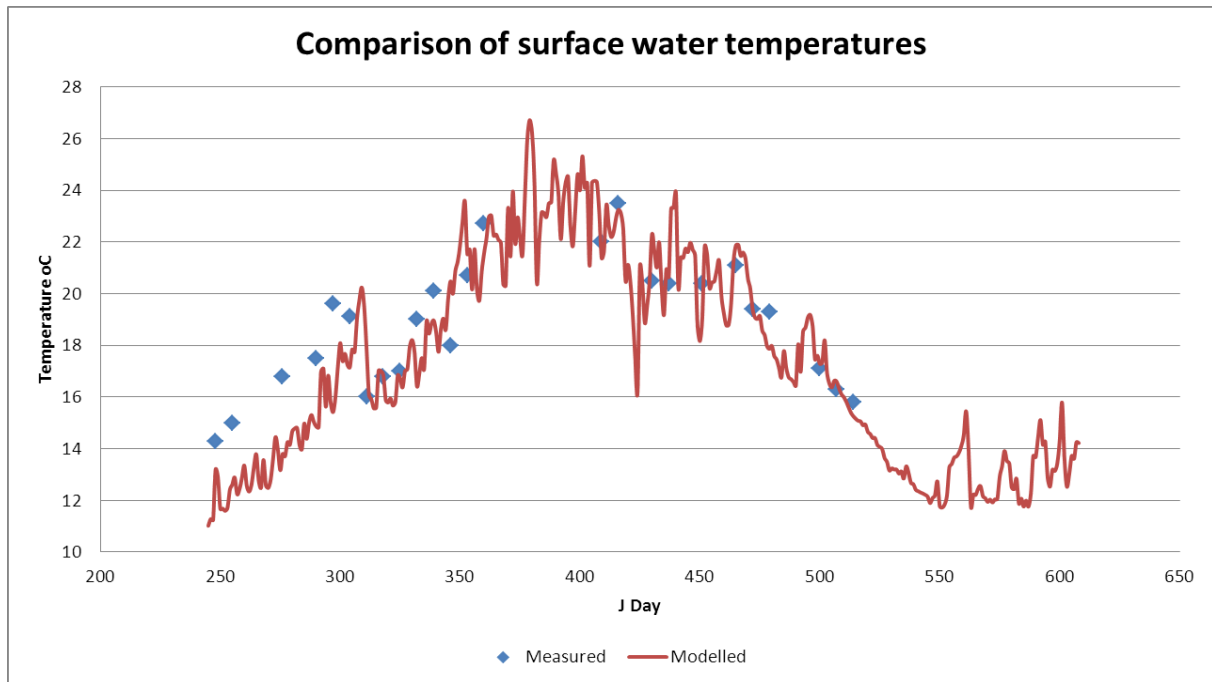


Figure 36 Surface water temperature compared with measured data

The modelled water temperature agreed well with the measured water temperature for the period 2 September 1996 to 1 September 1997. Overall, the trends between the modelled and actual measurements agreed thus confirming that the hydrodynamics of the dam are reproduced by the model and that it was sufficiently accurate to proceed. For the purpose of this study, it was deemed unnecessary to calibrate further as this study investigated the relative changes for projected climate change. It was noted that since no profile temperature measurements were made there was no way of knowing the accuracy of the model for incremental depths.

The seven measured water quality variables of concern were available from the DWA HIS database. These included chlorophyll-a, chlorine as tracer data, NH_4 , PO_4 , Si, Total P and NO_2+NO_3 . These constituents are grab samples and are collected near the dam wall on an irregular basis.

4.2.3 Ortho phosphorus comparison

When modelling algae, the phosphate concentration (PO_4) was probably the most affected water quality constituent because it was constantly being recycled from one form to another as shown previously in Figure 14. Total phosphorus, although not a conservative, was less dynamic than phosphate and was often treated as a pseudo-conservative substance (Cole and Wells, 2008). In this model setup, the sinks for phosphate included the outflows and photosynthetic process while the sources included the inflows, respiration and the decay of organic material including dead algae (organic sediments).

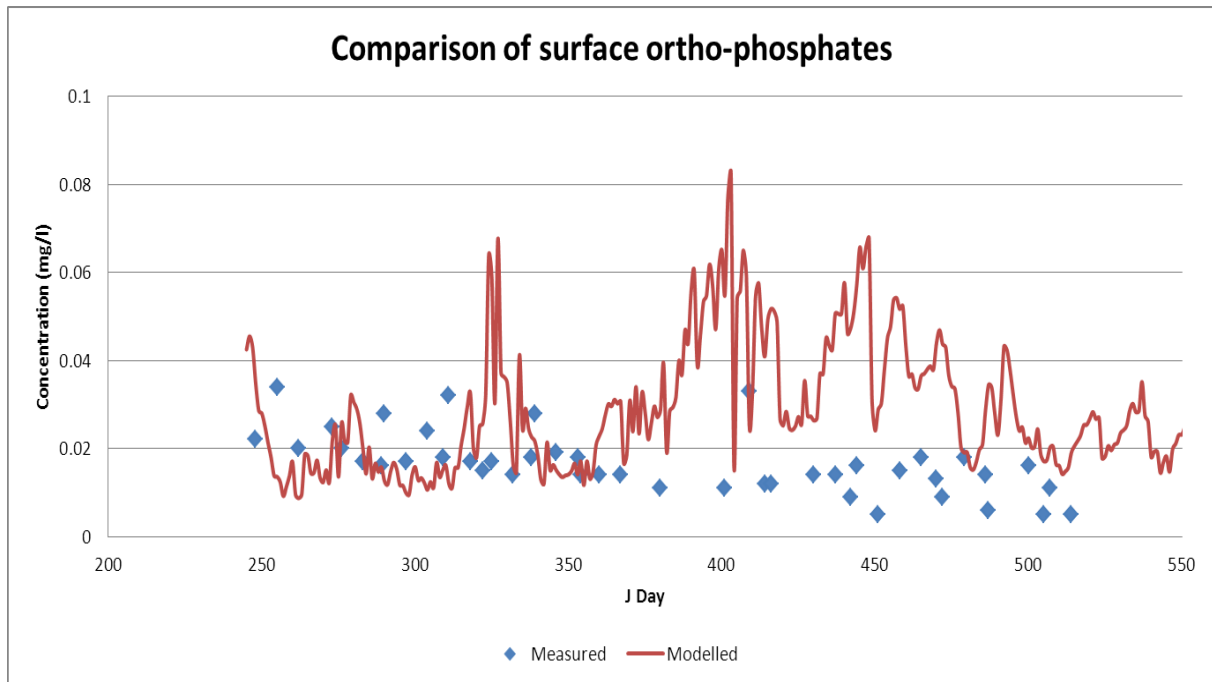


Figure 37 Comparison of simulated phosphate with sampled values

From Figure 37 it was seen that the model predicted the concentration of P in the dam well in spite of not having the additional withdrawal pipeline. The model however seemed to exaggerate the peaks. It was thought the difference could be attributed to the measured value being a composite depth sample and the modelled concentration was for the entire segment. In spite of the difference, the concentrations were well represented by the modelled values.

4.2.4 Ammonium and nitrite-nitrate comparison

It was expected that algal growth would be dependent on the amount of nitrogen available, either in the form of ammonium or nitrate-nitrites. The modelled results compared to measured samples are shown in Figure 38 and Figure 39. When comparing these figures to Figure 40 it was seen that the algal growth was greatest for larger concentrations of ammonium and nitrites-nitrates. Overall, the modelled data simulates the measured data satisfactorily. The discrepancies could be attributed to the measured value being a depth composite and the modelled concentration was laterally averaged for the entire segment.

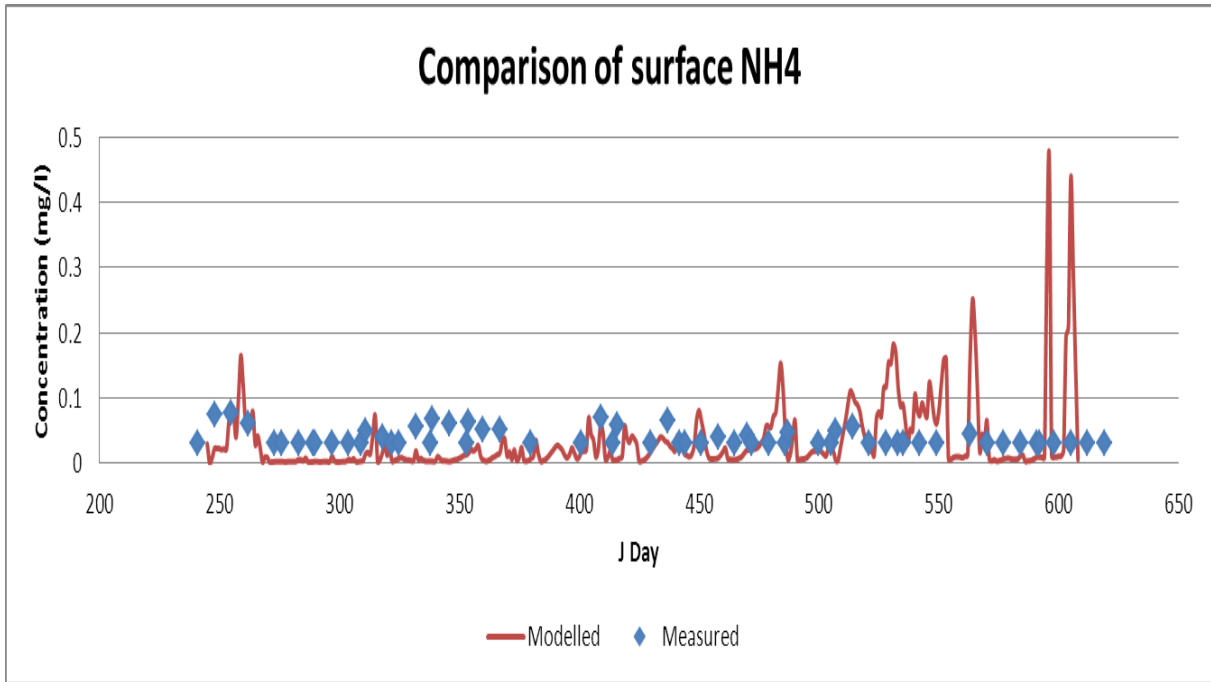


Figure 38 Comparison of modelled ammonium with sampled values

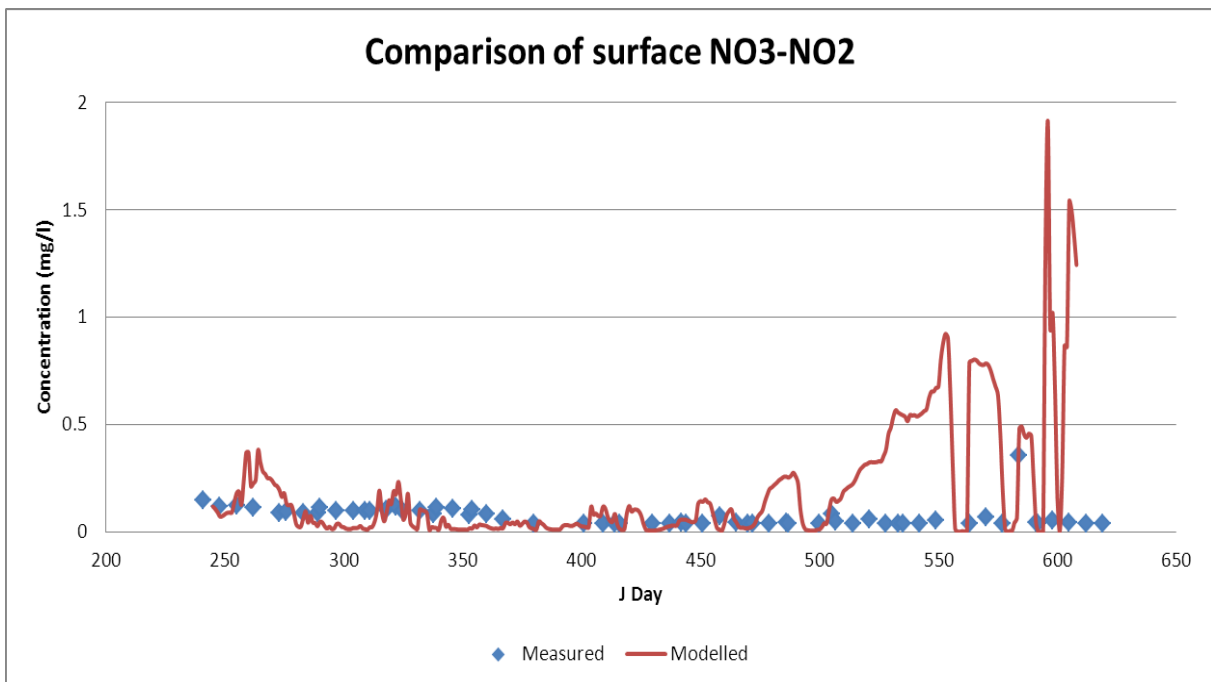


Figure 39 Comparison of Nitrite-nitrate with sampled values

4.2.5 Chlorophyll-a comparison

From the DWA HIS database it was seen that only total chlorophyll-a was measured and Figure 40 compares measured to modelled values. The algal growth was similar to that being measured with some discrepancies and the model produced chlorophyll-a concentrations similar to the measured values.

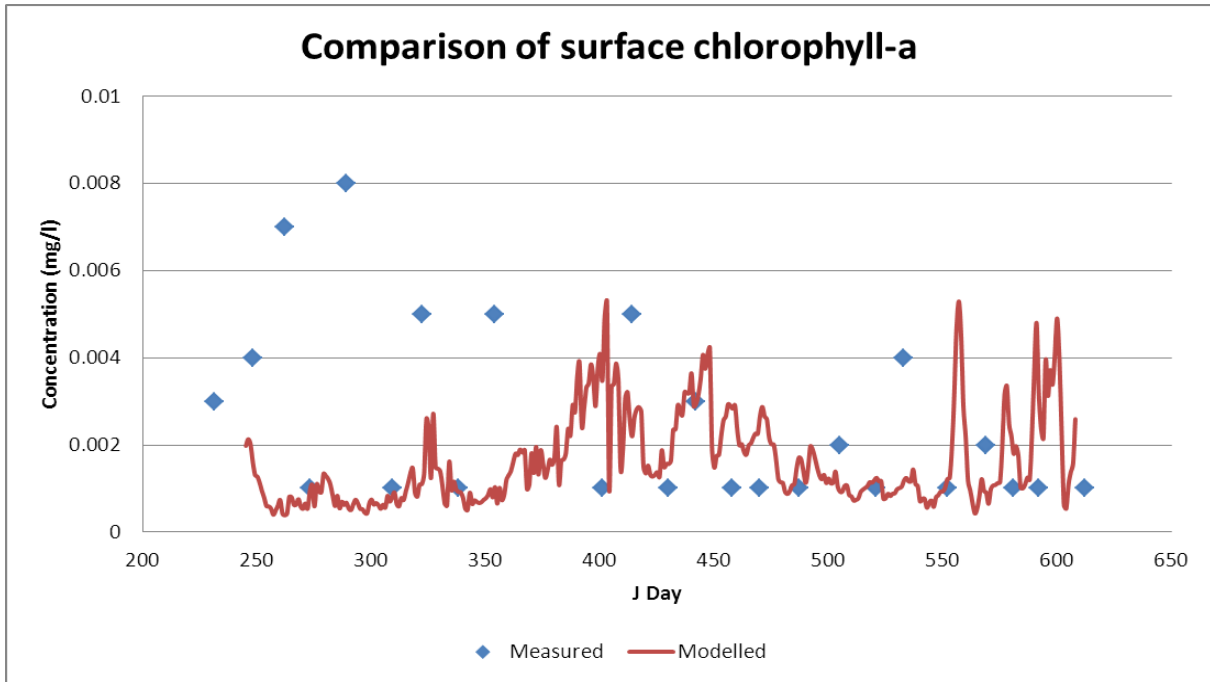


Figure 40 Comparison of chlorophyll-a with sampled values

The discrepancies could be because measured concentrations are a composite value of various samples at the surface and depth, at the dam wall. The modelled results are only for the surface layer and the entire dam wall was treated as one area as the model was laterally averaged. In spite of this, the algal growth was well represented by the model in the context of low concentrations being modelled.

4.2.6 Conservative tracer tracking

The addition of a conservative tracer was to ascertain whether a sizeable source or sink of water had been omitted from the dam in form of inflows, outflows, sources or sinks. From Figure 41 it was seen that the concentration of the modelled tracer mimics that of the measured values adequately. It may be concluded that the transport processes were modelled sufficiently accurate in order to proceed.

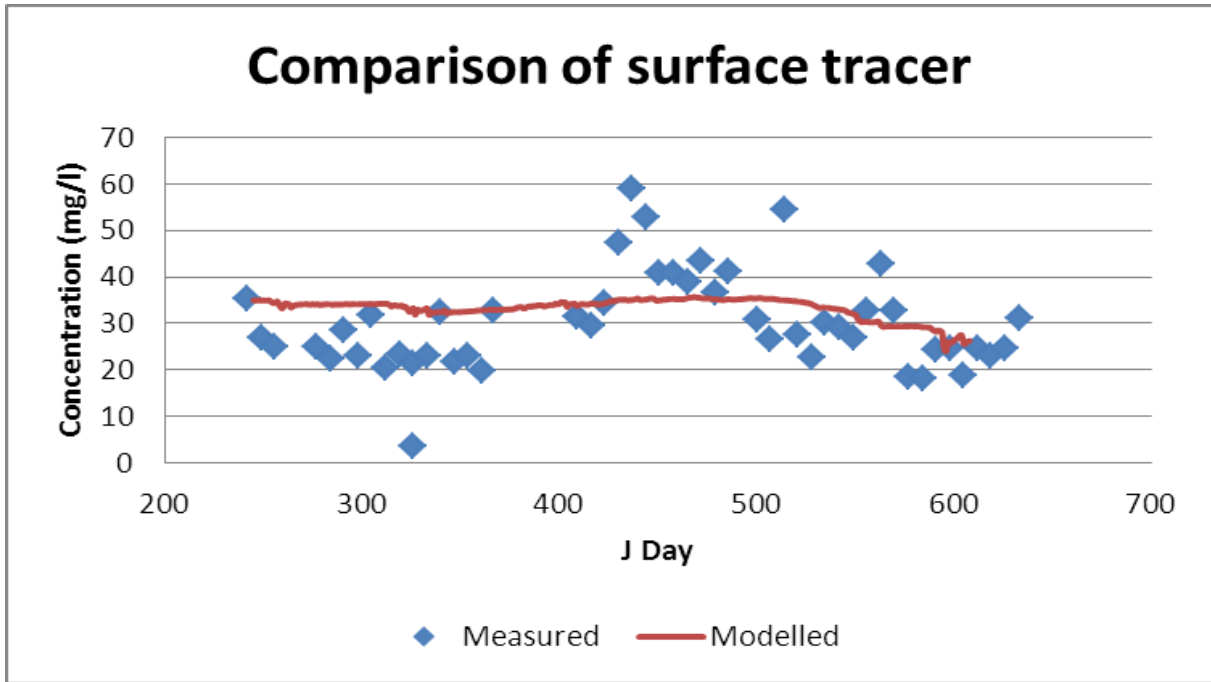


Figure 41 Comparison of modelled tracer to sampled values

4.2.7 Validation of the assumption of complete mixing of Voëlvlei Dam

For this study, it was assumed that Voëlvlei was polymictic i.e. it was stratified during the day but is too shallow to exhibit seasonal stratification as well as being well mixed by the prevalent winds. To validate this, a tracer profile was plotted of the dam at segment 11 (the MWTP extraction point) for a series of depths as shown in Figure 42.

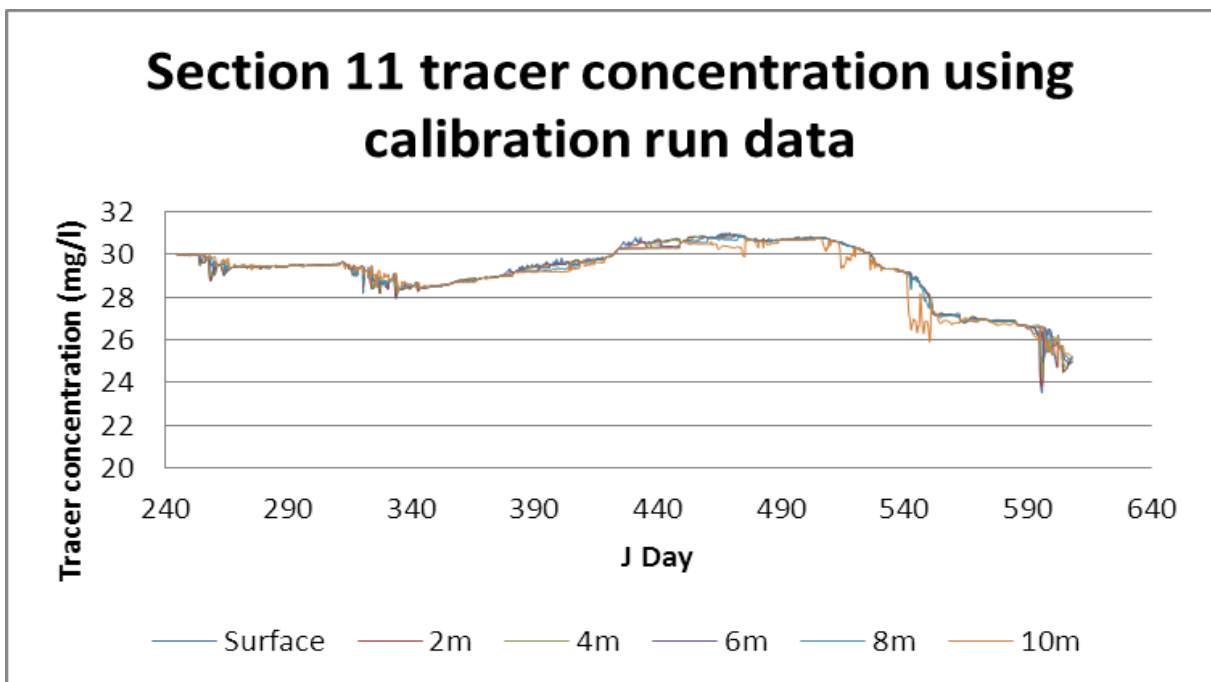


Figure 42 Tracer profile at segment 11 for various depths using calibration data

Thus, the assumption of complete mixing was vindicated as the tracer has equal concentration for a vertical profile in Voëlvlei Dam for the entire run period of 1 year. The applicability of this assumption was justified by the profile tracer concentration plot for a 20-year run as shown in Figure 43.

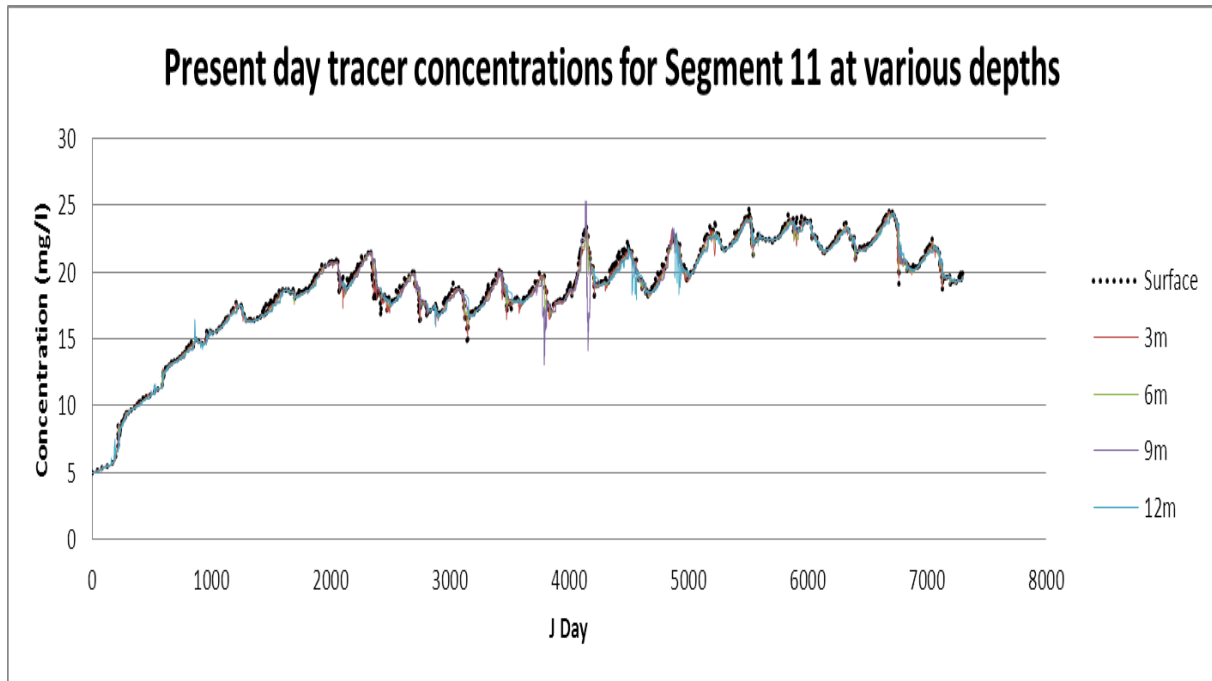


Figure 43 Vindication of the fully mixed assumption

For the entire 20-year simulation, a tracer concentration was plotted at various depths as shown in Figure 43 using the present day CCC climate change data. From this figure, it was seen that tracer concentration was relatively uniform for the various depth for the entire period, thereby justifying the assumption that Voëlvlei was fully mixed for the simulation period.

To investigate whether the dam was stratified for any significant period in winter or summer, the present day CCC air temperature and water temperature at various depths for a 20 year period was plotted. The result is shown in Figure 44.

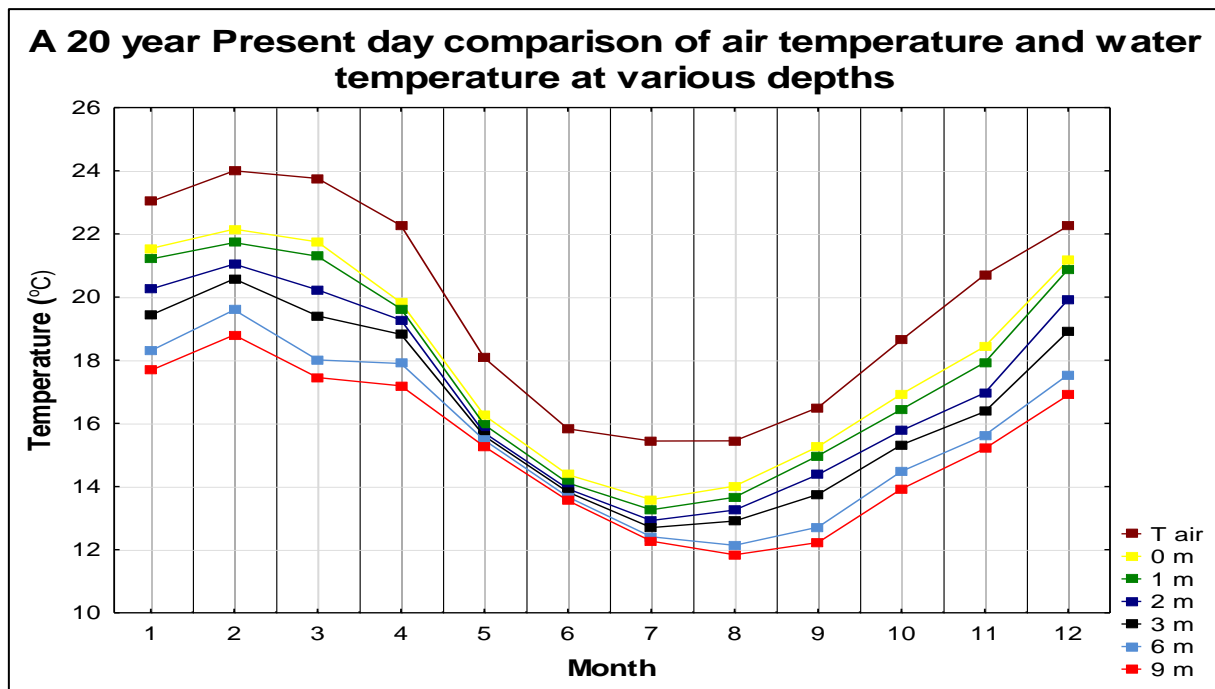


Figure 44 Present day air temperature driving Voëlvlei Dam water temperature

This figure shows that the monthly mean air temperature was warmer than the mean simulated surface water temperature. Upon examining the water temperatures, it was seen that the deeper water was cooler than the surface. This could be attributed to less penetration of incident solar radiation due to scattering as well as to increased mass of algae on the surface and at the surface interface the greatest heat transfer occurs, ensuring that the surface was warmer than water below. The temperature decrease with depth was linear for each month in contrast to stratified systems where the temperature changes stepwise, hence it was assumed that if stratification does occur it was not for a significant period, as it does not show in the figure. The vertical temperature variation was greater in summer than that of winter, implying that during winter the entire segment has nearly the same temperature from surface to bottom.

Thus, it may be valid to assume that Voëlvlei Dam was fully mixed and not stratified for any significant length of time.

4.3 DWA Target Water Quality Ranges

The South African Water Quality Guidelines Field Guide, Volume 8 of the South African Water Quality Guidelines series, is a compilation of all the different Target Water Quality Ranges (TWQR) for all the different water use sectors dealt with in volumes one to seven. These include Domestic Water Use (Volume 1), Recreational Water Use (Volume 2), Industrial Water Use (Volume 3), Irrigation Water Use (Volume 4), Livestock Watering (Volume 5), Aquacultural Water Use (Volume 6) and Aquatic Ecosystems (Volume 7).

The TWQR for a particular constituent and water use was defined as the range of concentrations or levels at which the presence of the constituent would have no known adverse or anticipated effects on the fitness of the water assuming long-term continuous use, and for safeguarding the

health of aquatic ecosystems. For the aquatic ecosystems guidelines the TWQR was not a water quality criterion as it was for other water uses, but rather a management objective that has been derived from quantitative and qualitative criteria.

The following tables are a summary of the TWQR field guide with specific emphasis on the constituents modelled for water quality.

Table 10 TWQR for the modelled water quality constituents

Constituent	TWQR			
	Aquatic ecosystem	Full contact recreational use	Human consumption	Other
Phosphate	<0.025mg/l	N/A		<0.1 mg/l for aquaculture
Ammonium	0-1 mg/l N has no health or aesthetic effects	N/A	0-1 mg/l	0-0.025 mg/l for cold water aquaculture 2-0.3 mg/l for warm water aquaculture
Nitrate-nitrite	0-6 mg/l N has no adverse health effects	N/A	0-6 mg/l for both species	0-100 mg/l for nitrite 0-10 mg/l nitrate for livestock watering
Dissolved oxygen	80-120% saturation	N/A	N/A	6-9 mg/l for cold water species and 5-8 mg/l warm water species for aquaculture
Dissolved silicon	N/A	N/A	N/A	0-150 mg/l for selected industries
Algae	See Table 11	0-15 mg/l	0-1 µg/l chl-a 0-50 algal cells/l 0-0.8 µg/l Microcystis	<6 µg/l Microcystis for livestock watering

Table 11 TWQR for all algae

Algal range ($\mu\text{g/l chl-a}$)	Effects
TWQR 0-1	Negligible risk of taste and odour
1-15	Slight green colouration of water at concentrations above 7 $\mu\text{g/l}$. Taste and odour problems can occur
Blue-green algae (cells/ml)	
TWQR 0-50	No health effects are experienced
50-14000	Possible chronic effects associated with long term ingestion
14000-42000	Possible acute hepatotoxic effects
>42000	Significant risk of acute and chronic effects
Microcystis range ($\mu\text{g/l}$)	
TWQR 0-0.8	No health effects expected
0.8-1	Possible chronic effects associated with long term ingestion
>1	Possible acute hepatotoxic effects

These limits were used to quantify the effect of the water quality variables for the climate study and their relative changes as influenced by climate change.

Once the model for Voëlvlei Dam had been implemented and the results for the validation and calibration period was compared to measured values and deemed to be of sufficient accuracy, the process of establishing a baseline present day scenario was undertaken. Following this, the effect of climate change would be completed and the present day scenario would be compared to the future scenarios with specific emphasis on algal growth.

5 THE CLIMATE CHANGE MODELLING RESULTS AND ANALYSIS

The CE-QUAL-W2 model was run with meteorological input data (air temperature, dew point temperature, wind-speed and direction, cloud cover and solar radiation) from the four climate models (CCC, CNRM, ECH and IPSL) and trends were noted from each of the runs and compared. For this study 1/1/1971-31/12/1990 represented the present time, 1/1/2046-31/12/2065 was the intermediate future and 1/1/2081-31/12/2100 was the distant future as seen in Figure 45.

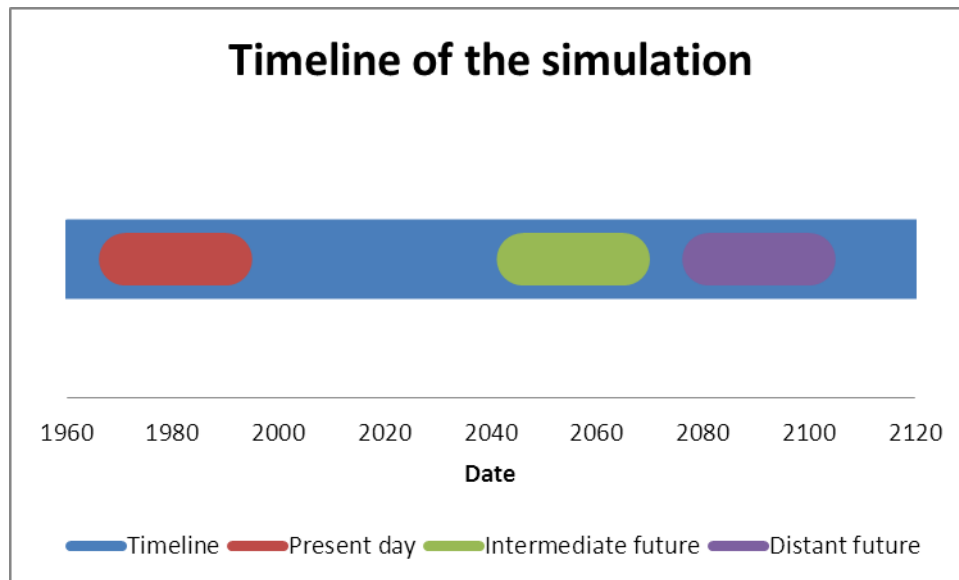


Figure 45 The timeline for climate change study

This figure shows that the period from the present day to the intermediate future was substantially longer than from the intermediate future to the distant future. This was a result of the climate change studies, which predicted an acceleration of climate change effects for the later part of the century due to the increased anthropogenic loadings. Any change from present day to intermediate future would happen at a slower pace than that from intermediate future to distant future.

The main objective of this study is to determine the long-term effect of climate change on surface water quality and the subsequent effect on eutrophication of surface water of Voëlvlei Dam and the resultant algal growth and possible algal succession. The present day simulations were used as the basis for comparison to the intermediate future and distant future scenarios, effectively highlighting changes caused by climate change. This procedure was considered accurate as it was validated and the present day quantification simulations for one year compared favourably to the actual measured data for Voëlvlei Dam. Climate model inter-variation would also be discussed, as it was clear that different climate models predicted varying climate change.

The more important site on the dam was considered the withdrawal site for the MWTW for Cape Town on segment 11 and hence all outputs and discussions were concentrated on this area.

High algal concentrations are indicative of poor water quality and that algal growth was affected by temperature, light and nutrients. In the event of climate change, the air temperature was expected

to increase as well as anthropogenic loadings. Thus to identify the variable that managers and operators of large dams could control to limit poor water quality with respect to algal growth consisted of:

- Identification of factors affecting algal growth;
- Quantification by how much it affects algal growth; and
- Identification of possible sources for reduction of these variables.

Of the factors mentioned in Section 2.4, temperature and light are two of the variables that are to impractical to try to manipulate to control algal growth. It was only nutrients, which may be removed before it enters the catchment and receiving waters that would limit algal growth.

5.1 THE PRESENT DAY SCENARIO

The model had been calibrated previously and was now run for 20 years using the provided climate model data as meteorological input. The inflows, withdrawals and wind-speed are kept the same for each year of the simulation.

The factors that limit algal growth are water temperature and solar radiation, if all other factors such as light, nutrients and dissolved oxygen are in abundance (Wetzel, 2001). Solar radiation emitted by the sun was relatively constant and the incident solar radiation over Voëlvlei Dam was affected largely only by cloud cover. Thus, the only factors that directly affect surface water temperature were air temperature (by conduction) and short-wave solar radiation and their relative contributions were to be assessed.

5.1.1 Air temperature

Carbon dioxide (CO₂), methane (CH₄), chlorofluorocarbons (CFCs), nitrous oxides (NO_x) and water vapour (H₂O) in the atmosphere allow the passage of shortwave solar radiation from the sun onto the earth surface, whilst absorbing the re-radiated radiation from the earth allowing the heating of the earth and the air. This heating was dubbed the *Greenhouse Effect* (Carter et al., 1994).

Four GCMs' were statistically downscaled to RCMs' over Voëlvlei Dam and these climate models predict amongst others, air temperature. The mechanism of the greenhouse effect would heat the air from the present day temperatures to a higher future temperature. It was postulated that this increase would alter the state of dams and contribute to worsening water quality by increasing algal biomass concentrations at the current cultural eutrophication rate.

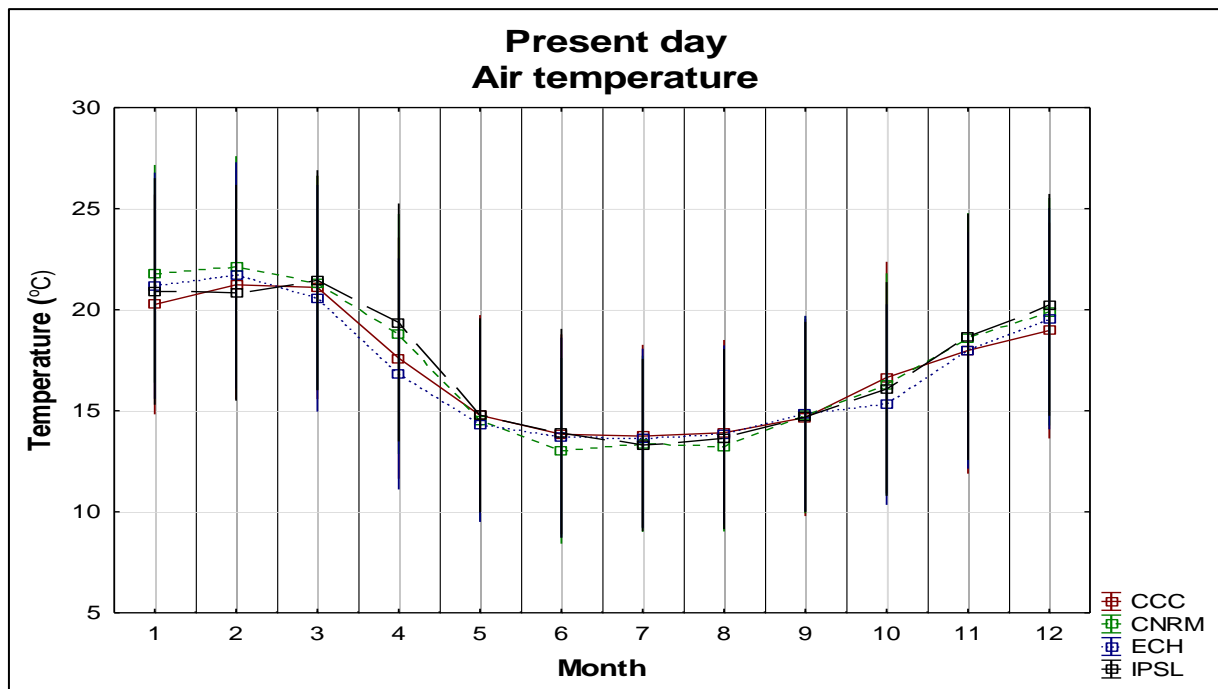


Figure 46 Present day mean air temperature predictions

Figure 46 and Table 12 show that all four climate models predicted similar mean monthly air temperatures for the 20 year present day simulation period. This mean temperature included day and nighttime temperatures. The inter-variation between climate models was minimal but they could be ranked in order of increasing present day temperatures as ECH, CCC then CNRM and IPSL models.

Table 12 Present day mean air temperature (°C)

	Jan	Feb	Mar	Apr	May	Jun	Jul	Aug	Sep	Oct	Nov	Dec
CCC	20.3	21.2	21.1	17.6	14.8	13.8	13.7	13.9	14.7	16.6	18.0	19.0
CNRM	21.8	22.1	21.3	18.8	14.5	13.0	13.4	13.2	14.8	16.3	18.6	19.9
ECH	21.2	21.7	20.6	16.8	14.3	13.7	13.6	13.8	14.9	15.3	18.0	19.6
IPSL	20.9	20.8	21.5	19.4	14.8	13.9	13.3	13.6	14.7	16.1	18.7	20.2

The mean monthly air temperatures of the four climate models were similar in magnitude and cycle. The colour represents the magnitude with red being greater than green. Winter was May to July and summer was December to March. The annual mean temperature of all the models was 17.2 °C, which was expected to increase with climate change into the future because of the greenhouse effect. There was almost a 7 °C difference between winter and summer.

5.1.2 Solar radiation

Each of the present day climate models predicted similar levels of solar radiation as shown in Figure 47 for the 20-year modelling period. It was discussed by Wetzel (2001) and DeNicola (1996) that solar radiation was the major driver for diurnal surface water temperature and hence algal growth, with all the other factors that may affect algal growth being equal. Thus, water

temperature may limit algal growth even in the presence of abundant nutrients and light, which may favour growth.

All organisms have a temperature range at which optimal growth occurs, thus their life cycles are directly linked to temperature. Temperature primarily affects the algal photosynthetic metabolism by controlling the enzyme reaction rate of the algae and an optimum temperature for each species was observed (DeNicola, 1996). Thus, diurnal algal growth was directly influenced by solar radiation intensity.

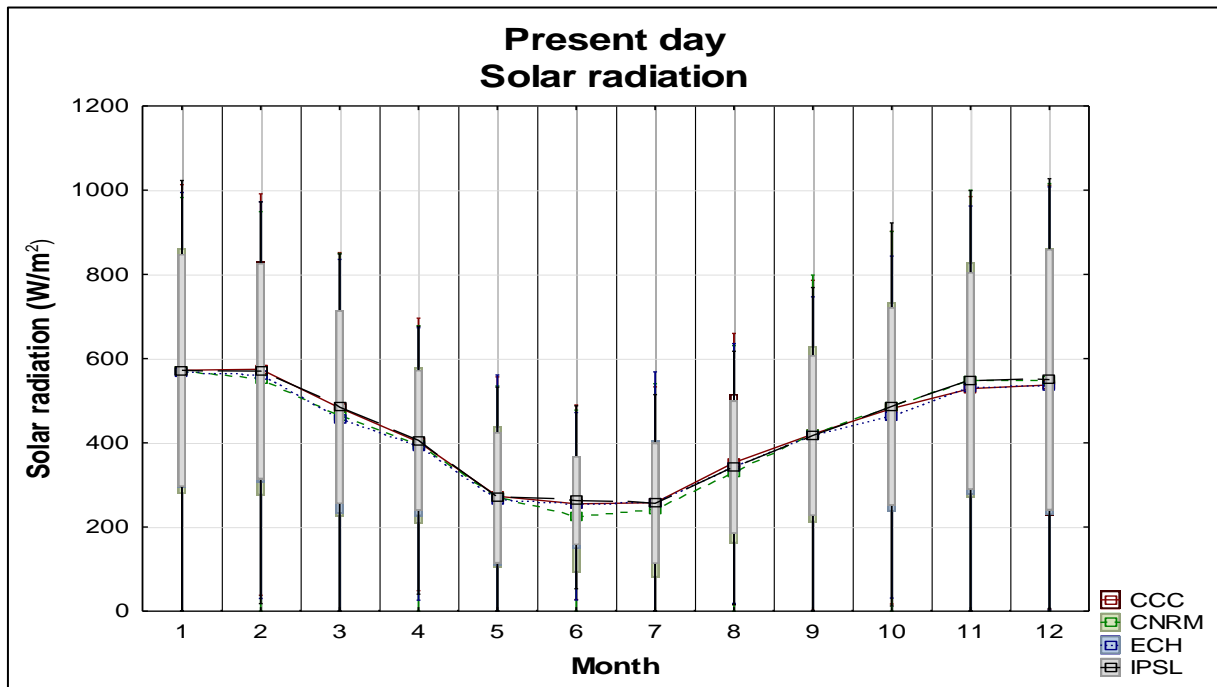


Figure 47 Present day solar radiation

Figure 47 and Table 13 show the mean monthly daily solar radiation for the 20 year present day simulation period for each of the four climate change models over Voëlvlei Dam. This figure had a similar shape as that for air temperature.

Table 13 Present day mean monthly daytime solar radiation (W/m²)

	Jan	Feb	Mar	Apr	May	June	July	Aug	Sep	Oct	Nov	Dec
CCC	572.41	574.81	482.98	401.93	272.96	255.17	257.74	353.15	420.71	481.32	528.79	537.51
CNRM	570.46	550.86	463.63	393.87	271.20	224.97	241.44	329.92	420.39	485.71	548.43	548.74
ECH	567.62	560.20	457.54	390.07	265.55	253.29	258.58	341.92	417.73	463.23	530.32	533.86
IPSL	572.12	570.31	484.59	406.02	269.51	262.68	256.26	342.25	417.40	486.36	547.11	550.12

From this table and figure, it was seen that the climate models agreed well with each other. Summer was December, January and February, whilst winter was June, July and August for the Western Cape Province, the location of Voëlvlei Dam. The solar radiation was on average almost double in summer to that of winter, which was attributed to the longer daylight hours during summer. The phenomena of higher solar radiation in summer should have a marked effect on the

diurnal temperature of the dam (Wetzel, 2001 and others) and its influence along with air temperature will be addressed in the following sections.

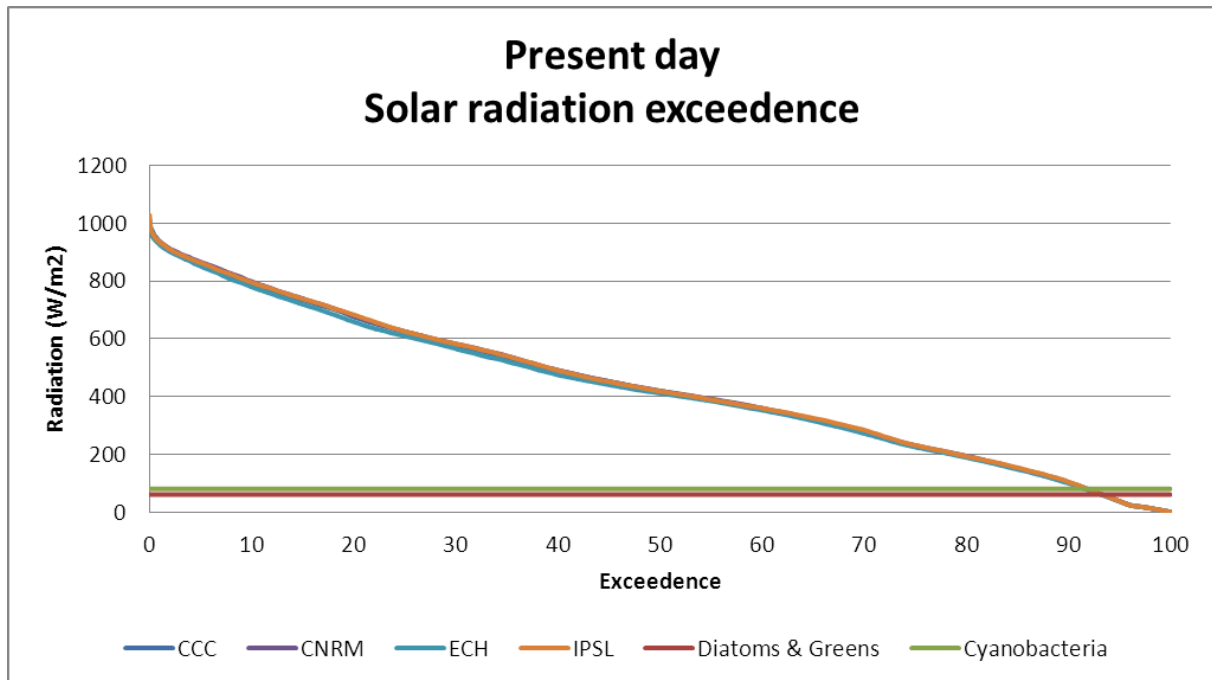


Figure 48 Present day solar radiation exceedance for light saturation

To investigate the effect of solar radiation on the light saturation of algal groups modelled, Figure 48 shows that for approximately 93% of the simulation period the solar radiation exceeded the maximum algal light intensity for maximum photosynthetic rate for all the algal groups. This implied that only for 7% of the time, the light intensity allowed for the maximum algal growth. This was a consequence of the choice of algal constants but these values were supported by literature. This would imply that these particular algal groups prefer less sunny conditions i.e. they prefer shade.

The four climate models agreed in solar radiation magnitude and its peaks were greater in summer than winter.

5.1.3 Wind-speed and direction

Wind-speed and direction was not by CSAG (UCT) and was a limitation. CE-QUAL-W2 requires wind-speed and direction as part of its meteorological data input to predict water quality. In the absence of this, wind-speed and direction was replicated from past data. For 1971 the recorded wind-speed and direction from 1 January 1971 to 31 December 1971 was repeated for the 20 years of all the simulation periods including the intermediate and future events, in the absence of any downscaled data. This should not be a problem as the study was to show changes in eutrophication due to varying climate conditions.



Figure 49 The N-S orientation of Voelvlei Dam

Figure 49 shows that the reach of Voelvlei Dam was almost exactly oriented in a NS direction and the subsequent effect of the prevalent wind over the dam was investigated.

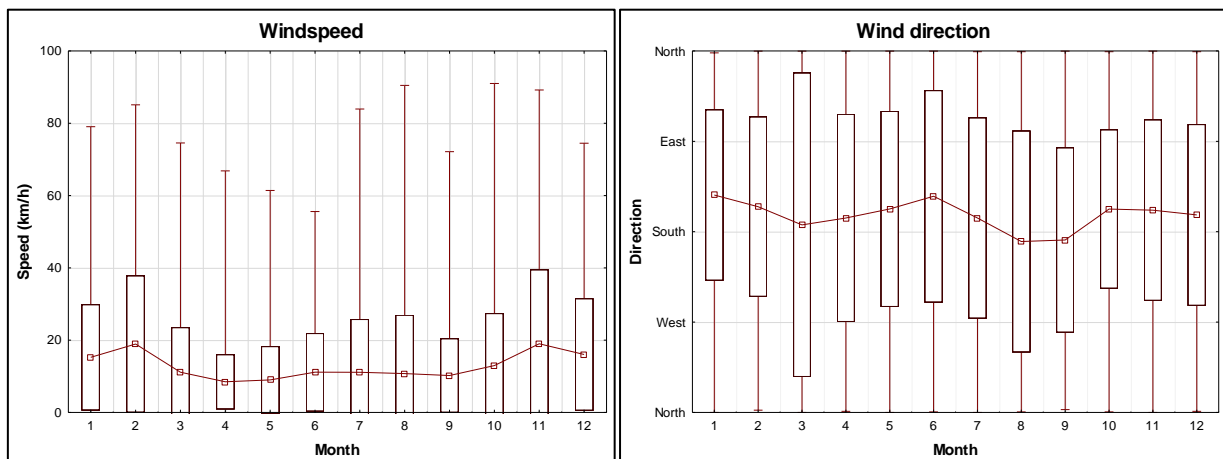


Figure 50 Wind-speed and direction over Voelvlei Dam

From Figure 50 it was seen that the predominant annual wind was between south and south-west and thus somewhat along the S-N axis and was strongest during summer. Since the dam was relatively shallow (10-15m) this wind and the hydraulics of the dam caused complete mixing as confirmed by the tracer concentrations as seen in Figure 42 previously.

5.1.4 Surface water temperature

Wetzel (2001), DeNicola (1996) and others argue that solar radiation was the major driver for surface water temperature, thus the following two figures shows the surface water temperature of segment 11 for the present day 20 year climate models.

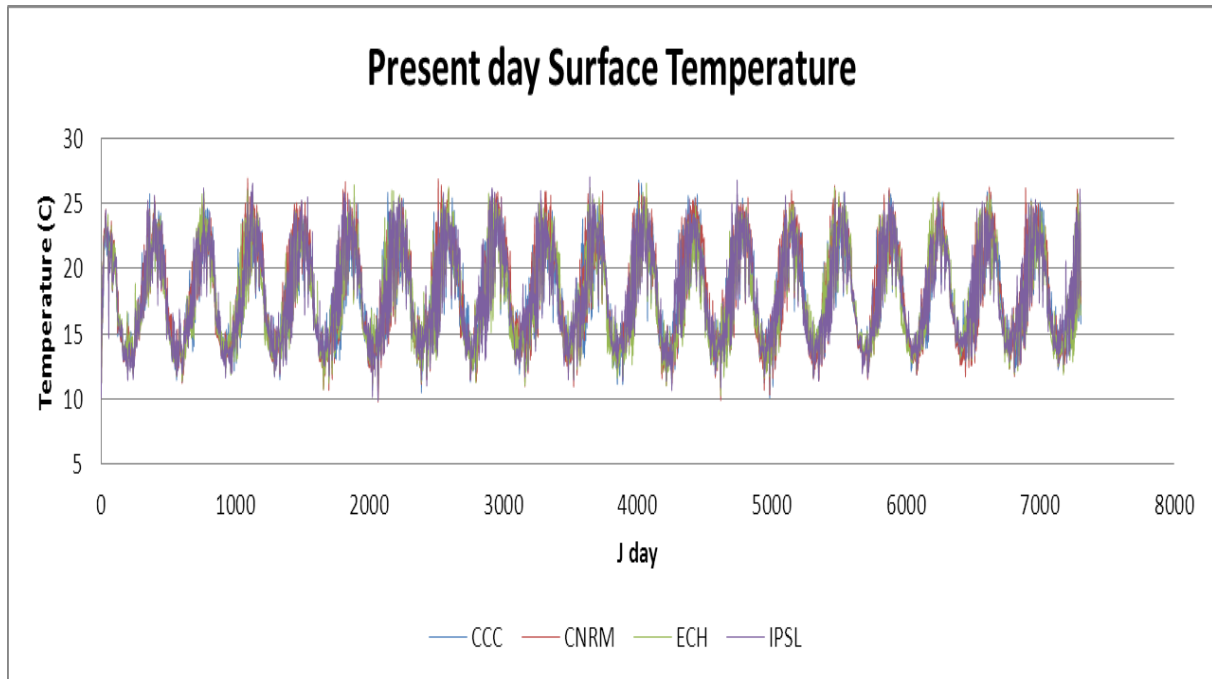


Figure 51 Surface water temperatures at segment 11

This figure shows the seasonal temperature fluctuations coinciding with the peaks and troughs of Figure 51 as well as the agreement between the various climate models producing similar surface water temperatures at segment 11. If the 20 year present day simulation period was further subdivided into monthly segments the following figure results.

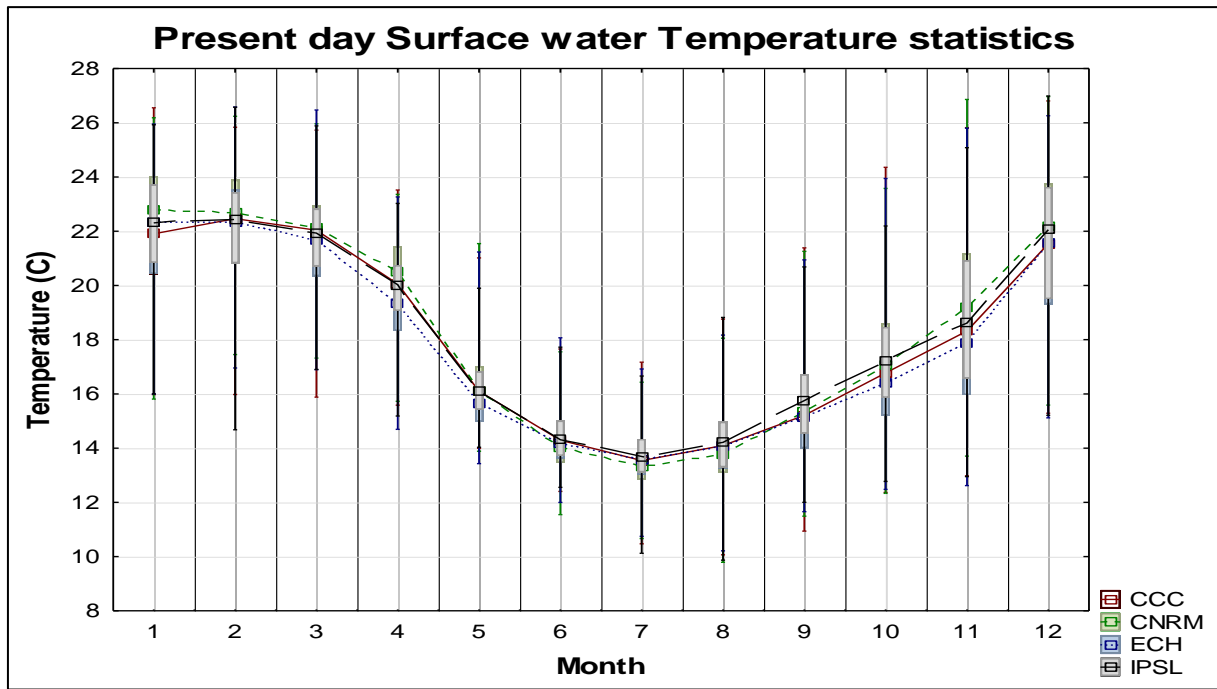


Figure 52 The monthly surface water temperature for segment 11

When comparing Figure 47 and Figure 52 a confirming relationship was observed in that months with high solar radiation had high surface water temperatures. There was a notable temperature drop between April and May and this was considered the onset of winter just as there was a notable temperature increase from November to December signalling the onset of summer. These trends are verified by all four climate change models. From this, it was deduced that an increase in solar radiation would increase the surface water temperatures and consequently may cause an increase in the number of algal blooms if all other conditions (nutrients, turbidity etc.) are favourable. This cycle would predict the annual seasonal blooms in the dam.

Table 14 Present day mean surface water temperature (°C)

	Jan	Feb	Mar	Apr	May	June	July	Aug	Sep	Oct	Nov	Dec
CCC	21.6	22.2	21.7	19.8	16.3	14.4	13.6	14	15.3	16.9	18.4	21.2
CNRM	22.4	22.5	22.0	20.3	16.3	14.1	13.4	13.7	15.3	17.2	19.1	21.7
ECH	22.0	22.2	21.4	19.3	15.8	14.3	13.6	14.0	15.2	16.5	18.1	21.3
IPSL	22.1	22.1	21.7	19.8	16.2	14.4	13.7	14.1	15.7	17.2	18.8	21.6

Table 14 shows that the surface water temperature of Voëlvlei Dam was on average 5.3°C warmer in summer than winter with an annual surface water temperature of 18°C. All four climate models showed similar trends and values. Thus, it was expected that if all conditions are favourable, then an increase in the concentration of algae be expected in the summer period due to the average summer surface water temperature coinciding within the temperature rate multipliers for the diatoms, greens and cyanobacteria modelled in Voëlvlei Dam (Table 9).

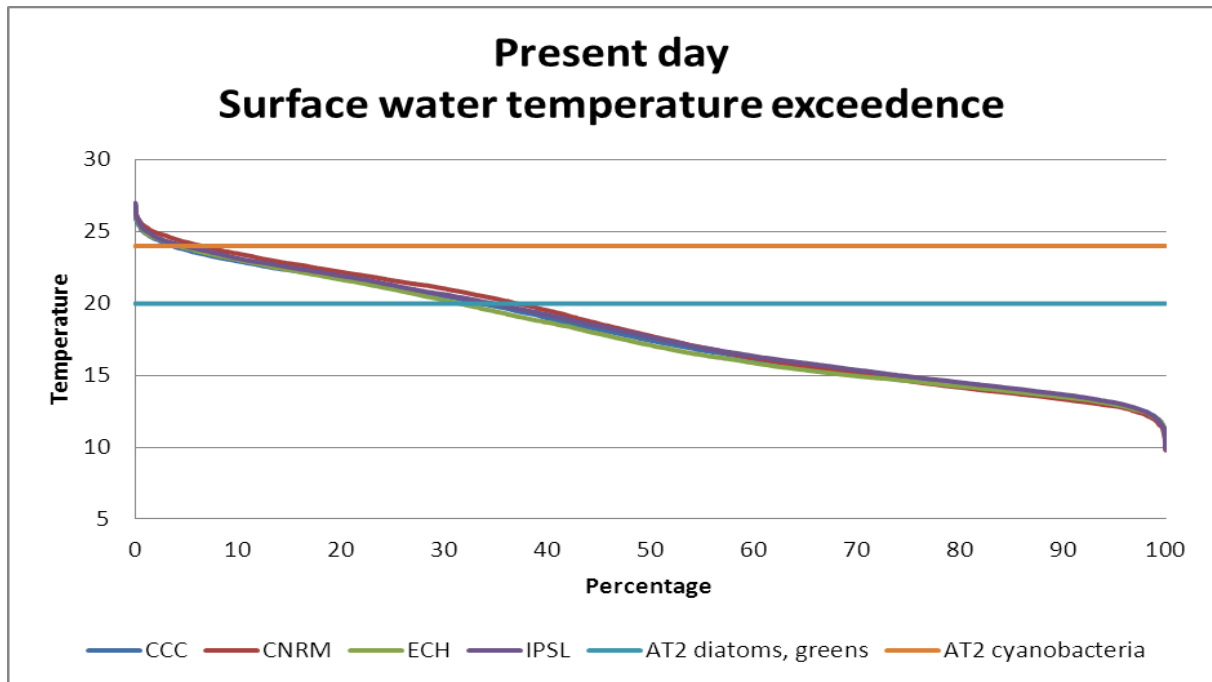


Figure 53 Present day surface water temperature exceedance plot

To establish the probability of the types algal blooms, an exceedance plot (Figure 53) was produced showing the algal temperature growth multipliers. The temperature rate multiplier for diatoms and greens that set the lower temperature limits (AT2) for maximum growth was exceeded between 33 and 38% of the simulation time. Cyanobacteria have a higher maximum temperature growth rate and this temperature was exceeded between 5 and 8% of the time of the 20-year simulation at segment 11. It was hereby expected that diatoms and green algae could be present in Voëlvlei Dam for up to 38% of the time and cyanobacteria up to 8% of the time, due to the temperature being favourable for their growth.

The higher solar radiation of summer caused higher surface water temperatures in summer than winter.

5.1.5 Surface water elevation

The factors affecting surface water elevations were:

- Inflow;
- Withdrawals; and
- Evaporation.

The inflows and withdrawals were kept the same for each year as well as for each model, thereby implying that only evaporation could change water levels due to climate change. The surface water elevation for the 20-year present day period was shown in the following figure as well as its monthly values. The various undulations are a result of the inflow and withdrawals and the inter-variation between climate models was a result of the evaporative differences between models.

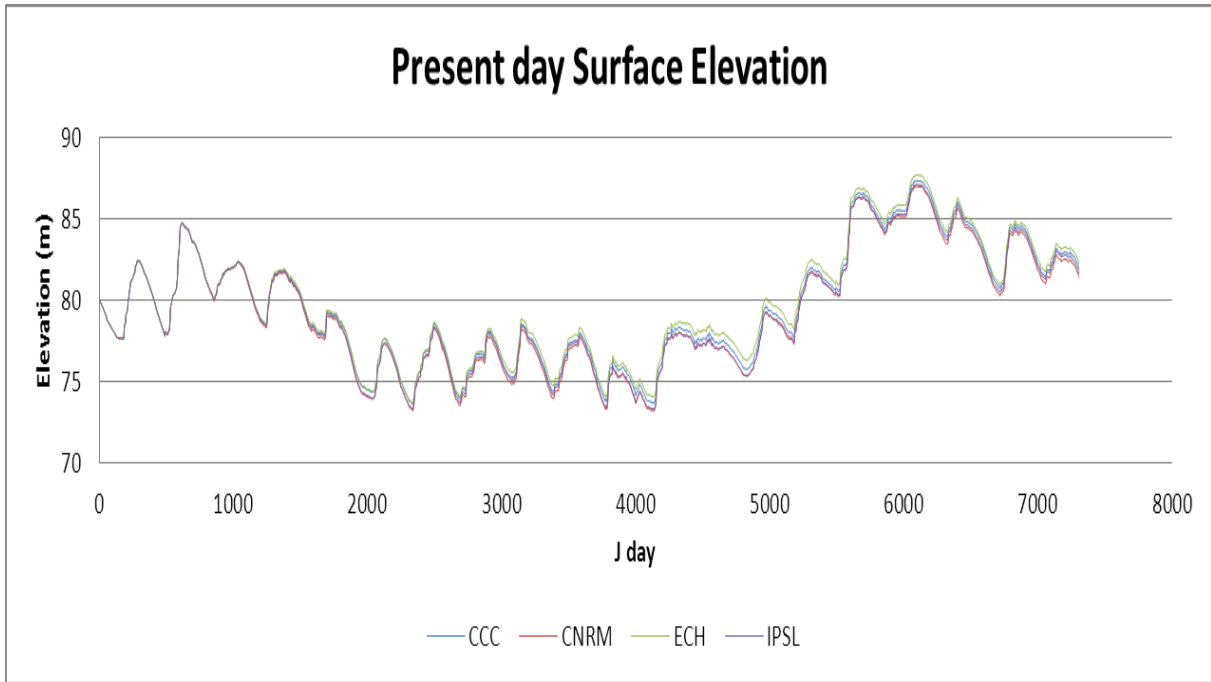


Figure 54 Present day surface water elevations

Figure 54 shows close agreement within all the climate models for the 20 year present day simulation period. The surface water level discrepancies are attributed to the inter-climate model air temperature and solar radiation variations causing varying rates of evaporation and subsequent different surface elevations.

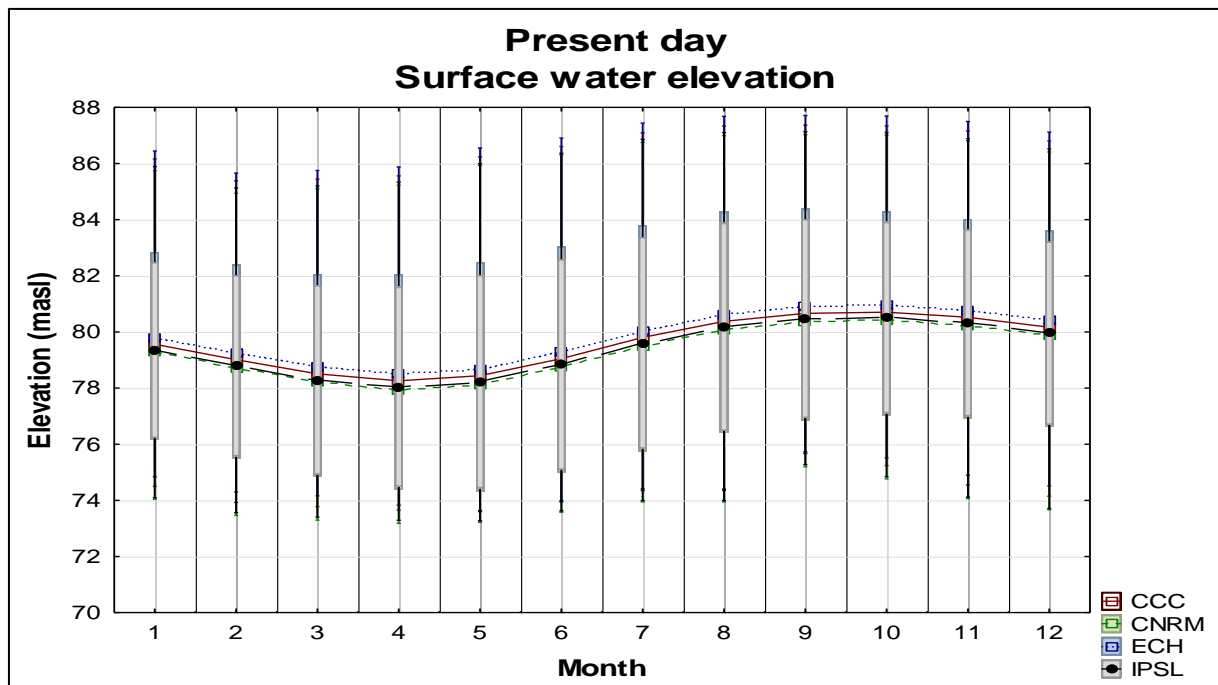


Figure 55 The monthly surface water elevations

Figure 55 and Table 15 show the monthly surface elevations as well as the inter-variation between climate models for the current set of inflow and withdrawals into Voëlvlei Dam during the period of

the simulation. It was seen that the air temperature difference between climate models was similar and that the subsequent surface water elevations were relatively small.

Table 15 Present day mean surface water elevations (masl)

	Jan	Feb	Mar	Apr	May	June	July	Aug	Sep	Oct	Nov	Dec
CCC	79.6	79.0	78.5	78.3	78.4	79.0	79.8	80.4	80.7	80.7	80.5	80.2
CNRM	79.3	78.7	78.2	77.9	78.1	78.7	79.5	80.1	80.4	80.4	80.2	79.9
ECH	79.8	79.2	78.7	78.5	78.7	79.3	80.0	80.6	80.9	80.9	80.8	80.4
IPSL	79.4	78.8	78.3	78.0	78.2	78.8	79.6	80.2	80.5	80.5	80.3	80.0

The dam showed the lowest level at the end of summer and onset of autumn, corresponding to March and April and this continued until the rains of late autumn and early winter inflow whereby the capacity was augmented.

It was seen that the dam has a stable monthly surface elevation that oscillates by about 2 masl on a monthly basis and that all the climate models agreed well with each other.

5.1.6 Algal nutrient inflow concentrations

Voëlvelei Dam is an off-channel dam and water is diverted to it from the Klein Berg and Twenty Fours Rivers. The only water quality constituents pertinent to this study were measured on an irregular basis was the surface concentrations of PO₄, ammonium, nitrite-nitrates and dissolved silicon at the dam wall.

The total inflow of PO₄, NH₄ and NO₃ is shown in Figure 56 and it shows that the concentration of phosphates and ammonium entering the dam was stable but that the nitrite-nitrate concentration fluctuates on a monthly basis, probably due to it being downstream of a municipal wastewater treatment plant (MWWTP). The inflow concentration of phosphates and nitrogen was of adequate concentration so that it was not considered to be limiting for algal growth.

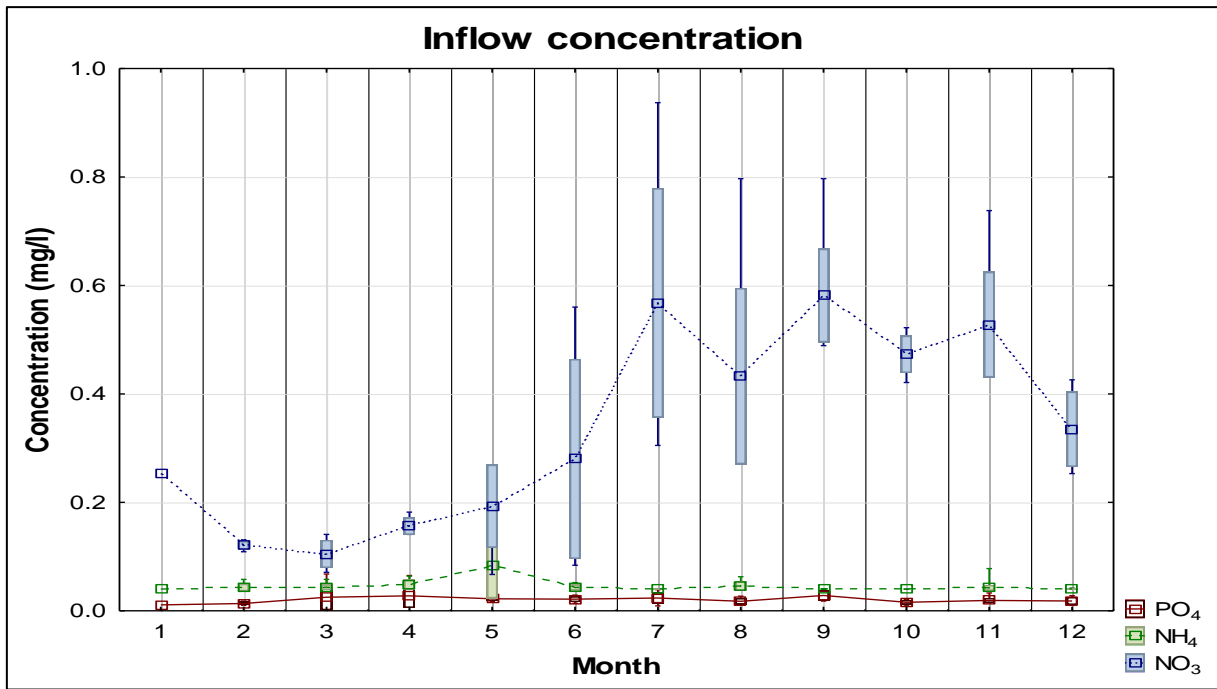


Figure 56 Constituents concentration in the inflow of Voëlvlei Dam

The dissolved silicon inflow concentration for the two inflow canals shown in Figure 57 fluctuates monthly but the overall concentration was not low enough to be limiting for diatom growth.

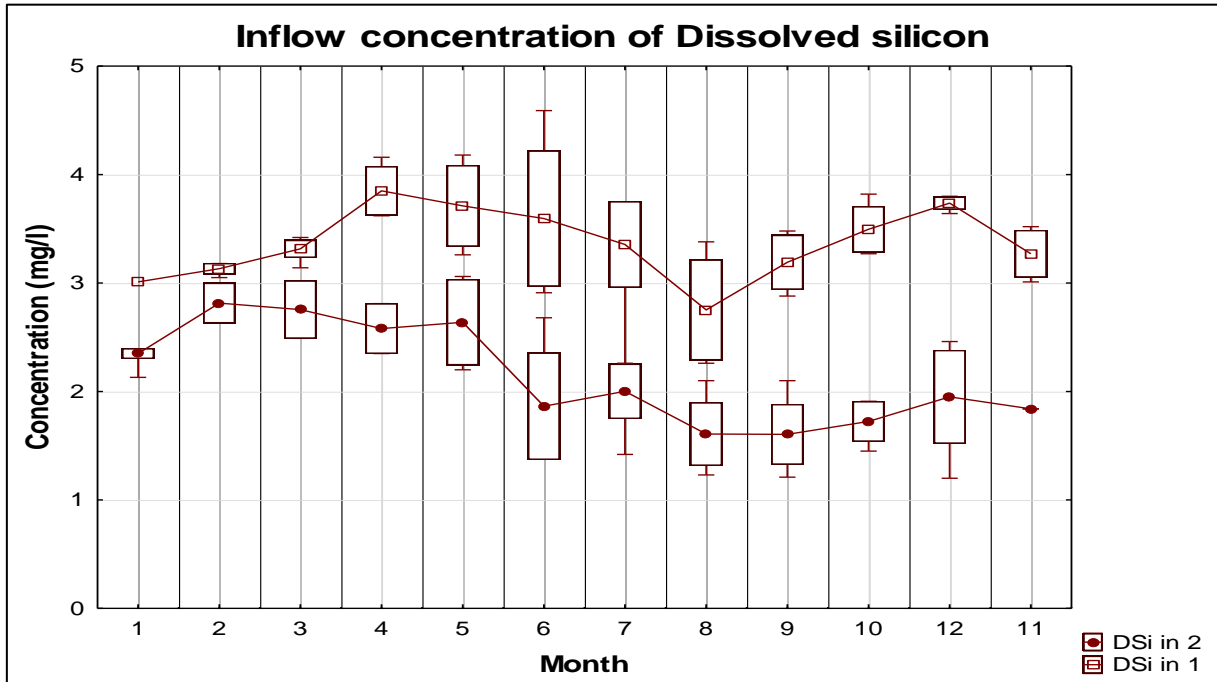


Figure 57 Dissolved silicon inflow concentration

These inflow concentrations and volumes would not change for the intermediate future and distant future simulations thus allowing for a direct comparison with the only effect on the surface water being that of air temperature change. This allowed for a direct comparison of climate change

influence on Voëlvlei Dam, as it assumed that the current set of operating parameters would be valid.

5.1.7 Ortho-Phosphorus concentration

The phosphorus concentration within the dam was influenced by various factors such as inflow and withdrawal quantities as well as assimilation by the various algae as it was the limiting nutrient for algal growth. The fluxes affecting in-dam phosphorus concentrations are shown in Figure 14 as used by the CE-QUAL-W2 model. The present day ortho-phosphorus concentration for Voëlvlei Dam of the four climate models was shown in Figure 58, Figure 59 and Table 16.

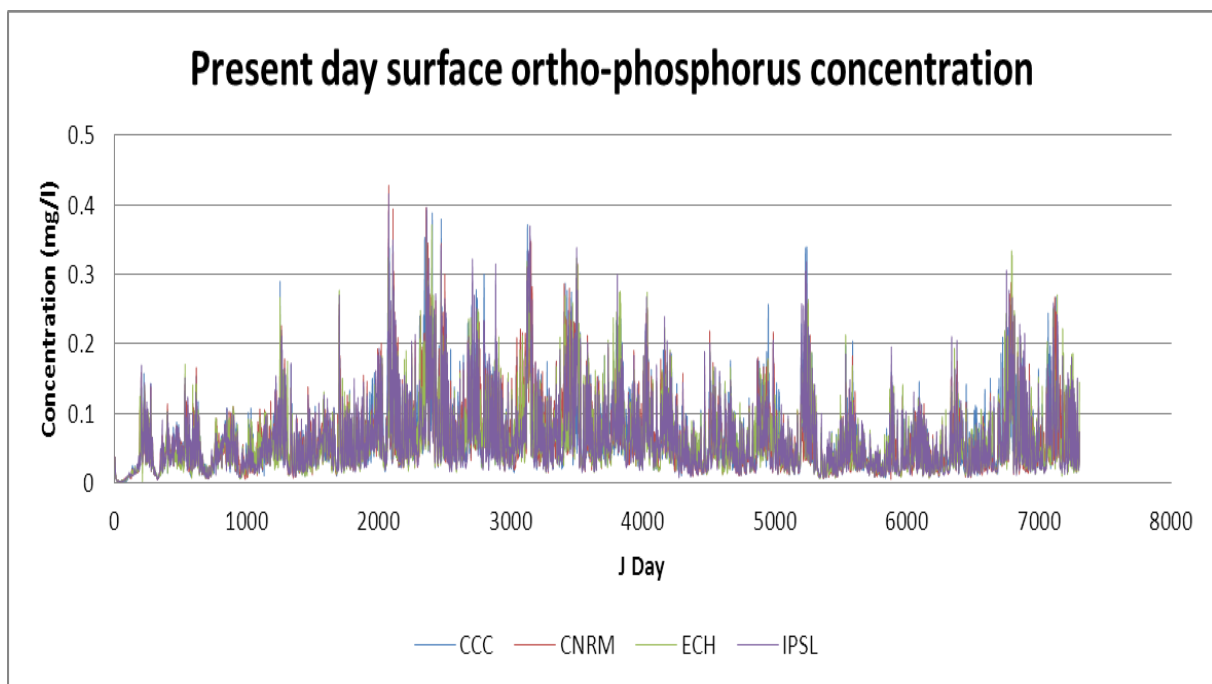


Figure 58 Present day ortho-phosphorus concentration at segment 11

The phosphorus concentrations agree well using the recorded set of inflow and withdrawals from Voëlvlei Dam. This shows that the inter-climate sink of phosphorus was the same as all the climate models agree well with each other. The average concentration was shown in Figure 59 and was well above the level of 0.025 mg/l set by DWA in 1985 (DWA, 2011).

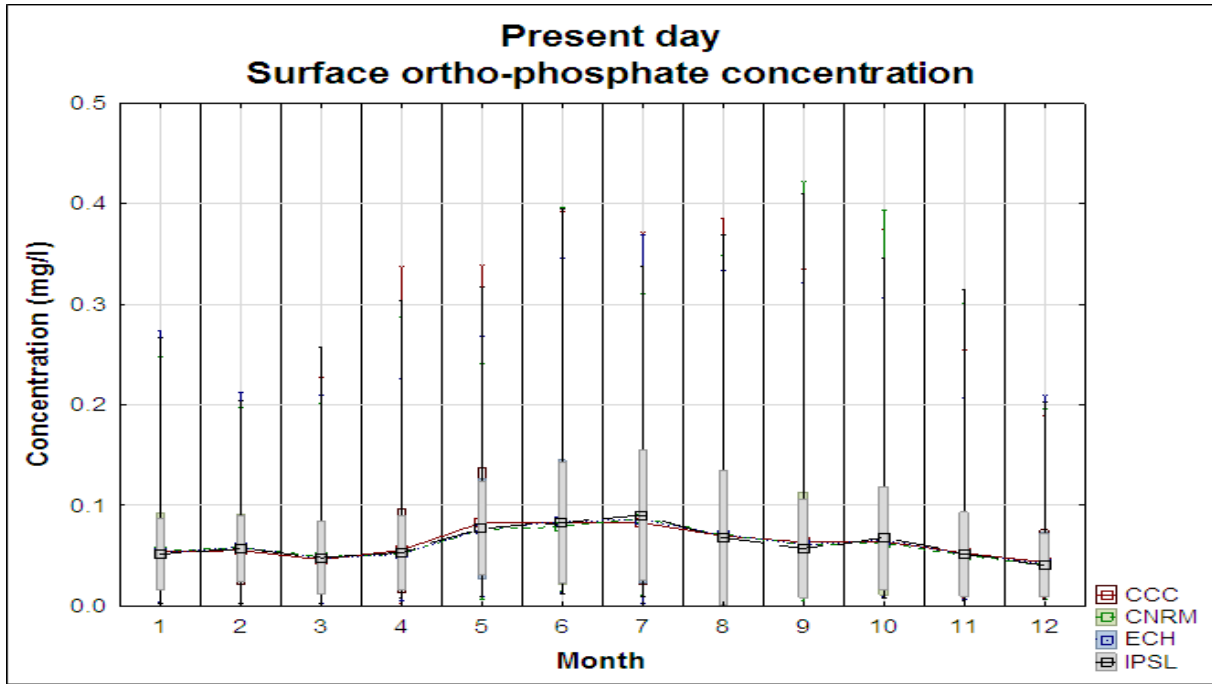


Figure 59 The present day monthly ortho-phosphorus concentration

Table 16 Present day mean surface ortho-phosphorus concentration (mg/l)

	Jan	Feb	Mar	Apr	May	Jun	Jul	Aug	Sep	Oct	Nov	Dec
CCC	0.054	0.055	0.046	0.055	0.083	0.083	0.083	0.070	0.063	0.064	0.053	0.044
CNRM	0.055	0.058	0.049	0.052	0.076	0.079	0.087	0.070	0.062	0.063	0.051	0.041
ECH	0.053	0.058	0.047	0.052	0.076	0.084	0.086	0.071	0.061	0.065	0.052	0.042
IPSL	0.052	0.057	0.048	0.053	0.077	0.083	0.090	0.068	0.057	0.067	0.051	0.040
Monthly mean	0.053	0.057	0.048	0.053	0.078	0.082	0.087	0.070	0.061	0.065	0.052	0.042

It was clear that phosphorus has an annual cycle with maximum concentrations reached during winter and the concentration was sufficiently high enough so as not to limit algal. From Table 8 it was seen that the phosphorus half saturation constants for diatoms are 0.002 mg/l, greens 0.38 mg/l and cyanobacteria 0.011 mg/l. The half saturation was defined as the concentration at which the uptake of phosphorus was half the maximum rate, thereby limiting algal growth. From Table 16 it was seen that these values are always exceeded except for that of the greens. This would imply that on average green algae growth was phosphorus limited for segment 11 at the surface. The corollary was that should the phosphorus loading increase, the growth of green algae could become unabated.

If algal blooms were to be controlled, it would be imperative to abate the inflow of phosphorus into Voëlvlei Dam. This would be achieved by lowering the inflow concentrations via legislation and applying new technologies or cleaner production to the WWTP upstream to the dam of phosphates as well as eliminating non-point sources.

The mean level of 0.025mg/l of phosphorus (DWA limit) in the dam was always exceeded for the duration of the present day simulation. Only green algae may become limited as its phosphorus half saturation constant was seldom exceeded.

5.1.8 Nitrogen concentration

Nitrogen was an abundant element in nature and is an essential building block of proteins and a constituent of chlorophyll. The sources of N with respect to water quality tests are ammonia (NH_3), ammonium (NH_4^+), nitrites (NO_2^-) and nitrates (NO_3^-) as well as atmospheric N, which are fixed by certain algae. From the aspect of eutrophication, it was very seldom that nitrogen is the limiting nutrient within a water-body as it is so abundant.

Ammonia was produced by the decomposition of organic matter that contains ammonia as well as being a constituent of sewage and industrial effluents. Nitrite occurs naturally as an anion in fresh and sea waters, whereas anthropogenically it was introduced to receiving waters as wastes from aquaculture, sewage effluents and industrial effluents. Nitrates are scarce in natural water sources as they are constantly being depleted by the process of photosynthesis, converting nitrates to organic nitrogen. For the purpose of this study, both ammonium and nitrites were included in the inflow into Voëlvlei Dam.

5.1.9 Ammonium concentration

Ammonia exists in two forms in nature (ammonium and ammonia) and the equilibrium concentrations are governed largely by pH (Chapra, 2008). Figure 60, Figure 61 and Table 17 shows the surface ammonia concentration at segment 11 of Voëlvlei Dam for the 20-year present day simulation.

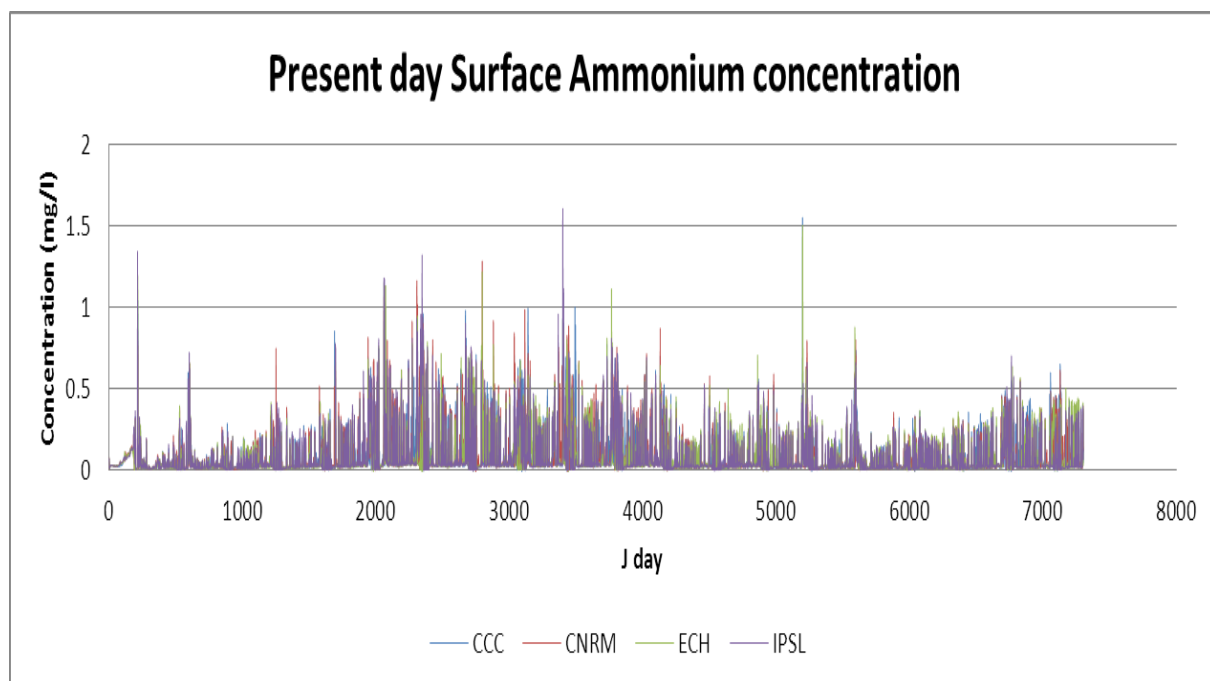


Figure 60 The present day ammonium concentration for Voëlvlei Dam

Cyanobacteria such as *Anabaena* sp. and others can utilise the nitrogen present in the atmosphere for growth and hence it was not seen as limiting for their growth (Dallas and Day, 2004) and for this study, they were modelled as nitrogen fixing. From an eutrophication management aspect, it is easier to manage and police the anthropogenic loading of a water system so that the subsequent abatement of eutrophication may take place but the case for nitrogen management was not easy or practical as it is abundant in the system. Nitrogen was essential for growth but rarely a limiting growth element for algae.

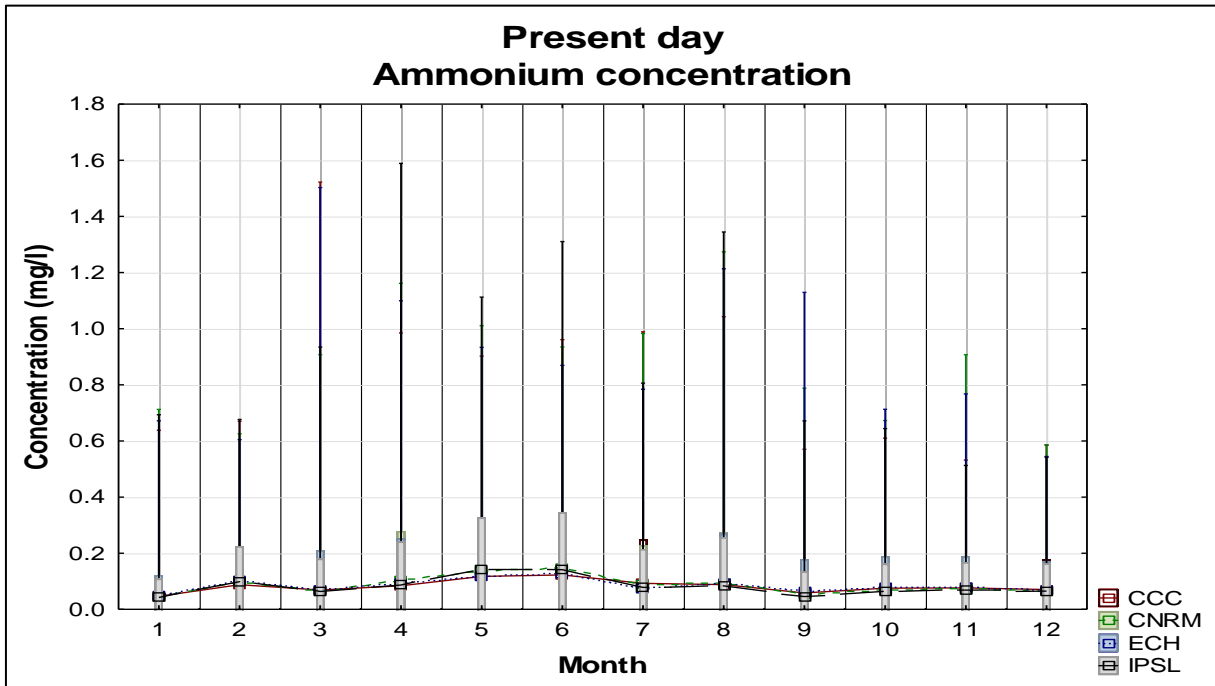


Figure 61 The monthly present day ammonium concentration

From Figure 61 and Table 17 it was seen that the surface ammonium concentration was a maximum during May and June and was in sufficient concentration so as not to limit algal growth. The climate models also show little inter-variability and the results compare well with each other.

Table 17 Present day mean surface ammonium concentration (mg/l)

	Jan	Feb	Mar	Apr	May	June	July	Aug	Sep	Oct	Nov	Dec
CCC	0.046	0.088	0.069	0.084	0.118	0.123	0.093	0.088	0.058	0.076	0.076	0.071
CNRM	0.046	0.096	0.063	0.105	0.136	0.149	0.086	0.093	0.056	0.068	0.073	0.065
ECH	0.049	0.101	0.068	0.095	0.115	0.125	0.076	0.094	0.064	0.078	0.077	0.067
IPSL	0.042	0.098	0.064	0.087	0.142	0.141	0.078	0.084	0.046	0.064	0.069	0.065

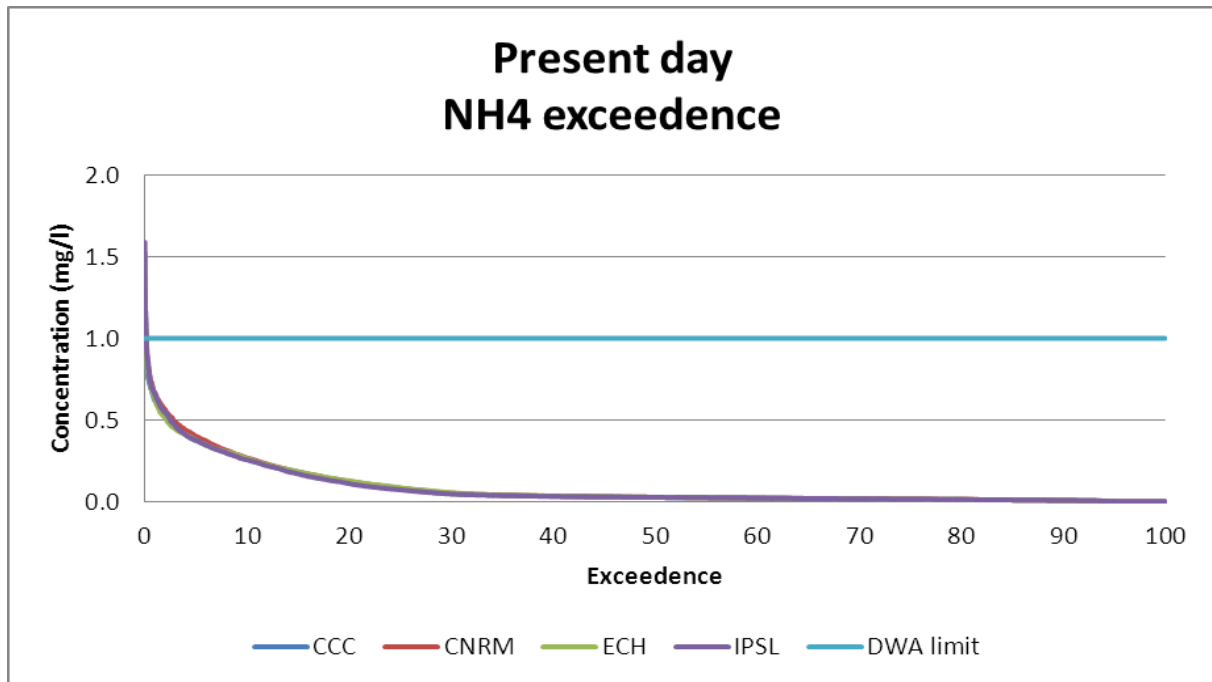


Figure 62 Present day surface ammonium exceedance plot

The guideline limit for ammonium in surface water is set at 1mg/l by DWA and Figure 62 shows the exceedance plot for this limit. The figure shows that the surface ammonium concentration never exceeded the DWA limit of 1mg/l for any relevant time.

5.1.10 Nitrate-nitrite concentrations

Figure 63, Figure 64 and Table 18 show the surface Nitrite-nitrate concentrations for segment 11 for the present day 20-year simulation. It was assumed that low concentrations of nitrite-nitrates was due to assimilation by algae as well as redistribution in the water column (Figure 15).

The figures show an increase in concentrations at the surface during the winter months as well as close agreement for the climate models.

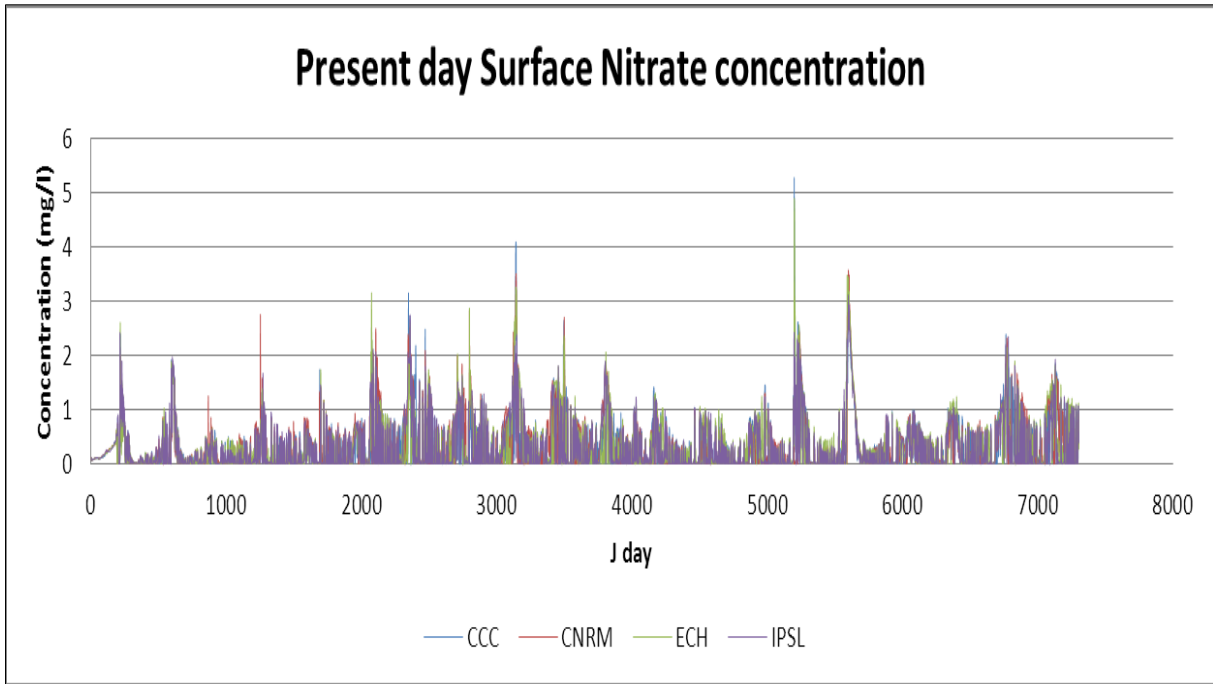


Figure 63 Present day nitrite-nitrate concentrations

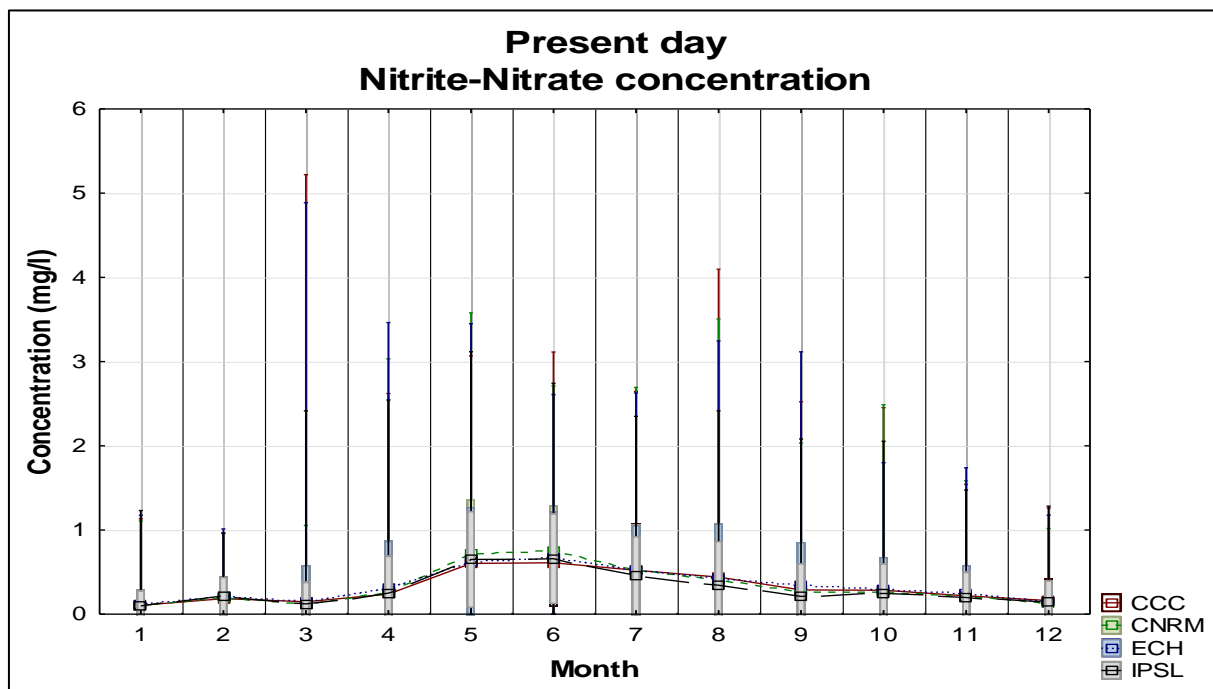


Figure 64 Monthly present day Nitrite-Nitrate concentrations

Table 18 Present day mean surface Nitrite-Nitrate concentration (mg/l)

	Jan	Feb	Mar	Apr	May	June	July	Aug	Sep	Oct	Nov	Dec
CCC	0.105	0.185	0.147	0.239	0.603	0.611	0.522	0.441	0.288	0.284	0.218	0.161
CNRM	0.105	0.204	0.116	0.264	0.715	0.746	0.522	0.409	0.260	0.263	0.208	0.136
ECH	0.112	0.214	0.152	0.314	0.622	0.676	0.524	0.432	0.345	0.297	0.241	0.148
IPSL	0.099	0.205	0.123	0.25	0.65	0.659	0.454	0.345	0.211	0.246	0.198	0.142

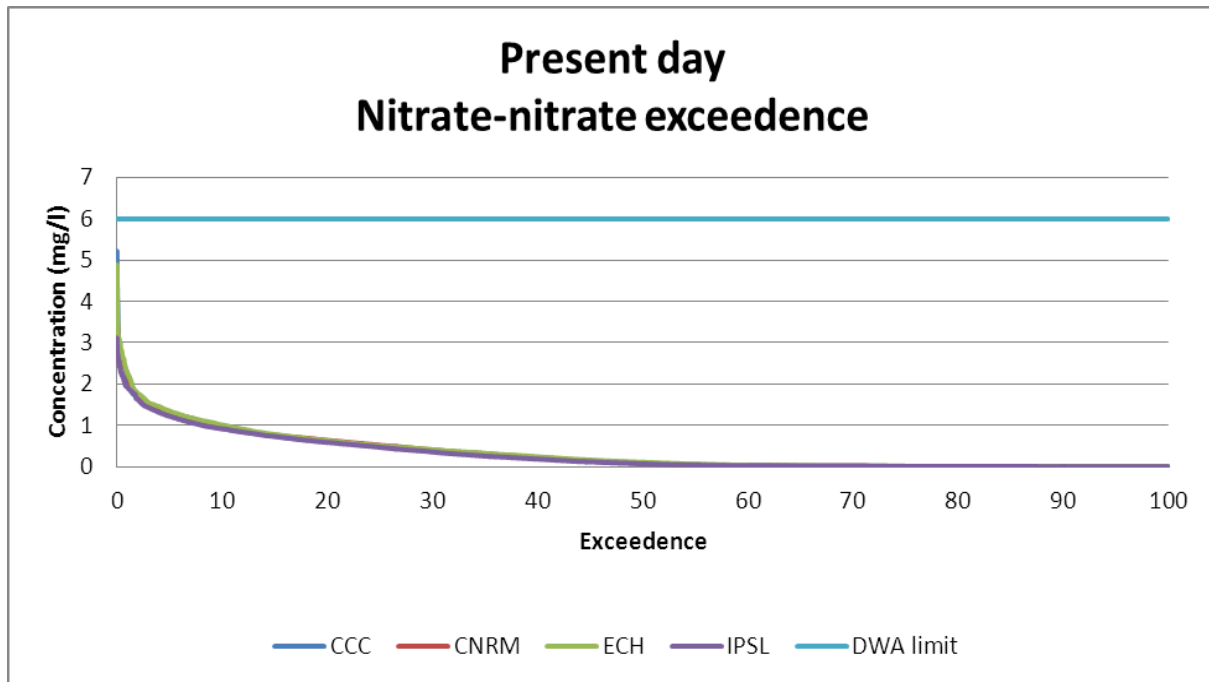


Figure 65 Present day surface nitrate-nitrite exceedance plot

The guideline limit of 6mg/l of nitrite-nitrate as set by DWA was never exceeded for the present day simulation runs. This plot is shown in Figure 65.

5.1.11 Total nitrogen concentration and the half-saturation constant

The algal half-saturation constant for nitrogen is defined as the nitrogen concentration (ammonium + nitrate/nitrite) at which the uptake rate was one-half the maximum rate. This represents the upper concentration at which algal growth was proportional to nitrogen and algal growth was nitrogen limited below this value. Table 19 gives the mean monthly surface nitrogen concentration. The nitrogen half-saturation constant was 0.01, 0.14 and 0 for diatoms, green algae and cyanobacteria respectively. From this, it was seen that only green algae could become growth limited by surface nitrogen.

Table 19 Total surface mean monthly nitrogen concentration

	Jan	Feb	Mar	Apr	May	June	July	Aug	Sep	Oct	Nov	Dec
CCC	0.151	0.273	0.216	0.323	0.721	0.734	0.615	0.529	0.346	0.360	0.294	0.232
CNRM	0.151	0.300	0.179	0.369	0.851	0.895	0.608	0.502	0.316	0.331	0.281	0.201
ECH	0.161	0.315	0.220	0.409	0.737	0.801	0.600	0.526	0.409	0.375	0.318	0.215
IPSL	0.141	0.303	0.187	0.337	0.792	0.800	0.532	0.429	0.257	0.310	0.267	0.207

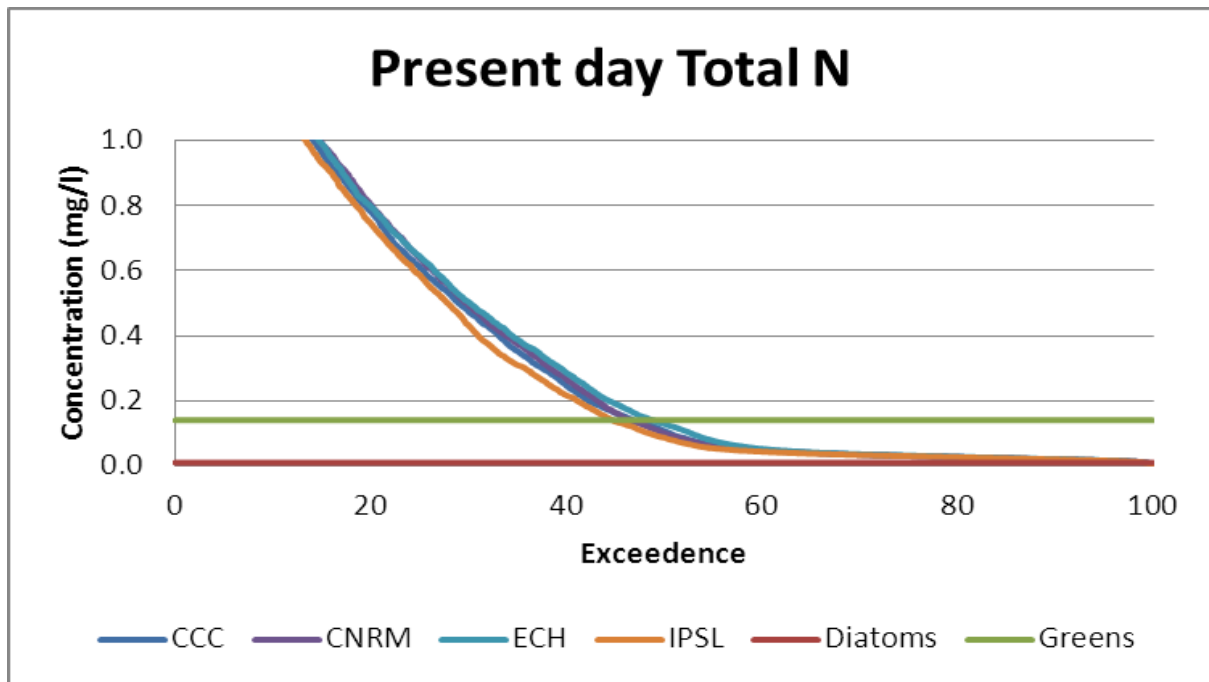


Figure 66 Present day total nitrogen half-saturation exceedance plot

From the exceedance plot in Figure 66 green algae growth was limited, as its half-saturation was not exceeded at the surface. Thus between 50 and 45% of the time this species of green algae was growth limited to half its maximum rate at the surface in the present day scenario. This would imply that if the total nitrogen concentration into the dam were to increase for the same conditions, the growth of green algae would be greater than currently presented.

5.1.12 Identifying the limiting nutrient

It had been established that the green algal species in Voëlvlei Dam was limited for both phosphorus and nitrogen concentration at the surface. DWA uses the standard that if N:P > 25:1 then there was no problem with water quality from an aspect of nutrient enrichment. If N:P < 10 then eutrophic conditions exist. If N/P > 10 then P limits algal growth and if N/P < 10 the N limits algal growth.

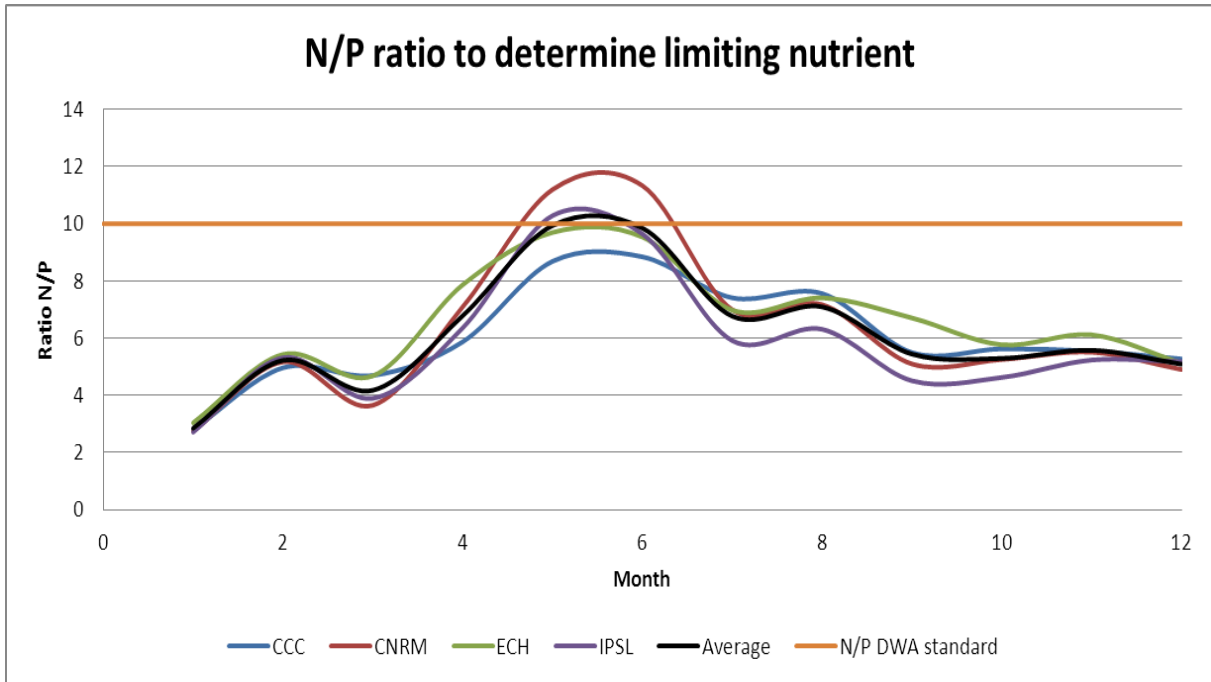


Figure 67 Present day limiting nutrient from DWA standards

From Figure 67 it can be seen that the dam was eutrophic and nitrogen limits algal growth for the entire year except during winter when it switches to phosphorus limited algal growth at the surface. Thus, the limiting nutrient was seasonal.

In order to control the growth of algae the only possible solution would be to limit the inflow of nutrients into the dam. It was thus deduced that to control the ingress of nitrogen into the dam would be unfeasible due to its natural abundance and the only realistic method to limit algal growth would be to limit the inflow of phosphorus into the dam down to a level where it becomes the limiting nutrient, thereby limiting algal growth.

5.1.13 Dissolved silicon concentration

The dissolved silicon concentration of the surface water for segment 11 is shown in Figure 68. For this study it is only diatoms that are silicon growth limited as both the green algae and cyanobacteria are capable of fixing nitrogen directly from the atmosphere and phosphorus was in abundance. The inflow concentration of dissolved silicon into Voëlvlei Dam is shown in Table 20 and graphically in Figure 57.

Table 20 Inflow concentration of dissolved silicon into Voëlvlei

Inflow	Mean (mg/l)	Minimum (mg/l)	Maximum (mg/l)	Std.Dev (mg/l).
1	3.385	2.26	4.59	0.453
2	2.050	1.20	3.06	0.535

The following figure shows that the dissolved silicon concentration is seasonal for the duration of the 20-year simulation period. It followed seasonal cycles with peaks and troughs, with the peaks occurring in winter.

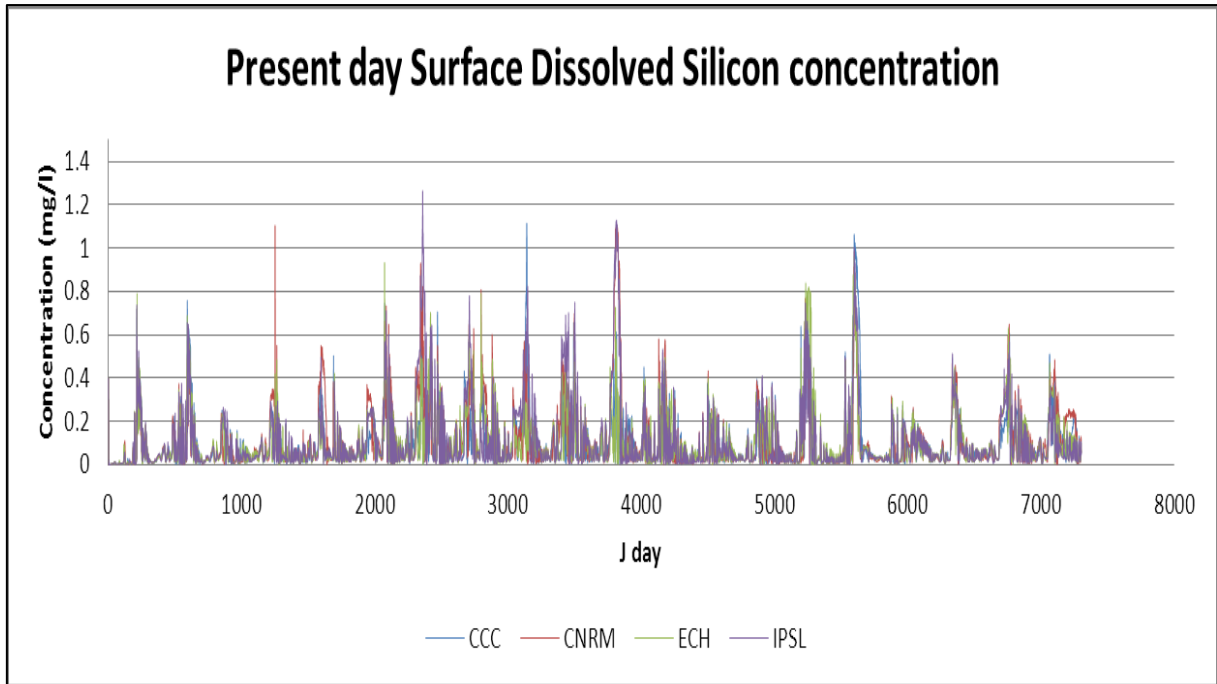


Figure 68 Present day silicon concentrations

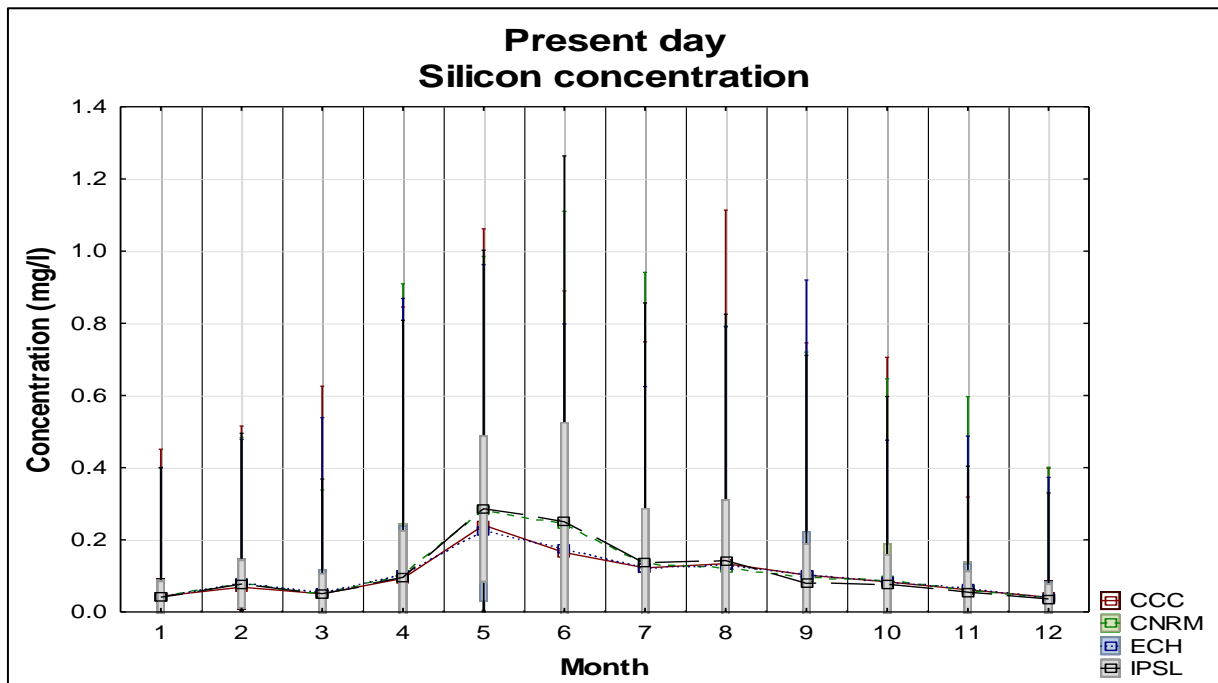


Figure 69 Monthly present day silicon concentrations

Figure 69 shows that the winter concentration of dissolved silicon was greater than that of summer, which meant that diatom growth should be silicon limited during summer and more growth during winter with favourable conditions for temperature and solar radiation.

Table 21 Present day mean monthly dissolved silicon concentration (mg/l)

	Jan	Feb	Mar	Apr	May	June	July	Aug	Sep	Oct	Nov	Dec
CCC	0.043	0.069	0.050	0.093	0.241	0.165	0.122	0.134	0.102	0.084	0.062	0.041
CNRM	0.043	0.080	0.050	0.105	0.280	0.244	0.134	0.120	0.097	0.088	0.062	0.037
ECH	0.043	0.080	0.055	0.102	0.223	0.177	0.120	0.128	0.103	0.084	0.066	0.039
IPSL	0.041	0.077	0.051	0.096	0.286	0.250	0.135	0.142	0.079	0.077	0.055	0.036

Diatoms are known to bloom in winter and from Figure 69 it was seen that the maximum silicon concentrations occur during winter months (May to August) thus not inhibiting diatom growth during the winter months.

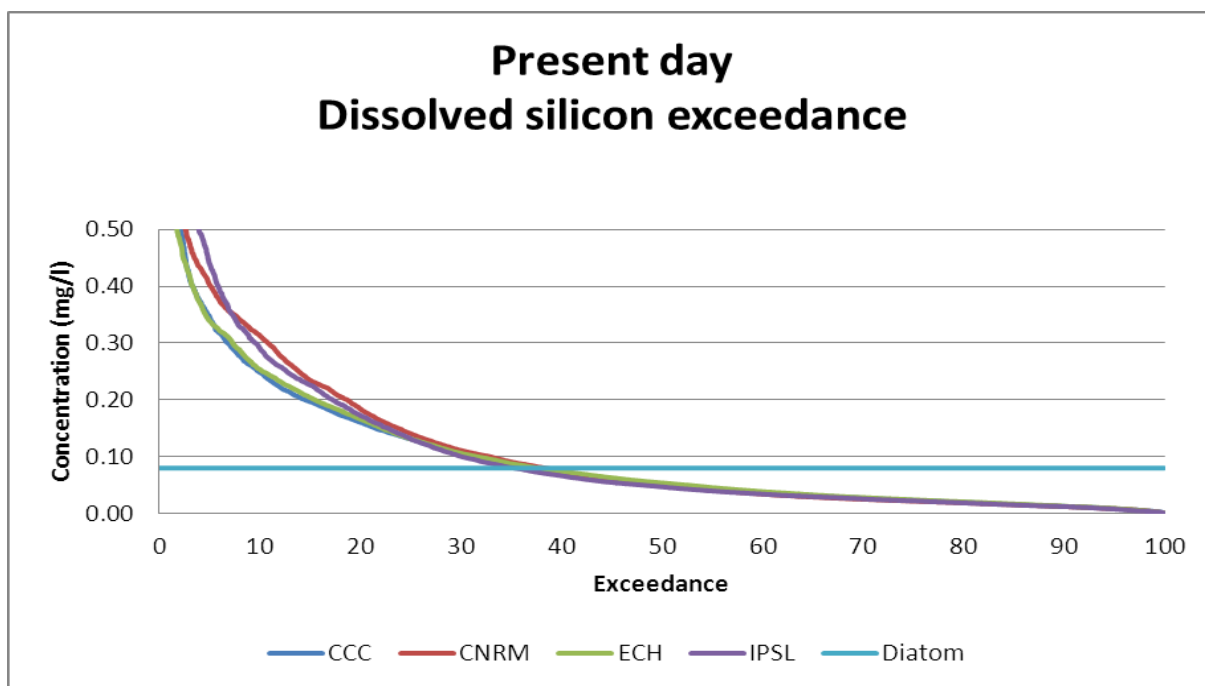


Figure 70 Present day dissolved silicon half-saturation exceedance plot

From the exceedance plot for dissolved silicon, it was seen that the concentration of surface dissolved silicon was lower than the half-saturation of 0.08 mg/l for approximately 63% of the 20 years. Thus, diatom growth was hampered by low levels of dissolved silicon and any increase in the inflow of dissolved silicon would allow for a greater growth rate of diatoms at the surface. The in-situ sources of dissolved silicon are algal respiration, anaerobic decay from the sediments and particulate silicon. Since none of these sources can be managed for a reduction in dissolved silicon the source reduction of silicon before it enters the dam seems a viable method to limit diatom growth.

5.1.14 Dissolved oxygen concentration

Similarly, the dissolved oxygen concentrations for the 20-year period, monthly and statistics are shown below. The inflow concentration of dissolved oxygen was 12.5 mg/l for both inflow canals for the duration of all the simulations.

From Figure 71 it is seen that the dissolved oxygen concentration is cyclic and greater concentration of dissolved oxygen is detected in winter. This was due to less dissociation of oxygen from the water because the water temperature was lower. The DWA TWQR level for dissolved oxygen was that it should not be less than 80% or greater than 120% of saturation levels. It was clear that the TWQR for dissolved oxygen was not met during the study period.

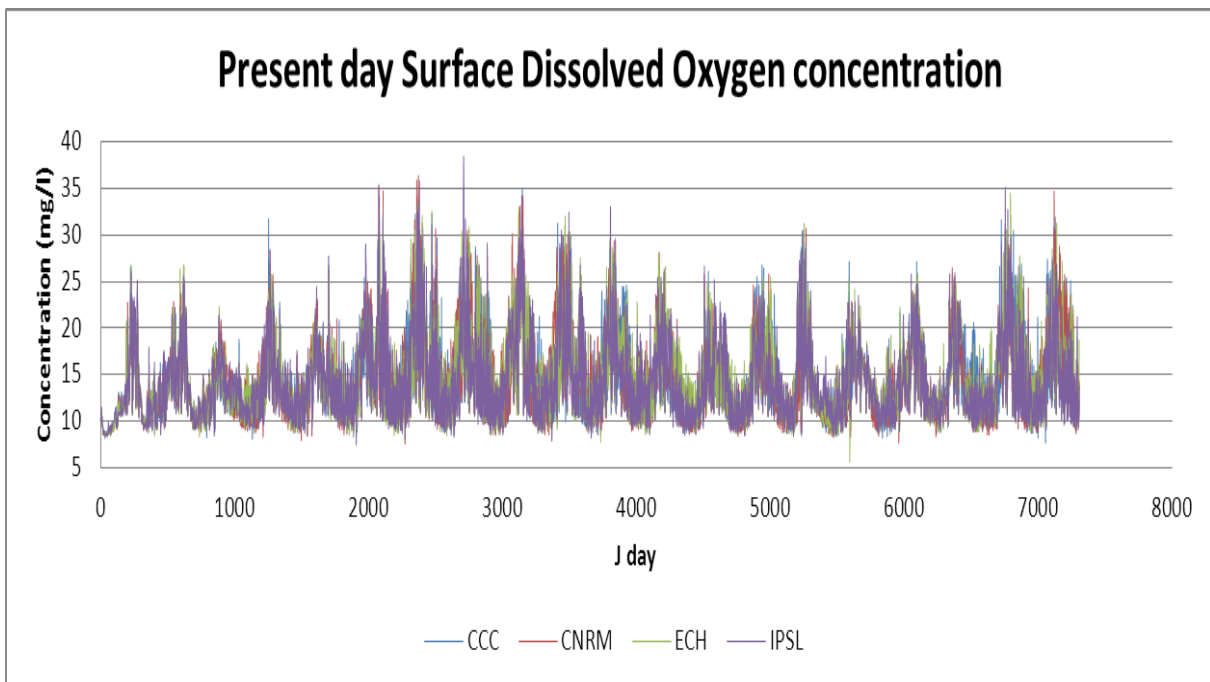


Figure 71 Present day dissolved oxygen concentration

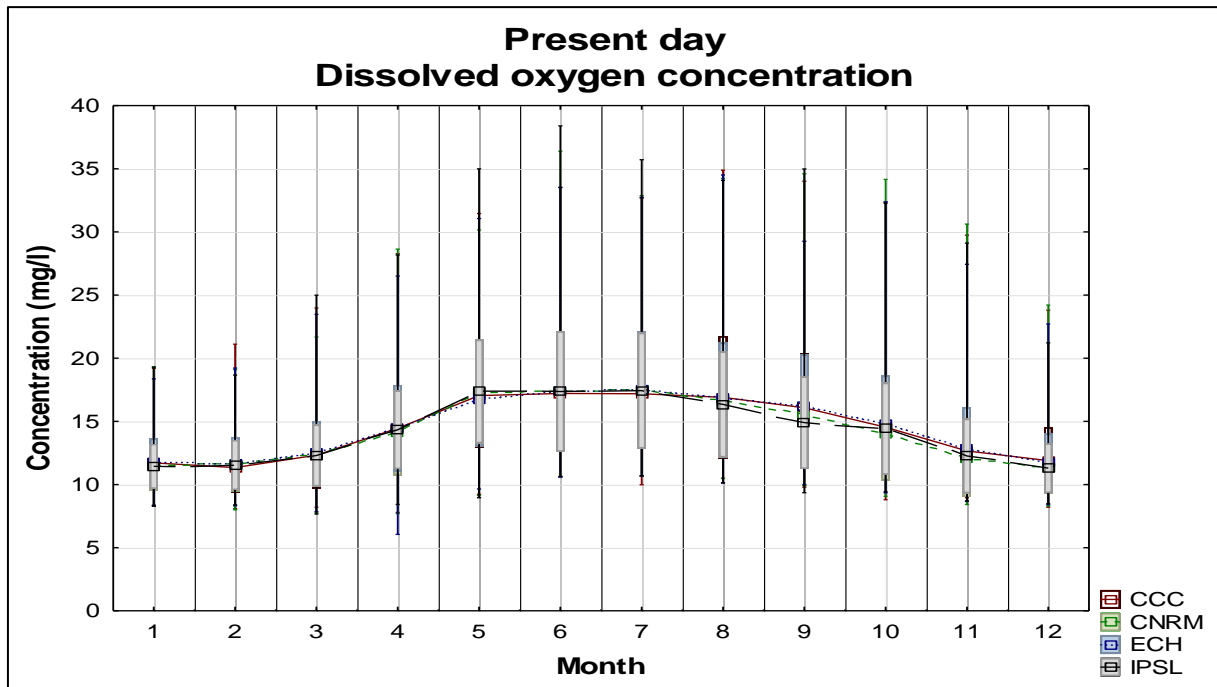


Figure 72 Monthly dissolved oxygen concentration

Table 22 Present day mean monthly dissolved oxygen concentration (mg/l)

	Jan	Feb	Mar	Apr	May	June	July	Aug	Sep	Oct	Nov	Dec
CCC	11.71	11.34	12.32	14.45	17.05	17.21	17.18	16.90	16.08	14.53	12.66	11.89
CNRM	11.49	11.61	12.41	14.13	17.26	17.36	17.47	16.60	15.51	14.01	12.06	11.28
ECH	11.70	11.68	12.50	14.47	16.80	17.37	17.50	16.83	16.18	14.78	12.86	11.74
IPSL	11.44	11.55	12.30	14.33	17.37	17.37	17.43	16.34	14.90	14.42	12.26	11.30

It was clear that the dam was supersaturated with dissolved oxygen for a greater part of the year, which needed further investigation and Figure 73 shows that for 30% of the simulation that the DO concentration was greater than 15mg/l, an unrealistically high concentration and had a maximum of 38 mg/l.

It was noted that the calibration of DO was not possible as there were no measured values to compare to. Calibration would involve assessing the aeration rate at the surface as well as the effect of the algal growth rates on the observed DO concentrations. A sensitivity analysis should show which parameters affected the DO concentrations and changes for calibration may be implemented.

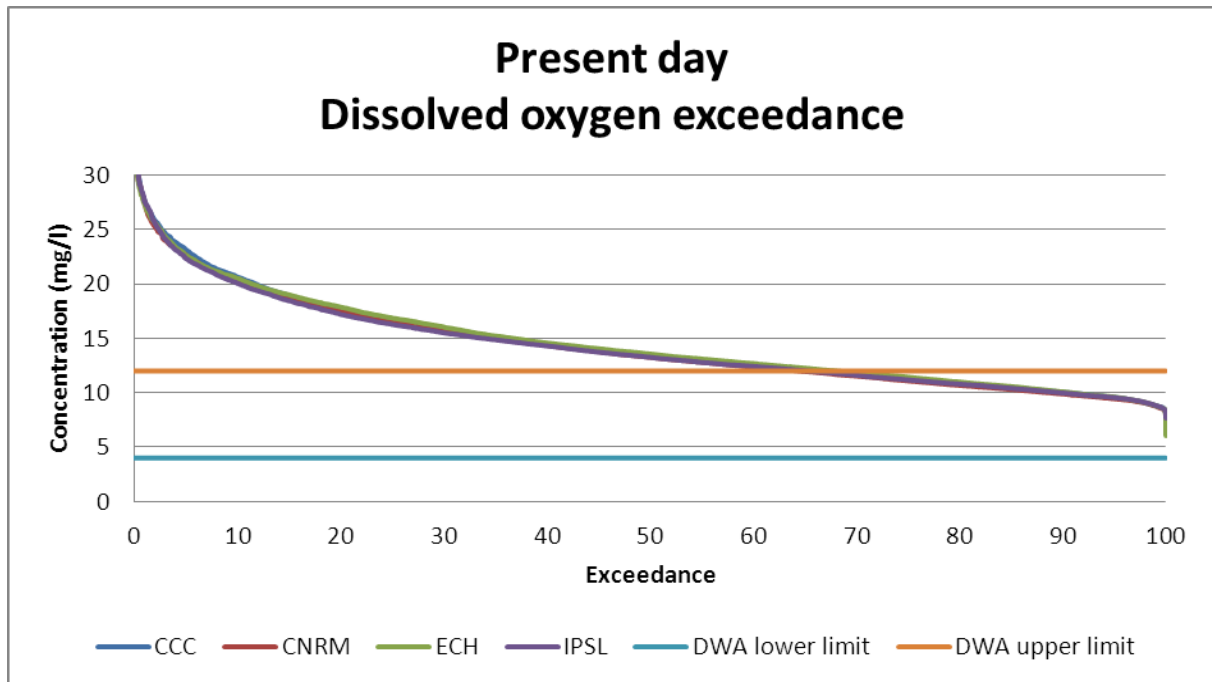


Figure 73 Present day surface dissolved oxygen exceedance plot

From the exceedance plot for surface dissolved oxygen it was seen that the DWA lower limit was never exceeded for the simulation period and that the upper limit of 120% saturation was exceeded 65% of the time. This happened in winter when the water temperature was cooler and less dissociation of oxygen from the water occurred.

In order to explain the high levels of super-saturation, the module of CE-QUAL-W2 that calculates DO was closer examined for viable sources of oxygen at the surface. Within the model, dissolved oxygen saturation was calculated as a function of water temperature and altitude of the dam. Figure 21 shows the fluxes for DO within the model and the only sources are photosynthesis and atmospheric transfer. The possible variable for the user to affect DO concentrations would be the algal growth constants, thereby directly affecting DO levels by varying the photosynthetic rate. As an exercise, the algal growth rates (AG) for the three groups were set as equal to 1 and the model rerun for the CCC present day. It was assumed that the one model (CCC) was representative of all four models as model inter-variance was negligible as seen in Figure 72.

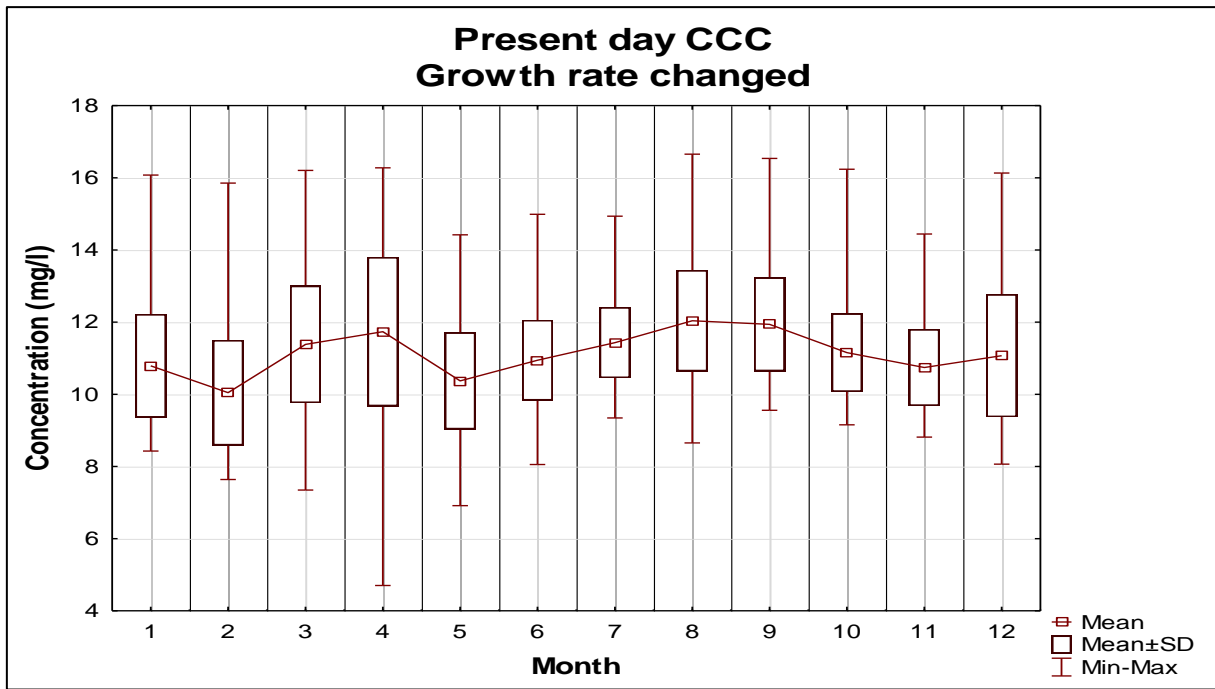


Figure 74 Effect of varied algal growth rates on dissolved oxygen

In comparing Figure 74 and Figure 72 it was seen that changing the algal growth rates the DO concentration levels are more representative of actual in-dam conditions. The problem with this approach in proceeding further was that the algal growth was now affected and not representative of in-dam conditions. The choice of algal growth rates and various parameters are critical for an accurate representation of in-dam conditions as previously mentioned.

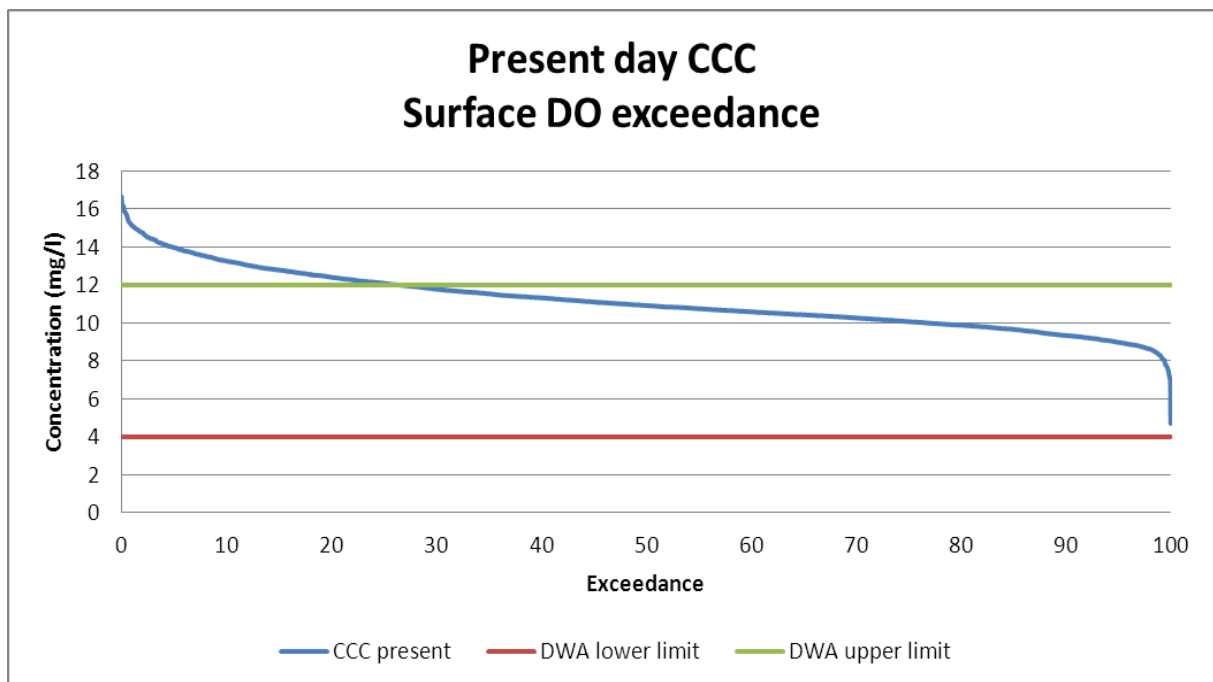


Figure 75 CCC present day DO exceedance levels

In comparing Figure 73 with Figure 75 it was seen that the DWA minimum level was not exceeded but that the upper limit was exceeded for at least 28% of the simulation. It was noted that although this was similar to the previous run but the maximum concentration was only 16.5mg/l of DO. This was considered a more realistic value for surface DO concentrations.

It was thus concluded that for the chosen algal parameters CE-QUAL-W2 predicted an unrealistic supersaturated surface DO concentration for the simulation and that by changing the algal parameters more realistic surface DO concentrations were obtained. Since this study is an investigation into the effects of climate change and comparative values were presented, it was considered that the initially presented present day DO concentrations are still valid in this context although noted to be an overestimation. The future DO concentrations would be shown as a change due to climate and thus were considered valid.

5.1.15 Total algal concentration

Algal growth is a function of temperature, light, and nutrients (Cole and Wells, 2008) and thus maximum algal growth occurs at or near the surface if the water-body was well mixed. The total algal concentration incorporating diatoms, greens and cyanobacteria are shown in the following figures for the present day simulation.

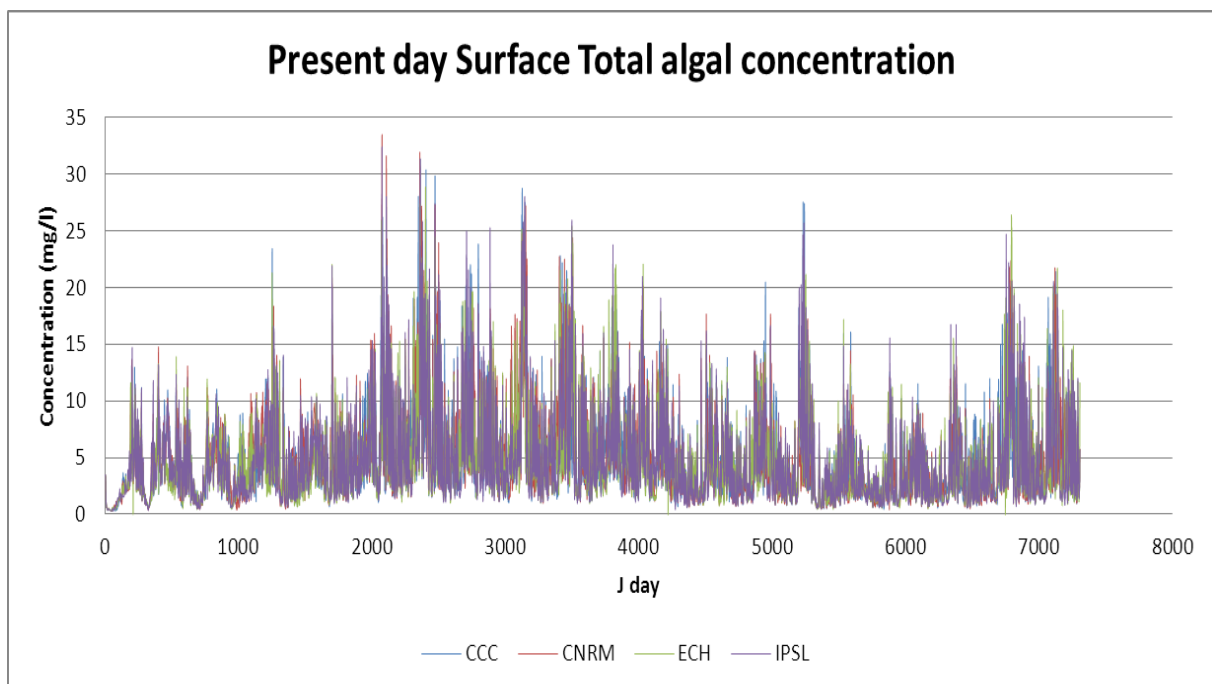


Figure 76 Present day total algal concentration

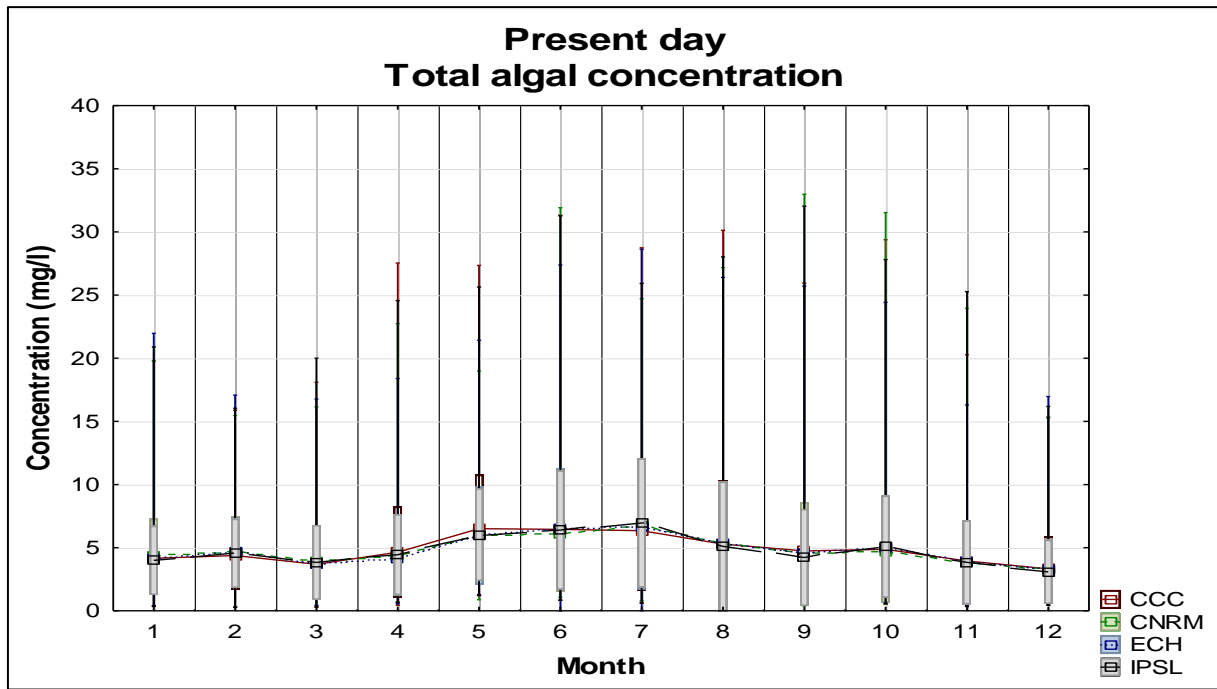


Figure 77 Monthly mean total algal concentration

Table 23 Present day mean monthly surface total algae concentration (mg/l)

	Jan	Feb	Mar	Apr	May	June	July	Aug	Sep	Oct	Nov	Dec
CCC	4.161	4.381	3.680	4.637	6.507	6.449	6.340	5.283	4.742	4.874	3.941	3.325
CNRM	4.309	4.712	3.915	4.370	5.939	6.136	6.714	5.297	4.572	4.700	3.805	3.225
ECH	4.166	4.637	3.738	4.109	5.964	6.546	6.621	5.314	4.564	4.962	3.905	3.228
IPSL	3.995	4.556	3.832	4.445	6.036	6.395	6.955	5.097	4.220	5.076	3.834	3.084

Figure 76 shows the total algal concentrations at the surface of segment 11 as well as the close agreement between the climate models. From Figure 77 it was seen that the mean total algal growth was greater for the winter months than for summer. It is known that diatoms blooms occur more often in winter (Cole and Wells, 2008) thus an investigation into which type of algae was dominant was conducted.

From the model parameterisation, diatoms and cyanobacteria shared lower light saturation values than greens, implying that they should grow better in winter than summer and conversely greens would grow better the entire year as it had the highest light saturation value and thereby could utilise the greater solar radiation of summer for photosynthesis.

In comparing the winter total algal concentration to that of summer, it was seen that winter had a greater concentration of algae with a drop in August attributed to an increase in the average solar radiation. This confirmed that the algae in Voëlvlei Dam are light sensitive and total algal growth was more in winter than summer.

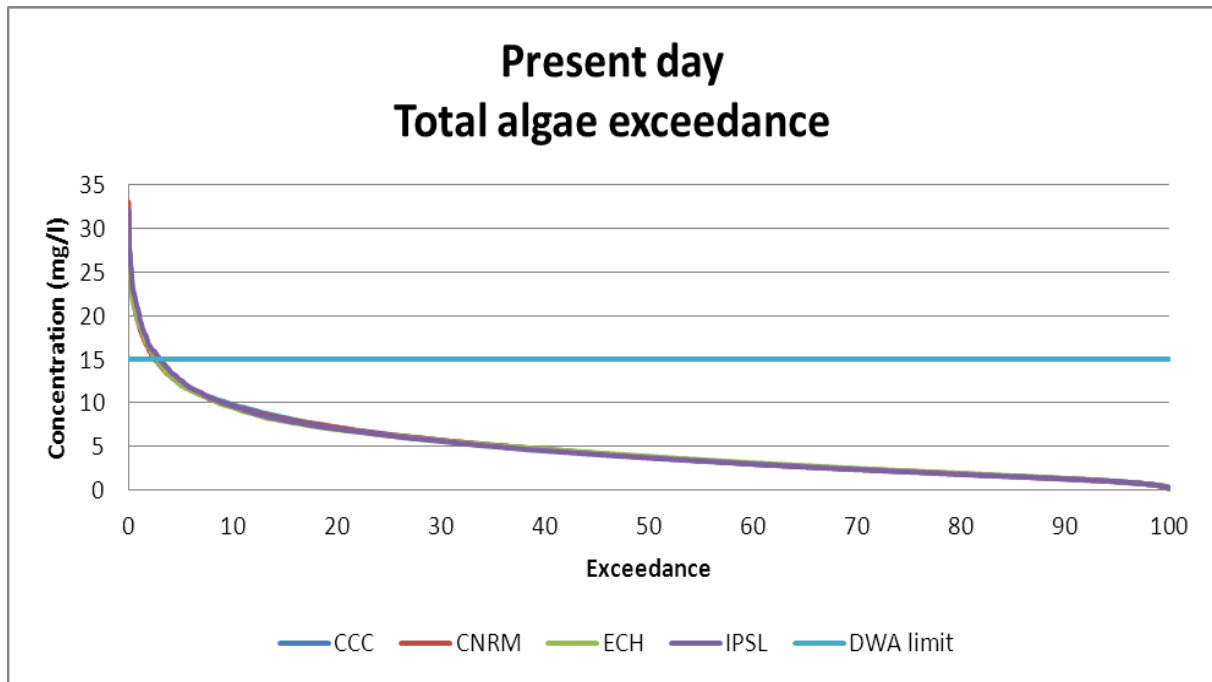


Figure 78 Present day total algae exceedance plot

From the exceedance plot, it was seen that the total surface algae concentration was greater than 15mg/l (DWA limit) for 3% of the simulation period, most probably during winter.

5.1.16 Diatoms concentration

It is known that diatoms have low light saturation values and tend to grow better in winter, as the winter water temperature was within its maximum growth rates. The following graph shows the diatom concentration for the 20-year period and it is noted that each of the peaks seen corresponded to winter.

Figure 79 shows the cyclic peaks of diatoms concentrations as well as the good agreement between the climate models for the present day.

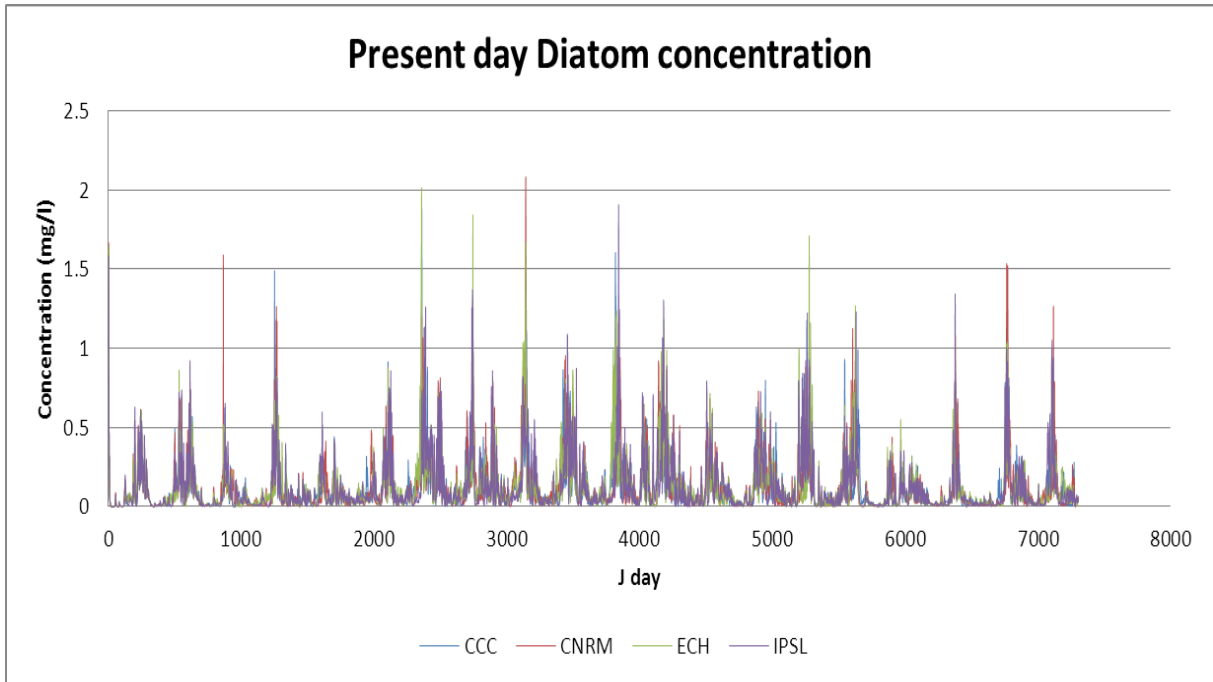


Figure 79 Present day diatom concentration

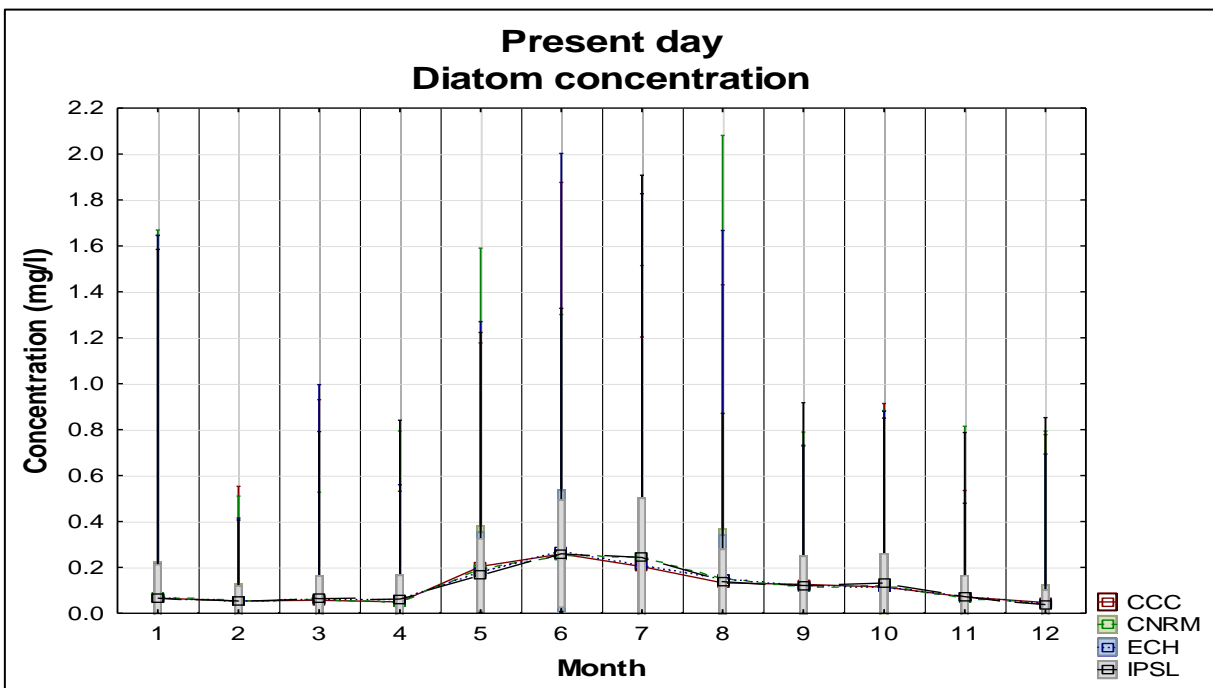


Figure 80 Monthly diatom concentration

Table 24 Present day mean monthly surface diatom concentration (mg/l)

	Jan	Feb	Mar	Apr	May	June	July	Aug	Sep	Oct	Nov	Dec
CCC	0.066	0.054	0.057	0.050	0.204	0.259	0.204	0.133	0.126	0.114	0.071	0.047
CNRM	0.071	0.055	0.062	0.051	0.191	0.250	0.248	0.152	0.113	0.117	0.069	0.043
ECH	0.069	0.052	0.062	0.058	0.179	0.272	0.210	0.149	0.123	0.114	0.072	0.039
IPSL	0.066	0.054	0.064	0.062	0.167	0.259	0.243	0.138	0.121	0.129	0.073	0.038

From Figure 80 and Table 24 it is seen that there was a much greater mean concentration of diatoms during the winter months as opposed to summer months. This is what was expected even though during summer the water temperature is high enough to promote maximum growth. This difference could solely be attributed to the diatoms lower light saturation inhibiting plant growth in the high solar radiation summer months. The temperature growth multipliers for diatoms predict that their growth should be limited in winter as the water temperature was below the levels for maximum algal growth. It was noted that there was good agreement within climate models.

5.1.17 Green algae concentration

The green algae for this study exhibits similar light saturation characteristics as the diatoms but have a higher temperature growth rate multiplier. Thus, it was expected to grow throughout the entire year and is shown in Figure 81.

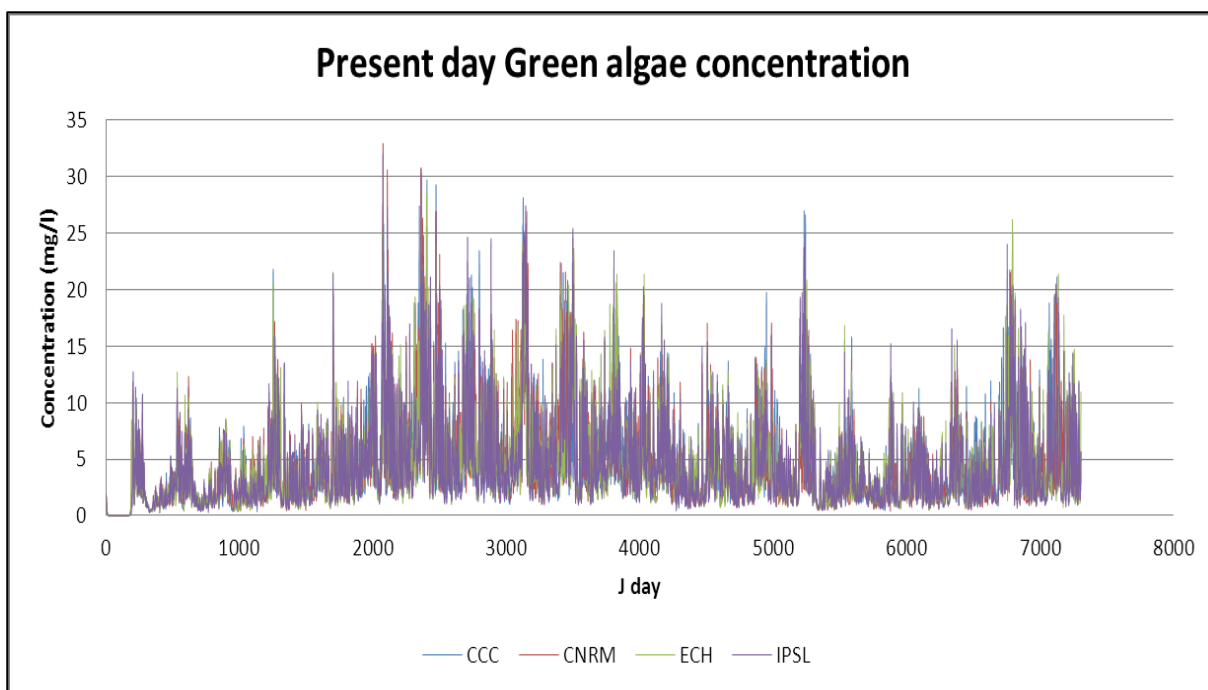


Figure 81 Present day green algae concentration

Green algae is the dominant species in Voëlvlei Dam as they have the greatest concentration and compared well to the total algae concentrations of Figure 79.

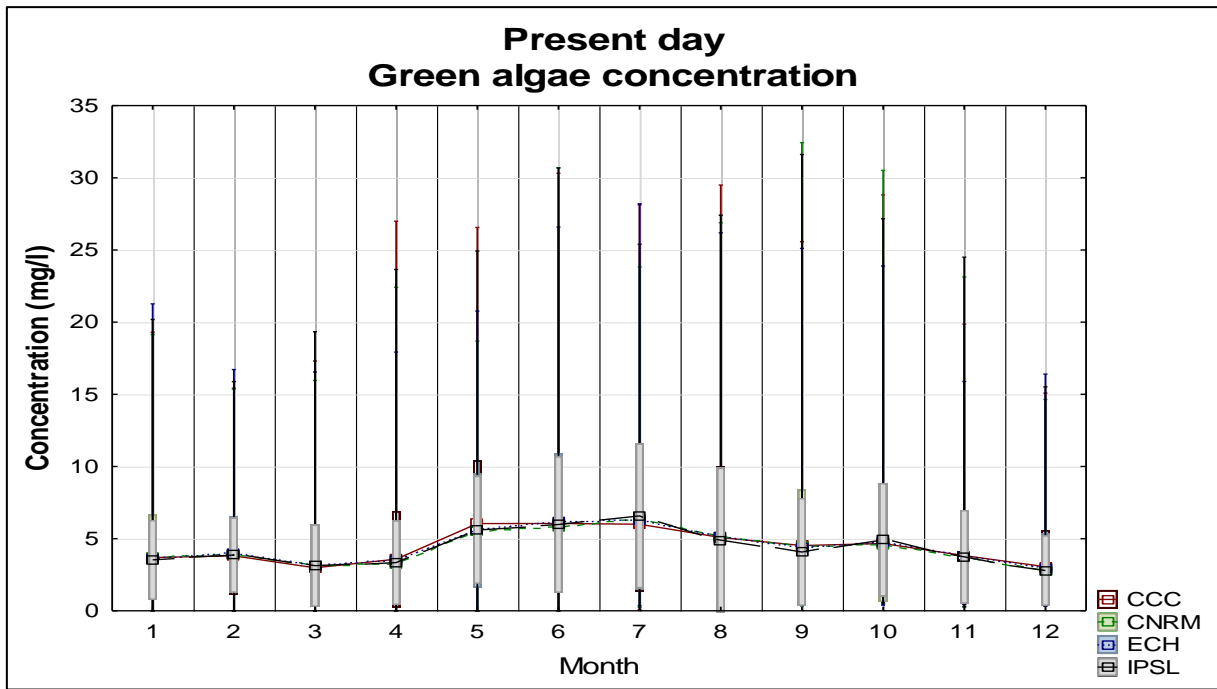


Figure 82 Present day monthly green algae concentration

When comparing Figure 82 to Figure 79 it is seen that the mean monthly green algae concentration is greater than that of the diatom concentration but the months of greatest growth is winter for both species.

Table 25 Present day mean monthly green algae concentration (mg/l)

	Jan	Feb	Mar	Apr	May	June	July	Aug	Sep	Oct	Nov	Dec
CCC	3.689	3.810	2.981	3.576	6.046	6.055	6.001	5.077	4.521	4.668	3.824	3.052
CNRM	3.713	3.920	3.177	3.280	5.494	5.766	6.374	5.095	4.439	4.556	3.695	2.806
ECH	3.620	3.951	3.135	3.508	5.577	6.158	6.329	5.100	4.355	4.725	3.772	2.944
IPSL	3.528	3.857	3.128	3.340	5.615	5.980	6.577	4.899	4.076	4.924	3.740	2.793

Table 25 compares the concentration of green algae in Voëlvlei Dam for the 20-year period. It is noteworthy that the winter period growth was greater than that of summer, which would seem counterintuitive, as the warmer water of summer should promote greater algal growth. This could be attributed to the lower light saturation of the species, thereby favouring winter growth.

5.1.18 Cyanobacteria concentration

The cyanobacteria modelled have high light saturation intensities relative to the diatoms and greens and are capable of utilising the extra light during summer for photosynthesis unlike the diatoms and greens. Thus, it was expected that maximum cyanobacteria concentrations should occur mainly in summer due to the additional light and warmer water. Figure 83 shows the cyanobacteria concentration for the 20-year simulation period.

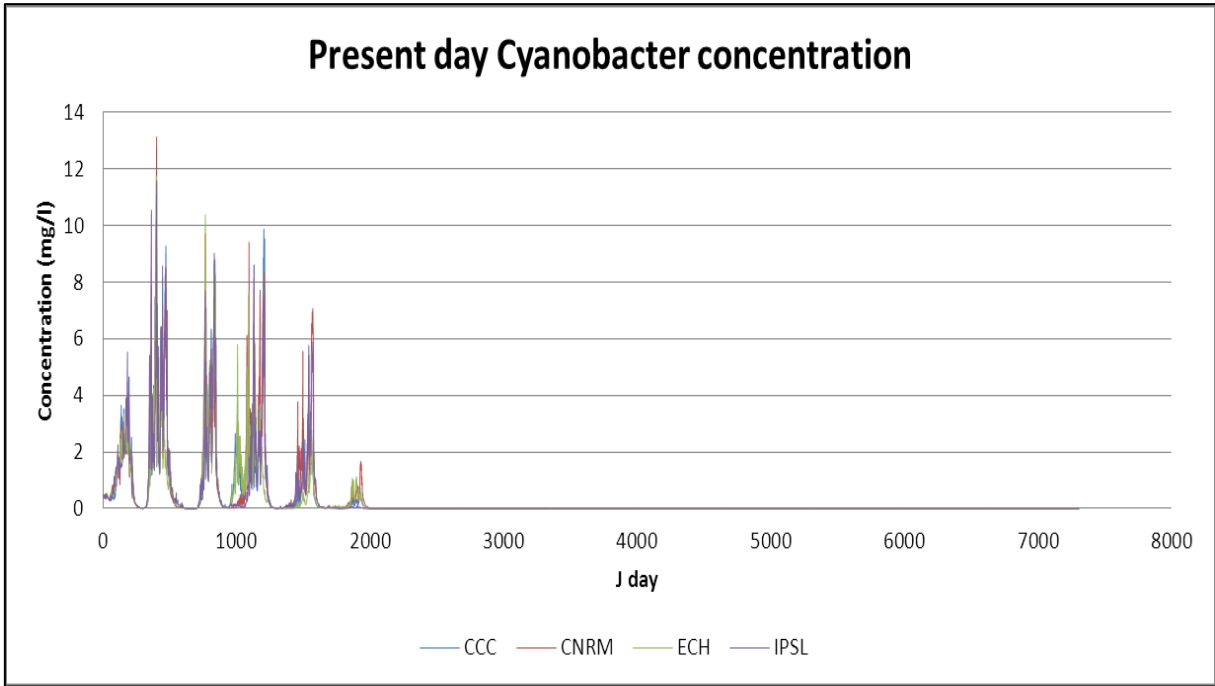


Figure 83 Present day cyanobacteria concentration

From this figure, it was deduced that for the present day that all climate models predict seasonal cyanobacteria blooms and this was confirmed by the monthly statistical values shown Figure 84 and Table 26.

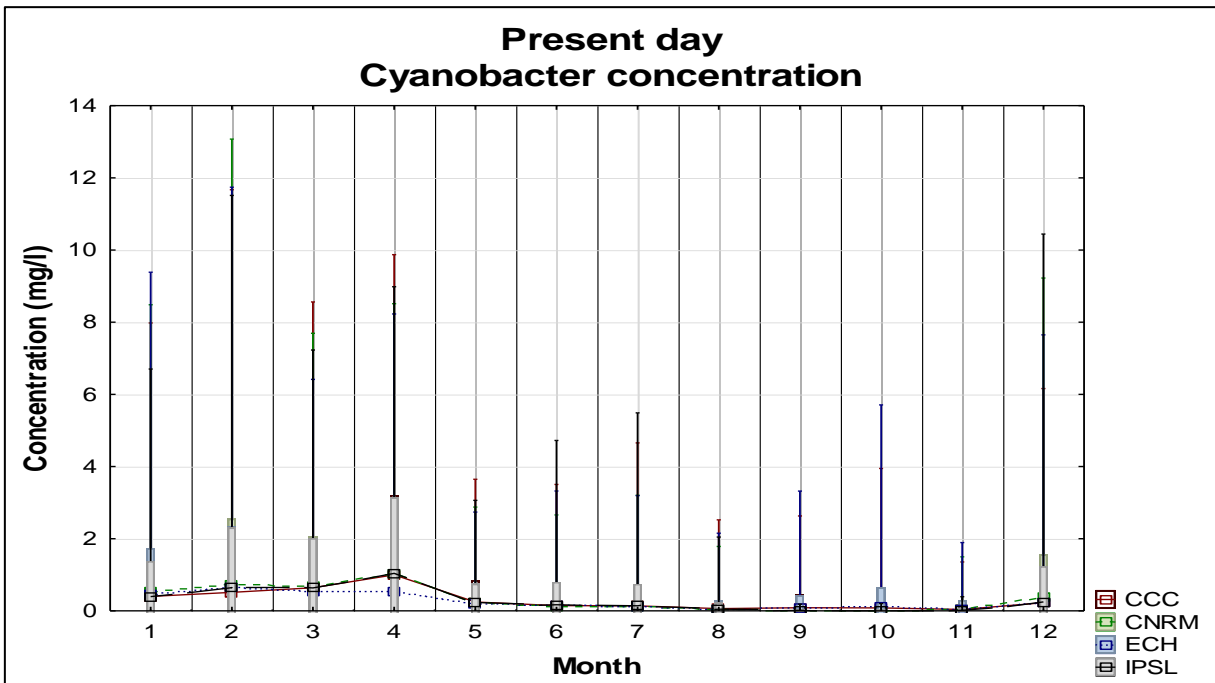


Figure 84 Present day monthly cyanobacteria concentration

The inter-variability between the climate models is evident but not excessive. Maximum mean values are during summer and autumn with a decrease during winter. This figure shows that

cyanobacteria is not present in the dam for the duration of the simulation but reaches maximum concentrations seasonally during summer, then dies off for the rest of the simulation. This would imply that conditions in Voëlvlei Dam were not favourable for the growth of cyanobacteria. This is still considered acceptable, as the aim of the study is to show changes in concentrations as a direct result of climate change.

Table 26 Present day mean monthly surface cyanobacteria concentration (mg/l)

	Jan	Feb	Mar	Apr	May	June	July	Aug	Sep	Oct	Nov	Dec
CCC	0.402	0.514	0.640	0.999	0.245	0.147	0.139	0.063	0.088	0.081	0.039	0.226
CNRM	0.519	0.728	0.671	1.039	0.241	0.131	0.100	0.039	0.010	0.020	0.034	0.377
ECH	0.472	0.630	0.536	0.533	0.195	0.146	0.107	0.058	0.076	0.114	0.058	0.244
IPSL	0.396	0.643	0.637	1.039	0.239	0.170	0.142	0.046	0.015	0.014	0.016	0.249

From the table it was seen that the mean summer to autumn cyanobacteria concentration is greater than that of winter as well as the summer maximum concentrations. This could be directly linked to the cooler waters during winter.

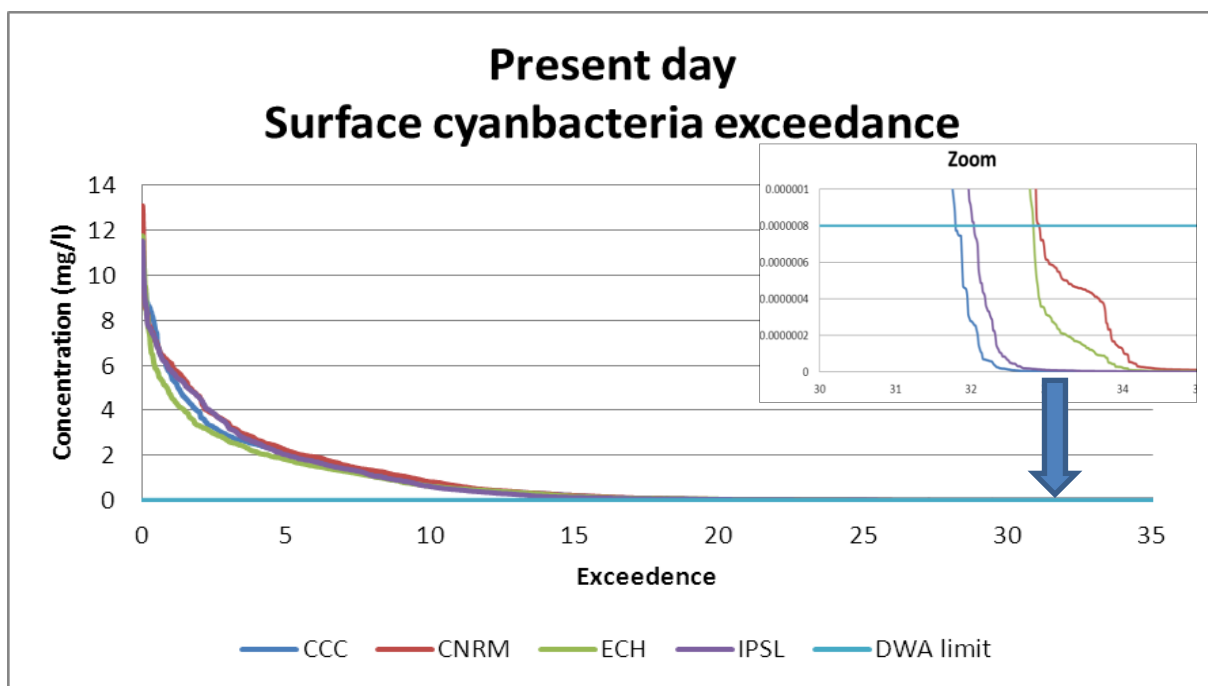


Figure 85 Present day surface cyanobacteria exceedance, DWA limits with zoom

From the exceedance plot, it was estimated that for the DWA limit of 0.8µg/l the surface cyanobacteria concentration in Voëlvlei Dam exceeded this limit about 32 to 33% of the simulation time depending on the climate model.

The accuracy of the prediction of the present day algal growth was not confirmed but was considered to be representative enough as the model had been calibrated and validated. The

outcome of this study was to firstly establish baseline conditions and then show changes induced by climate change on the baseline conditions in the ensuing sections.

5.1.19 Zooplankton growth

To investigate the effect of predation on diatoms and green algae, zooplankton was also modelled preferring diatoms and green algae over cyanobacteria and the resulting concentrations is shown in Figure 86. This figure resembles Figure 81 in shape and this was because green algae are present throughout the entire year and that zooplankton feed on them.

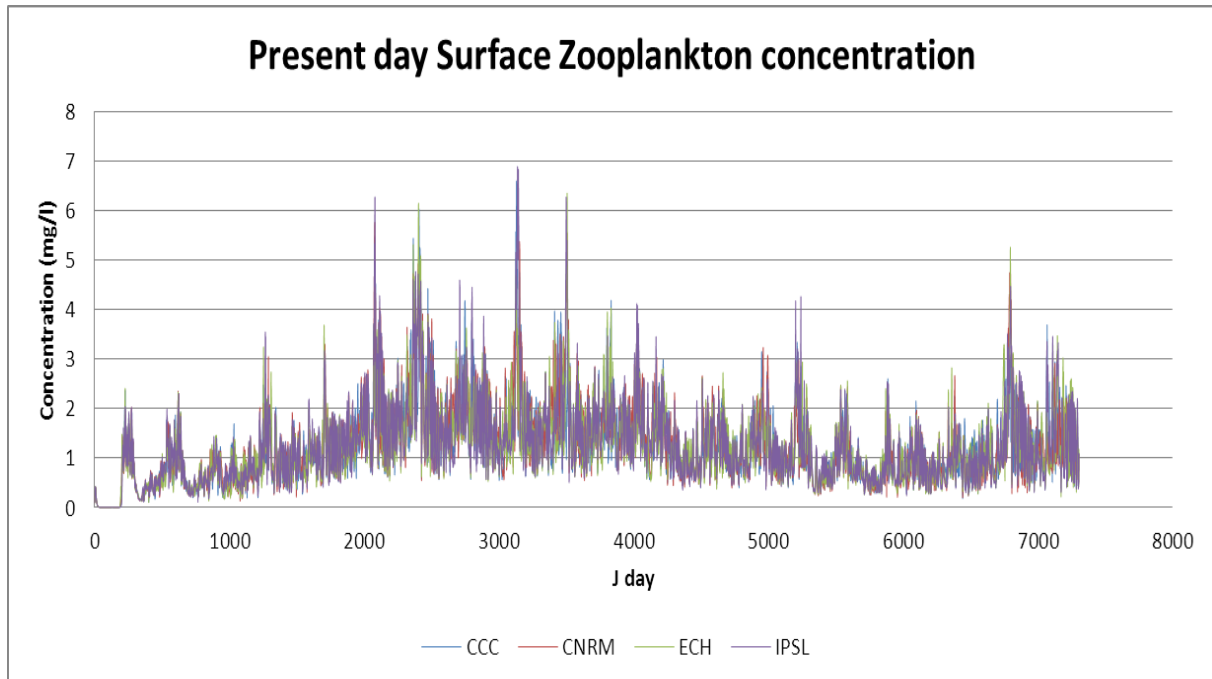


Figure 86 Present day zooplankton concentration

The following figure show the monthly averages of zooplankton concentration for the 20-year simulation period. It showed that zooplankton was present in Voëlvlei Dam throughout the entire year but at show a greater concentration during the winter months. This was probably due to the greater concentration of its diet, namely diatoms and green algae during these months.

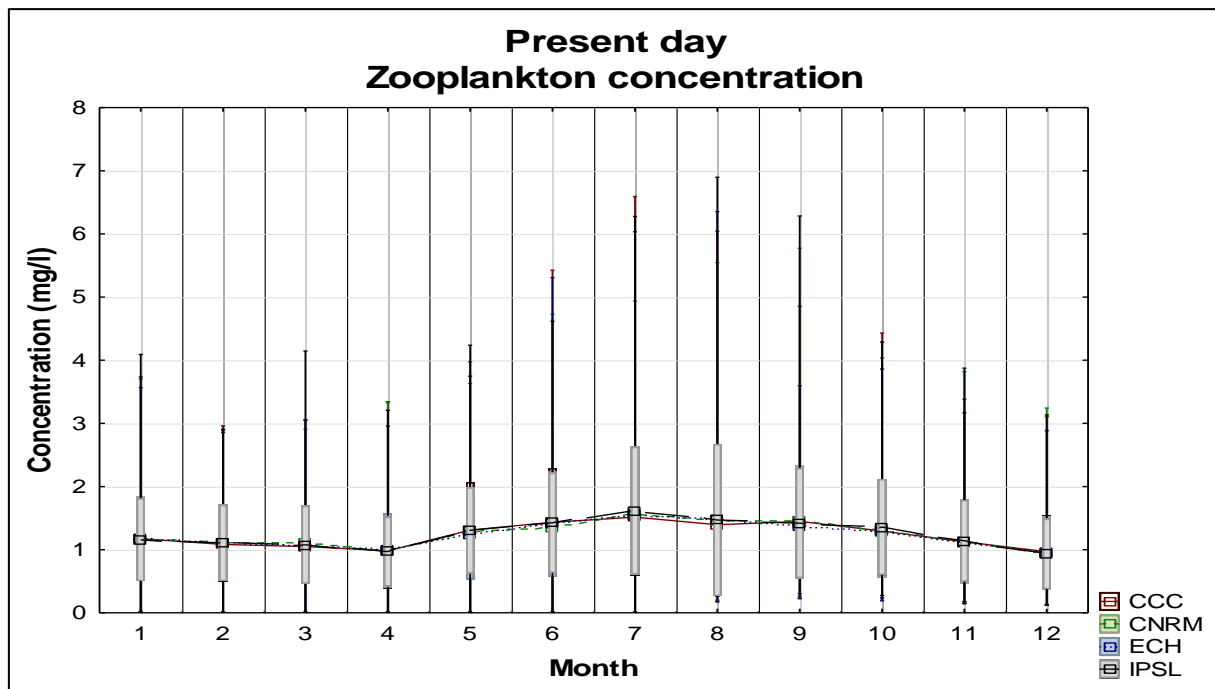


Figure 87 Present day monthly zooplankton concentration

Table 27 Present day mean monthly surface zooplankton concentration (mg/l)

	Jan	Feb	Mar	Apr	May	June	July	Aug	Sep	Oct	Nov	Dec
CCC	1.174	1.083	1.050	0.982	1.309	1.435	1.515	1.394	1.447	1.296	1.124	0.968
CNRM	1.177	1.113	1.115	0.975	1.273	1.339	1.570	1.448	1.456	1.304	1.134	0.946
ECH	1.178	1.113	1.069	0.996	1.240	1.404	1.556	1.470	1.376	1.279	1.119	0.953
IPSL	1.157	1.107	1.077	0.969	1.306	1.426	1.619	1.470	1.420	1.358	1.141	0.933

Table 27 shows the monthly statistics of zooplankton for the four climate models. Winter has the greatest mean surface zooplankton concentration as well as maximum concentrations, this being an indication that greater predation of diatoms and greens occurs during the winter months even though the zooplankton temperature growth rate was more suited to the summer months.

5.1.20 Eutrophication level

The trophic level indicator chosen for this study was the TRIX level, but its shortcoming was that it did not include secchi depth, which was not measured as part of this modelling process. This index characterised the trophic levels in coastal marine areas and was adopted by the Italian national legislation and is applied here as way of representing the trophic level. It was the linearization of chlorophyll-a concentration (ChA in $\mu\text{g}/\ell$), the dissolved oxygen concentration in percent (DO %), the total nitrogen ($N_{\text{min}} = N_{\text{nitrate}} + N_{\text{nitrite}} + N_{\text{ammonia}}$ in $\mu\text{g}/\ell$) and the total phosphorus (TP $\mu\text{g}/\ell$). CE-QUAL-W2 uses the ratio chlorophyll-a to total algae as 0.02. This was represented mathematically as:

$$TRIX = \frac{(\log(ChA + aDO\% + N\ min + TP) + 1.5)}{1.2} \tag{46}$$

From this the following trophic states of water was classified (Table 3).

Table 3 Categories of TRIX values

TRIX value	Trophic category
< 4	Low trophic level
4 - 5	Middle trophic level
5 - 6	High trophic level
6 - 8	Very high trophic level

From Pavluk and bij de Vaate, 2008:3602

The output of the study for mean monthly surface trophic level is shown in Figure 88 for the present day. Voëlvlei Dam is at the low trophic level with peaks into the middle trophic level mostly during winter.

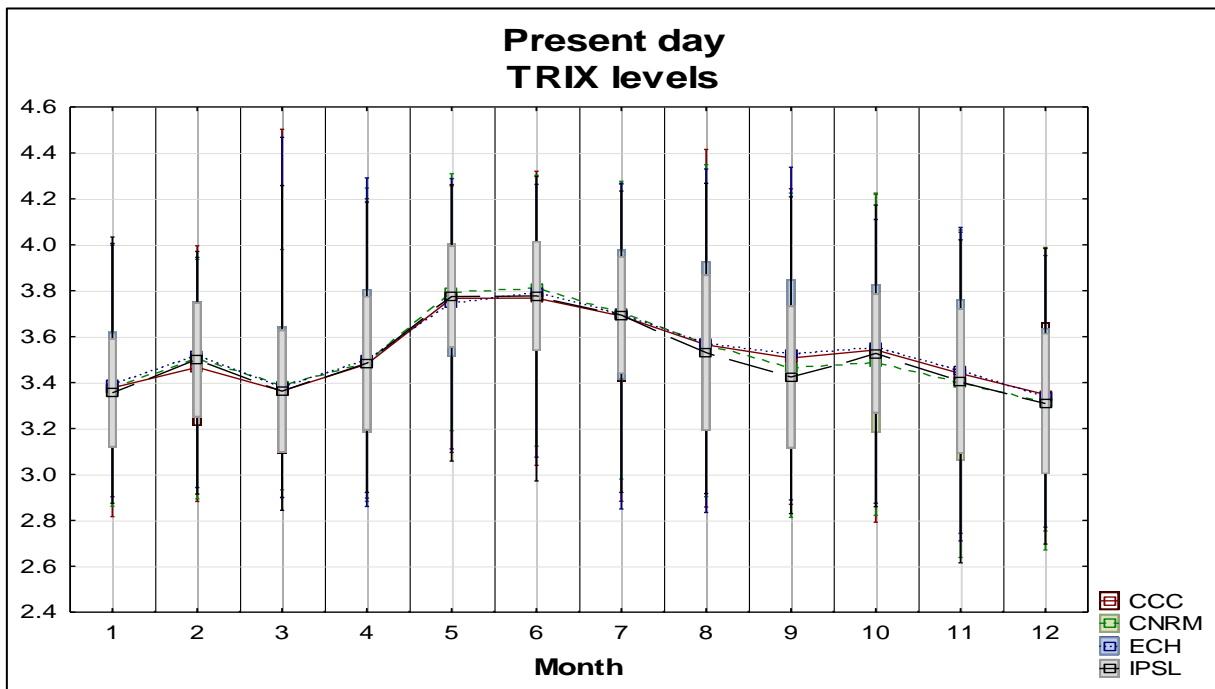


Figure 88 Present day TRIX level

Table 28 shows that the TRIX level of Voëlvlei Dam peaks during winter for all four present day climate models. It was expected that with climate change that this levels should increase due to changes in total algal concentration

Table 28 Present day monthly mean surface TRIX levels

	Jan	Feb	Mar	Apr	May	Jun	Jul	Aug	Sep	Oct	Nov	Dec
CCC	3.4	3.5	3.4	3.5	3.8	3.8	3.7	3.6	3.5	3.5	3.4	3.3
CNRM	3.4	3.5	3.4	3.5	3.8	3.8	3.7	3.6	3.5	3.5	3.4	3.3
ECH	3.4	3.5	3.4	3.5	3.7	3.8	3.7	3.6	3.5	3.6	3.5	3.3

IPSL	3.4	3.5	3.4	3.5	3.8	3.8	3.7	3.5	3.4	3.5	3.4	3.3
Monthly mean	3.4	3.5	3.4	3.5	3.8	3.8	3.7	3.6	3.5	3.5	3.4	3.3

When examining the formulae for TRIX (Equation 46) it was seen that every term increases during winter and thereby increasing the TRIX during winter. Thus, winter was considered the season of lowest water quality and greatest eutrophication for Voëlvlei Dam.

5.2 THE CLIMATE CHANGE SCENARIOS AND EUTROPHICATION LEVELS

Once the water quality for the preliminary present day climate had been established as the baseline, the effect of future climate change on the eutrophication of Voëlvlei Dam was investigated. This effect was determined by rerunning the water quality model, CE-QUAL-W2 but with the projected climate meteorological input data (air temperature, dew point temperature, wind-speed and direction, cloud cover and solar radiation) from the four climate change models (CCC, CNRM, ECH and IPSL). Water quality trends were noted from each of the runs and compared with the present day runs. For this study, 1/1/2046-31/12/2065 represented the intermediate future and 1/1/2081-31/12/2100 was the distant future. The CCC model only had present day and intermediate future climate data.

The inflow streams were not adjusted for increased temperature for the future runs but since the inflow was at segment 21 and the segment under study was segment 11, assuming that Voëlvlei was a well-mixed dam this was considered not a problem.

5.2.1 Air temperature

Once the mean monthly air temperature for the present day had been established, the effect of climate change on Voëlvlei Dam was quantified. The water quality model (CE-QUAL-W2) was rerun with the same initial conditions and parameters but with the intermediate future and distant future meteorological inputs. The intermediate future and distant future air temperature for each of the four climate change models is shown in Figure 89.

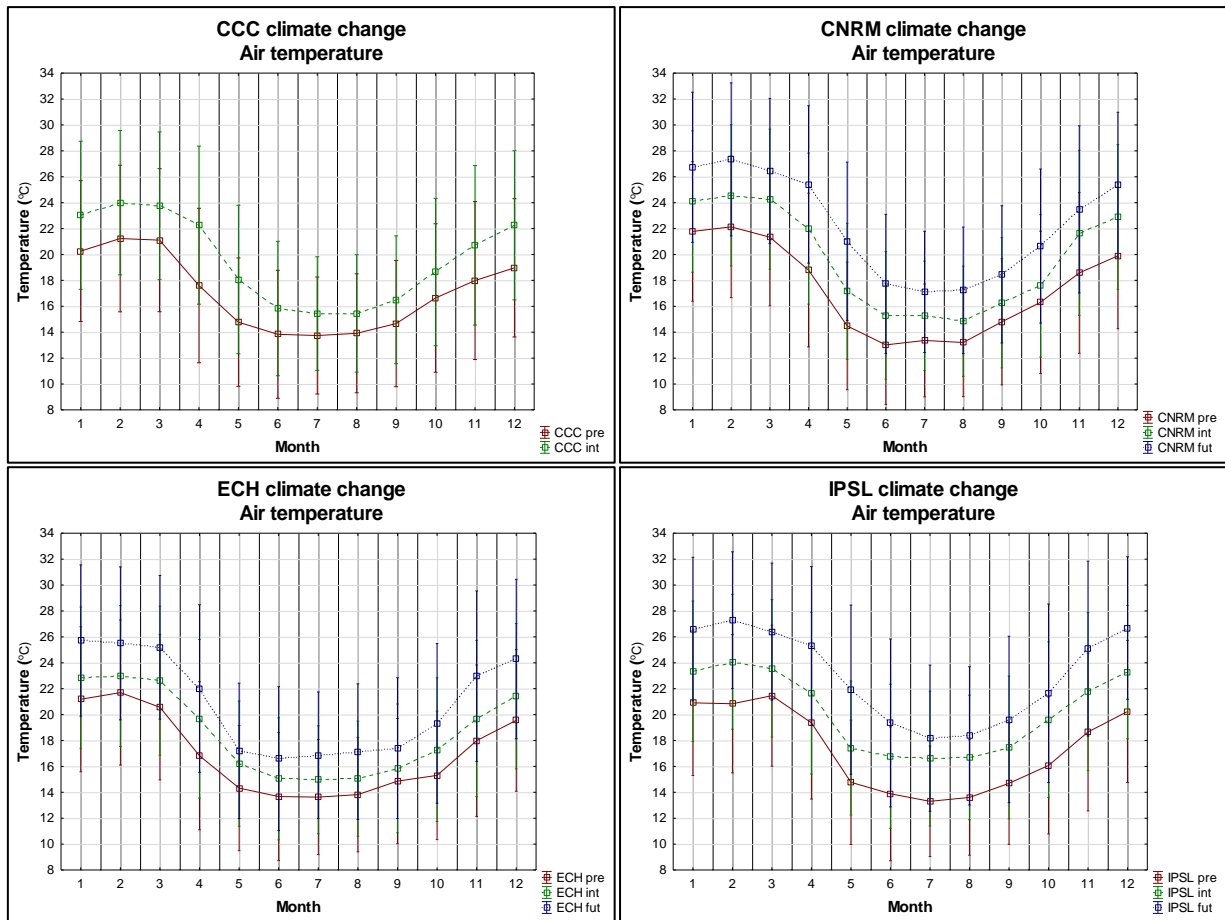


Figure 89 Climate change air temperature predictions

Figure 89 shows that the mean air temperature increased into the intermediate future and rose even higher into the distant future for all four climate models. This higher air temperature is expected to have a marked effect on the surface water temperature in the form of energy transfer at the surface interface, thereby increasing water temperature. The extent of this increase was investigated in conjunction with solar radiation, the other energy source that influences water temperature.

Table 29 Climate change mean monthly air temperature (°C)

	Jan	Feb	Mar	Apr	May	Jun	Jul	Aug	Sep	Oct	Nov	Dec
CCC												
CCC pre	20.3	21.2	21.1	17.6	14.8	13.8	13.7	13.9	14.7	16.6	18.0	19.0
Difference	2.7	2.8	2.7	4.7	3.3	2.0	1.7	1.5	1.8	2.0	2.7	3.3
CCC int	23.0	24.0	23.8	22.3	18.1	15.8	15.4	15.4	16.5	18.6	20.7	22.3
CNRM												
CNRM pre	21.8	22.1	21.3	18.8	14.5	13.0	13.4	13.2	14.8	16.3	18.6	19.9
Difference	2.3	2.5	3.0	3.2	2.7	2.3	1.9	1.6	1.5	1.3	3.1	3.0
CNRM int	24.1	24.6	24.3	22.0	17.2	15.3	15.3	14.8	16.3	17.6	21.7	22.9
CNRM int	24.1	24.6	24.3	22.0	17.2	15.3	15.3	14.8	16.3	17.6	21.7	22.9
Difference	2.6	2.7	2.1	3.4	3.8	2.4	1.8	2.4	2.2	3.1	1.8	2.5
CNRM fut	26.7	27.3	26.4	25.4	21.0	17.7	17.1	17.2	18.5	20.7	23.5	25.4
ECH												
ECH pre	21.2	21.7	20.6	16.8	14.3	13.7	13.6	13.8	14.9	15.3	18.0	19.6
Difference	1.7	1.3	2.0	2.9	1.9	1.3	1.4	1.2	0.9	2.0	1.7	1.8
ECH int	22.9	23.0	22.6	19.7	16.2	15.0	15.0	15.0	15.8	17.3	19.7	21.4
ECH int	22.9	23.0	22.6	19.7	16.2	15.0	15.0	15.0	15.8	17.3	19.7	21.4
Difference	2.8	2.5	2.6	2.3	1.0	1.6	1.9	2.1	1.6	2.0	3.3	2.9
ECH fut	25.7	25.5	25.2	22.0	17.2	16.6	16.9	17.1	17.4	19.3	23.0	24.3
IPSL												
IPSL pre	20.9	20.8	21.5	19.4	14.8	13.9	13.3	13.6	14.7	16.1	18.7	20.2
Difference	2.4	3.3	2.1	2.3	2.6	2.9	3.3	3.1	2.8	3.5	3.1	3.1
IPSL int	23.3	24.1	23.6	21.7	17.4	16.8	16.6	16.7	17.5	19.6	21.8	23.3
IPSL int	23.3	24.1	23.6	21.7	17.4	16.8	16.6	16.7	17.5	19.6	21.8	23.3
Difference	3.3	3.2	2.8	3.6	4.5	2.6	1.6	1.7	2.1	2.0	3.3	3.4
IPSL fut	26.6	27.3	26.4	25.3	21.9	19.4	18.2	18.4	19.6	21.6	25.1	26.7

From the table and the figure, it was seen that the mean monthly temperature increases when going from present day to intermediate day and was highest for the distant future scenario. The warmest months shown are the orange to red colours and the cooler months are greener. It was clear from this that May to September was the cooler months and November to April was the warmer months.

It was interesting to note that the change in mean air temperature in progressing from the present day to the intermediate future was similar of that from intermediate future to distant future. This was a consequence of the accelerated anthropogenic loading as the time span from present day (1971-1990) to intermediate future (2046-2065) was much greater than that of intermediate future to distant future (2081-2100) (Figure 45).

The climate models are ranked from the 'coolest' to the 'hottest' as ECH, CNRM then IPSL. This would imply that the ECH model produced the least change in air temperature and thus a

subsequent lower algal growth as compared to CNRM and the IPSL, which would have the maximum effect on algal growth.

The inter-variability between the climate models is now more evident and some discrepancies are noticed in Figure 89 and Table 29. The inter-variability arises from the climate models themselves in assigning different assumptions of greenhouse gas loadings to the atmosphere.

5.2.2 Solar radiation

Wetzel in 2001 and others had established the diurnal link between solar radiation and surface water temperature from the aspect of an energy balance. Increased water temperature was the direct result of the diurnal shortwave solar radiation on a water-body. Figure 47 showed the present day solar radiation over Voëlvlei Dam and it was seen that May, June, July and August has the lowest radiation values. Figure 90 shows the incident solar radiation over Voëlvlei Dam for climate change for the four climate change models.

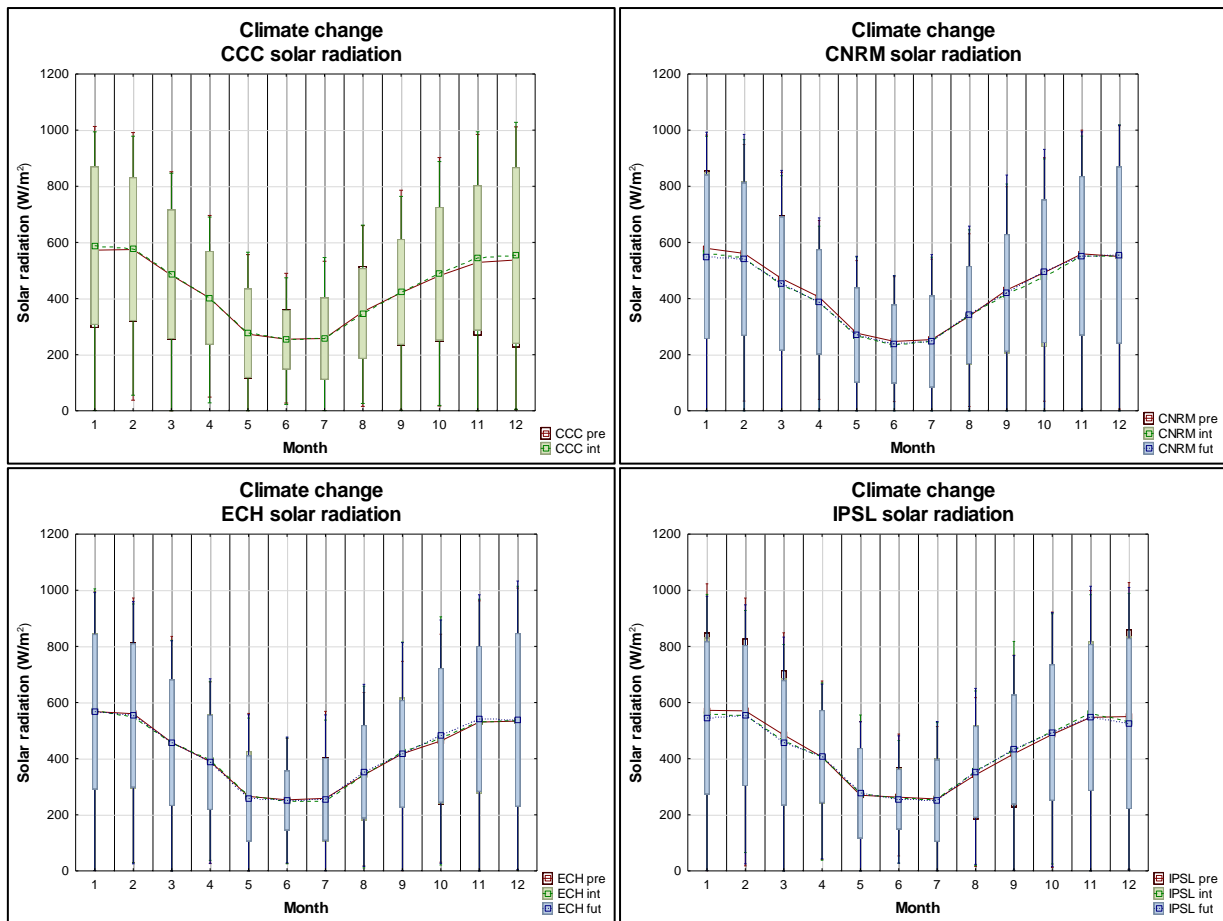


Figure 90 Mean monthly incident solar radiation over Voëlvlei Dam

Figure 90 shows that for the intermediate future and distant future climates the change in incident solar radiation was negligible over that of the present day for all four climate change models. This would imply that the effect of solar radiation of the present time and the future was similar and did not have a substantial impact on the growth of algae in the future. The months with the greatest

incident solar radiation were January and February for all climate models. When comparing the driving effect of air temperatures and solar radiation on surface water temperatures for future events, air temperatures had the greatest effect, as solar radiation remained unchanged for future climate change projections.

5.2.3 Surface water temperature changes

Long-term surface water temperature change had now been linked to air temperature increase due to climate change and the perceived changes due to diurnal fluxes are seen to be negligible within the four climate models used. Solar radiation influenced water temperature on a daily basis, but there was no nett climate change effect on solar radiation and thus it did not contribute to a long-term increase in water temperature. Essentially the long-term increases in surface water temperature were a result of increased air temperature, due to the greenhouse effect.

Figure 91 and Table 30 show the mean surface water temperature increase due to climate change into the intermediate future and distant future. It is seen that surface water temperature increases progressive for each month of the simulation period for all the future scenarios of climate change. If all other factors that support algal growth were favourable during this time then this increase in water temperature would have a marked increase in total algal growth in Voëlvlei Dam throughout the entire year. This premise is investigated further in the ensuing sections.

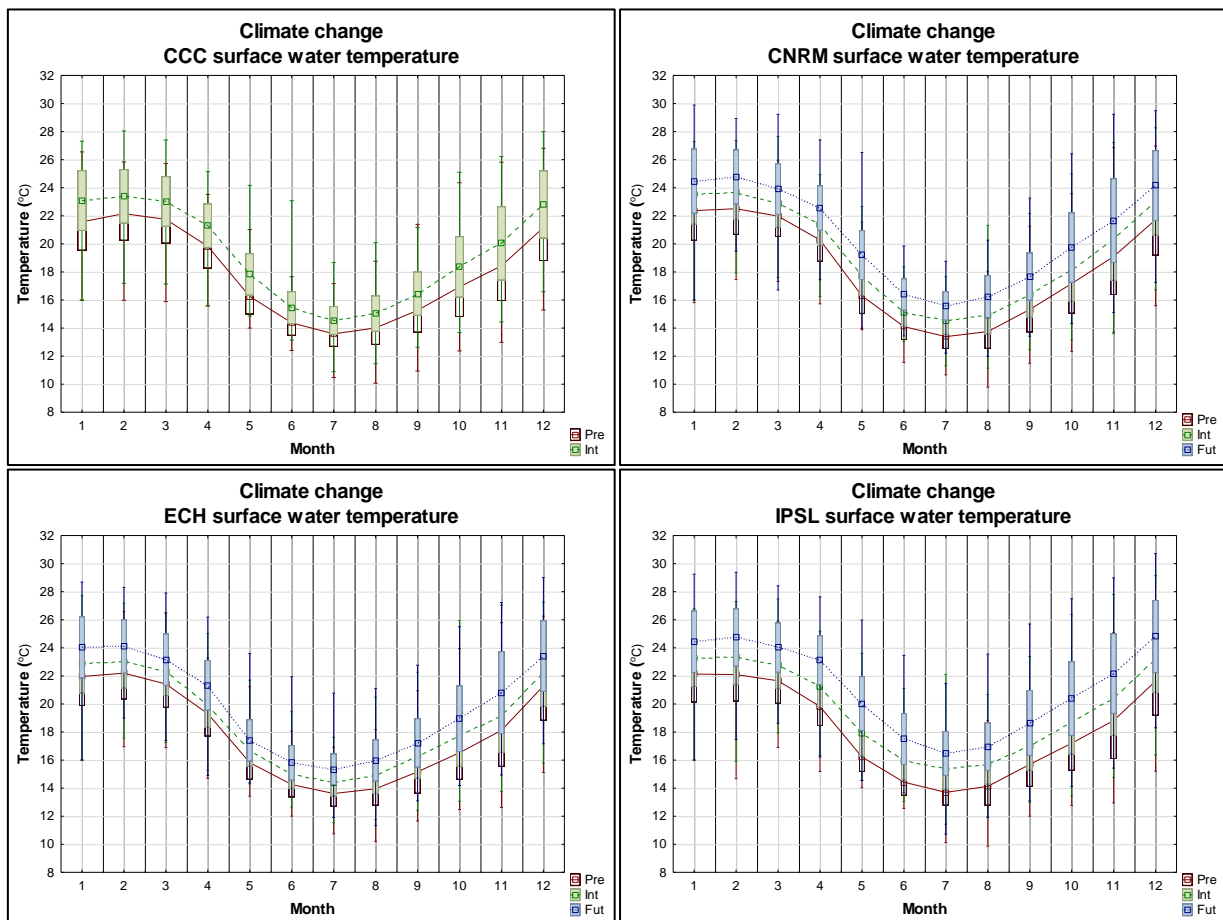


Figure 91 Climate change surface water temperature

It was clear that the mean surface water temperature increased from present day to distant future, with the intermediate future mean water temperatures between them.

Table 30 Climate change mean monthly surface water temperature (°C)

	Jan	Feb	Mar	Apr	May	Jun	Jul	Aug	Sep	Oct	Nov	Dec
CCC												
CCC pre	21.6	22.2	21.7	19.8	16.3	14.4	13.6	14.0	15.3	16.9	18.4	21.2
Difference	1.5	1.2	1.3	1.5	1.6	1.1	1.0	1.0	1.2	1.4	1.6	1.7
CCC int	23.1	23.4	23.0	21.3	17.8	15.5	14.6	15.0	16.4	18.4	20.0	22.8
CNRM												
CNRM pre	22.4	22.5	22.0	20.3	16.3	14.1	13.4	13.7	15.3	17.2	19.1	21.7
Difference	1.1	1.1	0.9	1.1	1.5	1.0	1.2	1.2	1.1	1.0	1.2	1.3
CNRM int	23.5	23.6	22.8	21.4	17.7	15.1	14.5	14.9	16.4	18.1	20.3	23.0
CNRM int	23.5	23.6	22.8	21.4	17.7	15.1	14.5	14.9	16.4	18.1	20.3	23.0
Difference	0.9	1.2	1.1	1.2	1.5	1.3	1.0	1.3	1.3	1.6	1.4	1.1
CNRM fut	24.5	24.8	23.9	22.6	19.2	16.4	15.6	16.2	17.7	19.7	21.7	24.2
ECH												
ECH pre	22.0	22.2	21.4	19.3	15.8	14.3	13.6	14.0	15.2	16.5	18.1	21.3
Difference	0.9	0.8	0.8	0.6	0.9	0.7	0.7	1.0	1.1	1.2	1.1	0.9
ECH int	22.9	23.0	22.3	19.9	16.7	15.0	14.4	14.9	16.3	17.7	19.2	22.2
ECH int	22.9	23.0	22.3	19.9	16.7	15.0	14.4	14.9	16.3	17.7	19.2	22.2
Difference	1.2	1.1	0.9	1.4	0.7	0.9	1.0	1.1	0.9	1.3	1.6	1.2
ECH fut	24.0	24.1	23.2	21.3	17.4	15.8	15.3	16.0	17.2	18.9	20.8	23.4
IPSL												
IPSL pre	22.1	22.1	21.7	19.8	16.2	14.4	13.7	14.1	15.7	17.2	18.8	21.6
Difference	1.1	1.2	1.1	1.5	1.7	1.5	1.6	1.6	1.3	1.5	1.6	1.6
IPSL int	23.2	23.3	22.7	21.3	17.9	16.0	15.3	15.7	17.0	18.7	20.4	23.2
IPSL int	23.2	23.3	22.7	21.3	17.9	16.0	15.3	15.7	17.0	18.7	20.4	23.2
Difference	1.2	1.4	1.3	1.9	2.1	1.5	1.1	1.2	1.6	1.7	1.8	1.6
IPSL fut	24.4	24.7	24.0	23.1	20.0	17.5	16.5	17.0	18.7	20.4	22.2	24.8

The accelerated trend of surface water heating due to climate change from intermediate future to distant future was also evident. From the table it was seen that the pattern for mean surface water temperatures follows that of mean air temperatures for monthly trends and climate change events, thereby consolidating the premise that air temperature was the driver for surface water temperature for this study.

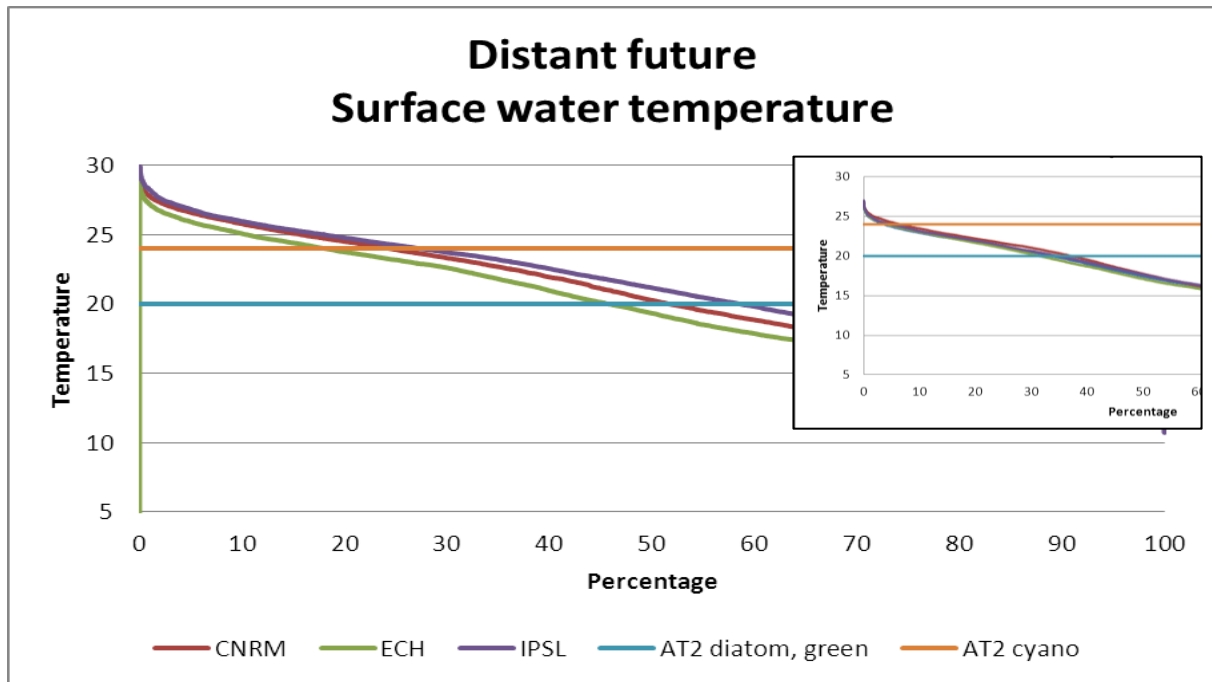


Figure 92 Distant future surface water temperature exceedance

Present day insert

To investigate the effect of increased water temperature on the algae growth an exceedance plot was constructed related to the algal growth rate multipliers. In comparing Figure 92 to Figure 53 and using Table 30 as a guide, it was seen that the mean surface water temperature increased by about 2°C with climate change. This had a direct effect on the perceived favourable growth rates of all algae in Voëlvlei Dam. For diatoms and greens, the favourable temperature was exceeded between 45-60% of the time, which was about double that of the present day, thereby implying twice as much blooms or greater concentrations for climate change. Similarly, for cyanobacteria the exceedance was 18-28%, which was 3 times greater than that of the present day.

It was noted that for the three distant future climate models, their surface water temperatures was more varied than for the present day and it is possible to rate their individual effect on the surface water temperature with ECH being the coolest and IPSL the hottest with CNRM the intermediate climate model.

5.2.4 Surface water elevations

It was expected that as the air temperature and surface water temperature increased, the rate of evaporation from Voëlvlei Dam would be greater for climate change. The result of fixing the inflow and withdrawals the same for the future simulations would be a decreased water level for the dam.

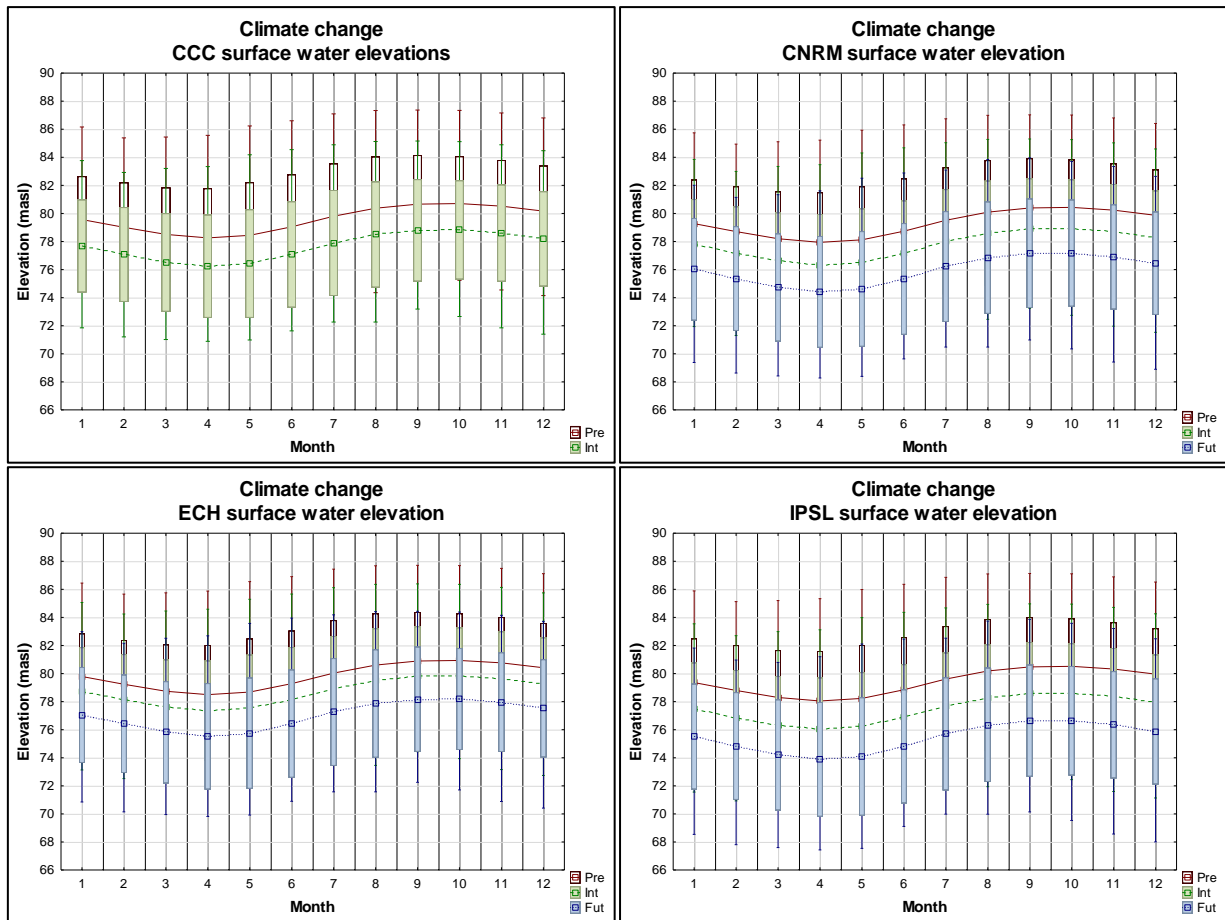


Figure 93 Climate change surface water elevations

The result is shown in Figure 93 and Table 31 where green represents a minimum and red a maximum. The mean monthly surface water levels was decreasing in going from present day to intermediate future and finally distant future scenarios at the accelerated rate explained before.

From Table 31, the mean monthly surface water levels decreased for future climate change scenarios due to increased air temperatures causing greater rates of evaporation. If the inflow concentration of constituents remained the same for climate change scenarios, which it did for this study, this phenomenon would concentrate all constituents in the dam as concentration was directly related to the volume of the dam, which was decreasing.

Table 31 Climate change surface water elevations (m)

	Jan	Feb	Mar	Apr	May	Jun	Jul	Aug	Sep	Oct	Nov	Dec
CCC												
CCC pre	79.6	79.0	78.5	78.3	78.4	79.1	79.8	80.4	80.7	80.7	80.5	80.2
Difference	-1.9	-1.9	-2.0	-2.0	-2.0	-2.0	-1.9	-1.9	-1.9	-1.9	-1.9	-2.0
CCC int	77.7	77.1	76.5	76.2	76.4	77.1	77.9	78.5	78.8	78.8	78.6	78.2
CNRM												
CNRM pre	79.3	78.7	78.2	77.9	78.1	78.7	79.5	80.1	80.4	80.4	80.2	79.9
Difference	-1.5	-1.5	-1.6	-1.6	-1.6	-1.6	-1.5	-1.5	-1.5	-1.5	-1.5	-1.6
CNRM int	77.8	77.2	76.6	76.3	76.5	77.2	78.0	78.6	78.9	78.9	78.7	78.3
CNRM int	77.8	77.2	76.6	76.3	76.5	77.2	78.0	78.6	78.9	78.9	78.7	78.3
Difference	-1.8	-1.8	-1.9	-1.9	-1.9	-1.9	-1.8	-1.8	-1.7	-1.8	-1.8	-1.9
CNRM fut	76.0	75.4	74.7	74.4	74.6	75.3	76.2	76.8	77.2	77.2	76.9	76.4
ECH												
ECH pre	79.8	79.2	78.7	78.5	78.7	79.3	80.0	80.6	80.9	80.9	80.8	80.4
Difference	-1.1	-1.1	-1.1	-1.1	-1.1	-1.1	-1.1	-1.1	-1.1	-1.1	-1.1	-1.1
ECH int	78.7	78.1	77.6	77.3	77.5	78.2	79.0	79.5	79.8	79.9	79.7	79.3
ECH int	78.7	78.1	77.6	77.3	77.5	78.2	79.0	79.5	79.8	79.9	79.7	79.3
Difference	-1.7	-1.7	-1.8	-1.8	-1.8	-1.7	-1.7	-1.7	-1.7	-1.7	-1.7	-1.7
ECH fut	77.1	76.4	75.8	75.5	75.7	76.4	77.3	77.9	78.2	78.2	78.0	77.5
IPSL												
IPSL pre	79.4	78.8	78.3	78.1	78.2	78.8	79.6	80.2	80.5	80.5	80.3	80.0
Difference	-1.9	-1.9	-2.0	-2.0	-2.0	-2.0	-1.9	-1.9	-1.9	-1.9	-1.9	-2.0
IPSL int	77.5	76.9	76.3	76.0	76.2	76.9	77.7	78.3	78.6	78.6	78.4	78.0
IPSL int	77.5	76.9	76.3	76.0	76.2	76.9	77.7	78.3	78.6	78.6	78.4	78.0
Difference	-2.0	-2.0	-2.1	-2.1	-2.1	-2.1	-2.0	-2.0	-2.0	-2.0	-2.0	-2.1
IPSL fut	75.5	74.8	74.2	73.9	74.1	74.8	75.7	76.3	76.6	76.6	76.4	75.9

In conclusion, if the dam were to be operated at the current inflows and withdrawal rates for the future, the surface water levels would decrease due to increased evaporation from the dam. This effective decrease will be discussed in the following sections.

5.2.5 Ortho-Phosphorus concentration

The phosphorus concentration within the dam was influenced by various factors such as inflow and withdrawal as well as assimilation by the various algae as it was the limiting nutrient for algal growth. The future inflow concentration of phosphorus was kept the same as was for the present day scenario. The future in-dam surface concentration of phosphorus was shown for the four climate models in Figure 94.

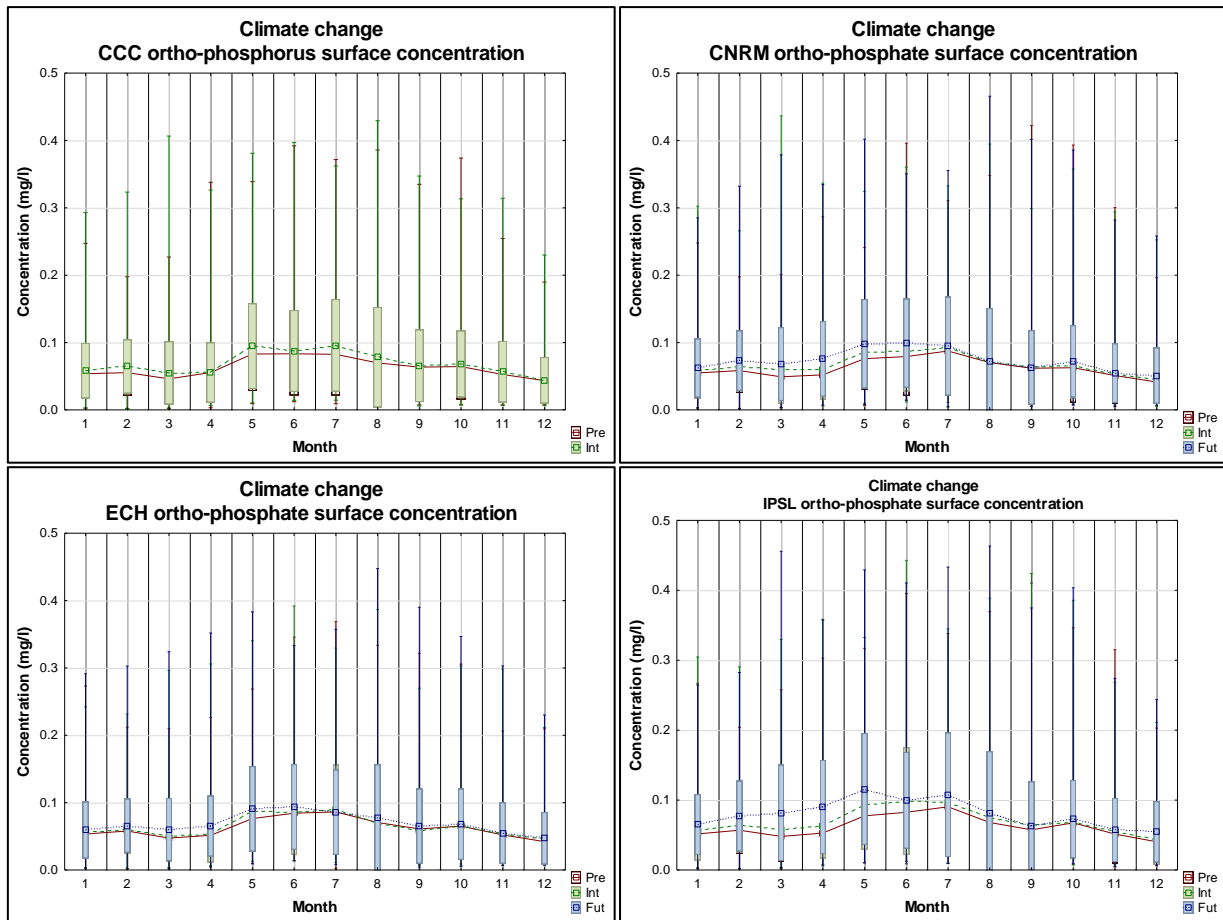


Figure 94 Climate change surface phosphate concentration

From Figure 94 it was seen that the surface phosphate concentration increased for all model with climate change with inter-variability between climate models likened to that of water temperature. Since the inflow of phosphorus into the dam was kept the same for the future events the plausible reasons for the increase in surface concentration was amongst others:

- Increased upwelling of the phosphorus from the organic sediments due to wind action and lower surface water levels; and
- Concentration of the phosphates in the dam due to evaporation of water

Table 32 Climate change phosphate concentration (mg/l)

	Jan	Feb	Mar	Apr	May	Jun	Jul	Aug	Sep	Oct	Nov	Dec
CCC												
CCC pre	0.054	0.055	0.046	0.055	0.083	0.083	0.083	0.070	0.063	0.064	0.053	0.044
Difference	0.004	0.010	0.009	0.000	0.012	0.005	0.013	0.008	0.002	0.004	0.004	0.000
CCC int	0.058	0.065	0.055	0.055	0.095	0.088	0.096	0.078	0.065	0.068	0.057	0.044
CNRM												
CNRM pre	0.055	0.058	0.049	0.052	0.076	0.079	0.087	0.070	0.062	0.063	0.051	0.041
Difference	0.004	0.006	0.010	0.008	0.010	0.008	0.005	0.001	0.002	0.002	0.003	0.004
CNRM int	0.059	0.064	0.059	0.060	0.086	0.087	0.092	0.071	0.064	0.065	0.054	0.045
CNRM int	0.059	0.064	0.059	0.060	0.086	0.087	0.092	0.071	0.064	0.065	0.054	0.045
Difference	0.003	0.009	0.009	0.016	0.012	0.012	0.003	0.001	-0.001	0.007	0.001	0.006
CNRM fut	0.062	0.073	0.068	0.076	0.098	0.099	0.095	0.072	0.063	0.072	0.055	0.051
ECH												
ECH pre	0.053	0.058	0.047	0.052	0.076	0.084	0.086	0.071	0.061	0.065	0.052	0.042
Difference	0.003	0.002	0.003	0.001	0.011	0.002	0.004	-0.001	-0.003	0.000	0.001	0.004
ECH int	0.056	0.060	0.050	0.053	0.087	0.086	0.090	0.070	0.058	0.065	0.053	0.046
ECH int	0.056	0.060	0.050	0.053	0.087	0.086	0.090	0.070	0.058	0.065	0.053	0.046
Difference	0.003	0.006	0.010	0.012	0.004	0.008	-0.004	0.007	0.007	0.003	0.002	0.001
ECH fut	0.059	0.066	0.060	0.065	0.091	0.094	0.086	0.077	0.065	0.068	0.055	0.047
IPSL												
IPSL pre	0.052	0.057	0.048	0.053	0.077	0.083	0.090	0.068	0.057	0.067	0.051	0.040
Difference	0.005	0.007	0.009	0.010	0.016	0.016	0.007	0.007	0.008	0.001	0.004	0.003
IPSL int	0.057	0.064	0.057	0.063	0.093	0.099	0.097	0.075	0.065	0.068	0.055	0.043
IPSL int	0.057	0.064	0.057	0.063	0.093	0.099	0.097	0.075	0.065	0.068	0.055	0.043
Difference	0.008	0.013	0.025	0.027	0.023	0.001	0.010	0.006	-0.002	0.005	0.002	0.012
IPSL fut	0.065	0.077	0.082	0.090	0.116	0.100	0.107	0.081	0.063	0.073	0.057	0.055

From Table 32 it is seen that the mean monthly phosphorus concentration increased with climate change into the future. The order of increasing surface phosphorus concentration was ECH, CNRM then IPSL in terms of climate models. The only difference between these models was the air temperature difference that caused the lower surface water levels. Thus, the lower surface water levels have a concentrating effect on the surface phosphorus concentration. Increases in phosphorus were seen during summer and Voëlvlei Dam had the greatest climate change increases during autumn.

It was concluded that the concentration of phosphorus in Voëlvlei was sufficiently high enough that it never poses a limitation for algal growth from the present day to distant future climate projections. For this dam, a source reduction of phosphorus for the inflows would greatly reduce algal blooms in all climate change scenarios, based on the premise that phosphorus was the limiting nutrient for algal growth.

The sources of phosphorus that could contribute to an increase are increased concentration in the inflows, algal respiration, increased anaerobic release from sediments as well as decay of organic matter. Decreases are due to photosynthesis and system losses to withdrawal and adsorption/settling.

5.2.6 Ammonium concentration

For the future climate change events it was seen in Figure 95 and Table 33 that the surface concentration of ammonium was increased for all the climate models and that the mean monthly concentration was below the DWA limit of 1mg/l, although peaks beyond this did occur.. ECH, CNRM followed by the IPSL was the order in the air temperature increased as well as the order in which the surface concentration of ammonium.

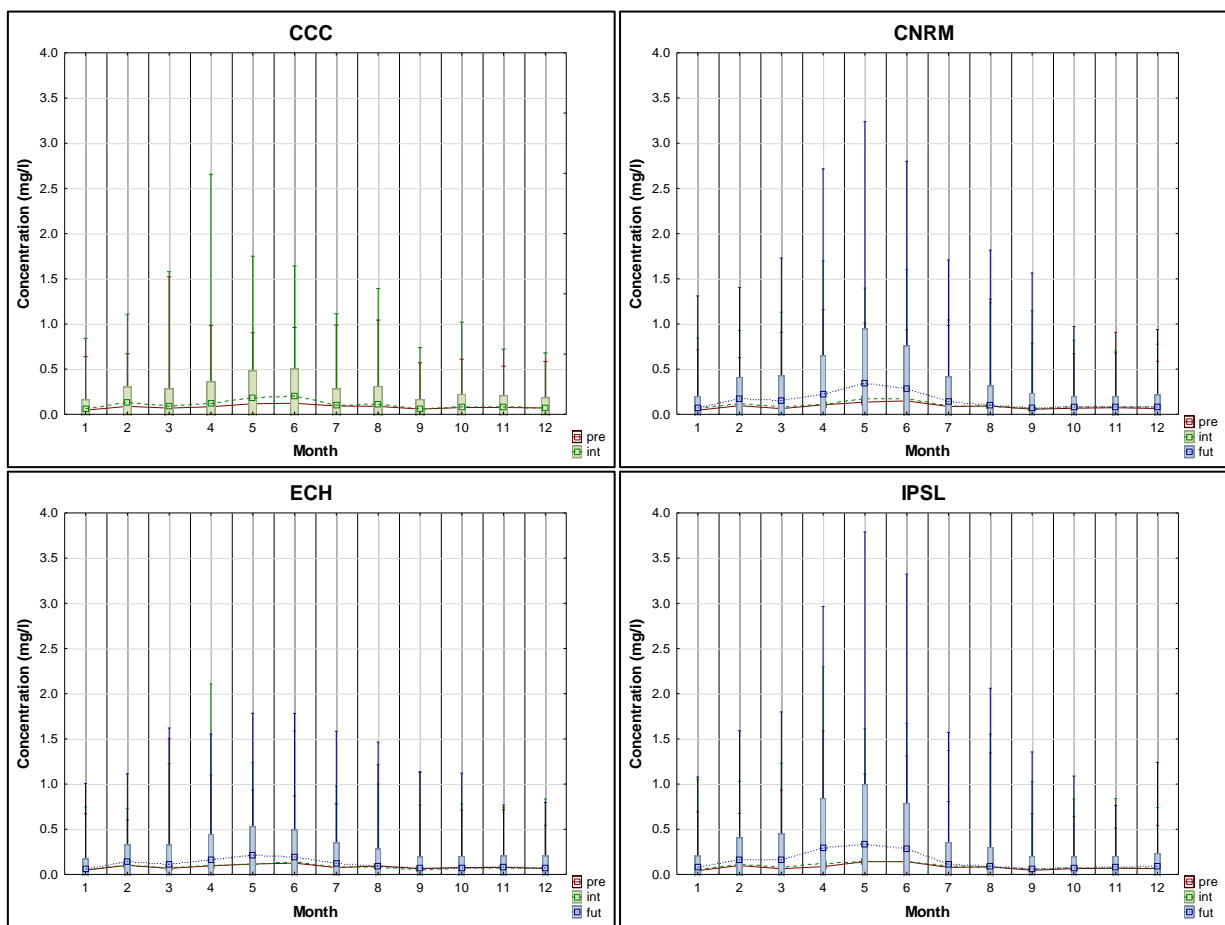


Figure 95 Climate change surface ammonium concentration

All models showed increases but the greatest increase occurred in going from intermediate future to distant future as shown by Table 33. An increase in ammonium was attributed to increased algal respiration, decay of dissolved organic material and anaerobic release from the sediments. System losses of ammonium were due to photosynthesis and nitrification to form the nitrite-nitrate complex ion.

Table 33 Climate change ammonium concentration (mg/l)

	Jan	Feb	Mar	Apr	May	Jun	Jul	Aug	Sep	Oct	Nov	Dec
CCC												
CCC pre	0.046	0.088	0.069	0.084	0.118	0.123	0.093	0.088	0.058	0.076	0.076	0.071
Difference	0.016	0.039	0.022	0.034	0.061	0.080	0.010	0.022	0.000	0.009	0.007	0.000
CCC int	0.062	0.127	0.091	0.118	0.179	0.203	0.103	0.110	0.058	0.085	0.083	0.071
CNRM												
CNRM pre	0.046	0.096	0.063	0.105	0.136	0.149	0.086	0.093	0.056	0.068	0.073	0.065
Difference	0.013	0.030	0.021	0.004	0.038	0.028	0.004	-0.001	0.001	0.010	0.007	0.012
CNRM int	0.059	0.126	0.084	0.109	0.174	0.177	0.090	0.092	0.057	0.078	0.080	0.077
CNRM int	0.059	0.126	0.084	0.109	0.174	0.177	0.090	0.092	0.057	0.078	0.080	0.077
Difference	0.015	0.042	0.066	0.118	0.167	0.106	0.053	0.011	0.016	-0.001	-0.003	0.004
CNRM fut	0.074	0.168	0.150	0.227	0.341	0.283	0.143	0.103	0.073	0.077	0.077	0.081
ECH												
ECH pre	0.049	0.101	0.068	0.095	0.115	0.125	0.076	0.094	0.064	0.078	0.077	0.067
Difference	0.003	0.003	0.001	0.008	0.002	0.021	0.009	-0.011	-0.012	-0.005	-0.002	0.009
ECH int	0.052	0.104	0.069	0.103	0.117	0.146	0.085	0.083	0.052	0.073	0.075	0.076
ECH int	0.052	0.104	0.069	0.103	0.117	0.146	0.085	0.083	0.052	0.073	0.075	0.076
Difference	0.011	0.036	0.046	0.062	0.092	0.043	0.041	0.012	0.016	0.001	0.003	0.000
ECH fut	0.063	0.140	0.115	0.165	0.209	0.189	0.126	0.095	0.068	0.074	0.078	0.076
IPSL												
IPSL pre	0.042	0.098	0.064	0.087	0.142	0.141	0.078	0.084	0.046	0.064	0.069	0.065
Difference	0.011	0.016	0.021	0.033	0.001	0.004	0.013	0.001	0.016	0.010	0.006	0.005
IPSL int	0.053	0.114	0.085	0.120	0.143	0.145	0.091	0.085	0.062	0.074	0.075	0.070
IPSL int	0.053	0.114	0.085	0.120	0.143	0.145	0.091	0.085	0.062	0.074	0.075	0.070
Difference	0.023	0.050	0.075	0.173	0.189	0.136	0.026	0.005	0.002	0.001	0.003	0.017
IPSL fut	0.076	0.164	0.160	0.293	0.332	0.281	0.117	0.090	0.064	0.075	0.078	0.087

5.2.7 Nitrite-nitrate concentration

The surface nitrate-nitrite concentration was shown in Figure 96 and Table 34. Some months showed a decrease in concentrations and other months showed an increase. The nitrite-nitrate complex was an intermediary and its losses are due to photosynthesis and de-nitrification to the water column. It was generated from ammonia by the process of nitrification.

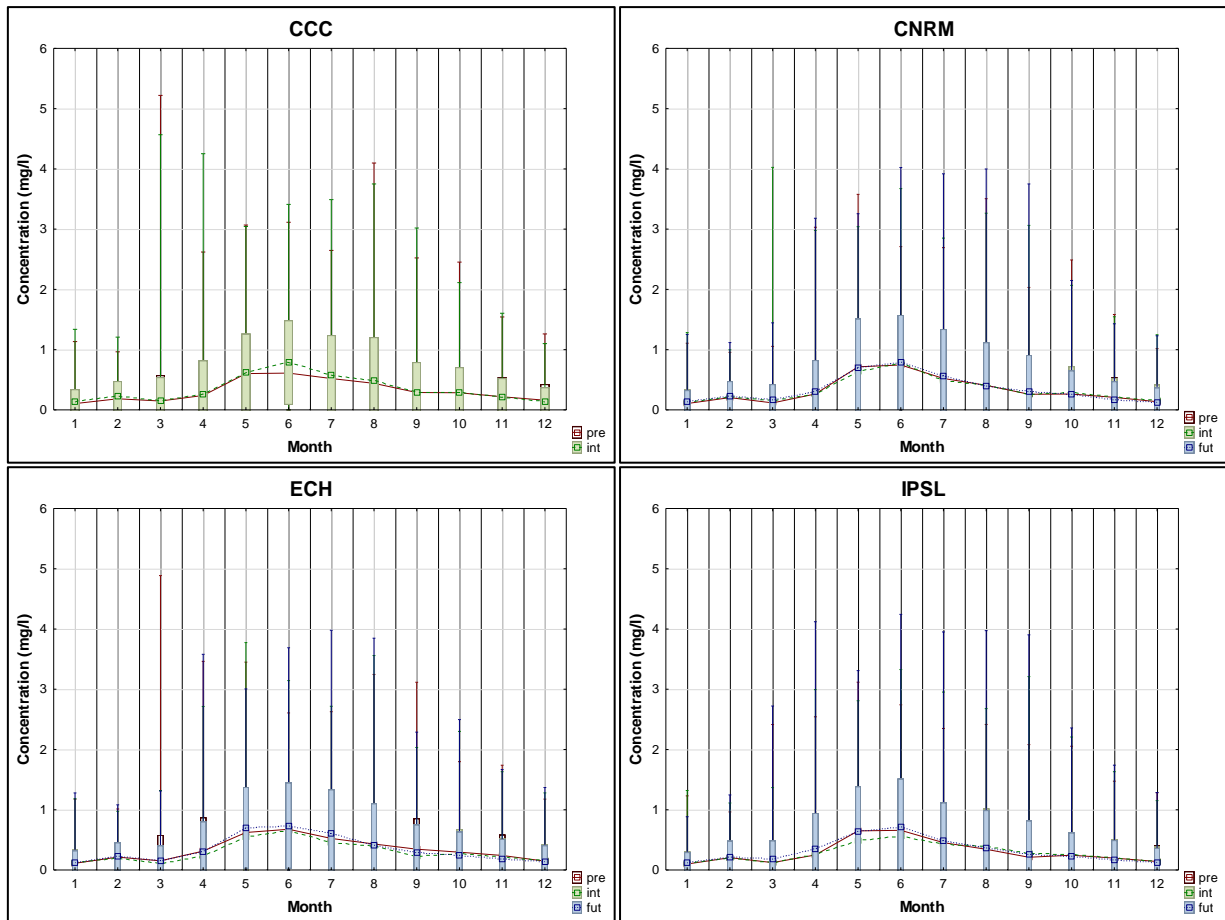


Figure 96 Climate change surface Nitrite-nitrate concentration

From Figure 96 it is seen that the future surface concentrations remain relatively unchanged when compared to present day surface concentrations, with winter having the higher concentrations.

Table 34 Climate change nitrite-nitrate concentration (mg/l)

	Jan	Feb	Mar	Apr	May	Jun	Jul	Aug	Sep	Oct	Nov	Dec
CCC												
CCC pre	0.10	0.19	0.15	0.24	0.60	0.61	0.52	0.44	0.29	0.28	0.22	0.16
Difference	0.03	0.03	0.00	0.02	0.02	0.18	0.06	0.05	0.00	0.01	-0.01	-0.03
CCC int	0.13	0.22	0.15	0.26	0.62	0.79	0.58	0.49	0.29	0.29	0.21	0.13
CNRM												
CNRM pre	0.11	0.20	0.12	0.26	0.72	0.75	0.52	0.41	0.26	0.26	0.21	0.14
Difference	0.02	0.01	0.03	0.00	-0.08	0.03	-0.03	0.00	0.00	0.03	0.00	0.01
CNRM int	0.13	0.21	0.15	0.26	0.64	0.78	0.49	0.41	0.26	0.29	0.21	0.15
CNRM int	0.13	0.21	0.15	0.26	0.64	0.78	0.49	0.41	0.26	0.29	0.21	0.15
Difference	0.00	0.02	0.02	0.05	0.07	0.01	0.08	-0.01	0.04	-0.04	-0.04	-0.02
CNRM fut	0.13	0.23	0.17	0.31	0.71	0.79	0.57	0.40	0.30	0.25	0.17	0.13
ECH												
ECH pre	0.11	0.21	0.15	0.31	0.62	0.68	0.52	0.43	0.35	0.30	0.24	0.15
Difference	0.01	-0.01	-0.04	-0.08	-0.07	-0.03	-0.06	-0.03	-0.12	-0.02	-0.03	0.00
ECH int	0.12	0.20	0.11	0.23	0.55	0.65	0.46	0.40	0.23	0.28	0.21	0.15
ECH int	0.12	0.20	0.11	0.23	0.55	0.65	0.46	0.40	0.23	0.28	0.21	0.15
Difference	0.00	0.02	0.05	0.08	0.15	0.09	0.14	0.02	0.06	-0.04	-0.02	-0.01
ECH fut	0.12	0.22	0.16	0.31	0.70	0.74	0.60	0.42	0.29	0.24	0.19	0.14
IPSL												
IPSL pre	0.10	0.21	0.12	0.25	0.65	0.66	0.45	0.34	0.21	0.25	0.20	0.14
Difference	0.01	-0.01	0.01	0.01	-0.16	-0.09	-0.03	0.06	0.07	0.01	-0.01	-0.01
IPSL int	0.11	0.20	0.13	0.26	0.49	0.57	0.42	0.40	0.28	0.26	0.19	0.13
IPSL int	0.11	0.20	0.13	0.26	0.49	0.57	0.42	0.40	0.28	0.26	0.19	0.13
Difference	0.01	0.02	0.05	0.08	0.15	0.14	0.07	-0.04	-0.02	-0.03	-0.02	0.00
IPSL fut	0.12	0.22	0.18	0.34	0.64	0.71	0.49	0.36	0.26	0.23	0.17	0.13

When examining Figure 97 it is seen that the exceedance of total surface N does not vary significantly for climate change. This would imply that total surface N concentration did not affect the growth of green algae from an increased limiting aspect, for the climate change period.

The concentration of total surface N increased similarly to that of air temperature with the different climate models i.e. ECH, CNRM then IPSL.

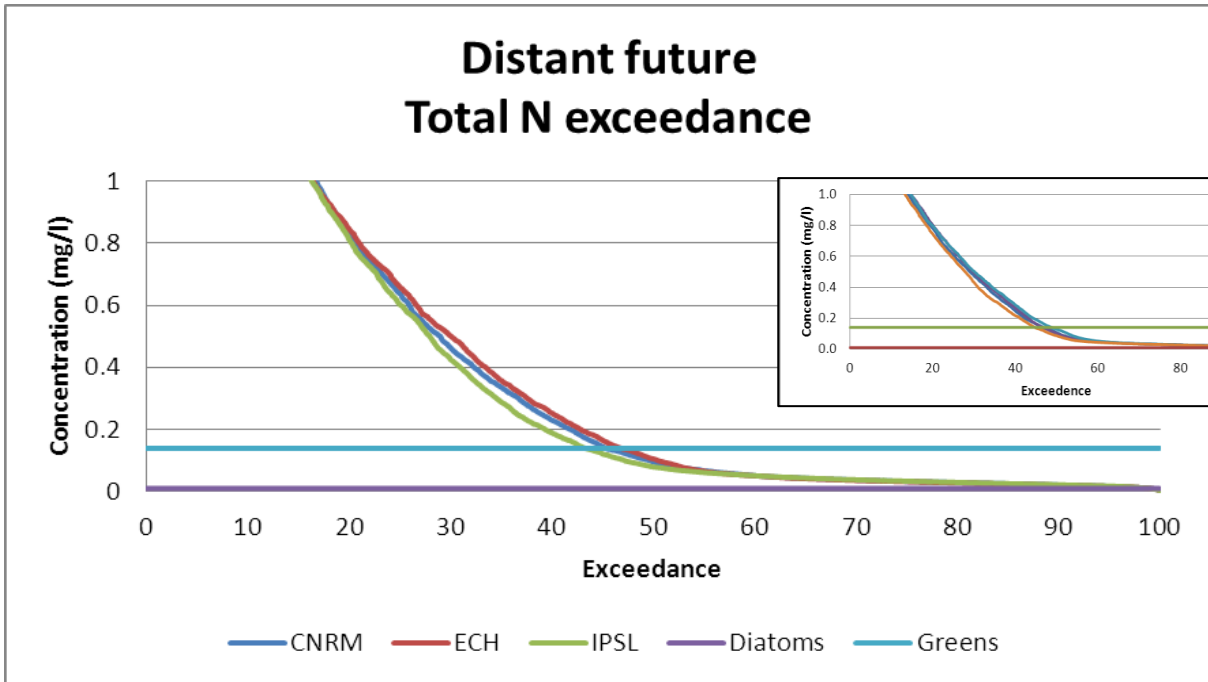


Figure 97 Distant future total surface N exceedance
Present day insert

5.2.8 Dissolved silicon

It had been established that only diatoms are silicon limited for growth and when comparing Figure 98 and Table 35 to the present day, it is seen that the mean monthly surface dissolved silicon concentration increases for future events and winter had the greatest concentration. It was noted that the surface dissolved silicon concentration does not exceed the DWA limit of 150mg/l.

The inter-variability of the climate models is evident but was within the same order of magnitude. The greatest increases are seen when progressing from intermediate future to the distant future. This increase seemed to be directly related to the climate model as the least change was seen with the cooler models and the greatest with the hottest model, namely the IPSL model.

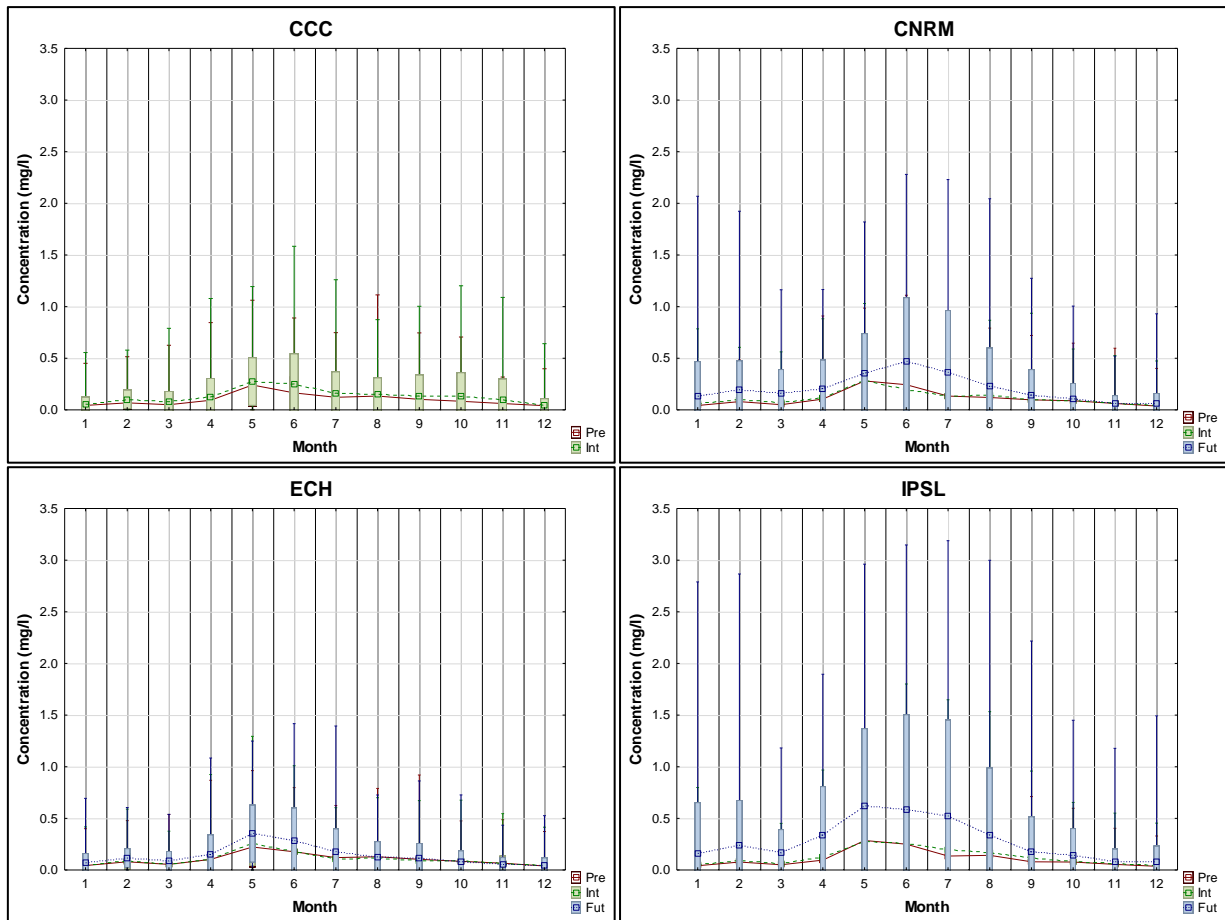


Figure 98 Climate change surface dissolved silicon concentration

The inter-variability is shown in the Table 35 and the dissolved silicon increases with climate change except for the ECH model, which was seen to be a cooler model than the other models. This would imply that the climate model that project warmer air temperatures would result in greater concentrations of surface dissolved silicon and the possibility for greater diatom growth.

Table 35 Climate change dissolved silicon concentration (mg/l)

	Jan	Feb	Mar	Apr	May	Jun	Jul	Aug	Sep	Oct	Nov	Dec
CCC												
CCC pre	0.043	0.069	0.050	0.093	0.241	0.165	0.122	0.134	0.102	0.084	0.062	0.041
Difference	0.013	0.033	0.029	0.028	0.033	0.087	0.041	0.013	0.033	0.046	0.039	0.004
CCC int	0.056	0.102	0.079	0.121	0.274	0.252	0.163	0.147	0.135	0.130	0.101	0.045
CNRM												
CNRM pre	0.043	0.080	0.050	0.105	0.280	0.244	0.134	0.120	0.097	0.088	0.062	0.037
Difference	0.020	0.017	0.024	0.009	0.000	-0.047	-0.003	0.019	0.005	0.002	0.000	0.008
CNRM int	0.063	0.097	0.074	0.114	0.280	0.197	0.131	0.139	0.102	0.090	0.062	0.045
CNRM int	0.063	0.097	0.074	0.114	0.280	0.197	0.131	0.139	0.102	0.090	0.062	0.045
Difference	0.070	0.098	0.089	0.093	0.072	0.272	0.232	0.088	0.043	0.016	0.000	0.016
CNRM fut	0.133	0.195	0.163	0.207	0.352	0.469	0.363	0.227	0.145	0.106	0.062	0.061
ECH												
ECH pre	0.043	0.080	0.055	0.102	0.223	0.177	0.120	0.128	0.103	0.084	0.066	0.039
Difference	0.006	0.006	0.002	0.005	0.033	0.003	-0.011	-0.011	-0.012	0.002	-0.003	0.003
ECH int	0.049	0.086	0.057	0.107	0.256	0.180	0.109	0.117	0.091	0.086	0.063	0.042
ECH int	0.049	0.086	0.057	0.107	0.256	0.180	0.109	0.117	0.091	0.086	0.063	0.042
Difference	0.019	0.029	0.031	0.042	0.096	0.103	0.066	0.011	0.023	-0.003	-0.007	0.007
ECH fut	0.068	0.115	0.088	0.149	0.352	0.283	0.175	0.128	0.114	0.083	0.056	0.049
IPSL												
IPSL pre	0.041	0.077	0.051	0.096	0.286	0.250	0.135	0.142	0.079	0.077	0.055	0.036
Difference	0.016	0.014	0.014	0.025	-0.008	0.011	0.059	0.030	0.033	0.005	0.010	0.008
IPSL int	0.057	0.091	0.065	0.121	0.278	0.261	0.194	0.172	0.112	0.082	0.065	0.044
IPSL int	0.057	0.091	0.065	0.121	0.278	0.261	0.194	0.172	0.112	0.082	0.065	0.044
Difference	0.106	0.148	0.100	0.217	0.347	0.325	0.327	0.169	0.063	0.058	0.011	0.035
IPSL fut	0.163	0.239	0.165	0.338	0.625	0.586	0.521	0.341	0.175	0.140	0.076	0.079

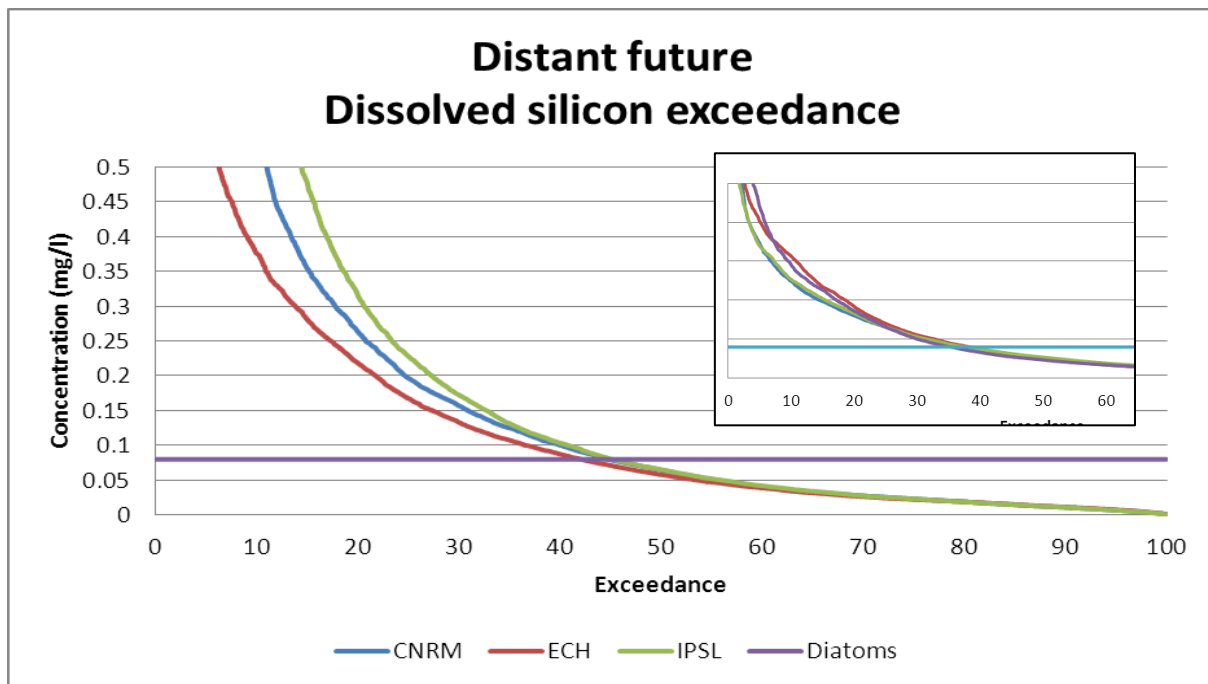


Figure 99 Distant future surface dissolved silicon concentration exceedance
Present day insert

From the exceedance plot of surface dissolved silicon with regards the half-saturation constant (0.08 mg/l) for diatoms it was seen that this had increased to 43-48% depending on the climate model. This would imply that the concentration of surface dissolved silicon was great enough to allow the maximum growth of diatoms for 43 % of the simulation period.

5.2.9 Dissolved oxygen

It was expected for the dissolved oxygen concentration that for the surface water it would decrease due to the increased water temperature causing greater dissociation of oxygen to the atmosphere. This phenomenon is shown in Figure 100 with climate change the concentration of dissolved oxygen in the surface water levels decreased. The figure also shows that the dissolved oxygen concentration was greatest during winter, when the water was cooler and could hold more oxygen as shown by the mean surface dissolved oxygen concentrations in Table 36.

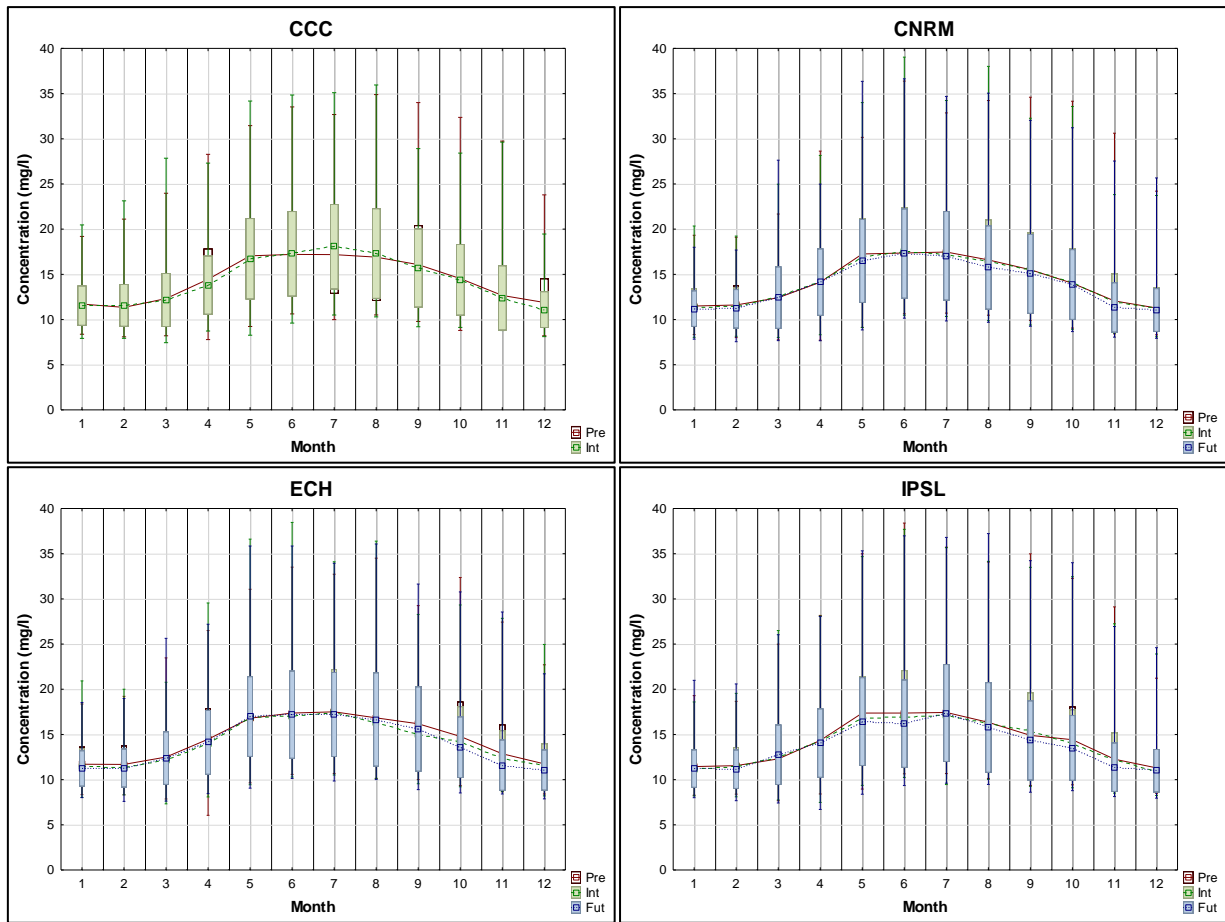


Figure 100 Climate change surface dissolved oxygen concentration

It has been noted that these dissolved oxygen concentrations were deemed very high and super-saturated and thus considered unrealistic but that this study allowed for a comparison due to climate change.

Table 36 Climate change dissolved oxygen concentration (mg/l)

	Jan	Feb	Mar	Apr	May	Jun	Jul	Aug	Sep	Oct	Nov	Dec
CCC												
CCC pre	11.71	11.34	12.32	14.45	17.05	17.21	17.18	16.90	16.08	14.53	12.66	11.89
Difference	-0.18	0.24	-0.16	-0.65	-0.31	0.08	0.90	0.40	-0.38	-0.12	-0.26	-0.80
CCC int	11.53	11.58	12.16	13.80	16.74	17.29	18.08	17.30	15.70	14.41	12.40	11.09
CNRM												
CNRM pre	11.49	11.61	12.41	14.13	17.26	17.36	17.47	16.60	15.51	14.01	12.06	11.28
Difference	-0.17	-0.21	0.20	0.01	-0.36	0.13	-0.26	-0.17	-0.01	0.05	-0.08	-0.06
CNRM int	11.32	11.40	12.61	14.14	16.90	17.49	17.21	16.43	15.50	14.06	11.98	11.22
CNRM int	11.32	11.40	12.61	14.14	16.90	17.49	17.21	16.43	15.50	14.06	11.98	11.22
Difference	-0.13	-0.20	-0.20	-0.01	-0.42	-0.20	-0.14	-0.67	-0.45	-0.19	-0.64	-0.17
CNRM fut	11.19	11.20	12.41	14.13	16.48	17.29	17.07	15.76	15.05	13.87	11.34	11.05
ECH												
ECH pre	11.70	11.68	12.50	14.47	16.80	17.37	17.50	16.83	16.18	14.78	12.86	11.74
Difference	-0.25	-0.29	-0.38	-0.45	0.07	-0.37	-0.04	-0.53	-1.20	-0.58	-0.55	-0.22
ECH int	11.45	11.39	12.12	14.02	16.87	17.00	17.46	16.30	14.98	14.20	12.31	11.52
ECH int	11.45	11.39	12.12	14.02	16.87	17.00	17.46	16.30	14.98	14.20	12.31	11.52
Difference	-0.21	-0.11	0.26	0.11	0.11	0.18	-0.25	0.36	0.62	-0.62	-0.71	-0.46
ECH fut	11.24	11.28	12.38	14.13	16.98	17.18	17.21	16.66	15.60	13.58	11.60	11.06
IPSL												
IPSL pre	11.44	11.55	12.30	14.33	17.37	17.37	17.43	16.34	14.90	14.42	12.26	11.30
Difference	-0.30	-0.10	0.11	-0.02	-0.58	-0.41	-0.26	-0.16	0.51	-0.49	-0.15	-0.36
IPSL int	11.14	11.45	12.41	14.31	16.79	16.96	17.17	16.18	15.41	13.93	12.11	10.94
IPSL int	11.14	11.45	12.41	14.31	16.79	16.96	17.17	16.18	15.41	13.93	12.11	10.94
Difference	0.07	-0.31	0.32	-0.27	-0.37	-0.79	0.20	-0.41	-1.07	-0.41	-0.75	0.06
IPSL fut	11.21	11.14	12.73	14.04	16.42	16.17	17.37	15.77	14.34	13.52	11.36	11.00

From Table 36 it is seen that dissolved oxygen concentrations for the surface decreased with all climate models, especially during summer. The distant future showed the greatest changes due to increased water temperatures and increased algal growth. The inter-variability between the models was not significant and all models show a decrease in dissolved oxygen concentrations with projected climate change.

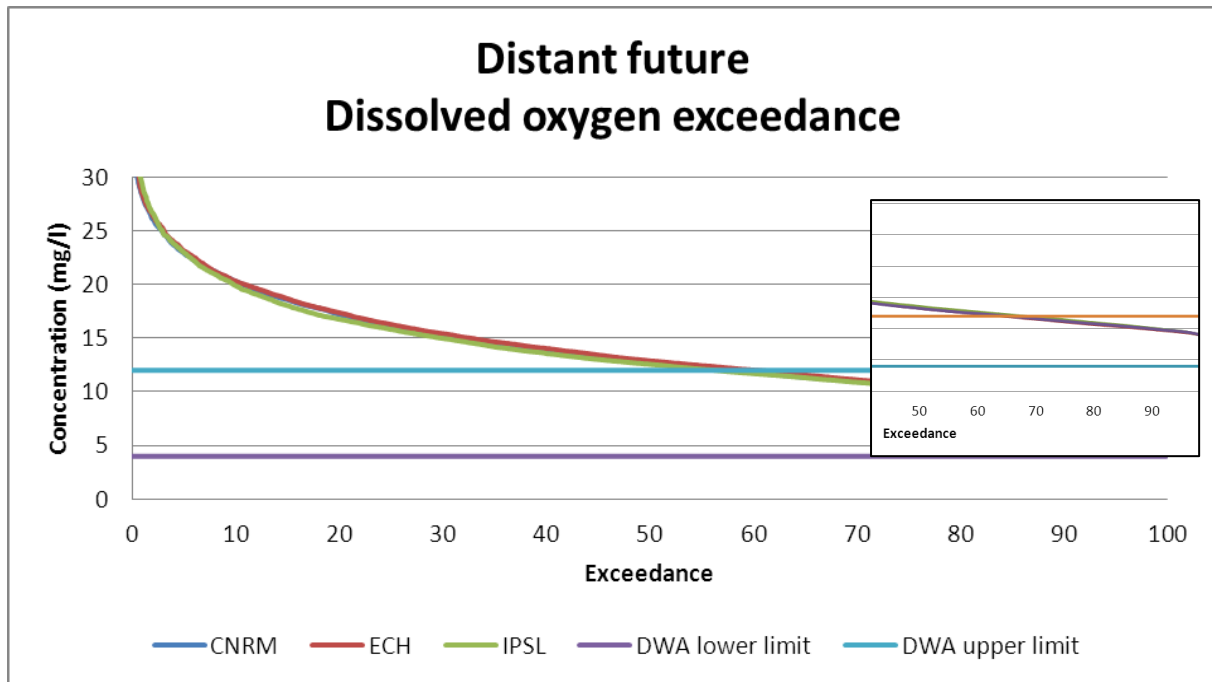


Figure 101 Distant future surface dissolved oxygen DWA limit exceedance plot

Present day insert

From the plot in Figure 101 it is seen that the surface dissolved oxygen exceedance has decreased from 65% in the present day to 58% in the distant future. This implies that for an additional 7% of the simulation period, that the surface dissolved oxygen was outside the TWQR limits set by DWA in the distant future as compared to the present day.

5.2.10 Total algae concentration

It is seen that with climate change the increased air temperatures would lead to increased surface water temperatures. To establish a link to this increased water temperature and algal blooms the total algae is plotted in Figure 102 for Voëlvlei Dam.

From Figure 102 it is seen that with climate change the mean monthly total algal concentration was greater than for the present day. This was attributed directly to the increased water temperature driving the growth of the algae.

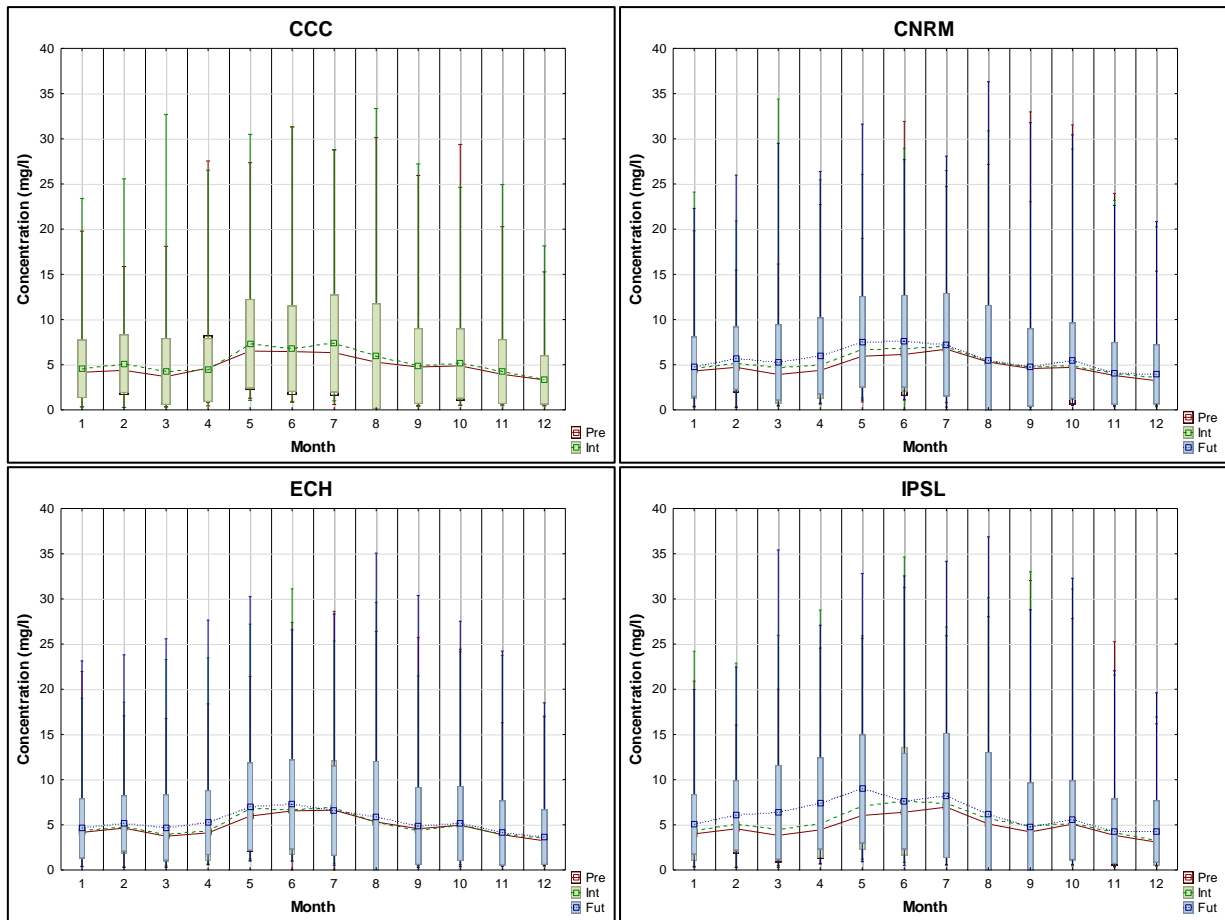


Figure 102 Climate change surface total algae concentration

It is seen that the mean monthly surface total algae concentration was greatest for winter and for climate change the concentration increased. Most of the increased concentration occurs late summer to autumn with the mean winter concentrations remaining relatively unchanged. This could imply a seasonal shift of algal blooms or algal succession.

Table 37 Climate change total algae concentration (mg/l)

	Jan	Feb	Mar	Apr	May	Jun	Jul	Aug	Sep	Oct	Nov	Dec
CCC												
CCC pre	4.16	4.38	3.68	4.64	6.51	6.45	6.34	5.28	4.74	4.87	3.94	3.33
Difference	0.38	0.73	0.57	-0.22	0.83	0.31	1.01	0.65	0.11	0.27	0.30	0.01
CCC int	4.54	5.11	4.25	4.42	7.34	6.76	7.35	5.93	4.85	5.14	4.24	3.34
CNRM												
CNRM pre	4.31	4.71	3.91	4.37	5.94	6.14	6.71	5.30	4.57	4.70	3.80	3.23
Difference	0.25	0.44	0.77	0.57	0.74	0.61	0.32	0.10	0.16	0.20	0.21	0.27
CNRM int	4.56	5.15	4.68	4.94	6.68	6.75	7.03	5.40	4.73	4.90	4.01	3.50
CNRM int	4.56	5.15	4.68	4.94	6.68	6.75	7.03	5.40	4.73	4.90	4.01	3.50
Difference	0.22	0.58	0.59	1.03	0.86	0.85	0.20	0.07	-0.02	0.55	0.04	0.44
CNRM fut	4.78	5.73	5.27	5.97	7.54	7.60	7.23	5.47	4.71	5.45	4.05	3.94
ECH												
ECH pre	4.17	4.64	3.74	4.11	5.96	6.55	6.62	5.31	4.56	4.96	3.91	3.23
Difference	0.22	0.14	0.24	0.25	0.82	0.11	0.32	-0.02	-0.22	0.03	0.06	0.33
ECH int	4.39	4.78	3.98	4.36	6.78	6.66	6.94	5.29	4.34	4.99	3.97	3.56
ECH int	4.39	4.78	3.98	4.36	6.78	6.66	6.94	5.29	4.34	4.99	3.97	3.56
Difference	0.23	0.37	0.73	0.89	0.25	0.59	-0.38	0.58	0.54	0.15	0.14	0.09
ECH fut	4.62	5.15	4.71	5.25	7.03	7.25	6.56	5.87	4.88	5.14	4.11	3.65
IPSL												
IPSL pre	4.00	4.56	3.83	4.44	6.04	6.40	6.95	5.10	4.22	5.08	3.83	3.08
Difference	0.39	0.52	0.68	0.74	1.11	1.20	0.49	0.61	0.66	0.09	0.31	0.19
IPSL int	4.39	5.08	4.51	5.18	7.15	7.60	7.44	5.71	4.88	5.17	4.14	3.27
IPSL int	4.39	5.08	4.51	5.18	7.15	7.60	7.44	5.71	4.88	5.17	4.14	3.27
Difference	0.67	0.97	1.87	2.20	1.83	0.03	0.81	0.45	-0.11	0.36	0.15	0.99
IPSL fut	5.06	6.05	6.38	7.38	8.98	7.63	8.25	6.16	4.77	5.53	4.29	4.26

Table 37 shows the mean monthly total algae concentration for climate change for the four climate models. The climate models predicted mean monthly increases with the maximum increases occurring during autumn to early winter. On average, the annual increase was 15.5%. The ECH model predicted the least increase as it was the climate model with the lowest increase in air temperature. The IPSL model predicted the greatest increase in algal concentration and it is the hottest of all the climate models. This confirms that the water temperature was the driver for surface algal growth when all other conditions were equal for algal growth such as nutrients and light.

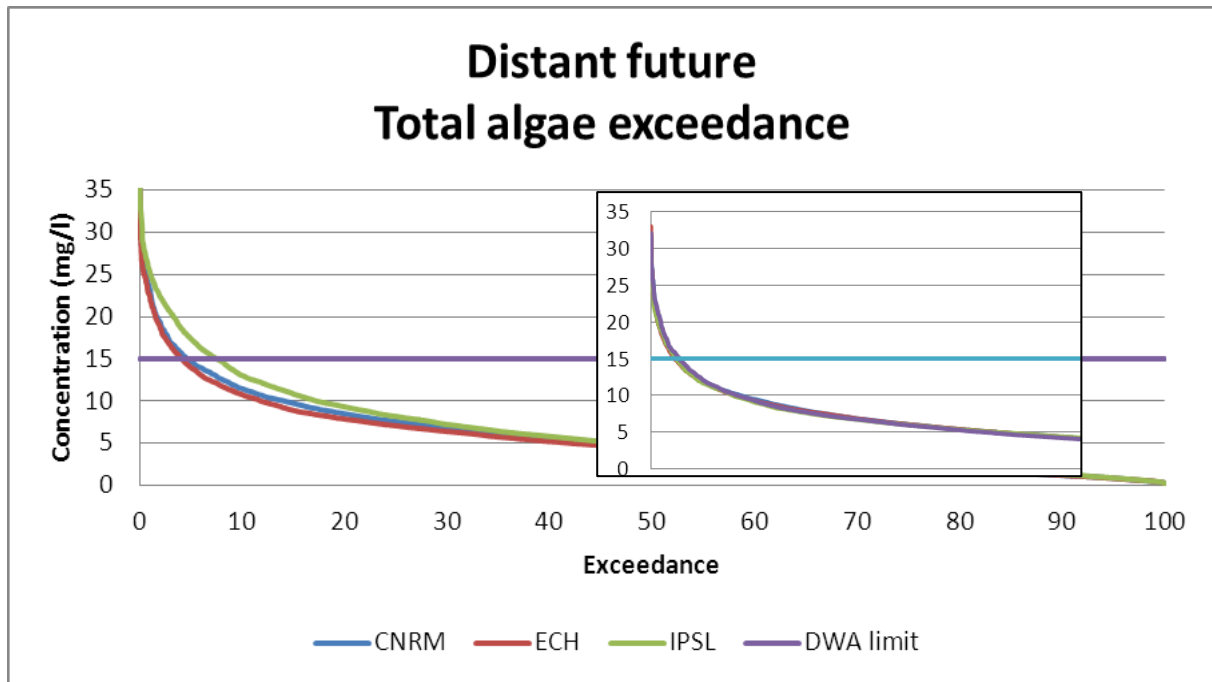


Figure 103 Distant future surface total algae DWA exceedance plot

Present day insert

Figure 103 show that the surface total algae would exceed the DWA limit of 15mg/l of total algae for the distant future by 3% to 5% for CNRM and ECH climate model and 8% for the IPSL climate model. This would imply a worsening of water quality with climate change.

An investigation into which species of algae (diatom, green or cyanobacteria) dominated in Voëlvlei Dam follows.

5.2.11 Diatom concentration

The mean annual increase in algal growth for climate change was predicted at 15.5% increase in algal concentration, what was required is to see which of the three species of algae, namely diatoms, green or cyanobacteria was responsible for this increase. From Figure 104 the surface concentration of diatoms increases especially autumn to winter due to increased water temperature, with the greatest concentrations during winter for all climate change models.

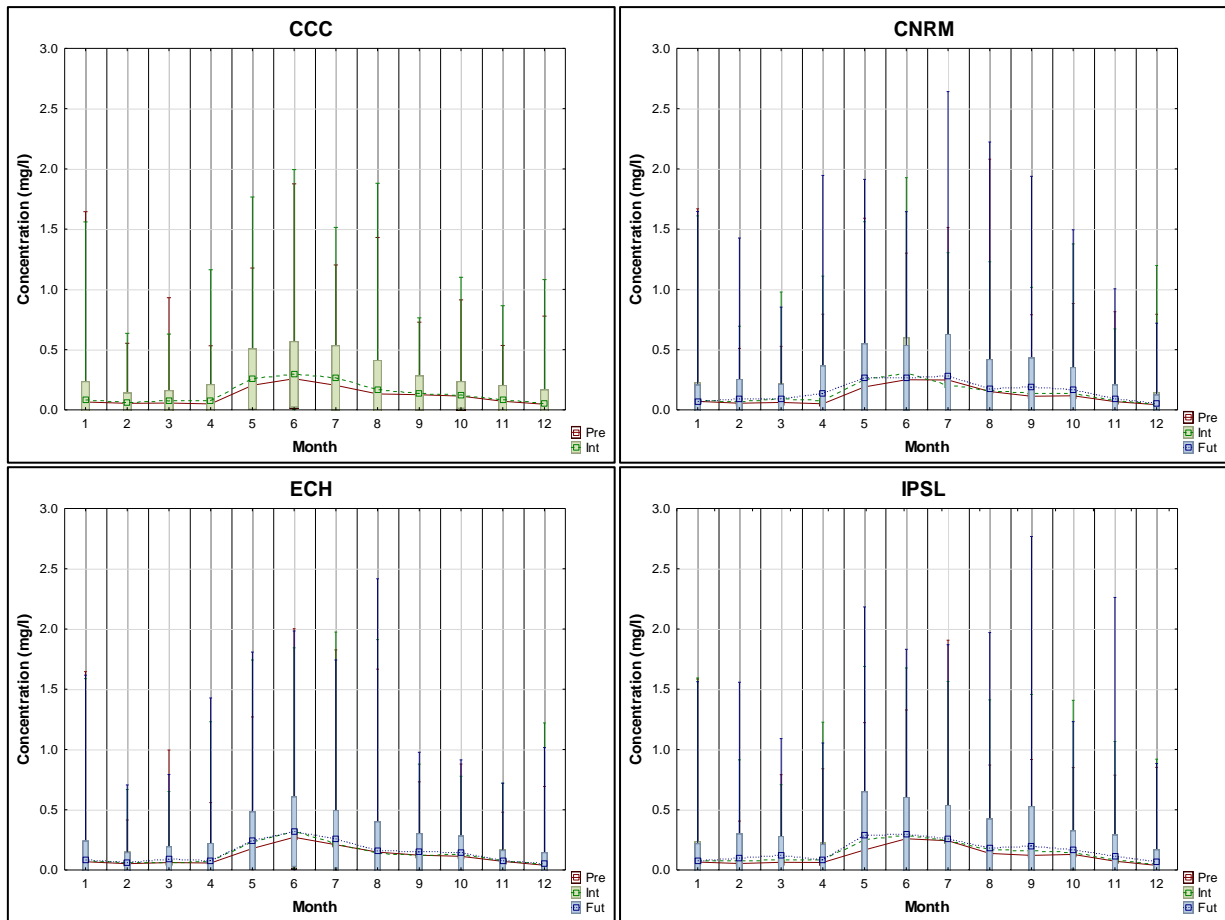


Figure 104 Climate change surface diatom concentration

From Table 38 it is seen that the monthly mean surface diatom concentration increases between 18.9% and 30% depending on the climate model used. The average annual mean surface diatom concentration increased by 24.6% for climate change. The months that showed the greatest increase were autumn and spring. This could be likened to a seasonal shift for diatoms and they have increased concentrations earlier in the year. This could mean a seasonal shift in the blooms of surface diatoms to autumn as well as a lengthening of the season of diatom blooms until late spring. This was a consequence of the increased air temperature that subsequently increased water temperature favouring growth of the diatoms.

Table 38 Climate change diatom concentration (mg/l)

	Jan	Feb	Mar	Apr	May	Jun	Jul	Aug	Sep	Oct	Nov	Dec
CCC												
CCC pre	0.066	0.054	0.057	0.050	0.204	0.259	0.204	0.133	0.126	0.115	0.072	0.047
Difference	0.016	0.009	0.017	0.031	0.051	0.037	0.062	0.032	0.012	0.010	0.016	0.009
CCC int	0.082	0.063	0.074	0.080	0.256	0.296	0.266	0.164	0.138	0.124	0.088	0.056
CNRM												
CNRM pre	0.071	0.055	0.062	0.051	0.191	0.250	0.248	0.152	0.113	0.117	0.069	0.043
Difference	0.008	0.013	0.027	0.022	0.063	0.052	-0.042	0.008	0.024	0.021	0.006	0.005
CNRM int	0.079	0.068	0.089	0.073	0.254	0.302	0.206	0.161	0.137	0.138	0.075	0.048
CNRM int	0.079	0.068	0.089	0.073	0.254	0.302	0.206	0.161	0.137	0.138	0.075	0.048
Difference	-0.007	0.020	0.005	0.061	0.011	-0.035	0.073	0.012	0.051	0.028	0.014	0.004
CNRM fut	0.072	0.088	0.093	0.134	0.266	0.267	0.279	0.173	0.188	0.165	0.089	0.052
ECH												
ECH pre	0.069	0.052	0.062	0.058	0.179	0.272	0.210	0.149	0.123	0.114	0.072	0.039
Difference	0.004	0.011	0.000	0.010	0.054	0.044	0.008	-0.011	-0.003	0.015	0.006	0.010
ECH int	0.073	0.064	0.062	0.069	0.232	0.316	0.218	0.138	0.120	0.129	0.077	0.049
ECH int	0.073	0.064	0.062	0.069	0.232	0.316	0.218	0.138	0.120	0.129	0.077	0.049
Difference	0.010	0.001	0.026	0.011	0.010	0.002	0.039	0.022	0.029	0.012	-0.001	0.004
ECH fut	0.082	0.065	0.088	0.080	0.243	0.318	0.257	0.160	0.149	0.141	0.076	0.053
IPSL												
IPSL pre	0.066	0.054	0.064	0.062	0.167	0.260	0.243	0.138	0.121	0.129	0.073	0.038
Difference	0.013	0.022	0.020	0.020	0.085	0.030	-0.001	0.033	0.037	0.018	0.015	0.005
IPSL int	0.079	0.076	0.084	0.082	0.252	0.290	0.242	0.171	0.158	0.147	0.088	0.043
IPSL int	0.079	0.076	0.084	0.082	0.252	0.290	0.242	0.171	0.158	0.147	0.088	0.043
Difference	-0.001	0.025	0.039	0.002	0.037	0.006	0.017	0.011	0.044	0.020	0.025	0.023
IPSL fut	0.078	0.101	0.123	0.085	0.289	0.296	0.259	0.182	0.202	0.167	0.112	0.066

The ranking of the climate models is as that for air temperature, i.e. ECH, CNRM then CCC and IPSL for increasing concentrations of surface diatoms. The greatest increases occurred during autumn and spring. The surface growth of diatoms was significant as they were light limited and have low light saturation (61.2 W/m^2 for maximum photosynthetic rate) and limited to surface growth.

5.2.12 Green algae concentration

An investigation into the surface green algae concentration and its surface concentration is represented in Figure 105. The green algae concentration increased with climate change. As with the diatoms, the green algae also showed a season shift and lengthening of the bloom season. The green algae and diatoms share similar temperature rate multipliers but different growth rates thus similar growth was not expected.

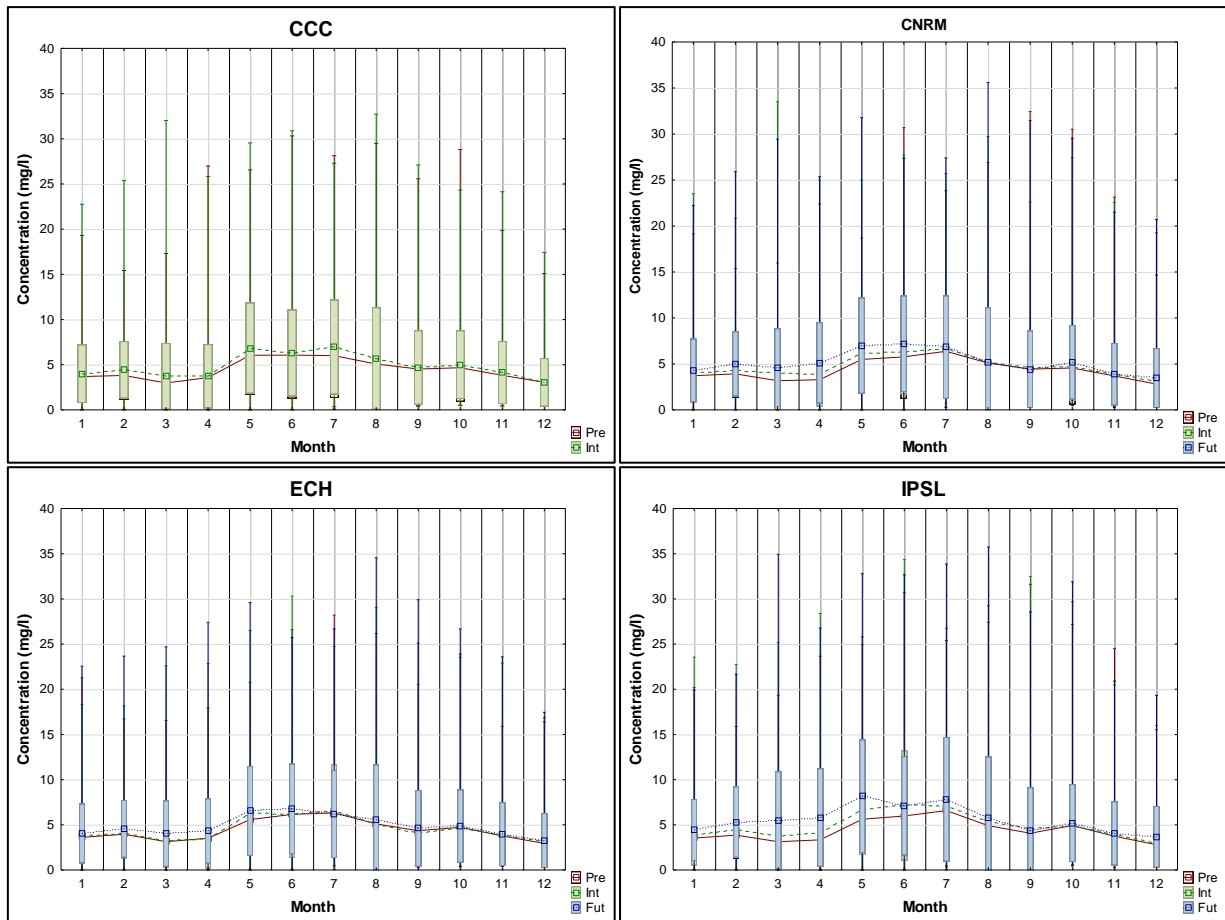


Figure 105 Climate change surface green algae concentration

The climate change produced an increase in the surface concentration of green algae. Table 39 shows the mean monthly surface concentrations of green algae with winter having the greatest concentrations and summer the lowest. The compounding effect of climate change evident as increases from present day to intermediate future was similar to that of intermediate future to distant future, albeit the timespan being much shorter.

Table 39 Climate change green algae concentration (mg/l)

	Jan	Feb	Mar	Apr	May	Jun	Jul	Aug	Sep	Oct	Nov	Dec
CCC												
CCC pre	3.69	3.81	2.98	3.58	6.05	6.06	6.00	5.08	4.52	4.67	3.82	3.05
Difference	0.30	0.63	0.75	0.15	0.79	0.24	0.96	0.61	0.17	0.33	0.31	0.01
CCC int	3.99	4.44	3.73	3.73	6.84	6.30	6.96	5.69	4.69	5.00	4.13	3.06
CNRM												
CNRM pre	3.71	3.92	3.18	3.28	5.49	5.77	6.37	5.09	4.44	4.56	3.70	2.81
Difference	0.29	0.41	0.79	0.62	0.67	0.53	0.35	0.05	0.10	0.10	0.17	0.28
CNRM int	4.00	4.33	3.97	3.90	6.16	6.30	6.72	5.14	4.54	4.66	3.87	3.09
CNRM int	4.00	4.33	3.97	3.90	6.16	6.30	6.72	5.14	4.54	4.66	3.87	3.09
Difference	0.29	0.69	0.62	1.22	0.82	0.88	0.11	0.00	-0.13	0.52	0.03	0.37
CNRM fut	4.29	5.02	4.59	5.12	6.98	7.18	6.83	5.14	4.41	5.18	3.90	3.46
ECH												
ECH pre	3.62	3.95	3.13	3.51	5.58	6.16	6.33	5.10	4.35	4.72	3.77	2.94
Difference	0.12	0.08	0.10	-0.06	0.71	0.06	0.29	-0.03	-0.26	-0.03	0.07	0.25
ECH int	3.74	4.03	3.23	3.45	6.29	6.22	6.62	5.07	4.09	4.69	3.84	3.19
ECH int	3.74	4.03	3.23	3.45	6.29	6.22	6.62	5.07	4.09	4.69	3.84	3.19
Difference	0.31	0.53	0.80	0.86	0.25	0.54	-0.44	0.54	0.52	0.17	0.12	0.07
ECH fut	4.05	4.56	4.03	4.31	6.54	6.76	6.18	5.61	4.61	4.86	3.96	3.26
IPSL												
IPSL pre	3.53	3.86	3.13	3.34	5.61	5.98	6.58	4.90	4.08	4.92	3.74	2.79
Difference	0.33	0.57	0.67	0.79	1.04	1.17	0.49	0.47	0.44	-0.05	0.26	0.17
IPSL int	3.86	4.43	3.80	4.13	6.65	7.15	7.07	5.37	4.52	4.87	4.00	2.96
IPSL int	3.86	4.43	3.80	4.13	6.65	7.15	7.07	5.37	4.52	4.87	4.00	2.96
Difference	0.56	0.88	1.70	1.68	1.51	-0.03	0.76	0.37	-0.16	0.32	0.06	0.71
IPSL fut	4.42	5.31	5.50	5.81	8.16	7.12	7.83	5.74	4.36	5.19	4.06	3.67

The greatest increases in green algae concentrations were in autumn and the least in late winter and spring, which signalled a seasonal shift. Thus, distant future climates produced excessive surface green algae from December until June and increased in the surface concentrations during winter and late summer.

5.2.13 Cyanobacteria concentration

The final group of algae studied for climate change was cyanobacteria concentrations. The climate change concentrations are shown in Figure 106 that is compared to the present day concentrations (Figure 83). For the intermediate future, some inter-variability between the climate models is evident as well as increased concentrations for cyanobacteria. For the distant future, cyanobacteria repopulates the dam but the result is climate model dependent. This difference highlighted the inter-variability between climate models as it showed an increase in some months

and a decrease in others for the various climate models. The mean monthly surface concentrations are shown in Figure 107.

Table 40 shows the mean monthly surface cyanobacteria concentration and the greatest occurs from December to May, corresponding to summer to autumn. The maximum surface concentration of cyanobacteria occurs during April, which was autumn.

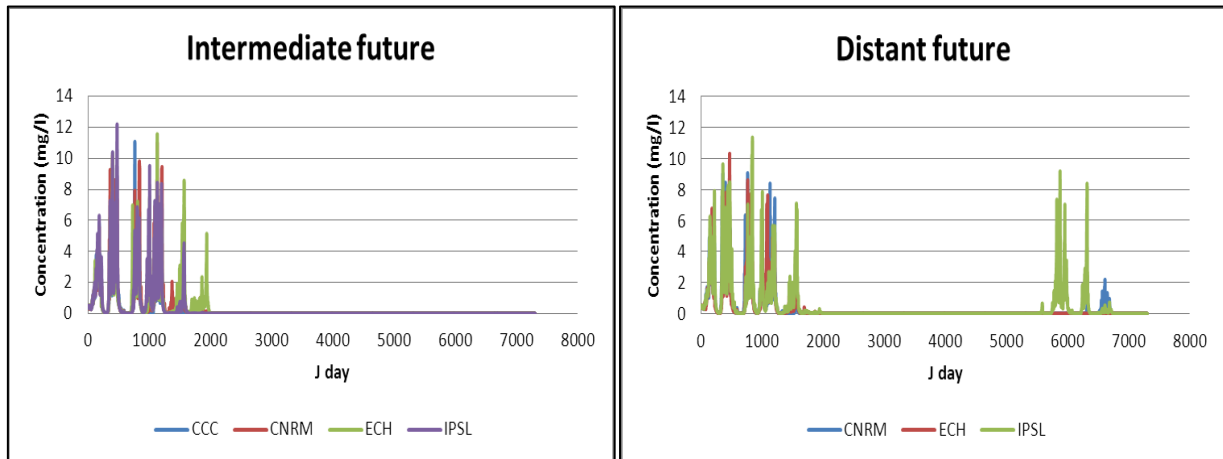


Figure 106 Climate change cyanobacteria concentrations

The inter-variability between the climate models was at its maximum as 2 models (ECH and CCC) show a decrease in cyanobacteria concentrations for the intermediate future, whilst 2 (CNRM and IPSL) show an increase in cyanobacteria concentrations. It is concluded that the hotter climate models favour cyanobacteria growth.

The light saturation for cyanobacteria was 60 W/m^2 and similar to that of the diatoms, thus similar surface growth patterns for the cyanobacteria was expected, but this did not materialise as the algal temperature growth rate multipliers and growth rates varied.

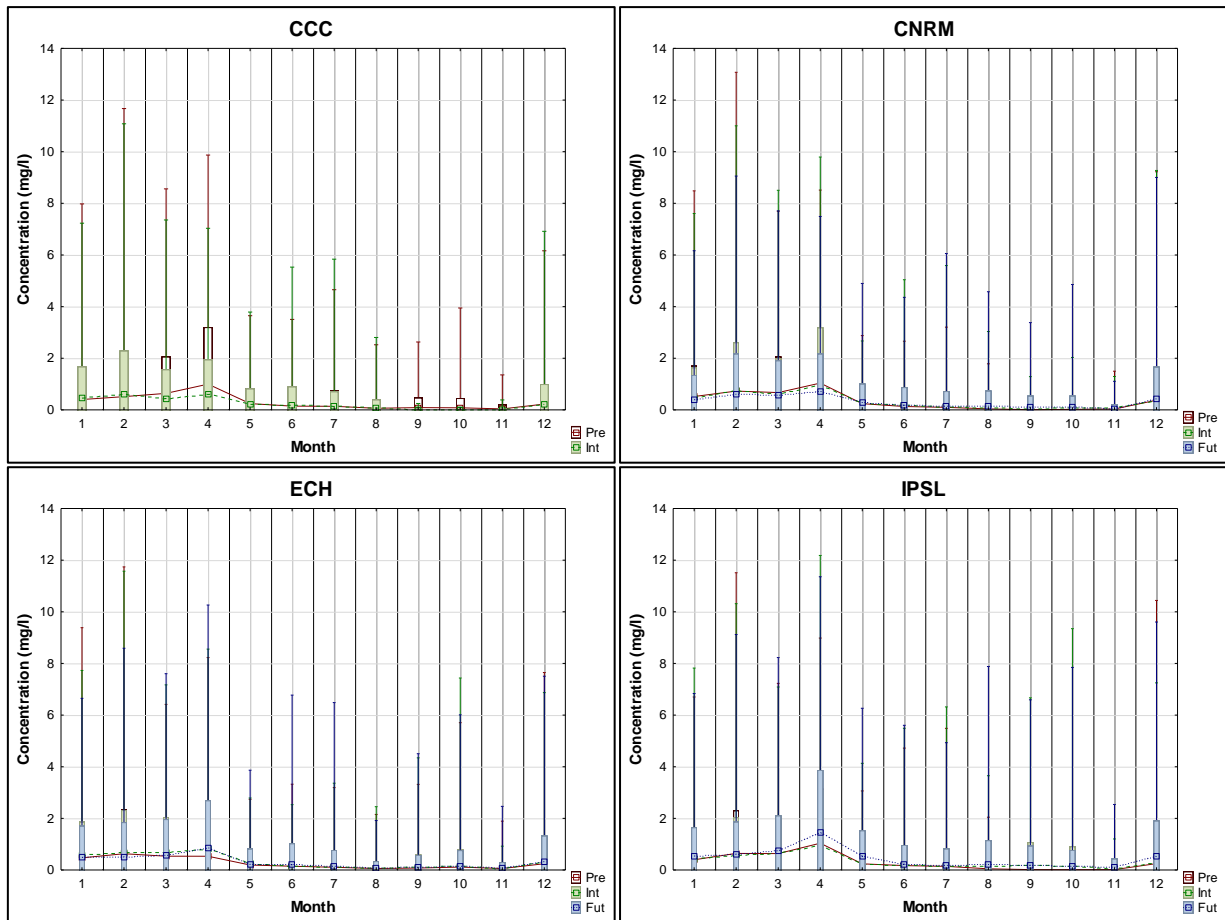


Figure 107 Climate change surface cyanobacteria concentration

From Figure 108 it is seen that the DWA limit for surface cyanobacteria concentration was exceeded by 30% to 53% in the distant future, depending on the climate model. Both warmer climate models, namely CNRM and IPSL showed an increase in this exceedance whereas the cooler models ECH and CCC showed a decrease in exceedance.

Table 40 Climate change cyanobacteria concentration (mg/l)

	Jan	Feb	Mar	Apr	May	Jun	Jul	Aug	Sep	Oct	Nov	Dec
CCC												
CCC pre	0.402	0.514	0.640	0.999	0.245	0.147	0.139	0.063	0.088	0.081	0.039	0.226
Difference	0.055	0.081	-0.198	-0.400	-0.013	0.034	-0.011	0.003	-0.080	-0.076	-0.028	-0.007
CCC int	0.457	0.595	0.442	0.599	0.232	0.181	0.128	0.066	0.008	0.005	0.011	0.219
CNRM												
CNRM pre	0.519	0.728	0.671	1.039	0.241	0.131	0.100	0.039	0.010	0.020	0.034	0.377
Difference	-0.045	0.012	-0.049	-0.076	-0.001	0.043	0.021	0.047	0.044	0.070	0.021	-0.018
CNRM int	0.474	0.740	0.622	0.963	0.240	0.174	0.121	0.086	0.054	0.090	0.055	0.359
CNRM int	0.474	0.740	0.622	0.963	0.240	0.174	0.121	0.086	0.054	0.090	0.055	0.359
Difference	-0.075	-0.135	-0.051	-0.268	0.046	0.010	0.013	0.061	0.050	0.003	-0.001	0.067
CNRM fut	0.399	0.605	0.571	0.695	0.286	0.184	0.134	0.147	0.104	0.093	0.054	0.426
ECH												
ECH pre	0.472	0.630	0.536	0.533	0.195	0.146	0.107	0.058	0.076	0.114	0.058	0.244
Difference	0.101	0.049	0.144	0.295	0.045	-0.009	-0.001	0.015	0.043	0.040	-0.006	0.075
ECH int	0.573	0.679	0.680	0.828	0.240	0.137	0.106	0.073	0.119	0.154	0.052	0.319
ECH int	0.573	0.679	0.680	0.828	0.240	0.137	0.106	0.073	0.119	0.154	0.052	0.319
Difference	-0.091	-0.167	-0.098	0.016	-0.015	0.062	0.028	0.007	-0.016	-0.019	0.013	0.007
ECH fut	0.482	0.512	0.582	0.844	0.225	0.199	0.134	0.080	0.103	0.135	0.065	0.326
IPSL												
IPSL pre	0.396	0.643	0.637	1.039	0.239	0.170	0.142	0.046	0.015	0.014	0.016	0.249
Difference	0.049	-0.082	-0.009	-0.081	-0.007	0.015	-0.003	0.111	0.182	0.130	0.026	0.019
IPSL int	0.445	0.561	0.628	0.958	0.232	0.185	0.139	0.157	0.197	0.144	0.042	0.268
IPSL int	0.445	0.561	0.628	0.958	0.232	0.185	0.139	0.157	0.197	0.144	0.042	0.268
Difference	0.107	0.059	0.115	0.499	0.286	0.047	0.026	0.058	-0.011	0.012	0.070	0.250
IPSL fut	0.552	0.620	0.743	1.457	0.518	0.232	0.165	0.215	0.186	0.156	0.112	0.518

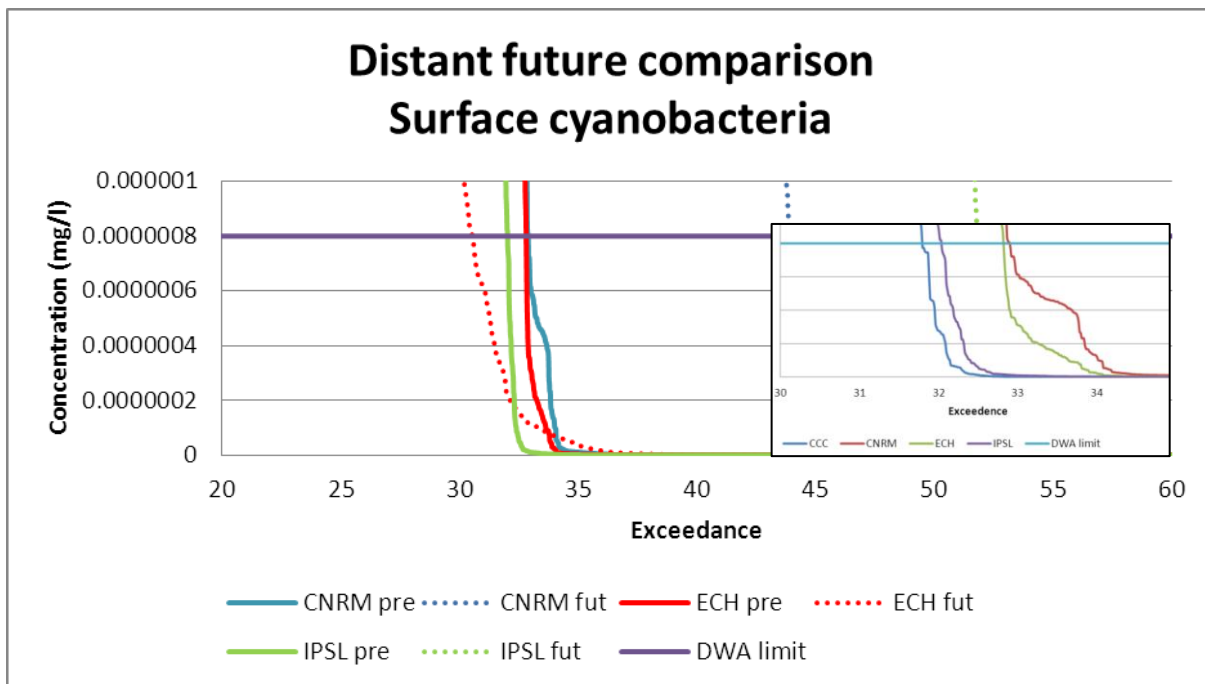


Figure 108 Distant future DWA cyanobacteria exceedance plot
Present day insert

5.2.14 The dominant algal group

It had now been established that with climate change the mean annual air temperature would increase by about 22% (Table 29) and this had a profound effect on the growth of algae in Voëlvlei Dam, in particular, it increased the surface concentrations of all algal groups present. The mean annual surface total algae increased by 15.5% (Table 30) because of a 24.6% increase in mean annual surface diatom concentrations, 15.5% increase in the mean annual surface green algae concentration and a 27.6% increase in the mean surface cyanobacteria concentration. This was shown graphically in Figure 109.

Thus, the dominant surface algal group in Voëlvlei Dam for the distant future is the green algal group, but the group with the greatest increase was the cyanobacteria at 27.7% mean annual increase in surface concentration.

In this study, algal succession was not found rather increases in the overall algal growth (Figure 109) as well as a seasonal shift for diatoms and greens. The cyanobacteria concentrations do not increase for the intermediate future but an increase is seen in the distant future projections. A discussion of the results follows in subsequent sections.

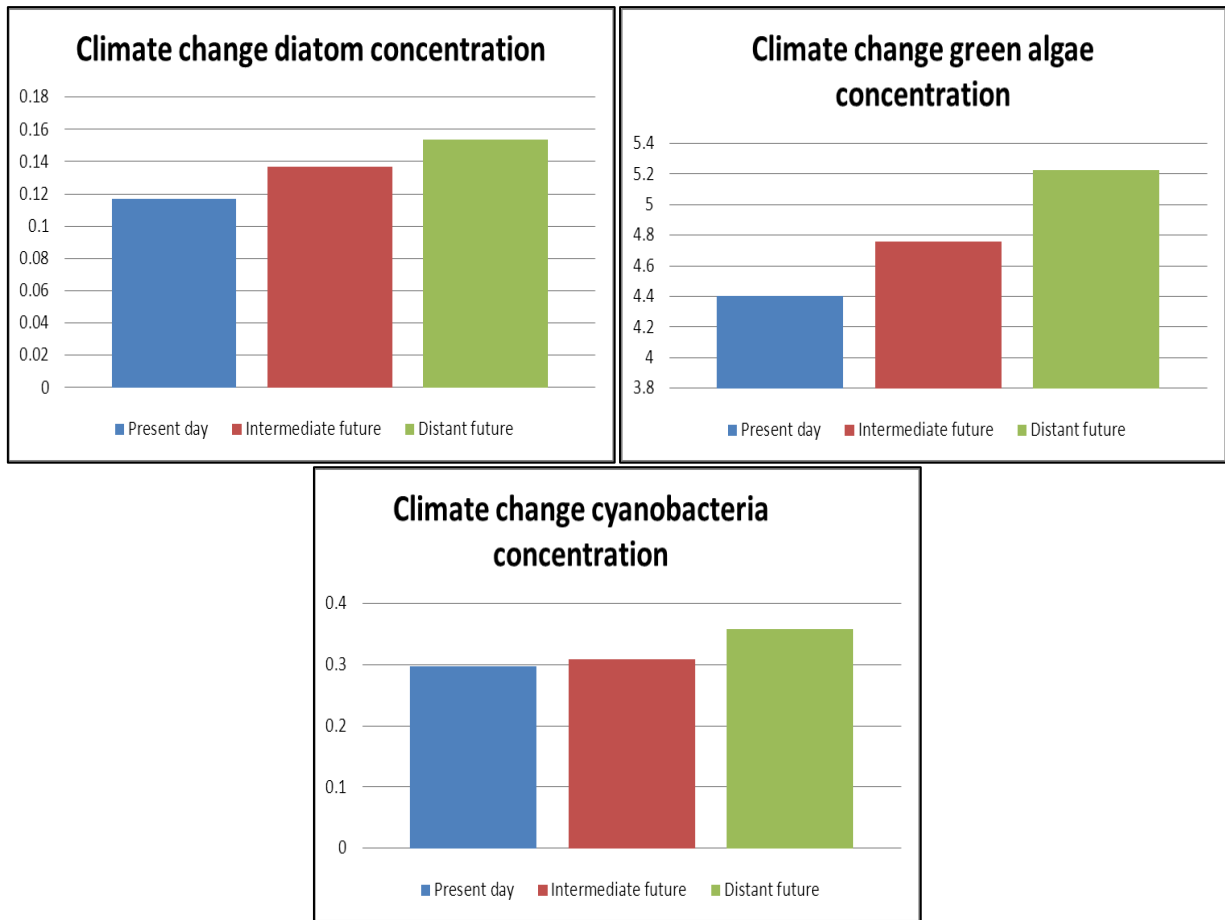


Figure 109 The effect of climate change on surface algal concentrations (mg/l)

5.2.15 Zooplankton concentration

The zooplankton in Voëlvlei Dam fed only on diatoms, green algae and other zooplankton present and since their surface concentration increased, it was expected that the surface concentrations of zooplankton should increase. For the purpose of this study, the predation of cyanobacteria by zooplankton was set to zero, i.e. zooplankton did not feed on cyanobacteria. The surface zooplankton concentration is shown in Figure 110 and climate models predict a greater concentration of surface zooplankton with maximum concentrations during winter.

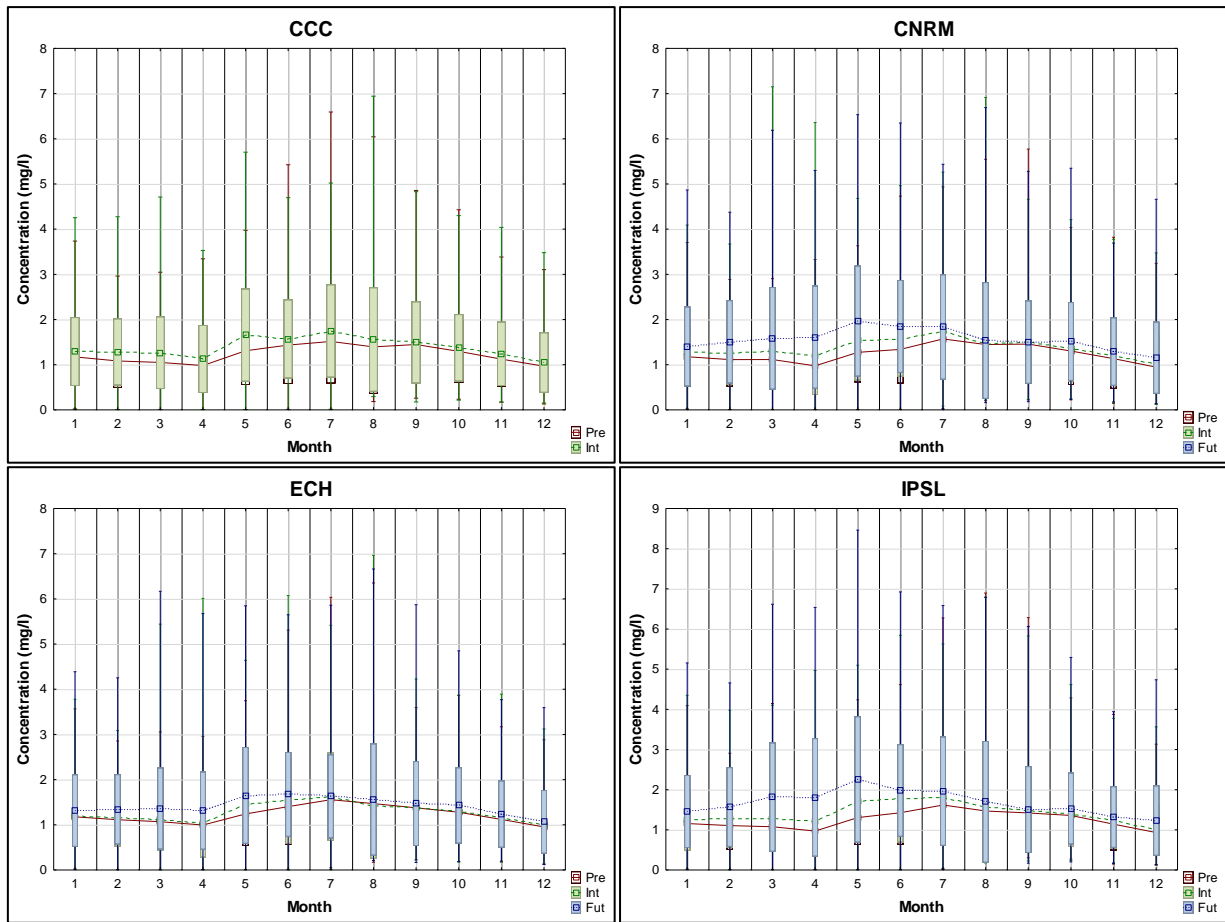


Figure 110 Climate change surface zooplankton concentration

It was expected that the greater concentrations of zooplankton would emulate that of diatoms and green algae and this emulations is shown in Table 41.

Table 41 Climate change zooplankton concentration (mg/l)

	Jan	Feb	Mar	Apr	May	Jun	Jul	Aug	Sep	Oct	Nov	Dec
CCC												
CCC pre	1.174	1.083	1.050	0.982	1.309	1.435	1.515	1.394	1.447	1.296	1.124	0.968
Difference	0.116	0.200	0.213	0.144	0.345	0.136	0.233	0.164	0.047	0.082	0.114	0.079
CCC int	1.290	1.283	1.263	1.126	1.654	1.571	1.748	1.558	1.494	1.378	1.238	1.047
CNRM												
CNRM pre	1.177	1.113	1.115	0.975	1.273	1.339	1.570	1.448	1.456	1.304	1.134	0.946
Difference	0.104	0.153	0.185	0.225	0.271	0.214	0.164	0.012	0.041	0.055	0.069	0.076
CNRM int	1.281	1.266	1.300	1.200	1.544	1.553	1.734	1.460	1.497	1.359	1.203	1.022
CNRM int	1.281	1.266	1.300	1.200	1.544	1.553	1.734	1.460	1.497	1.359	1.203	1.022
Difference	0.123	0.242	0.286	0.410	0.421	0.295	0.101	0.076	0.000	0.155	0.086	0.131
CNRM fut	1.404	1.508	1.586	1.610	1.965	1.848	1.835	1.536	1.497	1.514	1.289	1.153
ECH												
ECH pre	1.178	1.113	1.069	0.996	1.240	1.404	1.556	1.470	1.376	1.279	1.119	0.953
Difference	0.013	0.044	0.051	0.029	0.228	0.126	0.067	-0.042	0.012	0.025	0.042	0.048
ECH int	1.191	1.157	1.120	1.025	1.468	1.530	1.623	1.428	1.388	1.304	1.161	1.001
ECH int	1.191	1.157	1.120	1.025	1.468	1.530	1.623	1.428	1.388	1.304	1.161	1.001
Difference	0.123	0.188	0.241	0.288	0.184	0.144	0.008	0.131	0.082	0.126	0.075	0.066
ECH fut	1.314	1.345	1.361	1.313	1.652	1.674	1.631	1.559	1.470	1.430	1.236	1.067
IPSL												
IPSL pre	1.157	1.107	1.077	0.969	1.306	1.426	1.619	1.470	1.420	1.358	1.141	0.933
Difference	0.088	0.164	0.191	0.240	0.400	0.349	0.190	0.096	0.053	0.030	0.094	0.072
IPSL int	1.245	1.271	1.268	1.209	1.706	1.775	1.809	1.566	1.473	1.388	1.235	1.005
IPSL int	1.245	1.271	1.268	1.209	1.706	1.775	1.809	1.566	1.473	1.388	1.235	1.005
Difference	0.212	0.297	0.546	0.601	0.549	0.206	0.152	0.134	0.032	0.142	0.083	0.224
IPSL fut	1.457	1.568	1.814	1.810	2.255	1.981	1.961	1.700	1.505	1.530	1.318	1.229

5.2.16 Eutrophication level

The influence of climate change is seen to have implications for Voëlvlei Dam in the form of increased algal blooms and this had a direct effect on the surface TRIX levels. From Figure 111 and Table 42 it is seen the mean monthly TRIX levels increased for all climate models and the overall shape resembled that of the surface phosphorus concentration.

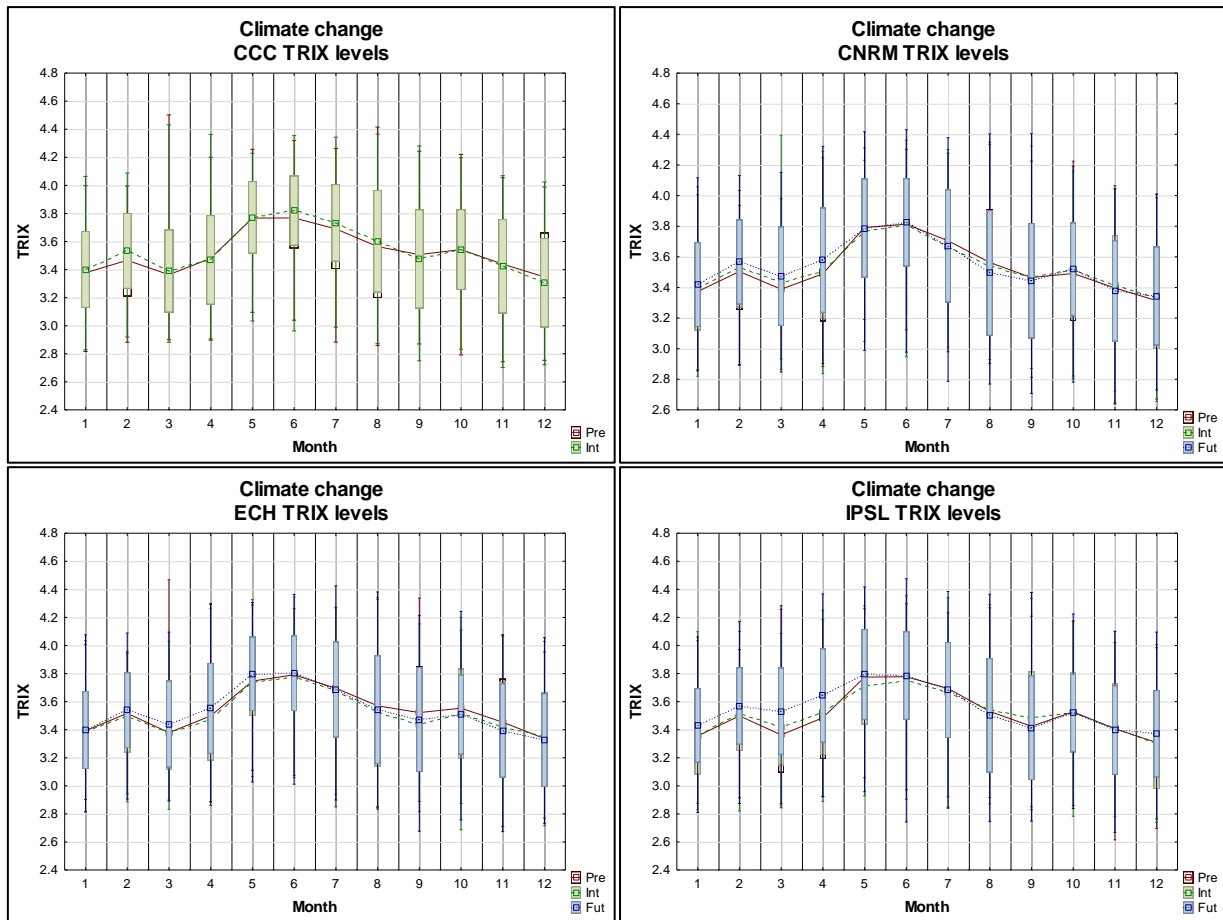


Figure 111 Climate change effect on the TRIX levels of Voëlvlei Dam

The inter-variability between climate models was apparent from these findings in that for differences for monthly TRIX levels for different climate model of the same time-period showed either an increase or decrease. TRIX levels showed increases mainly in late summer and autumn with decreases during winter and spring. In examining the equation that renders TRIX levels it was seen that:

$$TRIX = \frac{(\log(ChA + aDO\% + N \min + TP) + 1.5)}{1.2}$$

All the constituents increase for climate change effects except for the total nitrogen, which was negligible over that of the present day. It may be argued that the TRIX levels were significant as:

- The formulae was usually applied to marine waters and was adopted here as a guide
- It was applied here only to the surface water
- The formulae was of the logarithmic type which increases exponentially and any increase was significant
- The constituents were weighted equally
- It did not take water transparency into account

Even with its shortcomings, the TRIX levels provided a first estimate at the increase in trophic levels.

Table 42 Climate change effect on the surface TRIX level

	Jan	Feb	Mar	Apr	May	Jun	Jul	Aug	Sep	Oct	Nov	Dec
CCC												
CCC pre	3.38	3.47	3.36	3.48	3.77	3.77	3.69	3.56	3.51	3.54	3.44	3.35
Difference	0.02	0.07	0.03	-0.01	0.01	0.05	0.04	0.04	-0.03	0.00	-0.01	-0.04
CCC int	3.40	3.53	3.39	3.47	3.77	3.82	3.73	3.60	3.48	3.54	3.42	3.31
CNRM												
CNRM pre	3.37	3.50	3.39	3.49	3.79	3.81	3.71	3.56	3.46	3.49	3.40	3.31
Difference	0.02	0.03	0.04	0.01	-0.02	-0.01	-0.04	-0.02	0.00	0.02	0.02	0.02
CNRM int	3.40	3.53	3.43	3.50	3.77	3.81	3.67	3.54	3.47	3.52	3.42	3.33
CNRM int	3.40	3.53	3.43	3.50	3.77	3.81	3.67	3.54	3.47	3.52	3.42	3.33
Difference	0.02	0.03	0.04	0.08	0.02	0.02	0.01	-0.04	-0.02	0.00	-0.04	0.01
CNRM fut	3.42	3.57	3.47	3.58	3.79	3.83	3.67	3.49	3.45	3.52	3.38	3.34
ECH												
ECH pre	3.39	3.52	3.38	3.50	3.75	3.79	3.70	3.57	3.52	3.55	3.45	3.34
Difference	-0.01	-0.02	0.00	-0.03	-0.01	-0.02	-0.02	-0.05	-0.08	-0.04	-0.03	0.01
ECH int	3.39	3.50	3.38	3.47	3.74	3.78	3.68	3.52	3.44	3.51	3.42	3.35
ECH int	3.39	3.50	3.38	3.47	3.74	3.78	3.68	3.52	3.44	3.51	3.42	3.35
Difference	0.01	0.04	0.06	0.08	0.06	0.03	0.01	0.02	0.03	-0.01	-0.02	-0.02
ECH fut	3.40	3.54	3.44	3.55	3.80	3.80	3.69	3.54	3.47	3.51	3.39	3.33
IPSL												
IPSL pre	3.36	3.50	3.36	3.48	3.77	3.78	3.69	3.53	3.42	3.53	3.41	3.31
Difference	0.01	0.01	0.05	0.04	-0.06	-0.03	-0.03	0.01	0.06	-0.01	0.01	-0.01
IPSL int	3.36	3.51	3.42	3.52	3.71	3.75	3.66	3.54	3.48	3.52	3.41	3.30
IPSL int	3.36	3.51	3.42	3.52	3.71	3.75	3.66	3.54	3.48	3.52	3.41	3.30
Difference	0.07	0.06	0.12	0.12	0.08	0.04	0.02	-0.04	-0.07	0.00	-0.02	0.07
IPSL fut	3.43	3.57	3.53	3.64	3.79	3.79	3.68	3.50	3.41	3.52	3.40	3.37

6 DISCUSSION

The main objective of this study was to find any links between climate changes and water quality with specific emphasis on eutrophication of surface waters. It was postulated that with climate change that the air temperature would increase by between 2 and 4.5°C for southern Africa and this increase would heat the surface waters sufficiently to amplify the growth of algae within such waters. It was also postulated that the three groups of algae (namely diatoms, green and cyanobacteria) that are present, would experience varying rates of growth because of the increased water temperature with a preference for the warmer conditions. From a modelling aspect, this would be due to the temperature growth multipliers, which stipulate algal growth for different water temperatures. It was possible that seasonal shifts of the bloom season would become apparent with climate change. It was postulated that cyanobacteria would be the algal group that benefits the most from the increased water temperature with all other factors remaining constant, thereby allowing for the unabated growth of cyanobacteria and a greater frequency of harmful algal blooms.

Water temperature, pH, available light, turbidity, suspended solids (TSS), dissolved solids (TDS), nitrogen, phosphorus, salinity and trace elements influence water quality and algal growth. Water quality and algal growth is dependent on several variables for its lifecycle, such as conducive environmental conditions and nutrients, which for the purpose of this study may be categorised as:

- Water temperature and solar radiation;
- Availability of nitrogen within the water-body; and
- Availability of phosphorus within the water-body.

The present day study was conducted by utilising the water quality model CE-QUAL-W2 and establishing baseline water quality conditions for all the relevant factors that affect algal growth in the dam. The air temperature over the dam site was the classical southern hemisphere climate with summer being roughly December to February and winter May to July. The inflow and withdrawal quantity and quality as well as wind-speed and direction was constrained to be the same for each the simulation periods, namely present day, intermediate future and distant future thereby allowing for more controlled comparison as only the effect of increased temperature on the dam was investigated.

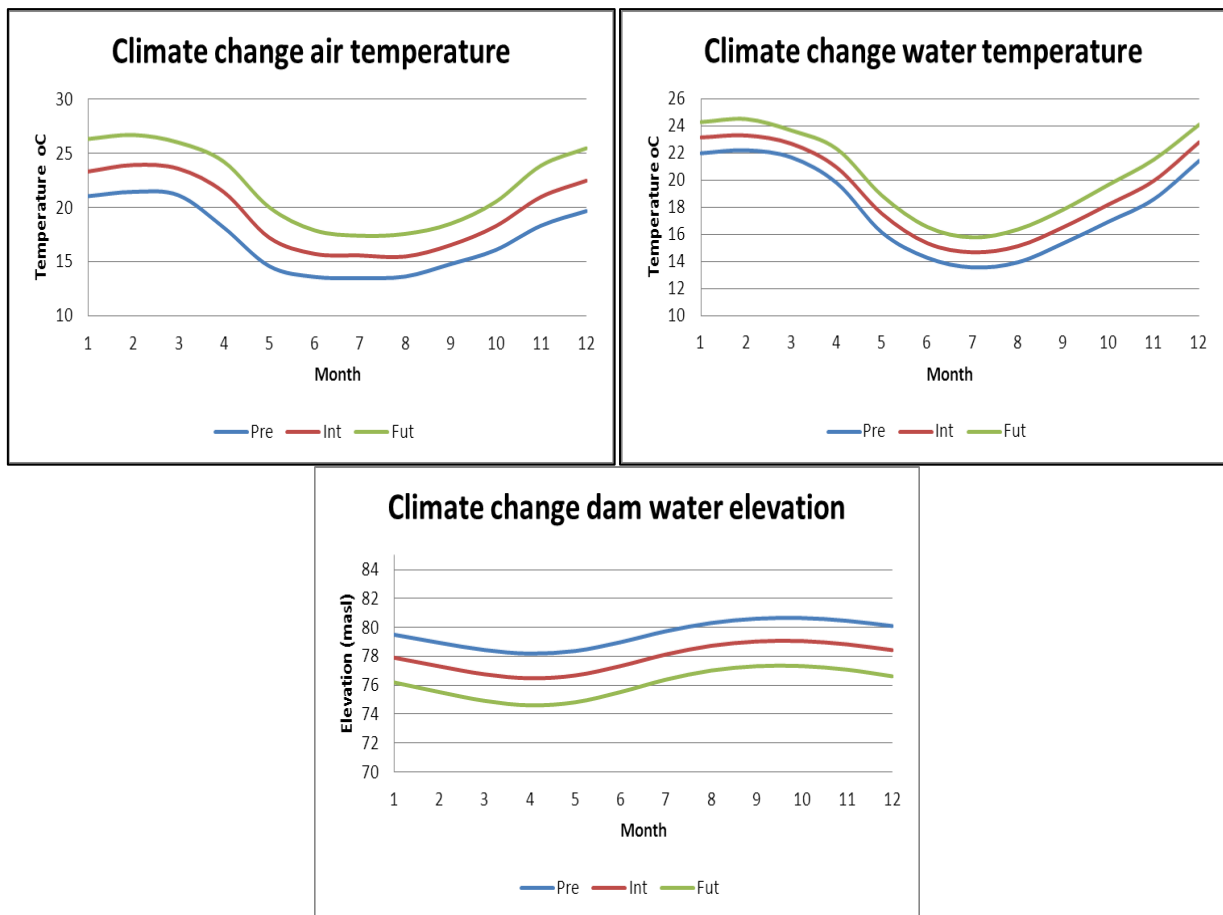


Figure 112 The mean monthly air temperature effect for Voëlvlei Dam

From Figure 112 the mean of the climate models show varying ranges of monthly air temperature increases, which drive an increase in surface water temperatures, which then affected the algal growth. The greatest increase in water temperature occurred during winter due to the heat transfer to the surface waters. It was thought that this would enhance algal growth especially the diatom growth in winter as well as start a shift towards earlier annual algal blooms. The inter-variability between climate models was small and they all predicted similar air temperatures for each of the time scenarios. The climate models were also ranked in order of coolest to hottest that being ECH, CNRM, CCC and then IPSL. This was a consequence of the anthropogenic assumptions used to generate the GCM. It was concluded that air temperature was the major driver for surface water temperatures and solar radiation was the diurnal driver.

Climate change heated the water and subsequently increased the evaporation rate. This heating should have the effect of enhancing algal growth as well as lowering the surface water level if the dam was to be operated at the present day levels. This heated water evaporated more in the distant future than the intermediate future a result of the increased water temperature. This poses a secondary problem for the Western Cape Province as it was a semi-arid area of the country and the effect of climate change was that its dam waters would evaporate faster in the future than at the current rate. For Voëlvlei Dam, this was not as important as other dams in the area as it was an off-channel dam. The dam's inflow is diverted as operations dictate.

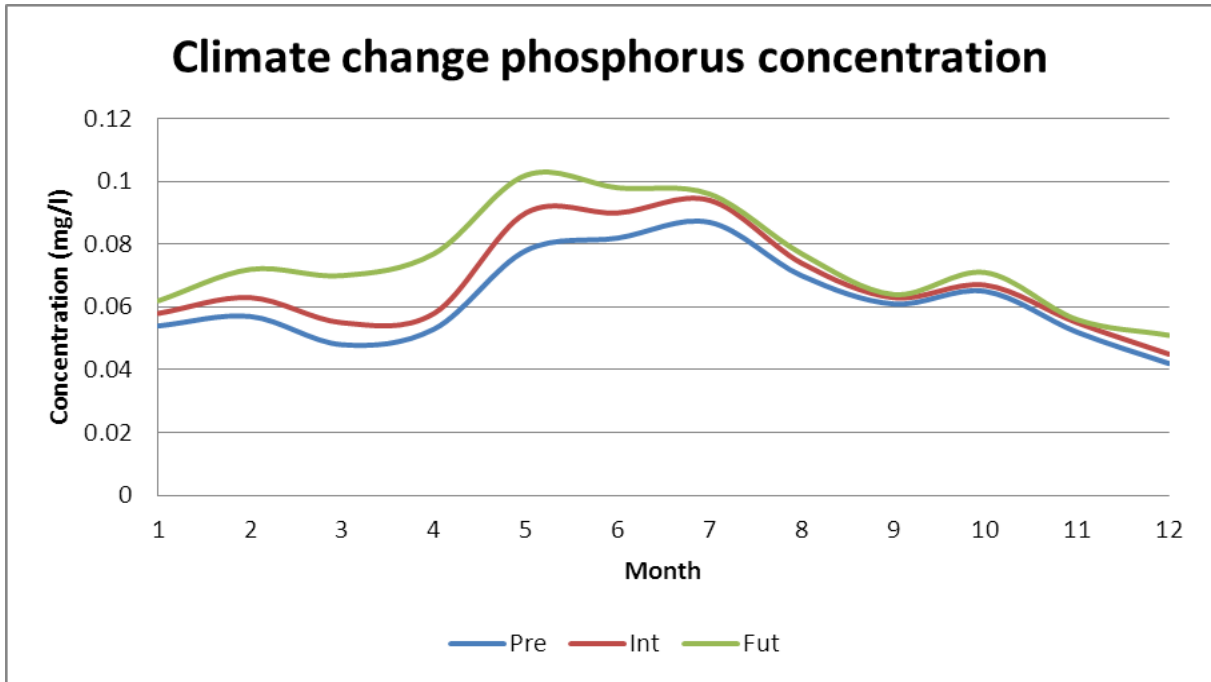


Figure 113 The mean monthly surface phosphorus concentration

Climate change heated the surface waters and lowered its surface level resulting in a concentration increase for the water quality constituents. Figure 113 shows the surface phosphates increased in all months, especially in autumn. This increase coupled with the warmer waters would enhance algal growth. When comparing this to Figure 56 it was seen that the increase was not due to increased concentrations in the inflow. The total algal growth was increased annually but especially during autumn, signalling a seasonal shift toward an earlier annual increased concentration of total algae as well as compounding the annual load in the dam.

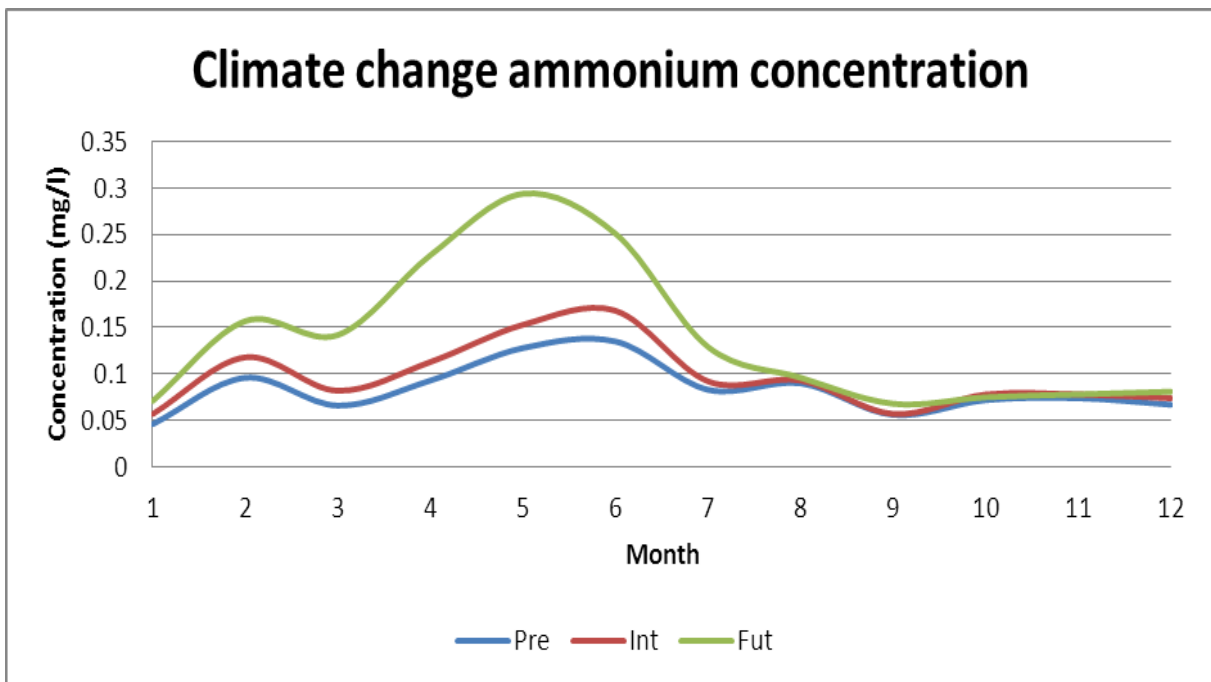


Figure 114 The mean monthly surface ammonium concentration

The surface ammonium is by the algae during photosynthesis so it was expected that for an increase in algal concentrations, the ammonium concentrations should decrease. From Figure 114 as the algal concentration increased, the concentration of surface ammonium also increased because of the concentrating effect of decreasing the surface water level. Annually this increase occurred mainly during autumn and winter with small changes and decreases during spring and summer. This increase along with the raised phosphorus concentrations during late summer and autumn, along with higher water temperatures would increase the algal growth at the surface during these months.

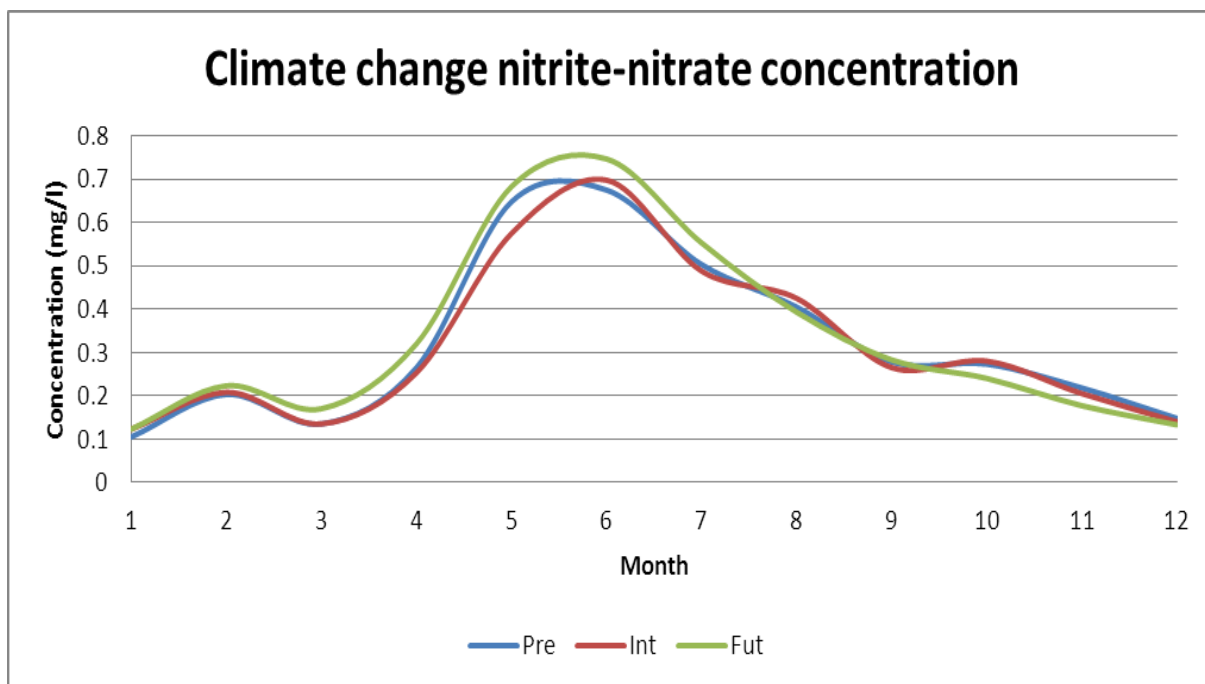


Figure 115 The mean monthly surface Nitrite-nitrate concentration

Nitrite-nitrates are an intermediate product as well as a source of nitrogen during photosynthesis. From Figure 115 the effect of climate change on nitrite-nitrates was very slight as the main source modelled was from the nitrification of ammonium. It was expected that for an increase in temperature and ammonium that the nitrification reaction would respond in an Arrhenius manner and produce more nitrite-nitrate but this was not so. It could be that the rate of generation of nitrite-nitrates was similar to its assimilation by algae, thereby producing relatively unchanged concentrations.

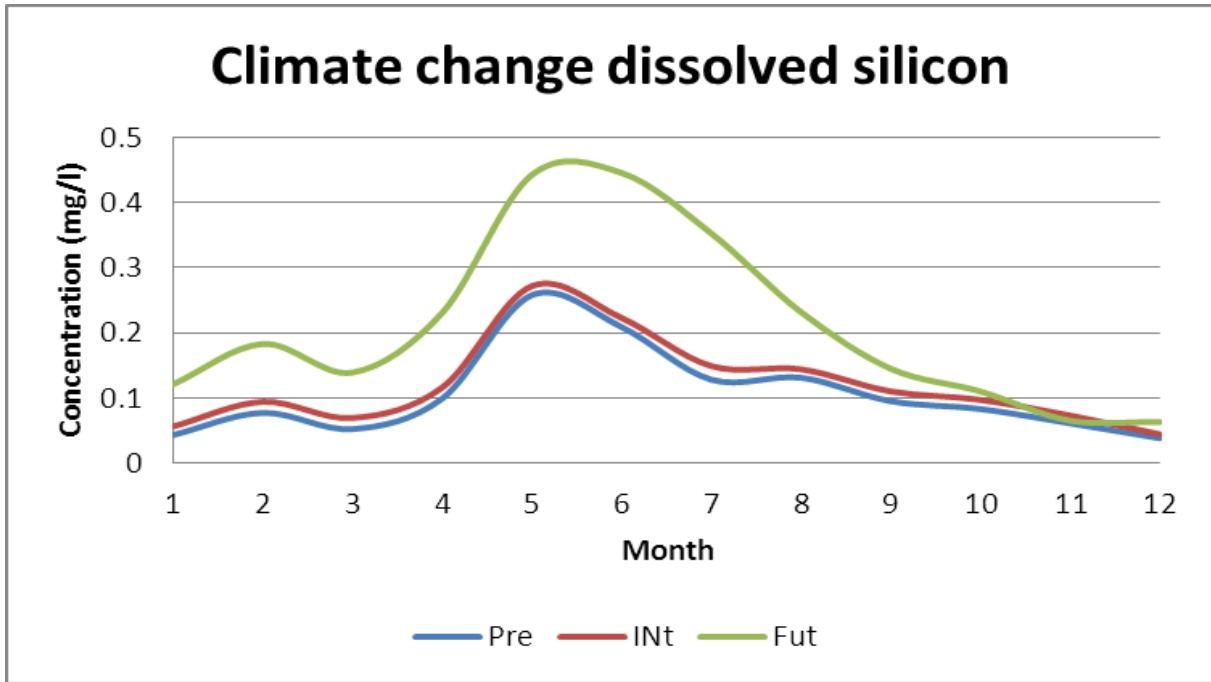


Figure 116 The mean monthly surface dissolved silicon concentration

Dissolved silicon is exclusively used by diatoms during photosynthesis. From Figure 116 the concentrating effect of evaporation was noted especially in autumn and winter for the intermediate and distant future. The greatest increases occur in the distant future for the entire year, especially winter. This would allow for diatom growth throughout the year and an earlier seasonal shift with diatoms was noted. Thus, the effect of warmer water due to climate change favours the growth of diatoms throughout the year in the distant future, with the greatest increases during autumn, signalling a seasonal shift to an earlier bloom of diatoms.

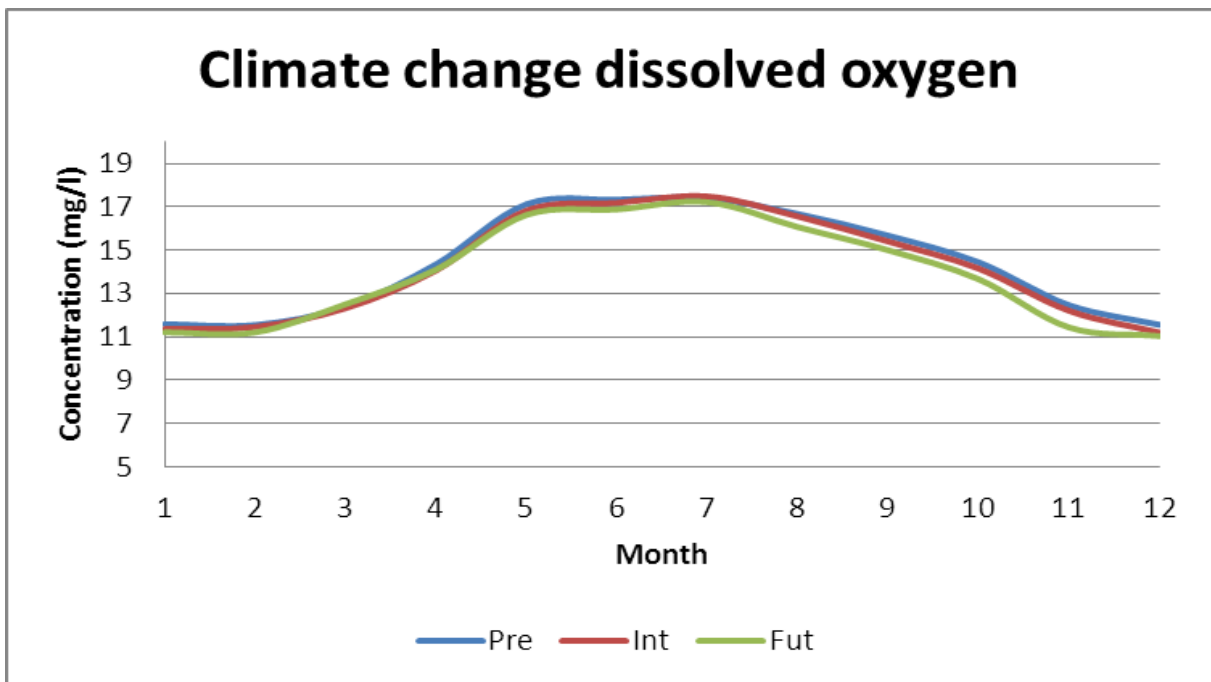


Figure 117 The mean monthly surface dissolved oxygen concentrations

The modelling of dissolved oxygen proved daunting, as the results were supersaturated dissolved oxygen concentrations. The only sources of dissolved oxygen are from the atmosphere and as a product of photosynthesis, with the photosynthesis rates being driven by the algal groups. From Figure 117 it was seen that the concentration of DO did not vary much with climate change as would be expected due to the warmer waters. This was attributed to the greater photosynthetic rates of the algae producing more oxygen. The results shown are critiqued as being too high and have been ascribed to the chosen algal growth rates. The selection of accurate algal growth rates was imperative for the quantification of algae in the dam and these are linked to the model output of dissolved oxygen. Varying the algal growth rates had the desired effect of lowering the DO concentrations but then the algal growth was adversely affected. This was not investigated further and it was not known if this was a problem in the water quality model or not.

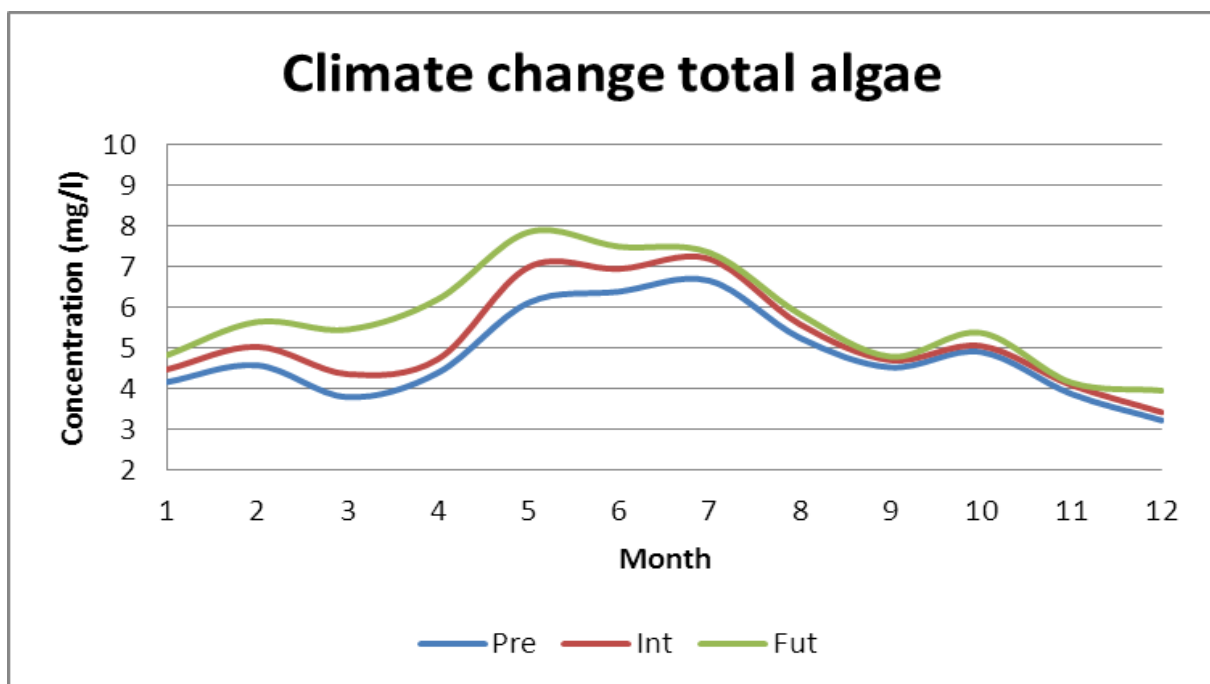


Figure 118 The mean monthly surface total algae concentrations

From Figure 118, climate change increased the total algae at the surface with a prominent shift earlier in the year for the distant future. This was a lengthening of the bloom season for total algae and it would persist for longer periods annually.

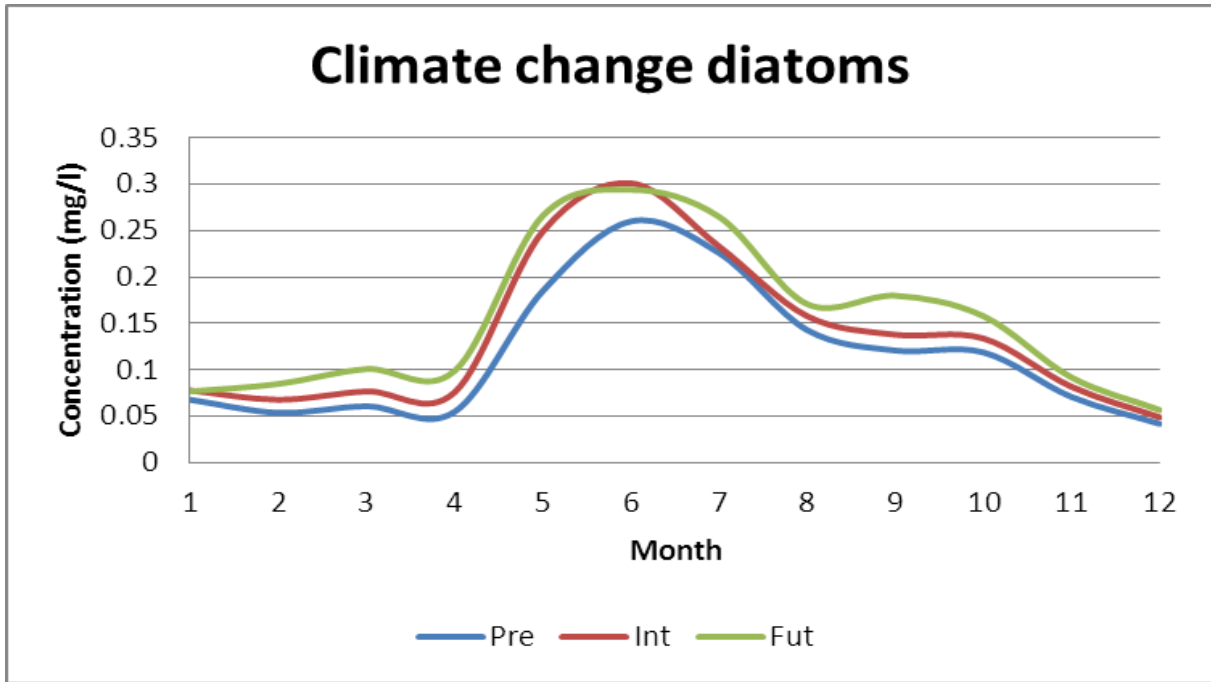


Figure 119 The mean monthly surface diatom concentrations

Total algae increased especially in the first half of the year for climate change and Figure 119 shows that diatoms concentrations would peak in winter but will also increase during the rest of the year. Diatoms are present in the dam for the entire year but are not responsible for the increased total algal due to its low concentrations.

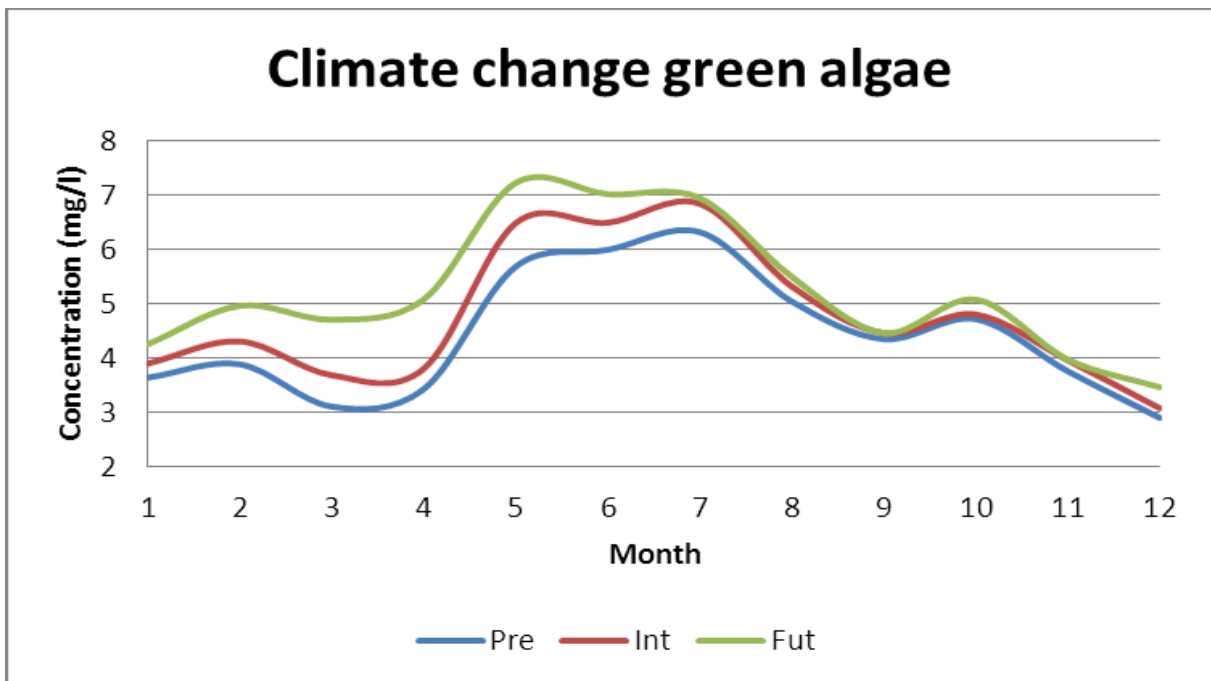


Figure 120 The mean monthly surface green algae concentrations

The green algae is the dominant group in the dam and are present in the highest concentrations when compared to diatoms and cyanobacteria as seen in Figure 120. The increase in its nutrients

throughout the year as well as the increased water temperature allows for unabated growth for the entire year with seasonal extensions earlier in the year during autumn, with climate change. The accelerated growth with climate change was clearly visible here as the increases during late summer and autumn are greater in the distant future than in the intermediate future.

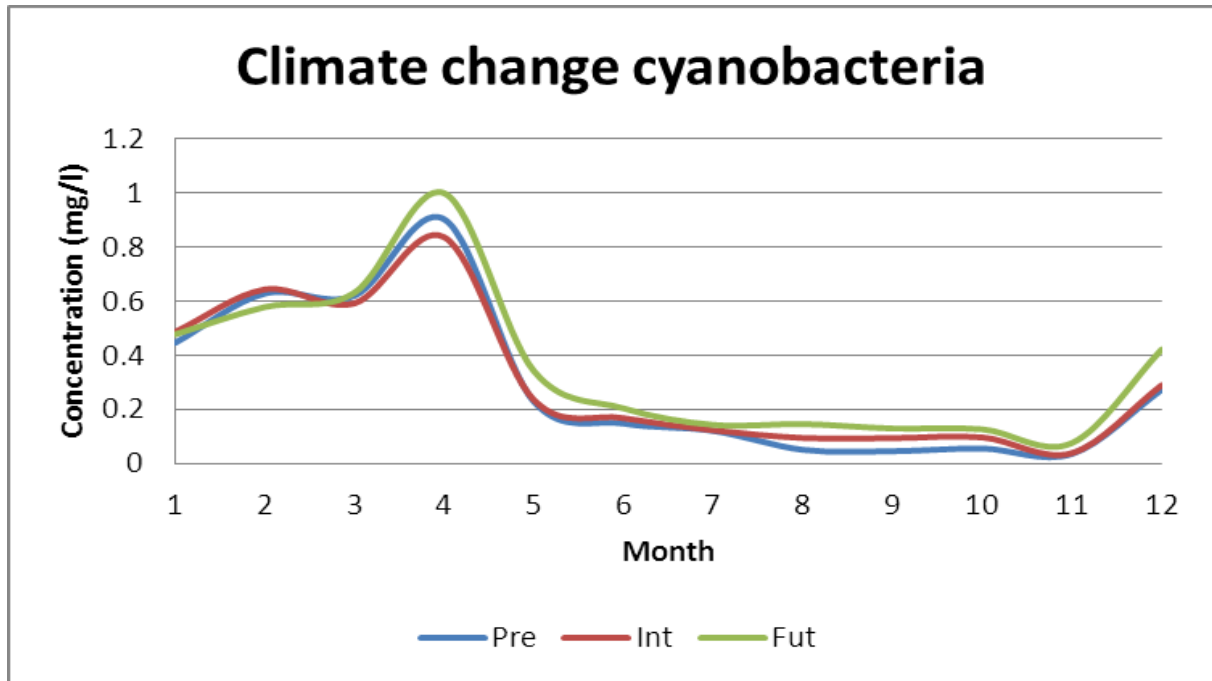


Figure 121 The mean monthly surface cyanobacteria concentrations

Cyanobacteria were present at the surface for the entire year at significant concentrations but with climate change their concentrations did not change significantly. It was expected to see larger growths and succession but this was not the outcome of this study. The current months of cyanobacteria blooms (January to May) will remain relatively unchanged but increases in incident of cyanobacteria blooms should occur during the current 'low' season for blooms (Autumn-August to November). It was therefore plausible that since Voëlvlei had a hazardous algal bloom HAB of *Anabaena* during December 2000 to May 2001 (Downing and Van Ginkel, 2004), that for the distant future it could still have this seasonal bloom as these months remain relatively unchanged but with climate change that blooms could also occur during spring. This would serve to lengthen the bloom season throughout the year. The result was inconclusive as the inter-variability between the climate models was the greatest for cyanobacteria, with 2 models showing an increase in surface cyanobacteria concentration and 2 a decrease in cyanobacteria concentration for intermediate and future time-period.

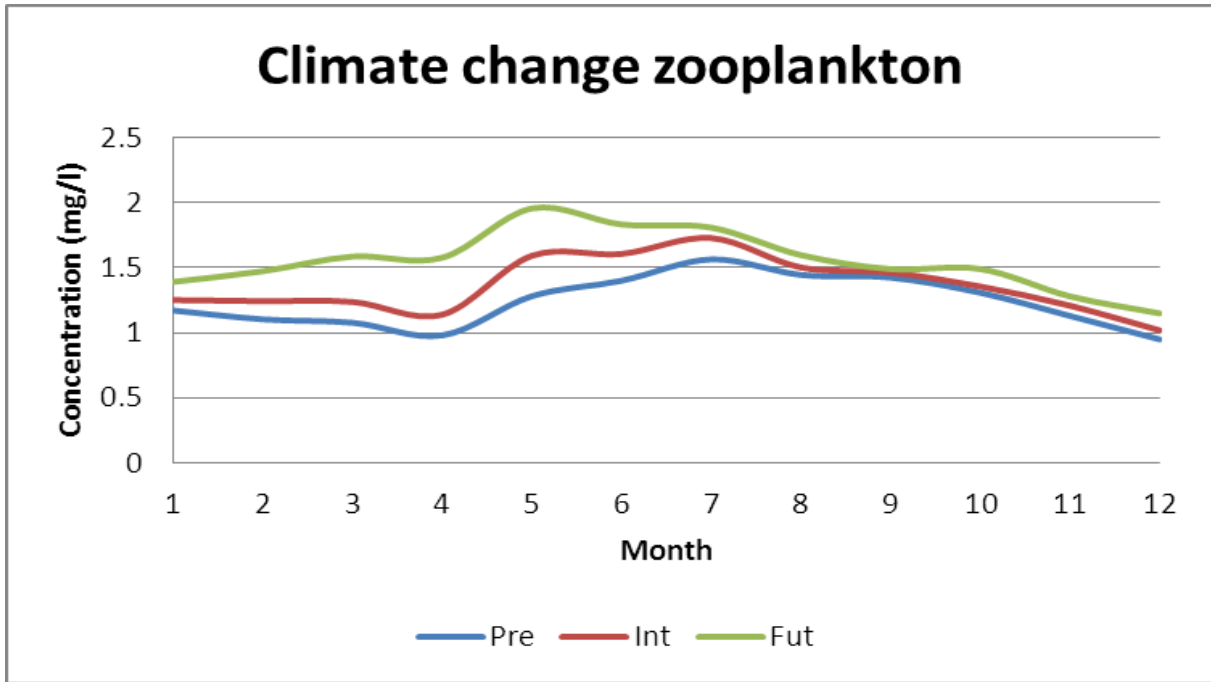


Figure 122 The mean monthly surface zooplankton concentrations

Along with the increase in total surface algae, it was seen that surface zooplankton concentration also increased. The zooplankton grazed on diatoms and green algae as their surface concentration increases for future climate the concentration of zooplankton subsequently increases.

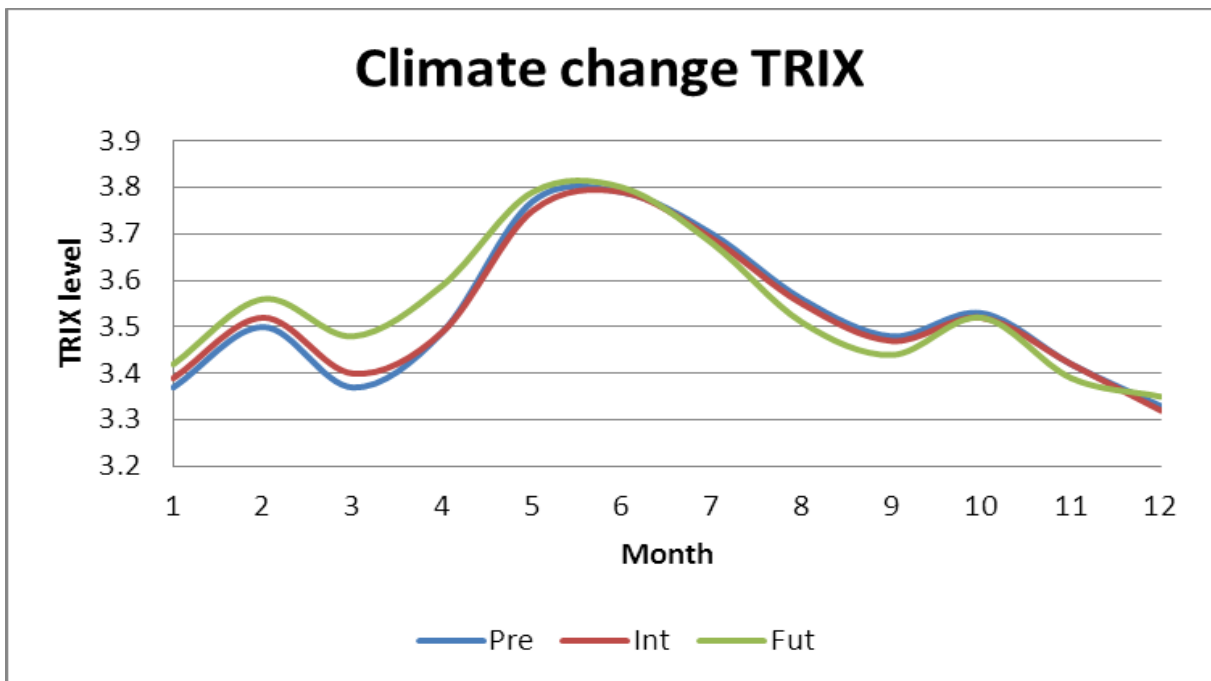


Figure 123 The mean monthly surface TRIX level

The influence of climate change was seen to have implications for Voëlvlei Dam in the form of increased algal blooms and this has a direct effect on the surface eutrophication level especially for

the distant future. For the distant future, a seasonal shift was observed and this is due to the decrease in DO and nitrite-nitrates in the latter half of the year at the surface. It was seen for climate change the mean monthly TRIX levels increased for all climate models with maximum in winter. With climate change, this level shifted its peak earlier in the year once again confirming a seasonal shift for worsening water quality.

The following table (Table 43) summarise the water quality of Voëlvlei Dam for the climate change events and a table summarising all the results is shown in the Appendix.

Table 43 Concise summary of water quality

	Jan	Feb	Mar	Apr	May	Jun	Jul	Aug	Sep	Oct	Nov	Dec
Air temperature (°C)												
Present day	21.05	21.45	21.13	18.15	14.60	13.60	13.50	13.63	14.78	16.08	18.33	19.68
Difference	2.28	2.48	2.45	3.28	2.63	2.13	2.08	1.85	1.75	2.20	2.65	2.80
Intermediate	23.33	23.93	23.58	21.43	17.23	15.73	15.58	15.48	16.53	18.28	20.98	22.48
Difference	3.01	2.78	2.43	2.81	2.81	2.18	1.83	2.09	1.98	2.26	2.89	2.99
Future	26.33	26.70	26.00	24.23	20.03	17.90	17.40	17.57	18.50	20.53	23.87	25.47
Difference	3.01	2.78	2.43	2.81	2.81	2.18	1.83	2.09	1.98	2.26	2.89	2.99
Overall change	5.28	5.25	4.88	6.08	5.43	4.30	3.90	3.94	3.73	4.46	5.54	5.79
Water temperature (°C)												
Present day	22.01	22.23	21.70	19.81	16.15	14.29	13.58	13.96	15.36	16.96	18.62	21.45
Difference	1.17	1.09	1.02	1.16	1.40	1.08	1.12	1.19	1.19	1.28	1.36	1.37
Intermediate	23.18	23.32	22.71	20.96	17.54	15.37	14.70	15.15	16.55	18.23	19.98	22.82
Difference	1.13	1.21	0.98	1.37	1.34	1.20	1.10	1.25	1.31	1.46	1.56	1.30
Future	24.31	24.53	23.69	22.33	18.88	16.57	15.80	16.39	17.85	19.69	21.54	24.12
Difference	1.13	1.21	0.98	1.37	1.34	1.20	1.10	1.25	1.31	1.46	1.56	1.30
Overall change	2.30	2.30	2.00	2.53	2.73	2.28	2.22	2.43	2.49	2.73	2.92	2.68
Total algae (mg/l)												
Present day	4.160	4.573	3.790	4.390	6.113	6.385	6.655	5.248	4.523	4.903	3.870	3.218
Difference	0.310	0.458	0.565	0.335	0.875	0.558	0.535	0.335	0.178	0.148	0.220	0.200
Intermediate	4.470	5.030	4.355	4.725	6.988	6.943	7.190	5.583	4.700	5.050	4.090	3.418
Difference	0.350	0.613	1.098	1.475	0.863	0.551	0.157	0.251	0.087	0.323	0.060	0.533
Future	4.820	5.643	5.453	6.200	7.850	7.493	7.347	5.833	4.787	5.373	4.150	3.950
Difference	0.350	0.613	1.098	1.475	0.863	0.551	0.157	0.251	0.087	0.323	0.060	0.533
Overall change	0.660	1.071	1.663	1.810	1.738	1.108	0.692	0.586	0.264	0.471	0.280	0.732
TRIX												
Present day	3.37	3.50	3.37	3.49	3.77	3.79	3.70	3.56	3.48	3.53	3.42	3.33
Difference	0.01	0.02	0.03	0.00	-0.02	0.00	-0.01	-0.01	-0.01	-0.01	-0.01	-0.01
Intermediate	3.39	3.52	3.40	3.49	3.75	3.79	3.69	3.55	3.47	3.52	3.42	3.32
Difference	0.03	0.04	0.08	0.10	0.05	0.02	-0.01	-0.04	-0.02	-0.01	-0.03	0.03
Future	3.42	3.56	3.48	3.59	3.79	3.80	3.68	3.51	3.44	3.52	3.39	3.35
Difference	0.03	0.04	0.08	0.10	0.05	0.02	-0.01	-0.04	-0.02	-0.01	-0.03	0.03
Overall change	0.04	0.06	0.11	0.10	0.02	0.02	-0.02	-0.04	-0.04	-0.01	-0.03	0.02

7 LIMITATIONS OF THIS STUDY

All water quality studies have inherent limitations especially where algal growth was to be simulated as algae adapts and modifies its growth to its environment and conditions. Some species are known to be motile which was virtually impossible to model accurately. This studies limitation was subdivided into:

- Model and data limitations; and
- Data limitations.

7.1 CE-QUAL-W2 MODEL LIMITATIONS

The model had successfully been applied to Voëlvlei in the past and the limitations were specifically on the model and not its application to Voëlvlei. From the aspect of hydrodynamics and transport, the models governing equations are laterally and layer averaged. Lateral averaging assumes lateral variations in velocities, temperatures, and constituents are negligible. This assumption may be inappropriate for large water-bodies exhibiting significant lateral variations in water quality. Eddy coefficients are used to model turbulence. Currently, the user must decide among several vertical turbulence schemes and select the one that was most appropriate for the type of water-body being simulated. The equations are written in the conservative form using the Boussinesq and hydrostatic approximations. Since vertical momentum was not included, the model may give inaccurate results where there was significant vertical acceleration (Cole and Wells, 2008).

Water quality interactions are, by necessity, simplified descriptions of an aquatic ecosystem that is extremely complex. This is especially so for modelling algae as they adapt to varying environmental conditions such as low light and nutrient sparse zones. Some species are capable of independent movement throughout the water column, something not modelled by CE-QUAL-W2. This could explain difference between the measured and modelled values of total algae, which was a surrogate for chlorophyll-a.

The model includes a user-specified sediment oxygen demand that was not coupled to the water column. SOD only varies according to temperature. The model does not have a sediment compartment that models kinetics in the sediment and at the sediment-water interface, i.e., a complete sediment diagenesis model. This places a limitation on long-term predictive capabilities of the water quality portion of the model (Cole and Wells, 2008). It was hoped that this limitation was carried forward by each of the modelling periods studied and that what was presented was still the difference in water quality for climate change. Future releases of CE-QUAL-W2 will include additional capabilities that will remedy this limitation (Cole and Wells, 2008) and version 3.7 has just been released (2012).

7.2 CLIMATE DATA LIMITATIONS

The availability of input data is not a limitation of the model itself. However, it is most often the limiting factor in the application or misapplication of the model. The GCMs employed in this study was of such coarse resolution (about 300km²) that they cannot be used directly for the

meteorological data. The GCMs are firstly downscaled statistically to regional level (RCMs). The advantage of this technique was that it was easily applied. One disadvantage of the statistical method of downscaling was that it relies on the availability of sufficient high-resolution data over long periods so that statistical relationships may be established. It was not possible to be sure how valid the statistical relations are for a climate-changed situation (Houghton, 2007; Quintana-Seguí et al., 2010).

In the absence of another type of downscaling such as dynamic downscaling, it was not possible to determine the accuracy of the downscaled data or compare it.

Wind-speed and direction was not supplied by CSAG (UCT) and was thus a limitation. CE-QUAL-W2 requires wind-speed and direction for meteorological data input to predict water quality. In the absence of this, wind-speed and direction was taken from past data. The recorded wind-speed and direction from 1 January 1971 to 31 December 1971 was repeated for the 20 years of all the simulation periods, in the absence of any downscaled data.

7.3 INFLOW AND WITHDRAWAL LIMITATIONS

The daily averaged inflow to the Dam was obtained from the DWA's Hydrological Information System (HIS) database. Outflows from Voëlvlei Dam consist of abstractions of raw water to supply the Voëlvlei (G1H070M01) and Swartland (G1H068M01) WTW. Water was also released via an outlet canal (G1H065A01) to the Berg River for run-of-river irrigation (DWA, 1999). An additional outflow to a pipeline was also operational but flow data for this gauging station (G1H069M01) was only available up to 1982. This pipeline was excluded from the simulation as it was deemed to have too little effect on the water quality.

Inflow water quality data was not as readily available as flow data, and was at best measured only on a weekly basis. Although a reasonably good water quality record exists at gauging station G1H029, it was not used. This was because the volume of water diverted from the Twenty-Four Rivers River was substantially greater than that diverted from the Leeu River and it was therefore assumed that the water quality of the Twenty-Four Rivers River would more representative of the water quality entering the Dam at G1H067. Similarly, gauging station G1H008 was representative of the water quality at G1H066. This choice could be vindicated by the fact that measured water quality variables and modelled water quality values were not vastly different as seen in the calibration section.

Since no inflow and outflow data was available for the predicted future scenarios it was proposed to use the current DWA HIS databases' flow-data from 1 January 1971 until 31 December 1990's (present scenario) for each of the subsequent intermediate and future simulations. This would assume that demand and allocation of the water resource does not change for the climate change periods.

7.4 ALGAL GROWTH RATES

For the study it was imperative that the growth of the three groups of algae namely diatoms, greens and cyanobacteria be modelled as accurately as possible so as to show changes with

climate change. The more important parameters were discussed in the parameterisation section (4.1.6) and summarised in Table 8. To predict the growth of algae these parameters have to be as accurate as possible for the species of algae present in the water-body under study. Finding some of these parameters proved difficult and futile in some instances and default values were used.

The choice of algal growth constant also affected the dissolved oxygen concentrations to such an extent that the dam became super-saturated at the surface for extended periods, which was not a reflection of reality. This also consolidated the fact that the choice of growth constant was extremely important and in-situ measurements should be collected for future studies.

7.5 GENERAL

For each run, the initial conditions were the same as the present day initial conditions. This allowed for a direct comparison of present day to intermediate future and distant future. In essence, for each simulation period it was the same original dam being subjected to climate change. What was absent was climate data from 1971 to 2100 so that the dam may be modelled for the entire period. This means that when the time of the simulation approaches 2045 the model has already run for over 50 years and the in-situ conditions are that of 2045. Currently the intermediate future and distant future initial conditions are that of the present day.

8 CONCLUSIONS

Numerous conclusions were drawn from this study and they may be subdivided into limitations and results.

8.1 STUDY LIMITATIONS

The GCMs employed in this study was of such coarse resolution (about 300km²) that they cannot be used directly for the meteorological data. The GCMs were firstly downscaled statistically to regional level (RCMs). The disadvantage of the statistical method of downscaling was that it relied on the availability of sufficient high resolution data over long periods so that statistical relationships may be established. It was not possible to be sure how valid the statistical relations are for a climate-changed situation (Houghton, 2007; Quintana-Seguí et al., 2010).

Wind-speed and direction was not supplied by CSAG (UCT) and was thus a limitation. CE-QUAL-W2 requires wind-speed and direction as part of its meteorological data input to predict water quality.

An additional outflow to a pipeline was operational but flow data for this gauging station (G1H069M01) was only available up to 1982. This pipeline was excluded from the simulation as it was deemed to have too little effect on the water quality when the calibration and validation was done.

Inflow water quality data was not as readily available as flow data, and was at best measured only on a weekly basis. No inflow and outflow data was available for the projected future scenarios and it was proposed to use flow-data from 1 January 1971 until 31 December 1990's (present scenario) for each of the subsequent intermediate and future simulations. This would assume that demand and allocation of the water resource did not change for the simulation periods.

In order to predict the growth of algae parameters had to be as accurate as possible. Finding some of these parameters proved difficult and futile in some instances and default values were used.

The choice of algal growth constant also affected the dissolved oxygen concentrations to such an extent that the dam became supersaturated at the surface for extended periods, which was not common in reality. This also consolidated the fact that the choice of growth constant was extremely important and in-situ measurements should be collected for future studies.

For each run, the initial conditions were the same as the present day initial conditions. This allowed for a direct comparison of present day to intermediate future and distant future. For each simulation period, it was the same original dam being subjected to climate change. What was absent was climate data from 1971 to 2100 so that the dam may be modelled for the entire period. This meant that when the time of simulation approached 2045 the model has already run for over 50 years and the in-situ conditions are that of 2045. Currently the intermediate future and distant future initial conditions are that of the present day.

8.2 WATER QUALITY MODELLING

The inter-variability between the four climate models was small and they all predicted similar air temperatures for each of the time scenarios studied. The climate models were also ranked in order of coolest to hottest that being ECH, CNRM, CCC and then IPSL. It was noted that the greatest increase in air temperature occurred during winter.

It was concluded that air temperature was the major driver for surface water temperatures and solar radiation was the diurnal driver.

Climate change affected the surface waters by heating the water and subsequently increased the evaporation rate of the water. This heated water evaporated more in the distant future than the intermediate future a result of the increased water temperature.

Once climate change has heated the surface waters of the dam, the water level dropped due to increased evaporation, an increase in the concentration of water quality constituents in the dam resulted.

The concentration of surface ammonium increased because of the concentrating effect of decreasing water level. Annually this increase occurred mainly during autumn and winter with small changes and decreases during spring and summer.

The effect of climate change on nitrite-nitrates was very slight as its main source was from the nitrification of ammonium. It was expected that for an increase in temperature and ammonium that the nitrification reaction would respond in an Arrhenius manner and produce more nitrite-nitrate but this was not so. It could be that the rate of generation of nitrite-nitrates was similar to its assimilation by algae.

It was seen that the concentration of DO did not vary much with climate change as would be expected due to the warmer waters. This was attributed to the greater photosynthetic rates of the algae producing more oxygen. Varying the algal growth rates had the desired effect of lowering the DO concentrations but then the algal growth was adversely affected.

Upon examining, the total surface algal growth it was seen that for climate change the concentration of total algae increased at the surface with a prominent shift earlier in the year for the distant future. This was a lengthening of the bloom season for total algae and it would persist for longer periods annually

Climate change favoured the growth of diatoms throughout the year in the distant future, with the greatest increases during autumn, signalling a seasonal shift to an earlier bloom of diatoms. Upon examining, the total surface algal growth it was seen that for climate change the concentration of total algae would increase at the surface with a prominent shift earlier in the year for the distant future. This was a lengthening of the bloom season for total algae and it would persist for longer periods annually. Diatoms were present in the dam for the entire year but were not responsible for the increased total algal due to its low concentrations.

The green algae were the dominant group in the dam and have the highest concentrations when compared to diatoms and cyanobacteria. The increase in its nutrients throughout the year as well as the increased water temperature allowed for an unabated growth for the entire year with seasonal extensions earlier in the year during autumn, with climate change. The accelerated growth with climate change was clearly visible as the increases during late summer and autumn are greater in the distant future than in the intermediate future.

Cyanobacteria are present at the surface for the entire year at significant concentrations but with intermediate and future climate change their concentrations did not change significantly for the chosen algal groups. The result for cyanobacteria was inconclusive as the inter-variability between the climate models was the greatest for cyanobacteria, with two models (IPSL and CNRM) showing an increase in surface cyanobacteria concentration and two models (CCC and ECH) a decrease in cyanobacteria concentration for intermediate and future time-period.

It was expected to see larger algal growths and algal succession but this was not the outcome of the study.

With the increase in total surface algae, zooplankton concentration increased with projected climate change.

The influence of climate change was seen to have implications for Voëlvlei Dam in the form of increased algal blooms and this had a direct effect on the surface eutrophication level especially for the distant future. For the distant future, a seasonal shift was observed and this was due to the decrease in DO and nitrite-nitrates in the latter half of the year at the surface.

For the distant future, a seasonal shift was observed in the trophic state and this was due to the decrease in DO and nitrite-nitrates in the latter half of the year at the surface. It was seen for climate change the mean monthly TRIX levels increased for all climate models with maximum in winter. With climate change, this level shifted its peak earlier in the year

9 RECOMMENDATIONS

This study concentrated on the water quality of the surface waters of Voëlvlei Dam. The study produced vast amounts of data and the limitation of presenting the surface waters only was vindicated for this dam as it was almost entirely mixed for the simulation time. The model used was CE-QUAL-W2, which is a two dimensional laterally averaged model which returns an acceptable solution. A more representative model would produce a true three dimensional solution but this would only be possible with using a three dimensional model and greater accuracy for inflow and withdrawals.

Surface water quality would deteriorate for climate change events with the decrease in dissolved oxygen and a lengthening of the total algal season. In order to prevent this phenomenon the most cost effective management of the problem would be to reduce the inflow of nutrients into the dam, especially that of phosphorus. What was required was source reduction at the facilities that discharge phosphorus into the catchment to limit its concentration in the dam.

Monitoring and measuring of all the channels into and out of Voëlvlei Dam should be implemented so that future models would be more accurate. This would include flow and water quality constituents.

Profile sampling of the water quality variables of concern would be required so that a profile of the dam may be compared thereby increasing the understanding of the hydrodynamics and the accuracy of the model predictions.

The algal parameters that govern its growth should be measured in a laboratory or in-situ for the species of algae in Voëlvlei Dam. These new values should then be used and the simulations rerun to ascertain whether the predictions differ markedly or not. This would also provide a quantitative analysis on the sensitivity of certain parameters as well as their effect on dissolved oxygen concentrations and algal growth.

Adopt a universal mathematical method of presenting the trophic level of a body of water. The TRIX level was a starting point but has its limitations, as it does not account for transparency. This would allow for direct comparisons of different water-bodies.

The complete meteorological data from 1971 to 2100 should be used for modelling. The model should be rerun with a complete set of meteorological data from 1971 to 2100 and all initial conditions should be pegged at 1971. Thus for example for 2045 the initial conditions was that of 31 December 2044.

No data on sedimentation was available, the dam was modelled in the absence of sedimentation, and since 2004, Voëlvlei Dam has become increasingly eutrophic due to re-suspension of sediments, which have not subsided (DWA, 2011). It was therefore imperative that sedimentation data be measured and incorporated and the simulation rerun to investigate this new effect on the eutrophication rate.

10 LIST OF REFERENCES

- Ahl, T., 1980, Eutrophication in relation to the load of pollution, *Progressive Water Technology*, 12:49-61
- Bergant, K., Bogataj, L. K., Trdan, S., 2006, Uncertainties in modelling of climate change impact in future: An example of onion thrips (Thrips Tabaci Lindeman) in Slovenia, *Ecological Modelling*, 194:244-255.
- Bowie, G.L., Mills, W.B., Porcella, D.B., Campbell, C.L., Pagenkopf, J.R., Rupp, G.L., Johnson, K.M., Chan, P.W.H., Gherini, S.A., and Chamberlin, C.E. 1985. *Rates, constants and kinetics formulations in surface water quality modelling: U.S. Environmental Protection Agency*, EPA/600/3-85/040
- Carter, T. R., Perry, M. L., Harasawa, H., Nishioka, S, 1994, *IPCC Technical Guidelines for Assessing Climate Change Impacts and Adaptations*, Department of Geography, University College London, United Kingdom, 1-72
- Cerco, C. F., Cole, T. M., 1995, Three-dimensional eutrophication model of Chesapeake Bay. Volume 1, U.S. Army Engineer Waterways Experiment Station, Vicksburg, Mississippi, 1994-05
- Chapra, S. C., 2008, *Surface water-quality modelling*, Illinois, Waveland Press Inc
- Chan, T.U., Hamilton, D. P., Robson, B. J., Hodges B. R., Dallimore, C., 2002, Impacts of Hydrological Changes on Phytoplankton Succession in the Swan River, Western Australia. *Estuaries and Coasts*, 25(6B)1406-1415
- Christensen, J. H., B. Hewitson, A. Busuioc, A. Chen, X. Gao, I. Held, R. Jones, R.K. Kolli, W.-T. Kwon, R. Laprise, V. Magaña Rueda, L. Mearns, C.G. Menéndez, J. Räisänen, A. Rinke, A. Sarr and P. Whetton, 2007: *Regional Climate Projections*. In: *Climate Change 2007: The Physical Science Basis. Contribution of Working Group I to the Fourth Assessment Report of the Intergovernmental Panel on Climate Change* [Solomon, S., D. Qin, M. Manning, Z. Chen, M. Marquis, K.B. Averyt, M. Tignor and H.L. Miller (eds.)]. Cambridge University Press, Cambridge, United Kingdom and New York, NY, USA (referenced as requested by document on IPCC website)
- Codd, G. A., Metcalf, J. S., Beattie, K. A., 1999, Retention of *Microcystis aeruginosa* and microcystin by salad lettuce after spray irrigation with water containing cyanobacteria, *Toxicon*, 37:1181-1185
- Codd, G. A., 2000, Cyanobacterial toxins, the perception of water quality and the prioritisation of eutrophication control, *Ecological Engineering*, March, 16:51-60
- Cole, T. M., Wells, S. A., 2008, CE-QUAL-W2: A two-dimensional, laterally averaged, Hydrodynamic and Water Quality Model, Version 3.6, Department of Civil and Environmental Engineering, Portland State University, Portland, OR.

Correll, D. L., 1998, The role of phosphorus in eutrophication of receiving waters: A review, March-April, *Journal of Environmental Quality*, 27:261-266

Correll, D. L., 1999, Phosphorus: a rate limiting nutrient in surface waters, *Poultry Science*, 78(5):674-682

Dai, A., Trenberth, K., Qian, T., 2004, A Global Dataset of Palmer Drought Severity Index for 1870–2002: Relationship with Soil Moisture and Effects of Surface Warming, *Journal of Hydrometeorology*, December, 5:1117-1130

Dallas, H. F., Day, J. A., 2004, The effect of water quality variables on aquatic ecosystems: a review, *WRC report no TT 224/04*, February, viii+222pp

DeNicola, D. M., 1996, Periphyton response to temperature at different ecological levels, *Algal Ecology*, 149-181pp

De Nobel, W.T., Huisman, Snoep, J.L. and Mur, L.R. 1997. Competition for phosphorus between nitrogen-fixing cyanobacteria *Anabaena* and *Aphanizomenon*. *FEMS Microbiology Ecology*, 24:259-267.

Department of Agriculture. 2006 – 2008. Potential First to Fourth Order Impacts of Climate Change on Agricultural Production in South Africa, and Adaptation Options. Funded by National Department of Agriculture and titled 'Climate Change: Mitigation and adaptation options for agricultural production'.

Downing, T. G., Van Ginkel, C. E., 2004, Cyanobacterial monitoring 1990-2000: Evaluation of SA data, *WRC report no 1288/1/04*, March, ix+44pp

Du Plessis, S., Kruskopf, M. M., Venter, A., Conradie, K. R., 2007, The role of nutrient utilisation and photosynthetic capacity in micro-algal bloom formation and the production of cyanotoxins, *WRC report no 1401/2/07*, October, xiii+72pp

DUFLOW, 2000, DUFLOW for Windows V3.3: DUFLOW Modelling Studio:User's Guide, Reference Guide DUFLOW, and Reference Guide RAM. Utrecht, The Netherlands, EDS/STOWA

DWA, 1996, *SOUTH AFRICAN WATER QUALITY GUIDELINES, Volume 1: Domestic use*, 2nd edition

DWA, 1996, *SOUTH AFRICAN WATER QUALITY GUIDELINES, Volume 2: Recreational Water Use*, 2nd edition

DWA, 1996, *SOUTH AFRICAN WATER QUALITY GUIDELINES, Volume 3: Industrial use*, 2nd edition

DWA, 1996, *SOUTH AFRICAN WATER QUALITY GUIDELINES, Volume 4: Irrigation*, 2nd edition

DWA, 1996, *SOUTH AFRICAN WATER QUALITY GUIDELINES, Volume 5: Livestock watering*, 2nd edition

DWA, 1996, *SOUTH AFRICAN WATER QUALITY GUIDELINES, Volume 6: Aquaculture*, 2nd edition

DWA, 1996, *SOUTH AFRICAN WATER QUALITY GUIDELINES, Volume 7: Aquatic ecosystems*, 2nd edition

DWA, 1996, *SOUTH AFRICAN WATER QUALITY GUIDELINES, Volume 8: Field guide*, 2nd edition

Department of Water Affairs and Forestry, South Africa. 2002. *Memorandum of Agreement between Department of Water Affairs and Forestry and the City of Cape Town for Water Supplied out of the Western Cape Water System Including the Berg Water Project*

Department of Water Affairs (DWA), 2011, Directorate Water Resource Planning Systems: Water Quality Planning, Resource Directed Management of Water Quality, Planning Level Review of Water Quality in South Africa. Sub-series No.WQP 2.0, Pretoria, South Africa.

Department of Water Affairs, 2011, Planning Level review of water quality in South Africa,

El Herry, S., Fathalli, A., Rejeb, A. J., Bouaïcha, N., 2008, Seasonal occurrence and toxicity of *Microcystis spp.* and *Oscillatoria tenuis* in the Lebna Dam, Tunisia, *Water Research*, 42:1263-1273

Thomann, R.V., D.M. Di Toro, D. M., Winfield, R. P., O'Connor, D. J., 1975. Mathematical Modelling of Phytoplankton in Lake Ontario, Part 1 – Model Development and Verification, U.S. Environmental Protection Agency, Office of Research and Development, ERL-Corvallis, Large Lakes Research Station, Grosse Ile, Michigan, EPA/660/3-75/005, 177 pp.

Fujihara, Y., Tanaka, K., Watanabe, T., Nagano, T., Kojiri, T., 2008, Assessing the impacts of climate change on the water resources of the Seyhan River Basin in Turkey: Use of dynamical downscaled data for hydrological simulations, *Journal of Hydrology*, 353:33-48

Genkai-Kato, M., Carpenter, S. R., 2005, Eutrophication due to phosphorus recycling in relation to lake morphology, temperature and macrophytes, *Ecology*, January, 85(1):210-219.

Goldman, J.C. and Carpenter, E.J. 1974. A kinetic approach to the effect of temperature on algal growth. *Limnology and Oceanography*, 19(5):756-766

Goldman, J. C., Porcella, D. B., Middlebrooks, E. J., Toerien, D. F., 1972, The effect of Carbon on algal growth- Its relation to eutrophication, *Water Research*, June, 6(6):637-679

Hansen, J., Sato, M., Ruedy, R., Kharecha, P., Lacis, A., Miller, R., Nazarenko, L., Lo, K., Schmidt, G. A., Russell, G., Aleinov, I., Bauer, S., Baum, E., Cairns, B., Canuto, V., Chandler, M., Cheng, Y., Cohen, A., Del Genio A., Faluvegi, G., Fleming E., Friend, A., Hall, T., Jackman, C., Jonas, J.,

Kelley, M., Kiang, N. Y., Koch, D., Labow, G., Lerner, J., Menon, S., Novakov, T., Oinas, V., Perlwitz, Ja., Perlwitz, Ju., Rind, D., Romanou, A., Schmunk, R., Shindell, D., Stone, P., Sun, S., Streets, D., Tausnev, N., Thresher, D., Unger, N., Yao, M., Zhang, S., 2007, Climate simulations for 1880–2003 with GISS model E, *Climate Dynamics*, 29:661–696

Harding, W., 2006, A research strategy for the detection and management of Algal Toxins in water sources, *Report to the Water Research Commission, WRC TT 277/06* June, xv+42pp

Harremoës, P., 1998, The challenge of managing water and material balances in relation to eutrophication, *Water, Science and technology*, 37(3):3-17

Hauer, F. R., Hill, W. R., 2007, *Methods in stream ecology*, 2nd edition, Elsevier press

Heisler, J., Glibert, P. M., Burkholder, J. M., Anderson, D. M., Cochlan, W., Dennison, W. C., Dortch, Q., Gobler, C. J., Heil, C. A., Humphries, E., Lewitus, A., Magnien, R., Marshall, H. G., Sellner, K., Stockwell, D. A., Stoecker, D. K., Suddleson, M., 2008, Eutrophication and harmful algal blooms: A scientific consensus, August, *Harmful Algae*, 8:3-13

Hewitson, B., Reason, C., Tennant, W., Tadross, M., Jack, C., MacKellar, N., Lennard, C., Hansingo, K., Walawege, R., Mdoka, M., 2004, Dynamic modeling of present and future climate systems, *WRC report no k5/1154*, vii+92pp.

Hodges, B.R., Dallimore, C., 2006, Estuary Lake and Coastal Ocean Model: ELCOM V2.2 Science, User's Manual, Centre for Water Research, Perth, 54 pp.

Holm, N.P., Armstrong, D.E. 1981. Role of nutrient limitation and competition in controlling the populations of *Asterionella Formosa* and *Microcystis aeruginosa* in semicontinuous culture. *Limnol. Oceanogr.*, 26(4):622-634.

Horne, A. J., Goldman, C. R., 1983, *Limnology*, 2nd edition, McGraw-Hill inc, New York, Chapter 22, 499-520

Houghton, J., 2007, *Global Warming: The complete briefing*, 3rd edition, Cambridge University Press, Cambridge,

Incropera, F. P., Thomas, J. F., 1977, A model for solar radiation conversion to algae in a shallow pond, *Solar Energy*, 20:157-165pp

IPPC, Integrated Pollution Prevention and Control, 2006, *Reference Document on Best Available Techniques for the Waste Treatments Industries*, August, <http://eippcb.jrc.es/reference/>.

IPCC home page: <http://www.ipcc.ch/index.htm>

IPCC, 2007: Summary for Policymakers. In: *Climate Change 2007: The Physical Science Basis. Contribution of Working Group I to the Fourth Assessment Report of the Intergovernmental Panel on Climate Change* [Solomon, S., D. Qin, M. Manning, Z. Chen, M. Marquis, K.B. Averyt, M. Tignor

and H.L. Miller (eds.)]. Cambridge University Press, Cambridge, United Kingdom and New York, NY, USA.

IPPC, 2006, Integrated Pollution Prevention: Reference document on Best Available Techniques for the Waste Treatment Industries.

Jiang, T., Chen, Y. D., Xu, C., Chen, Xia., Chen, Xi, Singh, V. P., 2007, Comparison of hydrological impacts of climate change simulated by six hydrological models in the Dongjian Basin, South China, *Journal of Hydrology*, 336:316-333.

Jeong, S., Yeon, K., Hur, Y., Oh, K., 2010, Salinity intrusion characteristics analysis using EFDC model in downstream of Geum River, *Journal of Environmental Science (China)*, 22(60):pp934-939

Jørgensen, S. E., 2008, *Ecosystems: Freshwater Lakes*, 1686-1689

Kamish, W., Rossouw, J. N., Petersen, A. M., 2007, *Development of strategies to address nuisance algal growth problems in Voëlvlei Dam*, report for the Department of Water affairs and Forestry by Ninham Shand, report number 6950/4382

Kay, A. L., Reynard, N. S., Jones, R. G., 2006, RCM rainfall for UK flood frequency estimation. I. Method and Validation, *Journal of Hydrology*, 318:151-162

Kgatuke, M. M., (2006), The internal variability of the regional climate model RegCM3 over southern Africa for the University of Pretoria. Unpublished Masters dissertation. Pretoria: University of Pretoria.

Kernan M., Battarbee R. W., Binney, H. A., (Eds) 2007, *Climate Change and Aquatic Ecosystems in the UK: science policy and management*. Proceedings of a meeting held at the Environmental Change Research Centre, University College London, 16 May 2007.

Khan, M. S., Coulibaly, P., Dibike, Y., 2006, Uncertainty analysis of statistical downscaling methods, *Journal of Hydrology*, March, 319(1-4):357-382

Kim, J., Jung, H-S., Mechoso, C. R., Kang, H-S., 2008, Validation of a multidecadal RCM hindcast over East Asia, *Global and Planetary Change*, 61:225-241

Knoesen, D., Schulze, R., Pringle, C., Summerton, M., Dickens, C., Kunz, R., (2009) *Water for the Future: Impacts of climate change on water resources in the Orange-Senqu River basin*. Report to NeWater, a project funded under the Sixth Research Framework of the European Union. Institute of Natural Resources, Pietermaritzburg, South Africa

Komatsu, E., Fukushima, T., Harasawa, H., 2007, A modelling approach to forecast the effect of long-term climate change on lake water quality, *Ecological Modelling*, 209:351-366

Kuo, J., Lung, W., Yang, C., Liu, W., Yang, M., Tang, T., 2006, Eutrophication modelling of reservoirs in Taiwan, *Environmental Modelling and Software*, 21:829-844

- Landman, W. A., Kgatuke, M., Mbedzi, M., Beraki, A., Bartman, A., Du Piesanie, A., 2006, Skill comparison of some dynamical and empirical downscaling methods for Southern Africa from a seasonal climate modeling perspective. *WRC report no 1334/1/06*, pp86
- Laprise, R., 2008, Regional climate modeling, *Journal of Computational Physics*, 227:3641-3666
- Lau, L., Young, R. A., McKeon, G., Syktus, J., Duncalfe, F., Graham, N., McGregor, J., 1999, Downscaling global information for regional benefit: coupling spatial models at varying space and time scales, *Environmental Modeling & Software*, 14:519:529
- Lee, S., Ni-Mesister, W., Toll, D., Nigro, J., Gutierrez-Magness, A. L., Engman, T., 2010, Assessing the hydraulic performance of the EPA's nonpoint source water quality assessment decision support tool using North American Land Data Assimilation System (NLDAS), *Journal of Hydrology*, 387(3-5):pp212-220
- Litchman, E. 2000. Growth rates of phytoplankton under fluctuating light. *Freshwater biology*, 44:223-235
- Limno-Tech, 2002, Descriptive inventory of models with prospective relevance of impacts of water withdrawals. Prepared for Great Lakes Commission
- Lin, C.K., Schelske, C.L. 1979. Effects of nutrient enrichment, light intensity, and temperature on growth of phytoplankton from Lake Huron. EPA-600/3-79-049.
- Ludwig, A., Matlock, Ma., Haggard, B. E., Matlock, Mo., Cummings, E., 2008, Identification and evaluation of nutrient limitation on periphyton growth in headwater streams in the Pawnee Nation, Oklahoma, *Ecological Engineering*, 32:178-186
- May, W., 2007, The simulation of the variability and extremes of daily precipitation over Europe by the HIRHAM regional climate model, *Global and Planetary Change*, 57:59-82
- Meisner, J. D., Goodier, J. L., Regier, H. A., Shuter, B. J., Christie, W. J., 1987, An assesment of the effects of climate warming on great lakes basin fishes, *Journal Great Lakes Res.*, 13(3):340-352
- Merel, S., Clement, M., Thomas, O., 2010, State of the art on cyanotoxins and their behaviour towards chlorine, *Toxicon*, 55(4), April:677-691
- Mortimer, C.H. 1956. The oxygen content of air-saturated fresh waters, and aids in calculating percentage saturation. *Intern. Assoc. Theoret. Appl. Commun.* No 6.
- Moss, R. H., (ed) 2007, Improving information for managing an uncertain future climate, *Global Environmental Change*, 17:4–7

- Nielsen, E. J., 2005, Algal succession and nutrient dynamics in Elephant Butte reservoir, Unpublished masters dissertation, Brigham Young University
- Nitsche, N. C., 2000, Assessment of a hydrodynamic water quality model, DUFLOW, for a winter rainfall river, MSc Engineering thesis, University of Stellenbosch
- Oberholster, P. J., Ashton, P. J., 2008, An overview of the current status of water quality and eutrophication in South African rivers and reservoirs, State of the nation report, *Parliamentary grant deliverable*, March, 1-15
- Oberholster, P. J., Botha, A-M., Myburgh, J. G., 2009, Linking climate change and progressive eutrophication to incidents of clustered animal mortalities in different geographical; regions of South Africa, *African Journal of Biotechnology*, November, 8(21):5825-5832
- Owuor, K., Onkonkwo, J., Van Ginkel, C., Scott, W., 2007, Environmental factors affecting the persistence of toxic phytoplankton in the Hartbeespoort dam, *WRC report no 1401/3/07*, October, xi+77pp
- Pannell, D. J., Michael A. Ewing, M. A., 2006, Managing secondary dryland salinity: Options and challenges, *Agricultural Water Management*, February, 80(1-3):41-56
- Pavluk, T., bij de Vaate, A., 2008, Ecological Indicators: Trophic Index and Efficiency, pp 3602-3608
- Peltzer, P. M., Lajmanovich, R. C., Sánchez-Hernandez, J. C., Cabagna, M. C., Attademo, A. M., Basso, A., 2008, Effects of agricultural pond eutrophication on survival and health status of *Scinax nasicus* tadpoles, *Ecotoxicology and Environmental Safety*, July, 70:185-197
- Perry, R. H., Green, D., 1985, *Perry's Chemical Engineers' Handbook*, 6th edition, McGraw-Hill,
- Prinsloo, J. F., Pieterse, A. J. H., 1994, Preliminary observations on the effect of increased concentration of total dissolved salts on growth and photosynthetic effects of different algal species, *Water SA*, July, 20(3):219-222
- Quayle, L. M., Dickens, C. W. S., Graham, M., Simpson, D., Goliger, A., Dickens, J. K., Freese, S., Bignaut, J., 2010, Investigation of the positive and neagative consequences associated with the introduction of zero-phosphate detergents into South Africa, *WRC report TT 446/10 xvi+159pp*
- Quintana-Seguí, P., Ribes, A., Martin, E., Habets, F., Boé, J., 2010, Comparison of three downscaling methods in simulating the impact of climate change on the hydrology of the Mediterranean basins, *Journal of Hydrology*, 383:111-124.
- Rosenzweig, C., G. Casassa, D.J. Karoly, A. Imeson, C. Liu, A. Menzel, S. Rawlins, T.L. Root, B. Seguin, and P. Tryjanowski, 2007, Assessment of Observed Changes and Responses in Natural and Managed Systems. In M.L. Parry, O.F. Canziani, J.P. Palutikof, P.J. van der Linden, and C.E. Hanson (eds.), *Climate Change 2007: Impacts, Adaptation and Vulnerability, Contribution of*

Working Group II to the Fourth Assessment Report of the Intergovernmental Panel on Climate Change. Cambridge, UK: Cambridge University Press.

Rossouw, J. N., 2000, The extension of management oriented models for eutrophication control, *WRC Report No 266/1/01* xiii+69pp

Rossouw, J. N., Harding, W. H. & Fatoki, O. S., 2008, A guide to catchment-scale eutrophication assessments for rivers, reservoirs and lacustrine wetlands, *WRC report TT 352/08*, April, xv+158pp

Schulze, R.E., 2004, Modelling as a Tool in Integrated Water Resources Management : Conceptual Issues and Case Study Applications. Water Research Commission, Pretoria, RSA. WRC Report 749/1/04. pp 258. (ISBN 1-77005-143 -0).

Schulze, R.E., 2005, Climate Change and Water Resources in Southern Africa: Studies on Scenarios, Impacts, Vulnerabilities and Adaptation. Water Research Commission, Pretoria, RSA, WRC Report 1430/1/05. pp 470.

Schulze, R. E., 2006, Climate change and water resources in Southern Africa, *WRC report no 1430/1/05*, liv+compact disc

Schulze, R.E. 2007. Climate Change and the Agriculture Sector in South Africa: An Assessment of Findings in the New Millennium. University of KwaZulu-Natal, Pietermaritzburg, RSA, School of Bioresources Engineering and Environmental Hydrology, *ACRUcons Report*, 55. pp 71.

Schulze, R.E., 2007, Some foci of integrated water resources management in the 'South' which are oft forgotten by the 'North'. *Water Resources Management*, 21, 269-294.

Schulze, R.E., 2007, South African Atlas of Climatology and Agrohydrology. Funded by the WRC (Report 1489/1/06) and titled 'Development of interactive updated and updateable, extended Atlas of South African Agroclimatology and Agrohydrology'.

Schulze, R.E., (Ed) 2008, *South African Atlas of Climatology and Agrohydrology*. Water Research Commission, Pretoria, RSA. pp535 (On interactive DVD).

Snaddon, C. D., Davies, B. R., 1999, An assessment of the ecological effects of inter-basin water transfer schemes (IBTs) in dryland environments, *WRC report no 665/1/00*, xxviii+113pp

Sellner, K. G., Lacouture, R. V., Parrish, C. R., 1988, Effects of increasing salinity on a cyanobacteria bloom in the Potomac River estuary, *Journal of Plankton Research*, 10(1):49-61.

Talling, J.F. 1955. The relative growth rates of three plankton diatoms in relation to underwater radiation and temperature. *Ann. Bot. N.S.*, 19:329-341

Tamiya, H.T., Sasa, T., Nikei, T. and Ishibashi, S. 1965. Effects of variation of daylength, day and night temperatures, and intensity of daylight on the growth of *Chlorella*. *J. of General and Applied Microbiology*, 4:298-307

Thomann, R.V., Di Toro, D. M., Winfield, R.P., O'Connor, D. J., 1975, *Mathematical Modelling of Phytoplankton in Lake Ontario, Part 1 – Model Development and Verification*, U.S. Environmental Protection Agency, Office of Research and Development, ERL-Corvallis, Large Lakes Research Station, Grosse Ile, Michigan. EPA/660/3-75/005, 177 pp.

Timbal, B., McAvaney, B.J., 2000, A downscaling procedure for Australia. *Bureau Meteorology Research Centre, Research Report No. 78*, Bur. Met. Australia

Trenberth, K.E., P.D. Jones, P. Ambenje, R. Bojariu, D. Easterling, A. Klein Tank, D. Parker, F. Rahimzadeh, J.A. Renwick, M. Rusticucci, B. Soden and P. Zhai, 2007, *Observations: Surface and Atmospheric Climate Change. In: Climate Change 2007: The Physical Science Basis. Contribution of Working Group I to the Fourth Assessment Report of the Intergovernmental Panel on Climate Change* Cambridge University Press, Cambridge, United Kingdom and New York, NY, USA.

Tsujimura, S and Okubo, T. 2003. Development of *Anabaena* blooms in small reservoirs with dense sediment akinete population, with special reference to temperature and irradiance. *Journal of plankton research*, 25(9):1059-1067

Tyson, P. D., Preston-Whyte, R. A., 2000, *The weather and climate of Southern Africa*. Oxford: Oxford University Press.

Van Ginkel, C., 2002, Trophic status assessment, Executive summary, www.DWA.gov.za/iwqs/eutrophication/NEMP/default.htm, June, i-xvii

Van Nguyen, V., Wood, E. F., 1979, On the morphology of summer algae dynamics in non-stratified lakes, *Ecological modeling*, 6(1979):117-131pp

Vézie, C., Rapala, J., Seitsonem, J., Sivonen, K., 2002, Effect of Nitrogen and Phosphorus on Growth of Toxic and Nontoxic *Microcystis* Strains and on Intracellular Microcystin Concentrations, *Microbial Ecology*, June, 43(4):443-454

Versteeg, H. K., Malalasekera, W., 1995, *An introduction to computational fluid dynamics*, Longman Group limited, Longman House, Essex, England

Vuren, M.J. and Grobbelaar, J.U. 1982. Selection of algal species for use in open outdoor mass cultures. *Water SA*, 8(2):86-91

Walmsley, R. D., 2000, Perspectives on eutrophication of surface waters: policy/research needs in South Africa, *WRC Report no KV129/00*, v+60 pp

Water Research Commission. 1995 and updates. Development of the ACRU Modelling System, Funded by the WRC (Project 270, Report TT 70/95 and others) and titled 'Hydrological Systems Model Development'.

Water Research Commission. 2004. Modelling as a Tool for Integrated Water Resources Development. Funded by the WRC (Project K/749) and titled 'Modelling the Benefits of Integrated Catchment Management'.

Water Research Commission. 2005. Climate Change and Water Resources in Southern Africa. Funded by the WRC (Report 1430/1/05) and titled 'Climate Change and Water Resources in Southern Africa'.

Wetzel, R. G., 2001, *Limnology, Lake and river ecosystems*, 3rd edition, London, Academic press

WHO, 2003, Guidelines for safe recreational water environments, Volume 1, Coastal and fresh waters, http://www.who.int/water_sanitation_health/dwg/en/, ISBN 92 4 154580 1

Wotton, R. S., 1995, Temperature and lake-outlet communities, *Journal of Thermal Biology*, 20(1/2):121-125pp

11 APPENDIX

Summary of the mean climate change modelling results

	Jan	Feb	Mar	Apr	May	Jun	Jul	Aug	Sep	Oct	Nov	Dec
Air temperature (°C)												
Present day	21.05	21.45	21.13	18.15	14.60	13.60	13.50	13.63	14.78	16.08	18.33	19.68
Difference	2.28	2.48	2.45	3.28	2.63	2.13	2.08	1.85	1.75	2.20	2.65	2.80
Intermediate	23.33	23.93	23.58	21.43	17.23	15.73	15.58	15.48	16.53	18.28	20.98	22.48
Difference	3.01	2.78	2.43	2.81	2.81	2.18	1.83	2.09	1.98	2.26	2.89	2.99
Future	26.33	26.70	26.00	24.23	20.03	17.90	17.40	17.57	18.50	20.53	23.87	25.47
Overall change	5.28	5.25	4.88	6.08	5.43	4.30	3.90	3.94	3.73	4.46	5.54	5.79
Water temperature (°C)												
Present day	22.01	22.23	21.70	19.81	16.15	14.29	13.58	13.96	15.36	16.96	18.62	21.45
Difference	1.17	1.09	1.02	1.16	1.40	1.08	1.12	1.19	1.19	1.28	1.36	1.37
Intermediate	23.18	23.32	22.71	20.96	17.54	15.37	14.70	15.15	16.55	18.23	19.98	22.82
Difference	1.13	1.21	0.98	1.37	1.34	1.20	1.10	1.25	1.31	1.46	1.56	1.30
Future	24.31	24.53	23.69	22.33	18.88	16.57	15.80	16.39	17.85	19.69	21.54	24.12
Overall change	2.30	2.30	2.00	2.53	2.73	2.28	2.22	2.43	2.49	2.73	2.92	2.68
Surface water elevation (masl)												
Present day	79.50	78.94	78.44	78.19	78.37	78.98	79.74	80.31	80.61	80.65	80.46	80.10
Difference	-1.58	-1.63	-1.68	-1.70	-1.69	-1.65	-1.61	-1.58	-1.58	-1.59	-1.63	-1.68
Intermediate	77.91	77.31	76.76	76.48	76.68	77.33	78.13	78.73	79.03	79.06	78.83	78.43
Difference	-1.72	-1.77	-1.84	-1.87	-1.86	-1.80	-1.74	-1.71	-1.71	-1.72	-1.75	-1.81
Future	76.20	75.53	74.92	74.61	74.82	75.53	76.39	77.02	77.32	77.33	77.08	76.62
Overall change	-3.30	-3.41	-3.52	-3.57	-3.55	-3.45	-3.34	-3.30	-3.29	-3.32	-3.38	-3.49
Phosphates (mg/l)												
Present day	0.054	0.057	0.048	0.053	0.078	0.082	0.087	0.070	0.061	0.065	0.052	0.042
Difference	0.004	0.006	0.008	0.005	0.012	0.008	0.007	0.004	0.002	0.002	0.003	0.003
Intermediate	0.058	0.063	0.055	0.058	0.090	0.090	0.094	0.074	0.063	0.067	0.055	0.045
Difference	0.005	0.009	0.015	0.019	0.011	0.008	0.002	0.003	0.001	0.005	0.001	0.007
Future	0.062	0.072	0.070	0.077	0.102	0.098	0.096	0.077	0.064	0.071	0.056	0.051
Overall change	0.009	0.015	0.023	0.024	0.024	0.015	0.009	0.007	0.003	0.006	0.004	0.009
Ammonium (mg/l)												
Present day	0.046	0.096	0.066	0.093	0.128	0.135	0.083	0.090	0.056	0.072	0.074	0.067
Difference	0.011	0.022	0.016	0.020	0.026	0.033	0.009	0.003	0.001	0.006	0.005	0.006
Intermediate	0.057	0.118	0.082	0.113	0.153	0.168	0.092	0.093	0.057	0.078	0.078	0.074
Difference	0.015	0.040	0.059	0.116	0.141	0.083	0.036	0.004	0.011	-0.002	-0.001	0.008
Future	0.071	0.157	0.142	0.228	0.294	0.251	0.129	0.096	0.068	0.075	0.078	0.081
Overall change	0.025	0.062	0.076	0.136	0.166	0.117	0.045	0.006	0.012	0.004	0.004	0.014
Nitrate-nitrite (mg/l)												
Present day	0.105	0.203	0.135	0.265	0.648	0.675	0.503	0.405	0.278	0.273	0.218	0.148
Difference	0.018	0.005	0.000	-0.013	-0.073	0.023	-0.015	0.020	-0.013	0.008	-0.013	-0.008

Intermediate	0.123	0.208	0.135	0.253	0.575	0.698	0.488	0.425	0.265	0.280	0.205	0.140
Difference	0.001	0.016	0.035	0.068	0.108	0.049	0.066	-0.032	0.018	-0.040	-0.028	-0.007
Future	0.123	0.223	0.170	0.320	0.683	0.747	0.553	0.393	0.283	0.240	0.177	0.133
Overall change	0.018	0.021	0.035	0.055	0.036	0.072	0.051	-0.012	0.006	-0.033	-0.041	-0.014
Silicon (mg/l)												
Present day	0.043	0.077	0.052	0.099	0.258	0.209	0.128	0.131	0.095	0.083	0.061	0.038
Difference	0.014	0.018	0.017	0.017	0.015	0.014	0.022	0.013	0.015	0.014	0.012	0.006
Intermediate	0.056	0.094	0.069	0.116	0.272	0.223	0.149	0.144	0.110	0.097	0.073	0.044
Difference	0.065	0.089	0.070	0.116	0.171	0.224	0.204	0.088	0.035	0.013	-0.008	0.019
Future	0.121	0.183	0.139	0.231	0.443	0.446	0.353	0.232	0.145	0.110	0.065	0.063
Overall change	0.079	0.107	0.087	0.132	0.186	0.237	0.225	0.101	0.049	0.026	0.003	0.025
Dissolved oxygen (mg/l)												
Present day	11.585	11.545	12.383	14.345	17.120	17.328	17.395	16.668	15.668	14.435	12.460	11.553
Difference	-0.225	-0.090	-0.058	-0.277	-0.295	-0.142	0.085	-0.115	-0.270	-0.285	-0.260	-0.360
Intermediate	11.360	11.455	12.325	14.068	16.825	17.185	17.480	16.553	15.398	14.150	12.200	11.193
Difference	-0.147	-0.248	0.182	0.032	-0.198	-0.305	-0.263	-0.489	-0.401	-0.493	-0.767	-0.156
Future	11.213	11.207	12.507	14.100	16.627	16.880	17.217	16.063	14.997	13.657	11.433	11.037
Overall change	-0.372	-0.338	0.124	-0.245	-0.493	-0.448	-0.178	-0.604	-0.671	-0.778	-1.027	-0.516
Total algae (mg/l)												
Present day	4.160	4.573	3.790	4.390	6.113	6.385	6.655	5.248	4.523	4.903	3.870	3.218
Difference	0.310	0.458	0.565	0.335	0.875	0.558	0.535	0.335	0.178	0.148	0.220	0.200
Intermediate	4.470	5.030	4.355	4.725	6.988	6.943	7.190	5.583	4.700	5.050	4.090	3.418
Difference	0.350	0.613	1.098	1.475	0.863	0.551	0.157	0.251	0.087	0.323	0.060	0.533
Future	4.820	5.643	5.453	6.200	7.850	7.493	7.347	5.833	4.787	5.373	4.150	3.950
Overall change	0.660	1.071	1.663	1.810	1.738	1.108	0.692	0.586	0.264	0.471	0.280	0.732
Diatoms (mg/l)												
Present day	0.068	0.054	0.061	0.055	0.185	0.260	0.226	0.143	0.121	0.119	0.071	0.042
Difference	0.010	0.014	0.016	0.021	0.063	0.041	0.007	0.016	0.017	0.016	0.011	0.007
Intermediate	0.078	0.068	0.077	0.076	0.249	0.301	0.233	0.158	0.138	0.134	0.082	0.049
Difference	-0.001	0.017	0.024	0.023	0.017	-0.007	0.032	0.013	0.041	0.023	0.011	0.008
Future	0.077	0.085	0.101	0.099	0.266	0.294	0.265	0.171	0.180	0.158	0.092	0.057
Overall change	0.009	0.031	0.040	0.044	0.081	0.033	0.039	0.029	0.059	0.039	0.021	0.015
Greens (mg/l)												
Present day	3.638	3.885	3.105	3.428	5.683	5.993	6.320	5.043	4.348	4.718	3.758	2.898
Difference	0.260	0.423	0.578	0.375	0.803	0.500	0.523	0.275	0.113	0.088	0.203	0.178
Intermediate	3.898	4.308	3.683	3.803	6.485	6.493	6.843	5.318	4.460	4.805	3.960	3.075
Difference	0.356	0.656	1.024	1.278	0.742	0.528	0.104	0.179	0.000	0.272	0.013	0.388
Future	4.253	4.963	4.707	5.080	7.227	7.020	6.947	5.497	4.460	5.077	3.973	3.463
Overall change	0.616	1.078	1.602	1.653	1.544	1.028	0.627	0.454	0.113	0.359	0.216	0.566
Cyanobacteria (mg/l)												
Present day	0.447	0.629	0.621	0.903	0.230	0.149	0.122	0.052	0.047	0.057	0.037	0.274
Difference	0.040	0.015	-0.028	-0.065	0.006	0.021	0.002	0.044	0.047	0.041	0.003	0.017

Intermediate	0.487	0.644	0.593	0.837	0.236	0.169	0.124	0.096	0.095	0.098	0.040	0.291
Difference	-0.010	-0.065	0.039	0.162	0.107	0.036	0.021	0.052	0.037	0.030	0.037	0.132
Future	0.478	0.579	0.632	0.999	0.343	0.205	0.144	0.147	0.131	0.128	0.077	0.423
Overall change	0.030	-0.050	0.011	0.096	0.113	0.057	0.022	0.096	0.084	0.071	0.040	0.149
Zooplankton (mg/l)												
Present day	1.172	1.104	1.078	0.981	1.282	1.401	1.565	1.446	1.425	1.309	1.130	0.950
Difference	0.080	0.140	0.160	0.160	0.311	0.206	0.164	0.058	0.038	0.048	0.080	0.069
Intermediate	1.252	1.244	1.238	1.140	1.593	1.607	1.729	1.503	1.463	1.357	1.209	1.019
Difference	0.140	0.229	0.349	0.438	0.364	0.227	0.081	0.095	0.028	0.134	0.072	0.131
Future	1.392	1.474	1.587	1.578	1.957	1.834	1.809	1.598	1.491	1.491	1.281	1.150
Overall change	0.220	0.370	0.509	0.597	0.675	0.433	0.244	0.153	0.066	0.182	0.152	0.200
TRIX												
Present day	3.37	3.50	3.37	3.49	3.77	3.79	3.70	3.56	3.48	3.53	3.42	3.33
Difference	0.01	0.02	0.03	0.00	-0.02	0.00	-0.01	-0.01	-0.01	-0.01	-0.01	-0.01
Intermediate	3.39	3.52	3.40	3.49	3.75	3.79	3.69	3.55	3.47	3.52	3.42	3.32
Difference	0.03	0.04	0.08	0.10	0.05	0.02	-0.01	-0.04	-0.02	-0.01	-0.03	0.03
Future	3.42	3.56	3.48	3.59	3.79	3.80	3.68	3.51	3.44	3.52	3.39	3.35
Overall change	0.04	0.06	0.11	0.10	0.02	0.02	-0.02	-0.04	-0.04	-0.01	-0.03	0.02